# Protein and Cell Interaction with Bone Substitute Materials

**Dara McCreary**

Submitted for the Degree of Doctor of Philosophy,
Department of Biomedical Engineering

University College London,
Stanmore Campus & Research Department of Materials & Tissue,
Royal National Orthopaedic Hospital,
Stanmore,
HA7 4LP
United Kingdom.

I, Dara McCreary confirmed that the work presented in this thesis is my own. Where information has been derived from other sources, I confirm that this has been indicated in this thesis.

**Acknowledgements**

This thesis would not be possible without Professor Blunn, who shared his knowledge, support, and supervision. Thank you, it was an honour of being part of your laboratory group.

Thank you to Mark Harrison and Rebecca Porter for both their technical support, for always having a friendly face and an open door throughout this thesis.

Thank you to everyone in the Zimmer Lab throughout the years, who were always there to bounce ideas off and for the endless supply of cakes.

Thank you to all my friends for listening and supporting me. Special thank you to Sinead who was always there whenever I needed support and advice.

Thank you to my Mother, Father, and the rest of my family for their love, support, and always believing in me. Without them, I would not be where I am today.

Finally, to Alex, who has been my rock throughout this process and has been there through the toughest moments and for the numerous cups of coffee during the late nights. Thank you for everything.

This student is registered as dyslexic / dyspraxic with UCL Student Disability Services.

Students with SpLDs have the option of attaching this electronic ‘sticker’ to any assessed coursework.

These stickers do not activate differential marking: they indicate to academic staff the nature of the student’s diagnosis and they refer staff to the following document:

Guidance for Academic Staff: Assessment of the work of students with specific learning difficulties – Dyslexia / Dyspraxia

http://www.ucl.ac.uk/disability/info-for-staff/dyslexia-marking-guidelines

In general, students with specific learning difficulties such as dyslexia and dyspraxia benefit from detailed and sensitive formative feedback, highlighting areas of their work that could be improved.

**Thesis Abstract**

Protein attachment to bone graft substitutes (BGS) is believed to influence the cell and tissue response to these materials. This thesis aimed was to investigate protein attachment to the surface of five commercial BGSs and to determine if this affected cellular response and osteoinduction *in vitro*. I hypothesised that differences in BGS composition would encourage different proteins to adhere and thereby influence subsequent cellular behaviour. Furthermore, I hypothesised that when selected proteins were coated onto the BGS surface, they would enhance cell proliferation and osteogenic differentiation.

No difference in mesenchymal stem cell differentiation was found on the different BGSs, but there was a significant increase in cell viability and proliferation on Inductigraft™ when compared with ApaPore™, Actifuse™, β-TCP™ and Orthoss® ($p$=0.001). Sintered discs of hydroxyapatite (HA) (ApaPore™) and silicate-substitute HA (SiHA) (Actifuse™ and Inductigraft™) were created to remove the influence of BGS morphology on cell behaviour and used to investigate the effect of silicon substitution on cell proliferation and osteogenic differentiation. The incorporation of Si significantly increased metabolic activity ($p$=0.001). Protein adhesion was measured following incubation with foetal calf serum for 30s, 1hr, 24hrs and 72hrs using SDS Page and micro BCA assays. Higher protein attachment was observed on Orthoss® compared to other BGSs. Mass spectrometry identified 106 adhered proteins and showed differences in the protein attachment profiles on the different BGSs.

To promote osteoinduction, proteins identified from the adhesion study, that could potentially affect osteoinduction, were selected (fibronectin, collagen type I alpha) and coated onto sintered HA. These proteins significantly increased cell metabolic activity ($p$=0.001; $p$=0.003). My study has shown that protein adhesion is essential, and it may be possible to select and coat proteins onto the BGS that will influence subsequent bone formation.

## Impact Statement

Bone defects occur due to congenital disability, trauma, infection or tumour. For thousands of years bone graft have been used; however, bone grafts, as we know them were not developed until the 17th century when Job Van Meekeren used *canine* bone to aid repair in an injured soldier.

More recently (2001), approximately half a million bone grafting procedures were performed in the United States and a further 2 million performed globally (Fernandez De Grado et al., 2018; Campana et al., 2014; Faour et al., 2011; Greenwald et al.; 2001). Overall majority of these procedures used autograft, known as the gold standard bone graft. However, there are other options available because of the limited supply of autograft and complications, including donor site morbidity. The other grafts include allograft; xenograft and bone graft substitutes (BGS). BGS include synthetic, inorganic or a combination of these.

Annually, the United States spends $2.5billion on bone grafts for approximately 3 million musculoskeletal procedures (Ashman and Philips, 2013). While in 2007, BGS cost €31.7 billion in Europe alone for musculoskeletal procedures, and this is expected to rise to €76.7 billion by 2050 (Karis et al., 2007).

The market of synthetic BGS is continually expanding; however, there is yet to be a graft developed that can match the performance of autografts. The first part of this thesis will compare five commercially available BGS's that have not been compared to one another previously. Four of which are synthetic BGS's (Actifuse™, ApaPore™, β-TCP™, and Inductigraft™) and one is a demineralised xenograft bone (Orthoss®). These BGSs were investigated for their potential to affect both cellular attachment and osteoinductive during *in vitro* experiments. These *in vitro* experiments will expand the current knowledge about these different grafts, which may be beneficial for future experiments and the selection of BGS for surgical procedures.

To date, there has been no large-scale investigation that explores protein attachment to BGS surfaces. The second part of this thesis will investigate the proteins that are adhering to the same five BGS's as in part one. Protein adherence to a BGS surface is known to be the first critical events to occur once the graft when submerged into biological fluids. These adhering proteins can cause the success or failure of the BGS. These proteins can be highly influenced by both chemical and physical composition of the different BGSs and have the potential to affect the subsequent interactions between the BGS and adhering cells. Novel techniques were developed to isolate and identify the adhered proteins before ranking them on their potential increase cellular attachment and osteoinductivity if adhered to BGS surfaces.

The final part of this thesis involved coating a selected BGS with either of the top two candidate proteins before seeding cells onto them to investigate whether these proteins could potentially increase cellular attachment or osteoinduction levels. The results

indicated that FINC had significantly increased both factors compared to non-coated BGS. These results could increase the potential of the BGS in aiding repair.

**Table of Contents**

## Table of Figures

**Table of Tables**

**Abbreviations**

| | |
|---|---|
| β-TCP | Beta Tricalcium phosphate |
| α-TCP | Alpha Tricalcium |
| ALP | Alkaline phosphatase |
| FETUA | Alpha-2-HS-glycoprotein |
| RGD | Arginylglycylaspartic acid |
| APCI | Atmospheric Pressure Chemical Ionization |
| BCA | Bicinchoninic Acid |
| BGS | Bone Graft Substitute |
| BMP | Bone Morphogenetic protein |
| CaP | Calcium Phosphate |
| CEMS | Centre of Excellence for Mass Spectrometry |
| CI | Chemical Ionization |
| COL1A1 | Collagen alpha-1 (I) chain |
| CO1A2 | Collagen alpha-2 (I) chain |
| DBM | Demineralised bone matrix |
| DD | Dense Disc |
| DMEM | Dulbecco's Modified Eagle Medium |
| EI | Electron Impact |
| ESI | Electrospray Ionization |
| ECM | Extracellular Matrix |
| FINC | Fibronectin |
| FACS | Fluorescence-activated cell sorting |
| FCS | Foetal calf serum |
| Hh | Hedgehog |
| HMDS | Hexamethyldisilazane |
| HSCs | Human stem cells |
| OH | Hydroxide |
| HA | Hydroxyapatite |
| KDA | Kilodalton |
| LC | Liquid Chromatography |
| LC-MS | Liquid Chromatography-Mass Spectrometry |
| MS | Mass Spectrometry |
| m/z | Mass-to-Charge |
| MALDI | Matrix Assisted Laser Desorption Ionization |
| MSC | Mesenchymal Stem Cells |
| OM | Osteogenic DMEM+ media |

| | |
|---|---|
| pNPP | p-Nitrophenyl Phosphate |
| P/S | Penicillin Streptomycin |
| PBS | Phosphate Buffered Saline |
| PLGA | Poly Lactic-co-Glycolic Acid |
| PAGE | Polyacrylamide |
| pH | Potential of Hydrogen |
| qPCR | Real-time Polymerase Chain Reaction |
| RANK | Receptor Activator of Nuclear Factor kappa-B |
| RANKL | Receptor Activator of Nuclear Factor kappa-B Ligand |
| RFU | Relative Fluorescence unit |
| SEM | Scanning Electron Microscope |
| TRFE | Serotransferrin |
| SiHA | Silicon-substituted hydroxyapatite |
| SDS | Sodium Dodecyl Sulfate |
| Std. | Standard |
| TMTs | Tandem Mass Tags |
| THRB | Thyroid Hormone Receptor Beta |
| TOF | Time of Flight |
| TGFβ | Transforming Growth Factor Beta |
| TCP | Tricalcium Phosphate |
| WST-1 | Water- Soluble Tetrazolium Salt-1 |
| Wt | Weight |
| XRD | X-ray Diffraction |

# Chapter 1
# Introduction

## 1.1 Aims and Hypothesis

This thesis aims is to investigate the protein attachment to bone graft substitute (BGS) and the possible role these proteins have on influencing the cell and tissue response to these materials. The overall aim of my thesis was to investigate protein attachment to the surface of five commercial BGS's and to decode if this affected cellular response and osteoinduction in vitro.

The general hypothesis was that differences in BGS composition would encourage different proteins and the amount of proteins to adhere to and influence subsequent cellular behaviour.

The novelty of this thesis is to investigate how proteins interact with five commercially available BGS and if these protein interactions determine *in vitro* cellular responses. Protein attachment to materials has been reported to be vital for determining cellular responses (Absolom et al., 1987; Yang et al., 2002; Sawyer et al., 2007; Schmidt et al., 2009). Whilst a plethora of research papers have investigated how BGS interact in vitro and in vivo (Coata et al., 2013; Yuan et al., 2010; Campion et al., 2010; Hayes et al., 2012; Ma et al., 2007; Wang et al., 2017), there is little attention on protein attachment. To date, there is no literature quantitatively comparing protein attachment.

### 1.1.2 Thesis chapters

Chapter One gives a physiochemical background of bone healing and BGS's. Focusing on the BGS's investigated in this thesis and the role of protein attachment to BGS. It also discusses some of the techniques used in this thesis.

Chapter Two started with the characterisation of MSCs isolated from ovine bone marrow aspirate using tri-lineage differentiation to show that the isolated cells were truly MSCs and not cell of other lineages extracted accidentally. The second investigation compared the osteoinductive potential of five different BGS's. The hypothesis was that scaffold porosity, topography and chemistry differ in each BGS and therefore affect the rate of cellular attachment, proliferation, viability, and differentiation towards osteoblasts been affected.

Chapter Three focus on the Orthoss® BGS product, which underperformed when investigated during Chapter Two and in comparison to published literature. This chapter .will investigate whether conditioning the BGS's before cell seeding could improve its performance. The hypothesis is that the Orthoss® BGS harms the seeded cells during *in vitro* experiments and that by conditioning the Orthoss® BGS in DMEM media in the presence of FCS may lead to the increase in both cellular attachment and proliferation.

Chapter Four investigates how the chemical composition of selected grafts can affect the quality of the cellular attachment and its osteoinductive potential. Two different BGS's

chemical compositions, which were compressed into a disc form to control their surface topography. The chemical composition of the discs: synthetic hydroxyapatite (HA) represented ApaPore™, and silicate-substituted hydroxyapatite (SiHA) was used for the production of both Actifuse™ and Inductigraft™. The hypothesis is that higher rates of proliferation and osteoblastic activity on the sintered discs of SiHA rather than HA.

Chapter Five considers protein attachment to BGS's before cellular attachment. Within seconds of placing a BGS into biological fluids, proteins would be attracted to it and begin to interact with its surface. These protein interactions are critical for the successful integration of the implant and the formation of bone tissue. The hypotheses for this chapter is that the amount of protein attached to the BGS varies depending on both the BGS and the time points investigated.

Chapter Six aims to identify the proteins that were attached over time to the surface of the five BGS using different methods of protein isolation and Mass Spectrometry (MS). Before ranking the proteins based on their potential to influence a multitude of factors, including cellular attachment and osteoinduction. The hypothesis was that there would be a difference in the number and quantity of proteins that adhere to different surfaces and the highest number of proteins would be found on the Si substituted BGS.

Chapter Seven investigate whether coating HA discs in the proteins identified in Chapter Six could increase the potential for the HA to influence subsequent the cellular attachment and osteoinductivity compared to non-coated HA disc's. The hypothesis is that the addition of proteins increases the number of cells that adhere to the surface of sintered HA discs and causing an increased rate of osteoinduction in the MSCs adhered too.

Chapter Eight discusses the overall conclusions and discuss recommendations for possible future work.

### 1.2 Bone Function and Physiology

Bone is a hard rigid, complex tissue that is the main component of the vertebrate's skeleton. Bone has many critical functions within human physiology; these include; structural support, locomotion, calcium homeostasis, an environment for haematopoiesis and the protection of soft tissue organs.

The adult human skeleton has 213 bones when excluding the sesamoid bones (Gray's Anatomy, 2004). The sesamoid bones are small bones that are embedded in tendons and found in locations where tendons pass over a joint. The remaining 213 bones include flat, short, and long forms.

The composition of bone consists of 80% cortical (compact) and 20% trabecular (cancellous) bone although for specific bones and regions these percentages can widely vary (Clarke, 2008; Augat et al., 2006). Cortical bone is a hard, heavily calcified dense arrangement that is involved in both structural support and protection. Trabecular bone anatomy has a lighter, less dense porous structure, which creates a large surface area

filled with bone marrow, and the metabolic activity increased (Walsh et al., 2014). The cortical bone is dense and surrounds the inner trabecular bone. The material components of the two types of bone are the same; however, they differ in their porosity and cellular organisation. Generally, in non-articulating regions of bone is surrounded by a cellular membrane known as periosteum while for cortical bone, the lining of the intramedullary cavity is endosteum (Clarke, 2008).

Bone strength is dependent on the quality and quantity of the bone tissue, while its composition is composed of both inorganic salts and organic matrixes (Viguet-Carrin et al., 2006; Florencio-Salva et al., 2015; Boskey et al., 2002). The composition of bone consists of 50-70% minerals, 20-40% organic matrix, and 5-10% water, with the remainder consisting of lipids (approximately <3%) (Clarke, 2008; Boskey, 2013). The 50-70% mineral is calcium phosphate that is arranged in a structure known as hydroxyapatite (Clarke, 2008; Boskey, 2013). The hydroxyapatite crystalline structure consists predominately of calcium phosphate, but calcium fluoride, calcium hydroxide and citrate can also be present (Hedges et al., 1992). There are several different mineral components, the most common of which is hydroxyapatite (HA) [$Ca_{10}(PO_4)_6(OH)_2$]. HA has a non-stoichiometric crystalline structure with crystal size lengths of approximately 40nm, a width of 25nm and a thickness of 1.5-3nm (Clarke, 2008; Dobelin et al., 2010; Gibson et al., 2000). Other mineral components present usually include small amounts of carbonate, magnesium and acid phosphate with missing hydroxyl groups (Clarke, 2008).

### 1.3 Bone Cells

Bone tissue is continually being remodelled. This process involves a wide array of cell types that have to be orchestrated for different functions ranging from the breaking down of damaged bone to the formation of new bone (Florencio-Salva et al., 2015; Clarke, 2008). The different cells types involved in these processes include osteoblasts, bone lining cells, osteocytes and osteoclasts (Buckwalter et al., 1996; Florencio-Salva et al., 2015). A network of both intracellular and extracellular molecular signalling manages these different processes, which are defined by their temporal and spatial sequence. These include; skeletal absorption and cellular differentiation followed by bone formation (Dimitriou et al., 2011). The process of bone formation and resorption are triggered concerning biochemical and mechanical stimuli (Rubin et al., 2006).

Bone marrow is the most common cell source of MSCs, but other tissues are now being explored, such as the periosteum, fat, muscle, cord blood, and embryonic or induced pluripotent stem cells (Colnot, 2011). Bone and bone marrow are anatomically contiguous but exhibit marked functional interdependence (Compston et al., 2002). Bone marrow is a viscous tissue that fills the cavities within the bone with a soft tissue containing a complex mixture of pluripotent stem cells (Gurkan et al., 2008). The pluripotent cells include both hematopoietic stem cells (HSCs) and mesenchymal stem cells (MSCs). HSCs are stem

cells that can undergo differentiation into all blood cells through the process of haematopoiesis. Whereas, MSCs have the potential to contribute to the regeneration of tissues such as bone, cartilage, muscle, adipose, tendons, and stroma (Garcia-Costro et al., 2008).

Tissues are regenerated by MSCs differentiating in response to biochemical cues that induce the cells to differentiate into osteoblasts, chondrocytes, myocytes, adipocytes, tenocytes and even neuronal cells (Caplan, 1991; Garcia-Costro et al., 2008; Franceschi, 1999; Logan, 2004). MSCs differentiation is a highly regulated process involving cell proliferation, migration, and finally, differentiation to a specific and distinctive phenotypic cell type (Minguell et al., 2016; Caplan, 1991). MSCs were first identified and isolated from bone marrow more than 40 years ago and can be found within adipose, peripheral blood, cord blood, liver and fetal tissues (Ullah et al., 2015; Friedenstein et al., 1970). MSCs are attractive candidates for biological cell-based tissue repair approaches due to their ability to be cultivated in high quantities *in vivo* while retaining their mesenchymal multilineage potential (Augello et al., 2010).

### 1.3.1 Osteoblasts

Osteoblasts form bone, play a role in controlling bone resorption, and are critical in fracture repair (Garg et al., 2017). Osteoblasts are differentiated from pluripotent MSCs and occur due to physical and biochemical stimulation from the surrounding bone and body fluid (Rutkovskiy et al., 2016). Osteoblasts cells exhibit various structural morphologies depending on their activity, ranging from polygonal preosteoblasts that are actively synthesising the bone matrix and become cells that are less active and more flattened in morphology, known as bone lining cells (Mallaval et al., 1999). The final stages where the cells become embedded within bone minerals and are known as osteocytes (Mallaval et al., 1999). The chemical signals include the circulating hormones; cytokines and growth factors that regulate the replication, proliferation and subsequent maturation of osteoblast to ensure bone of adequate strength can be produced (Rosenberg et al., 2012). Osteoblasts secrete the bone matrix proteins and synthesise the extracellular matrix or osteoid that is composed of collagenous and non-collagenous proteins (Florencio-Silva et al., 2015).

During fracture, healing the first bone that forms is woven bone, this due to the osteoblasts producing a matrix where the collagen fibres have a random orientation. During the fracture healing process, the woven bone is replaced by a new, stronger lamellar bone that produces aligned collagen fibres. The osteoblasts sit on the bone surface and secrete directionally secrete collagen fibres to produce osteoid, which is unmineralised. These cells also produce small extracellular vesicles in the osteoid called matrix vesicles that form the initial sites of hydroxyapatite crystal deposition. Following this initial crystal formation, HA then starts to form on the collagen fibres initially located into the so-called

“whole region” before the rate of deposition is accelerated and becomes more haphazard. The HA that is deposited is often poorly crystalline with a high carbonate content (Florencio-Silva et al., 2015).

Mature osteoblasts are eventually enclosed within the mineral matrix where they survive as osteocytes or the cells undergo apoptosis (Rosenberg et al., 2012). The enzyme alkaline phosphatase is believed to be critical in the mineralisation process. Extracellular inorganic pyrophosphate inhibits HA formation, and alkaline phosphatase (ALP) hydrolyses pyrophosphate and provides inorganic phosphate to promote mineralization (Golub et al., 2007).

### 1.3.2 Osteocytes

Once the osteoblasts become entrapped within the extracellular matrix, these cells differentiate into osteocytes (Aarden et al., 1994). This is evident in changes to both endoplasmic reticulum and Golgi apparatus, which consequently induces protein synthesis and secretion. Osteocytes are the most abundant cell types in bone (Bonewald, 2007) and are in contact with other osteocytes and with osteoblasts on the bone surface through a series of subtle channels in the bone called canaliculi. Fine cytoplasmic processes run within the canaliculi and connect to other cells through gap junctions. Being located within mineralised bone means that osteocytes are ideally positioned to respond to biomechanical and systemic signals; these interact with both osteoclast and osteoblasts (Florencio-Silva et al., 2015; Goldring, 2015). This allows for bone regulation, remodelling and adaption to mechanical loads (Goldring, 2015).

### 1.3.3 Osteoclasts

Osteoclasts are multinucleated bone-resorbing cells. The processes of bone resorption and new bone formation processes are balanced to maintain the adult skeleton. These cells can degrade mineralised matrices, including both bone and calcified cartilage (Henriksen et al., 2011; Rosenberg et al., 2012).

Osteoclasts can resorb mineralized tissues such as bone. When this occurs, osteoclasts have to attach to a mineralised surface and isolated from the extracellular environment before resorption. This process causes the dissolution of mineral crystallites that lowers the surrounding pH, which in turn causes the production of proteolytic enzymes (Primarily: cysteine proteinases and matrix metalloproteinases (MMPs)). The MMPs are then released before the collagenous matrix being digested. Once the fragments are then ingested into the cell before the subsequently excreted at the basolateral membrane (Everts et al., 2006; Chambers 2000). Recent studies suggest osteoclasts control bone formation and bone quality (Boyce et al., 2009; Henriksen et al., 2011). Osteoclast activation involves RANKL/RANK signalling, and the production of pro-inflammatory cytokines and chemokine is for regulating the inflammatory process (Walsh et al., 2014;

Pagliari et al., 2015). The contact between RANKL found on the osteoblast surfaces and RANK on the pre-osteoclast surfaces are required for cellular differentiation (Boyce et al., 2008; Mohamed et al., 2008).

### 1.4 Apatite formation

Biological apatite is an inorganic calcium phosphate salt, which can develop at a nanoscopic scale (within the range of smaller than 500Å) and is a critical component of hard tissues within vertebrate calcified tissues (Liu et al., 2013; Dorozhkin 2011). The apatite crystals formed can be flexible, can accommodate chemical substitutions before precipitating CaP's ions (LeGeros 1993; Wopenka and Pasteris 2005; Liu et al., 2013). The production of an apatite layer on biomaterials can contribute to the biomaterials ability to connect chemically and biologically to bone tissue, termed osseointegration (Hench and Wilson, 1993; Patlolla et al., 2013 Ducheyne and Qiu 1999; Blockhuis et al., 2000; LeGeros 2008). The development of biological apatite onto a BGS surface is also be used as an in vitro measure of the potential success of the graft in terms of bioactivity (apatite forming capacity with simulated body fluid) (Liu et al., 2013; Drouet, 2013). The structure of apatite crystals formed gives them the ability to promote chemical substitutions and form a bond directly with bone tissue through the apatite layer (LeGeros 1993; Wopenka and Pasteris 2005; Liu et al., 2013). The addition of Si into the HA lattice has also been shown to affect bone cell behaviour ad change the physicochemical properties (Pietak et al., 2007). For more detail, go to section 1.8.6, where the differences in BGS are discussed.

### 1.5 Differentiation of MSCs to bone cells

Differentiation of MSCs involves the expression of critical proteins and genes (Franceschi, 1999; Logan 2004). If the differentiation of MSCs is to occur, several crucial signalling pathways must interact. These pathways include hedgehog (Hh), Wnt, Notch, bone morphogenetic proteins (BMP), and transforming growth factor-beta (TGFβ) (Hojo et al., 2013). Hh and Wnt pathways regulate both proliferation and apoptosis (Rosenberg et al., 2012). Notch signalling is required for the differentiation and function of both osteoblasts and osteoclasts (Regan et al., 2013). BMP proteins are part of the TGFβ superfamily (Chen et al., 2004) and are involved in regulating the maintenance of both postnatal bone and cartilage (Wu et al., 2016). When activated during remodelling or tissue injury, TGFβ leads to recruitment of stem cells and will influence their regulation (Zhen et al., 2014; Watabe et al., 2009; Augello et al., 2010; Zhao et al., 2011; Studer et al., 2012).

#### 1.5.1 Alkaline Phosphatase

The level of alkaline phosphatase (ALP) formation was measured to investigate the BGS osteoconductive potential. In bone, ALP is an enzyme that is involved in skeletal mineralisation (Sharma et al., 2014; Wuthier et al., 1985). ALP is present in many organisms ranging from bacteria to humans and can be found within the proteoglycan

membrane (Millan, 2006; McComb et al., 1979). Levels of ALP within cells have long been established as an accessible indicator of osteoblastic activity (Leung et al., 1993). ALP activity is used to indicate early osteoblastic differentiation (Stein et al., 1990. When there is an increase in ALP levels, that is an indicator of osteoblasts have matured towards the mineralisation phase (Stein et al., 1990). During the Sugawara et al. (2002) study, they showed that ALP activity was essential for bone formation to occur and when higher ALP levels occur, they usually are associated with increased amounts of bone formation. The evidence for ALP's roles in calcification can be noted in patients with hypophosphatasia (Golub and Boeze-Battaglia, 2007).

There is an initial peak of ALP production during osteogenic differentiation; however, the levels of ALP produced by the cells decreases as the cell begins to lay down minerals and the cells matures (Aubin, 2001; Huang et al., 2007; Thibault et al., 2010). There is also higher ALP gene expression during early bone tissue development; this expression declines during the later stages when other genes are upregulated, such as osteocalcin (Golub and Boeze-Battaglia, 2007). In their 1993 study by Leung et al., they noted an increased ALP activity of 94% during the healing process.

The skeletal ALP is anchored to the inositol-phosphate membrane that can be found on the outer surface of osteoblasts (Anh et al., 1998). Throughout this thesis, the ALP levels being discussed are the levels is the external released. The ALP levels investigated are released from the cell's surface by the glycan-inositol hydrolase and/or in the form of the membrane vesicles (Farlety et al., 1994).

### 1.6 Bone Development

During the early stages of embryonic development, the skeleton consists of fibrous membranes and hyaline cartilage. Early bone development can be affected by different expression levels of specific genes; these can influence the distribution and proliferation of important cells (Olsen et al., 2000).

The process of bone development refers to as ossification (Osteogenesis). Ossification occurs in two distinct stages during fetal development. After the first two months of fetal development, the same processes, which control adult bone formation and repair, kicks in and takes control of the final stages of fetal bone development.

The first stage is intramembranous ossification; this process starts during fetal development and continues into adolescence. During intramembranous ossification bone, the tissue is formed directly over mesenchymal tissues. This process occurs during the formation of the flat bones within the skull, mandible, maxilla, and clavicles (Long et al., 2013; Gilbert, 2000). The second type of ossification is endochondral. Endochondral ossification involves the generation of bone from a cartilaginous template, which is gradually replaced by osteoblasts producing bone (Mackie et al., 2008; Long et al., 2013). Endochondral ossification is involved in the development of diaphysis of short, long and

some of the irregular bones. After birth, secondary ossification begins place. Secondary ossification occurs in the formation of the epiphyses of long, flat and extremities of bones. The diaphysis (central shaft of a long bone) and epiphyses (round ends of the long bone) separate the growth zone of cartilage also referred to as an epiphyseal plate. Once skeletal maturity is reached, epiphyseal closure can occur, and during this, the cartilage is replaced by bone fusing the epiphysis and diaphysis.

### 1.7 Bone Remodelling

Bone has the ability to self-repair and can remodel without scar tissue formation. However, when there is a significant bony defect or underlying bone pathology, poor healing occurs, and there may be a requirement to intervene to encourage bone formation using bone graft substitutes. Bone remodelling is the adaption of the bone structure.

Bones of all sizes and shapes have the ability to remodelling to remove any damaged tissues. Bone retains its ability to change its internal structure during remodelling through a complex mechanical and biochemical signal pathway even after the skeleton is fully formed (Graham et al., 2013). This process allows new bone to replace old or damaged bone while preserving bone strength, allowing bone to adapt to mechanical changes, repairing damage, and maintaining mineral homeostasis (Clarke, 2008; Graham et al., 2013). The remodelling process is initiated by damage, which signals the production of osteocyte apoptosis (Seeman, 2009). The process of remodelling begins before birth and continues until death. The initiation of mineralisation requires two phases, including the removal of acid evolved during hydroxyapatite nucleation by the osteoblast epithelium enclosed in the mineralised matrix (Blair et al., 2017). Once deposited, the mineral undergoes maturation from amorphous calcium phosphate to hydroxyapatite with essential changes in mineral orientation and organisation depending on pH levels (Gadaleta et al., 1996; Blair et al., 2017).

There are differences between the remodelling processes of cortical and cancellous bone. Many of the same molecular mechanisms that occur during skeletal development are reactivated during bone healing (Gerstenfeld 2003). Cancellous bone remodelling involves four sequential phases (Clarke et al., 2008). These steps are initiated by recruitment and activation of osteoclasts to the bone surface, and then the removal of bone is started (Clarke et al., 2008). Once a threshold is met, the osteoclast activity stops, and the production of bone by osteoblasts begins (Clarke et al., 2008).

### 1.8 Bone Graft Substitutes

When a bone is damaged or diseased, self-regeneration is the most favourable method of repair; however, there are occasions where this might not occur naturally. These include trauma, infection, tumours or congenital disabilities. There are also some situations the

regeneration of bone is essential, and the use of BGS may be advantageous (Gao et al., 2016).

One of the earliest recorded BGS ever used was to repair a soldier's injuries performed by Job Van Meekeren in 1668, he used dog bone tissue to repair the soldier's cranial injury (Hiorting- Hansen, 2002).

Authors have compiled BGS into three distinct generations. The first generations of BGS materials were developed to match the physical properties as a natural bone with a minimal host response (Hench & Polak 2002; Navarro et al., 2008). The second generation of biomaterials was designed to be bioactive and be resorbed by the natural bone (Hench & Polak 2002; Henkel et al., 2013; Navarro et al., 2008). The third generation of newly designed biomaterials was developed not just to be osteoconductive but osteoinductive, which stimulates a molecular response from the adhering cells causing regeneration of bone (Henkel et al., 2013; Navarro et al., 2008). Third-generation biomaterials are currently being designed to stimulate specific cellular responses at the level of molecular biology (Hench & Polak 2002). This involved the development of a three-dimensional structure that allows cells to adhere and begin proliferation. It's physical characteristics, can facilitate increased nutrient, and vascular infiltration into the biomaterial (Yu et al., 2015). An example of this is Nukavarapu et al. (2011), who developed a biomaterial that can control factors that included oxygen tension, which can control osteogenic cellular survival. The addition of either bone marrow aspirate or osteoinductive materials was shown to increase the recruitment of progenitor cells and enhanced cellular differentiation (Yu et al., 2015; Yu et al., 2014; Bangio et al., 2010).

During the first decade of the twenty-first century, the concepts of bioactive materials and resorbable materials have converged; bioactive materials were developed to be resorbable and resorbable polymers were formed to support bioactivity. Molecular modifications were being made to resorbable polymer systems to elicit specific interactions with cell integrins and thereby direct cell proliferation, differentiation, extracellular matrix (ECM) production and organization. Third-generation bioactive glasses and hierarchical porous foams were being designed to activate genes that can stimulate the regeneration of living tissues. Two alternative routes of repair use the new molecularly tailored third-generation biomaterials — tissue engineering. Progenitor cells can be seeded on to molecularly modified resorbable scaffolds outside the body where the cells grow, become differentiated, and mimic naturally occurring tissues. These tissue-engineered constructs are then implanted into the patients to replace diseased or damaged tissues. The scaffolds can be resorbed and replaced by host tissues that ideally include viable blood supplies and nerves with time. The goal is to develop living tissue engineering (TE) constructs that can adapt to the physiological environment and provide repair or replacement for a defect.

*In situ* tissue regeneration aims to take advantage of the body's ability to regenerate, and these include inducing endogenous stem cells and specific tissues (Lee et al., 2016). BGS

can be designed to release specific ionic dissolution products that influence cell behaviour (Polo-Corrales et al., 2014). The cells produce additional growth factors in response to these ions (e.g. soluble Si, Ca, P and Na), which in turn stimulate bone regeneration (Hench 1998; Xynos et al., 2000a).

The surface reactions of BGS release these soluble Si, Ca, P and Na ions that give rise to both intracellular and extracellular responses at the interface of the glass with its cellular environment. This is discussed in more detail in **section** 1.8.5. However, the slow release of soluble ions from the material stimulates cell division and production of growth factors and ECM proteins.

### 1.8.1 Osteoconduction, Osteoinduction and Osteointegration

Bioactivity is often termed as a measure of the rate of osteointegration or apatite layer formation (Moore et al., 2001). The formation of apatite on the material's surface has linked to the osseointegration (Pan et al., 2010).

#### 1.8.1.1 Osteoconduction

Osteoconduction is a term used for a bone that is grown directly on the surface of a material and any pores on the material's surface (Albrektsson et al., 2001; Wilson-Hench et al., 1987). However, Glantz (1987) suggests that osteoconduction is a restrictive term that is not related to the biomaterial itself (Albrektsson et al., 2001; Glantz, 1987). Osteoconduction and osseointegration are both not dependent on biological factors; however, it acts in response to foreign materials. Both osteoconduction and osseointegration are connected, and the former won't occur without the latter (Kapoor et al., 2016; Albrektsson et al., 2001). In BGS's that is osteoconductive, there is an increased bonding between the natural bone tissue due to increase cellular and capillaries activities from the host bone (Hing, 2004; Campana et al., 2014). Osteoconduction requires cell adhesion, proliferation, and migration, as well as angiogenesis (Sponer et al., 2011).

#### 1.8.1.2 Osteoinduction

Osteoinductive BGS are often placed in the non-healing bone to increase the levels of bone healing (Ludwig et al., 2000; Campana et al., 2014). Osteoinduction is the process of osteogenesis and is an important part of normal bone healing processes (Albrektsson et al., 2001; Daculsi et al., 2013). Osteoinduction occurred when undifferentiated and pluripotent cells were induced to differentiate bone-forming cells known as osteoblasts (Ko et al., 2014; Logert-Avramoglou et al., 2004). Osteoinduction can be influenced by the chemistry and structure of a BGS, but this may not be a prerequisite for bone induction (Daculsi et al., 2013).

#### 1.8.1.3 Osteointegration

Osteointegration is the interaction between the living bone and the surface of the implant in terms of direct structural connection (Mavrogenis et al., 2009).

#### 1.8.1.4 Biocompatibility and Bioactivity

Biocompatible grafts are designed to a maintain balanced microenvironment, secure osteoinductivity, enable diffuse soluble factors, while being both flexible and able to maintain mechanical loading while still being anatomically accurate (Mravic et al., 2014; Billstrom et al., 2013; Ducheyne et al., 2012). Bioactivity describes the interactions between a BGS and the surrounding tissues and the influence that the graft has on the bone formation; this bioactivity effects on cellular attachment and differentiation (Blokhuis et al., 2011). An important factor is that the selected BGS is biocompatible with the recipients living tissue and does not induce an immunological rejection, therefore, causing a positive biological effect after being placed within the body.

### 1.8.2 Autografts, Allografts and Xenografts

The gold standard BGS has been autologous bone; this is due to the patient's own bone cells which do not cause an immunogenic reaction and which can contribute to the repair of bone. There is a wide range of BGSs currently available; these include autologous bone (patient's own), allogeneic bone (donor), demineralised bone (DBM), or synthetic BGS, which includes ceramics, composites, metals and polymers. For the promotion of bone growth, biological factors have were added to the repair site, and these include the addition of undifferentiated osteoblasts cells, growth factors and proteins (Wang et al., 2017). The patient or clinical requirement influences the selection of a specific BGS at the time. The BGS's should have the ability to orchestrate the repair and regeneration of the skeletal tissue by re-establishing the microenvironments.

#### 1.8.2.1 Autografts

Autografts are considered osteoinductive. Autologous bone has been well established as the gold standard; nonetheless, synthetic BGS has become a legitimate alternative. Autologous bone is bone taken from one point in the patient and transplanted to another point in the same patient's body. Autografts are normally transplanted from fresh cancellous, cortical bone tissue or a combination of both. These sites can include fibula, iliac crest or ribs. Autologous stem cells within the donated graft can be recruited and can induce the differentiation of the adhering MSCs towards the osteoblast lineage and aid the regeneration of bone tissues (Nair et al., 2013). However, autografts are in limited supply and can cause complications at the donor site, including hematomas, fracture and donor site pain (Delloye et al., 2007).

#### 1.8.2.2 Allografts

Allograft is a donor bone tissue harvested and implanted in a different recipient patient. Allograft is one of the most commonly BGSs used for large bone defects and currently comprises a third of BGS's used in the United States (Ashman and Philips et al., 2013). Allografts have been transplanted from cancellous, cortical or a demineralised bone matrix from living or cadaver donor to the patient. In some cases, the bone was produced from femoral heads when the hip has been replaced. In the 1980s, there were less than 10,000 cases of bone grafts, and it's raised to almost 1.5 million by 2006 in the United States (Ashman and Philips et al., 2013). In the majority of recent cases, the graft is processed and supplied as freeze-dried material that has been irradiated; however, the older cases involved fresh frozen graft was used.

#### 1.8.2.3 Xenografts

Xenografts are a graft harvested from one species and implanted into another species. Xenografts offer similar chemical and physical properties offered by allografts (Schwartz et al., 2000). Xenografts have been processed to remove attached antigens or proteins that may cause an immunogenic response. Both allografts and xenografts have excellent osteoconductive potential; however, they may still induce an immunogenic response due to being foreign tissues, and there is a risk of disease transmission (Amini et al., 2012). Freezing or freeze-drying allograft and xenograft can minimize the immune response and sterilization by gamma irradiation, or ethylene oxide minimizes the risk of disease transmission; however, this is known to reduce the osteogenic potential of the grafts (Gaston et al., 2007; Jahangir et al., 2008).

#### 1.8.2.4 Metal Implants

Metallic scaffolds also should be noted. Formed from a range of different materials; including titanium, alloys and stainless steel. These are used in situations, which require mechanical strength. Metallic implants are not osteoinductive or osteoconductive and additionally release ions that in some cases are toxic (Matassi et al., 2013; Dorati et al., 2017). However, there has been a focus on developing biologically active metallic surfaces to encourage osteointegration between the implant and host bone; these include the addition of calcium phosphate (CaP) to the metal surfaces that increase the biocompatibility and longevity of the implants (Zhang et al., 2014; Campbell, 2003)

### 1.8.3 Synthetic Bone Graft Substitutes

The aim of developing synthetic BGSs was to augment and replace autologous bone (Pietak et al., 2007). The market currently has a wide range of synthetic BGSs available for surgeons to choose from (Batt et al., 2012; Gao et al., 2016). The ideal properties of a BGS that were required include an ability to promote and stimulate osteogenesis,

osteoinduction and osteoconduction (Bauer et al., 2000; Lobo et al., 2010; Langstaff et al., 1999).

Around 60-70 % of commercially available BGS is in a granular form, and many research groups are currently investigating how granular architecture influences the biological response (Habraken et al., 2015). Surface topography and roughness is one topographical factor that influences several interactions, with increased surface roughness showing higher levels of integration (Wang et al., 2017; Lord et al., 2006). Surface roughness is essential for cell attachment and differentiation, with increased surface roughness, there is an increased available surface area for both protein and cellular to interact with (Agarwal and Garcia, 2015). However, osteoblasts are attracted to smooth surfaces in increased amounts, but the surface roughness can increase both differentiation and mineralization (Agarwal and Garcia, 2015).

BGS surface chemistry charge; tension and polarity are all critical in determining the hydrophobic and hydrophilic nature of the graft. The hydrophilicity of the BGS surface can influence the intermolecular interactions with surface proteins and the attraction of ions that also affect the surface interactions with the adhering cells. These are all critical in the rate of subsequent bone formation.

The porosity of the BGS scaffold has been proven to promote both cellular and vascular ingrowth into the graft, enabling mechanical fixation of the graft to the bone. Niederauer (1994), describes surface roughness of osteoceramic materials that affecting the surface wetting properties and this can affect cellular attachment by increasing focal contacts or indirectly by influencing serum protein adsorption before cellular attaching (Koutsoukos et al., 2000). While the surface topography can influence surface energy and can increase the polar components of the surface that can have knock-on effects of improving the cellular attachment of osteoblasts (Koutsoukos et al., 2000).

### 1.8.4 Characteristics of Bone Graft Substitutes

There are several design features that can be manipulated and potentially increase the success of BGS, these include changes to chemistry, shape, surface energy, roughness, protein attachment, permeability, macroporosity and strut porosity (Coathup et al., 2012; Campion et al., 2010; Hayes et al., 2012; Ma et al., 2007). These differences can influence the differentiation of stem cells to osteoblasts in vitro and bone induction in vivo (Coata et al., 2013; Yuan et al., 2010; Campion et al., 2010; Hayes et al., 2012; Ma et al., 2007; Wang et al., 2017). Even changes at the nanometre scale to the surface of the grafts could be critical in graft success and could affect its biological interactions (Lord et al., 2006). There is an established relationship between surface energy, surface chemistry, and topography, where changes to one of these parameters could affect the other characteristics and this may affect cell-surface attachment, cell orientation and spreading (Anselme et al., 2011; Abagnale et al., 2015). Other important factors, which affect the

response of the tissues to the BGS, includes proteins attracted to the implant surface (Hing et al., 2005).

#### 1.8.4.1 Nano-topography

Nano-topography has been reported to increase osteoblast attachment, proliferation and differentiation, leading to improved bone regeneration (Semal et al., 1999; Roach et al., 2005). Surface topography at the nanometre scale plays a crucial role, implants with increased surface roughness have increased affinity with bone compared to smooth surfaces and may be critical in enabling adsorption of proteins (Brydone et al., 2010). However, the precise nature of how nanostructures influence protein and cellular performance remains unclear. The surface topography and physiochemical properties of biomaterials are essential and affect the amount of protein and cellular attachment (Thevenot et al., 2008). A description of these differences of the selected BGS is discussed in more detail throughout **section** 1.91.

#### 1.8.4.2 Porosity

There has been a debate on the optimum “type” of porosity (Hing, 2005). Increasing the strut porosity has shown to increase bone growth into the graft and early neovascularization while maintaining structural strength (Campion et al., 2010).

The porosity of typical bone graft substitute materials are at several levels with macropores being defined as being those pores that are greater than >50μm while strut porosity is defined as pores of less than 50 μm (Coathup et al., 2012).

BGS macroporosity is engineered by deliberately forming the bone graft material around another material that is later removed. The strut porosity of a BGS allows cells to infiltrate into the graft and means that the cells predominantly surrounded by graft material rather than just attached to the graft surface which is a feature of the macroporosity (Bignon et al., 2003; Hing et al., 2005). For this reason, porosity is crucial to the success of the implant.

Optimizing the porosity can increase the BGS’s surface area, influencing the amount of protein and cellular attachment that occurs while allowing bone to be integrate into the implant. However, due to structural competence, it is not possible to increase the porosity, beyond a threshold. Porosity above a critical limit was associated with a decline in mechanical stability, and if the pores are too large, they may not provide sufficient surface area for cell attachment, but on the other hand, if the pores are too small, they may inhibit cellular migration and induce necrosis (Petrochenko et al., 2010). The surface topography affects the interacts with surface protein attachment that in turn, interact with integrin’s, and these mediate the cellular interactions will the BGS. These extracellular proteins can induce changes to the cell’s phenotypic expression, protein synthesis, and osteoblastic

activities: the BGS surface topography and porosity influences cellular migration, attachment and differentiation.

Microporosity is a consequence of sintering the bone graft and is associated with smaller pores that occur in the graft material that separates the larger pores. Increased strut porosity leads to increased osteoinduction levels (Coathup et al., 2012). The formation of porosity in BGS can occur in several ways. One way is to use polymer beads that maintain the pore space and the slurry coats the beads. Salt or sugar could be used instead of the beads and was dissolved, leaving a porous scaffolding CaP. Another way is to use the investment casting of CaP slurry onto polyurethane foam. A final method is to use bubbles of gas typically; hydrogen peroxide can be used to form pores within the CaP slurry. Yeast is used to generate the CO2 bubbles by a typical fermentation reaction to create porosity. All of these methods result in the formation of a porous CaP structure before been sintered at high temperatures (Babaie et al., 2018; Wood et al., 2001).

### 1.8.5 Bone Graft Substitutes Chemistry

There is a limit to the amount of human-derived bone available for bone grafting. Meaning that there is a requirement for both natural and synthetic bone mimetic for clinical situations involving bone regeneration. One natural BGS is coralline HA, formed from marine coral. Coralline HA has a similar structure to trabecular bone (Damien et al., 2004). The calcium carbonate coral structure is hydrothermally converted to hydroxyapatite (Damien et al., 2004). The benefit of coralline HA is associated with its morphology, biocompatibility, osteoconductivity and its ability to be a capable carrier of growth factors, which increase osteointegration of the graft (Damien et al., 2004).

Ceramic BGS are generally characterised by high mechanical stiffness (O'Brien, 2011). They have a high Young's modulus. Ceramics BGS have only been considered potential grafts since the 1960's due to their high stiffness and their brittle properties (Canillas et al., 2017). 70% of human bone is hydroxyapatite mineral, and for this reason, CaP bone graft materials predominate the bone repair industry (Habraken et al., 2015). The CaP BGS releases calcium and phosphate ions which can induce an osteoinductive response (Habraken et al., 2015; Habibovic et al., 2010). These ionic releases are dependent on the graft's composition and the surrounding environment; changes to either of these conditions can influence the rate of the grafts resorption and the biological responses. Either solubilisation or induced by macrophages or foreign body giant cells can cause graft resorption (Polo-Corrales et al., 2014).

#### 1.8.5.1 Synthetic Calcium Phosphate BGS

Synthetic CaP based BGS's have been developed using several different methods. These include the synthesis using a reaction of ammonium phosphate with either calcium nitrate or calcium hydroxide in a suspension before the addition of phosphoric acid. This forms a

slurry composition; this is then cast before being sintered. Sintering occurs at high temperatures to densify the slurry into a powder.

Studies have shown that CaP can be osteoinductive when implanted into animal models causing cells to differentiate (Amini et al., 2012). It's surface chemistry, topography, and lower crystallinity can increase cellular attachment, but it can also increase pH level and cytotoxicity, leading to lower the proliferation rates of the adhered cells (Chou et al., 2007). Increased porosity leads to higher protein attachment that in turn influences the surface physiochemical reactions and interactions of the BGS, which in turn affects cellular adhesion then, eventually the formation of a calcified matrix (Zheng et al., 2006).

#### 1.8.5.2 Additions of Si ion into synthetic Calcium phosphate BGS

Several cations including magnesium, sodium, silicon and strontium ions that can be substituted for the hydroxyl group of the HA bone mineral have been identified (Barrere et al., 2006). Silicon (Si) is essential for life being Si deficiency has shown to lead to decrease collagen formation in bone (Seaborn and Nielson 2002). Low Si levels will compromise mineralization and leading to poor collagen formation (Schwarz 1973; Carlisle 1980; Carlisle 1986; Jugldaohsingh 2004). Si substitution into HA promotes increased biological activity due to the transformation of material surfaces to a biologically equivalent apatite. This resulted in increasing the solubility of material due to the generation of a more electronegative surface and to a finer microstructure (Patel et al., 2002).

Some studies have shown that HA incorporating silicon into the HA structure, can lead to increased levels of bone formation and osteoblast cell activity (Polo-Corrales et al., 2014). The addition of either 0.8wt% or 1.5wt% of Si has shown lower crystallinity while increasing solubility (Szurkowska et al., 2017). When Si was added to HA and submerged into SBF was shown to increase nucleation and growth quicker (Szurkowska et al., 2017). They believed that 0.8wt% was the ideal amount of Si to add to HA as in human bones, there is <1% of Si (Szurkowska et al., 2017). Carlisle identified trace amounts of up to 1.0wt % of Si within the immature bone. Si is critical for the metabolic role in new bone formation (Voronkov 1997).

As early as 1966, Si studies have demonstrated the promotion of cross-linking of collagen (Meyer, 1966). SiHA placed in both *in vitro* and *in vivo* have led to increased interactions between bone and implant, improving osteointegration leading to the success of the implant (Regi and Arcos, 2004). It has been hypothesized that the Si within the material can stimulate angiogenesis of endothelial cells via the paracrine way and could stimulate fibroblasts to express angiogenic factors that subsequently activate the endothelial receptors to begin downstream cascades before finally stimulating endothelial cells to undergo angiogenesis (Li et al., 2013).

Gibson et al. (1999) demonstrated that the incorporation of Si ions into a phase-pure HA could stimulate osteoblast-like cell activity when compared to stoichiometric HA. Si can

directly affect the biomineralisation processes, cellular differentiation, proliferation, collagen synthesis, and calcification during early bone development (Lee et al., 2014; Patel et al., 2002). Gibson et al. (1998) showed that Si substitutes for the phosphorus ion during the aqueous precipitation associated with the chemical reaction between calcium hydroxide and orthophosphoric acid. Si substitution into the HA crystal lattice alters the surface charge (Botelho et al., 2006; Rashid et al., 2008). Price et al., (2013) described Si as having the ability to cause a higher rate of electronegative surface leading to increased bone formation, however others studies have suggested that Si is released as the graft is being absorbed, thus having the ability to affect osteoblastic differentiation and proliferation (Lerner and Liljenqvist, 2013).

The addition of soluble Si to *in vitro* cultures results in the upregulation of collagen synthesis, osteoblast metabolism, and differentiation (Reffitt, 2003; Brown 2003). While also having the potential to increase metabolic activity and proliferation of osteoblast-like cells (Zuo et al., 2009). The addition of Si had the ability to increasing bone mineralisation of MC3T3-E1 (Kim et al., 2013).

Additionally, this affects the wettability and surface charge when compared to HA alone (Guth et al., 2010). *In vitro* studies performed by Porter et al., (2004) suggested that the incorporation of silicate ions into HA promotes bone remodelling at the bone/HA interface (Porter et al., 2004; Hing et al., 2005). Other studies have also shown that HA incorporated with other ionic substitutes including $CO_3^{2-}$, $HPO_4^{2-}$, $Mg^{2+}$, $K^{+}$, $Na^{+}$, $Zn^{2+}$, $Mn^{2+}$, $F^{-}$, or $Cl^{-}$ have the ability to enhance the bioactivity when compared to HA alone (Laskus, 2017; Dorozhkin et al., 2010; Combes et al., 2016).

### 1.8.6 Surface wettability

Cellular adhesion and interactions with the surface influenced by surface hydrophobicity and free energy (Thevenot et al., 2008). The structure and chemistry of the BGS can influence fluid and BGS interactions. Material wetting is a nanoscopic event that causes contact angles (Xu et al., 2007). While also affecting protein absorption to the surface, their conformation and the subsequent biochemical cascades that can influence cellular activities (Vogler, 1998; Xu et al., 2007). This also influences ions released from the surface of the graft.

Surface wettability is described as in two ways, firstly how fluid to spread on a surface or secondly how the water interacts with the solid surface. BGS wettability can be either hydrophobic or hydrophilic, and both can be critical to the success of the BGS. Protein adsorption is a complex process involving hydrophobic, electrostatic, and van der Waals interactions as well as hydrogen bonding (Guo et al., 2018). Comparison studies have suggested that hydrophilic surfaces cause stronger interactions with protein adhesion (Hlady and Buijs, 1996). It has also been argued that hydrophilicity surfaces, however, it has also been argued that hydrophilicity surfaces do not block proteins from adhering (Xu

et al., 2007). Studies demonstrate that attaching of diluted serums proteins onto hydrophilic surfaces before cellular seeding can increase cellular attachment and cell spreading across the surfaces (Webb et al., 1998).

Competition between proteins and water on BGS surface is a critical component of protein adsorption; however, the effects of surfaces wettability on proteins adhesion is not always consistent and may affect "quality" and quantity of proteins that adsorption (Xu et al., 2007). Guo et al. (2018) investigated the influence on how surface charge and wettability may affect proteins adsorption attributes, kinetics, quantities, deformation, and reversibility. This enabled them to investigate how BSA is adhering to BGSs. They used the quartz crystal microbalance, which monitored dissipation and atomic force microscopy-based force spectroscopy on different surfaces. However, they were unable to determine whether surface charge or wettability was more dominant in affecting protein attachment due to the complexity of interacts between solids and liquids (Guo et al., 2018).

Proteins may undergo conformational changes due to both surface charge and hydrophobicity; this may increase the protein−surface interaction forces and the amount of protein adsorption. Nonetheless, Guo et al., (2018) were able to show that the hydrophobicity can cause deformation of the proteins, thus affecting how the proteins spread.

The surface charges can also affect the protein conformation changes and desorption. This could be affected by the ionic strength, which is a secondary charge to that of the surface hydrophobicity. Understanding this will enable advances in surface chemistry and properties leading to tailored directing the proteins-surface interactions.

#### 1.8.6.7 Dissolution of BGSs

Bioactive materials dissolve in equilibrium with natural apatite formation through interactions between the dissolving BGS and the surrounding tissues causing the new bone formation of new tissues. The opposite is also an issue as if they too little dissolution will lead to an inability for the graft to make space for new health bone formation; however, the graft may be retained to support the osteoblasts in the development of new bone (Yamada and Egusa, 2018).

The surface area can profoundly influence the dissolution rate of the graft to volume ratio, fluid convection, acidity and temperature (Dorozhkin, 2002). Dissolution release incorporates functional ions affecting bioactive and potentially osteoporotic properties. Understanding the dissolution rates can aid in improving the bioactivity of materials.

Dissolution can be broken down by enzymatic or chemical dissolution is critical for making space for the new bone development; however, it should be noted that if the dissolution occurs too quickly making the graft unstable before the new bone forms which can contribute to defective space formation (Yamada and Egusa, 2018). Enzymatic dissolution occurs through cells for osteoblasts that produce various isoforms of collagenase that will

breakdown the collagen matrix or tissue fluids degradation through hydrolysis. While, chemical dissolution continues to aid bone remodelling after the bioabsorption of BGS after in embedded, this occurs through chemical dissolution. Chemical dissolution may lead to apoptosis osteoclasts a subsequent inhibition of osteoclastic resorption due to excess calcium ions (Yamada and Egusa, 2018).

The dissolution of the material causes the absorption of increased levels of proteins, which also increase osteoblast adhesion (Coathup et al., 2013). This interaction occurs between the dissolving materials interacting with the surrounding materials that could mediate osteoblast cells (Porter et al., 2003).

Bioactivity of the HA materials such as in the ApaPore™ is believed to be associated with the release of both Ca and P ions during the dissolution, while precipitation of biological apatite layers (Porter et al., 2003; Coathup et al., 2013). Priya et al., (2010) discussed that high levels of dissolution graft formed from CaP composites causing the release both of Ca and P ions. This release of ions can induce increased levels of apatite formations onto the graft's surface. Priya et al., (2010) believed that this to process is an interlinked mechanism and this resorption of the graft influences the bone-bonding properties.

While the dissolution rate of the ceramic could be potentially be affected by the addition of Si could potential affect the rate of dissolution rate of the graft as it influences the structural composition, protein conformation, and topography (Wang, 2017). This is essential for the substituted materials can influence the rate of apatite dissolution and favouring osseointegration (Dalculsi et al., 1989; Porter et al., 2003). This has been shown to occur during in vivo and in vitro situations during *in vivo* conditions.

As noted before several times strut porosity is the difference between Actifuse™ and Inductigraft™. Inductigraft™ has the increased and strut porosity results in the largest surface area that contributes to the adsorption as well as to ion exchange and bone-like apatite formation by dissolution and re-precipitation. Porter et al., (2003), studies investigated *in vivo* dissolution comparing HA, 0.8wt% SiHA and 1.5wt% SiHA. Using high-resolution transmission electron microscopy, they were to illustrate that there was a higher level of dissolution 1.5wt% SiHA compared 0.8wt% SiHA, which was then higher than HA. They believed that this increased dissolution due to the addition of Si and the increased porosity (Porter et al., 2003).

Sha et al., (2011) a comparison was made with β-TCP™ to have shown to have an excellent rate of dissolution when in vivo environment after implantation. While with Orthoss® there currently no comparisons studies between and the other BGS investigate here, however, there is a comparison of xenografts and them. These studies showed that there was better osteointegration when compared to HA/β-TCP (Bagher et al., 2012). A study by Zivko et al., (2013) suggested that the dissolution of the Orthoss® surface and its osteogenic responses are highly depended on its concentration during in vitro experiments.

### 1.9 Bone Graft Substitutes and Protein Attachment

The addition of chemicals, proteins, peptides or cells could potentially affect the success rate of BGS (Polo-Corrales et al., 2014). How cells respond to the BGS surface has long been established as a secondary response (Amini et al., 2012). The initial response has been showed to be the absorption of a protein layer onto the surface, which occurs within seconds after immersion of the BGS into biological fluids (Hayes et al., 2012; Botelho et al., 2006; Deligianni et al., 2000). Within milliseconds of implantation into biological fluids, proteins start to adhere to the BGS surface and these proteins are critical in mediating both further protein attachment and future cellular response (Absolom et al., 1987; Yang et al., 2002; Sawyer et al., 2007; Schmidt et al., 2009). Proteins within the extracellular matrix influence this response and this fluctuation is depended on several factors such as the type of bone, age, gender, disease state and treatments associated with medical conditions (Florencio-Silva et al., 2015). However, it should be noted that cell signalling could also be affected by ions or peptides (Hing et al., 2005).

Several studies have demonstrated how optimising protein attachment can influence critical processes including cell attachment, cell spreading, proliferation and promotion of osteoinduction (Guth et al., 2011; Shelton et al., 1988). The attachment of specific and non-specific proteins could be prevented from attaching, leading to a reduction in an immunological response when implanted (Fang et al., 2005). To induce earlier osteoblast differentiation, protein attachment at the right time can be critical (Komori, 2006). Most of these previous studies have only been able to isolated individual or selected groups of proteins and investigated their potential in the osteoinductive pathway.

Proteins within the body are constantly interacting with both the bone, cells and any implanted structure (Heaney et al., 2008). The proteins that absorb initial have the ability to control subsequent cellular reactions (Chen et al., 2008; Anderson et al., 2008; Keselwsky et al., 2005). These cellular reactions are mediated by signal transduction within the cell that will affect gene expression and subsequently, cellular behaviour. The adhered proteins mask an otherwise potentially hostile surface (Wilson et al., 2005). By the time cells arrive at the BGS surface, the graft should have a monolayer of proteins. This means the arriving cells do not “see” the BGS surface but instead “see” a potential attractive layer of attached proteins (Schmidt et al., 2009). These proteins relay extracellular instructions causing a constructive response from the cells, possibly leading to further cellular recruitment and osteoinduction (Wilson et al., 2005).

The processes regulated by some of these absorbed proteins that attach to biomaterials can influence a phenotypic response. Osteoinductive agents are generally proteins, which can induce differentiation of pluripotent stem cells to osteogenic cells or induce stem cells to proliferate (Nandi et al., 2010; Perry 1999; Rabe et al., 2011; Sawyer et al., 2007; Shelton et al., 1988; Allen et al., 2006).

### 1.9.1 Physical and chemical properties of grafts affect Protein interactions

The surface topography and chemistry varies between different commercial BGS, and this can affect protein attachment by deciphering this it's hoped we can control on proteins could potentially enable a way to manipulate it and possibly develop superior BGS (Lord et al., 2006). This could be by optimising protein attachment that in turn influences critical processes of cells that range from attachment, spreading, proliferation, and pushing them towards the osteoinduction lineage (Guth et al., 2011; Shelton et al., 1988).

Proteins interact with BGS surface so the physical and chemical properties of the grafts could be critical in influencing the response of the proteins in terms of quantity and diversity (Rosengren et al., 2002; Schmidt et al., 2009; Wang et al., 2012; Chen et al., 2008).

As with cellular attachment, there are many different factors that could affect protein absorb to the graft surface; including chemical formula, surface topography and the amount of proteins in the surrounding fluid and tissues (Wang et al., 2012; Lord et al., 2006; Nath et al., 2006; Guth et al., 2010; Fang et al., 2005).

The chemical composition is also a critical factor in interacting with proteins by influencing the types of forces, which have the ability to govern interaction with proteins (Guth et al., 2010; Hing, 2005; Podaropoulos et al., 2009; Sawyer et al., 2007; Wang et al., 2012; Dee et al., 2002). Studies have demonstrated that synthetic BGS, developed from CaP, can attract proteins that other investigated (Sawyer et al., 2007; Wang et al., 2012; Guth et al., 2010; Hing, 2005; Podaropoulos et al., 2009). This is due to its chemistry affecting the electrostatic and hydrophobic levels of the surfaces (Wang et al., 2012).

The release of ions and surface charge of the BGS surface can influence the surrounding solution around the surface changing and can attract ions solution. These changes in the electrostatic attraction cause more acidic proteins to attach to the surface, whereas more basic proteins are attracted to P/OH sites (Wang et al., 2012). Thian et al. suggested that the increased protein adsorption to it SiHA surface was caused by the formation of a silicate network causing intracellular specific cellular interactions that could stimulate the bone mineralisation process (Thian et al., 2006a; Thian et al., 2006b; Dalgic et al., 2018). In Thain et al., (2006), they also believed that increasing the amount of Si content in samples led to the increased cellular organisation compared to controls; however, they noted that how Si affects the cellular activity required more investigated.

The surface topography affects this protein adsorption as the more exposed surface can lead to increased surface area for protein adsorption. The increased porosity leads to a larger surface area that could increase the quantity and possible variation in the protein attachment (Hing et al., 2005; Guth et al., 2010). As with the chemistry, the surface topography of BGS affects the speed that proteins attachment, which proteins adhere, their quantity and how they adhere leading to possible conformational changes to the protein (Dee et al., 2002; Hing et al., 2005). Other factors that can influence the diversity

of protein attachment include surface energy (Schmidt et al., 2009; Hing, 2005; Lampin et al., 1997).

### 1.9.2 Surrounding fluid protein concentrations

A critical factor that affects the amount of protein interaction with grafts is highly dependent on the concentration of proteins within fluids surrounding the implant (Wang et al., 2012; Nath et al., 2004). Variation of protein affinities to the BGS surface is critical, and competition encouraging variation (Hing et al., 2005). The Vroman effect shows that the protein adherence changes and over time, some proteins could detach from the surface while others attach. The first proteins to attach are usually those that have a high concentration, more mobile, but also have low surface adherence (Nath et al., 2004; Hing et al., 2005). These proteins can be usually replaced by proteins that are lower in concentration, less mobile but with a higher surface affinity (Nath et al., 2004; Hing et al., 2005).

## 1.10 Bone Graft Substitutes being investigated in this thesis

This thesis investigated five different commercially available BGSs and identified the proteins, which adhere to their surfaces and relate this to their osteoinductive potential. Four of which are synthetic BGSs: ApaPore™ (ApaTech, UK), Actifuse™ (ApaTech, UK), β-TCP™ (Pfizer, UK), Inductigraft™ (ApaTech, UK) and the fifth is commercial demineralised bovine bone scaffold, known as Orthoss® (Geistlich, Switzerland). There is a brief overall description of these BGSs layout in **Table** 1.1 below.

**Table 1. 1** The five commercial available bone graft substitute investigated.

| Substrate | Size | Macro Porosity* | Strut Porosity* | Chemistry | Suppliers |
|---|---|---|---|---|---|
| **Actifuse™** | 2-5mm | 50% | 5-15% | SiHA (8% Si) | ApaTech, Uk |
| **ApaPore™** | 2-5mm | 60% | 20% | Synthetic HA | ApaTech, Uk |
| **β-TCP™** | 2-5mm | 80% | 22.5% | β–Tricalcium phosphate | Pfizer, Uk |
| **Inductigraft™** | 1-2mm | 80% | 32% | SiHA (8% Si) | ApaTech, Uk |
| **Orthoss®** | 1-2mm | 80 | 10-20nm** | Deproteinised bovine bone | Geistlich, Swiss |

*****Coathup et al., (2013), defined porosity at the micrometre levels, with macropores, typically being between 100 to 200μm and strut porosity being <50um and having a diameter of between 1 to 10μm. **Kouroupis et al., 2013.

The BGS selected for this thesis were chosen due to their differences in a range of features, including physio-chemical, surface topography, micro, and macro-porosity. Actifuse™ is SiHA materials were selected to make a comparison to the HA material of

ApaPore™. This was done to compare the addition of the silicate substitution into the HA lattice. Two SiHA materials were selected to compare the differences in microporosity with Inductigraft™ having, an increased porosity compared to Actifuse™. Inductigraft™ has previously been described as osteoinductive. β-TCP™ was selected to give a measure of the different physio-chemical compared to the other HA materials. The final BGS of Orthoss® was select as a contrast to the synthetic BGS as it is a bio-derived BGS and developed from highly purified bovine natural HA.

### 1.10.1 ApaPore™

ApaPore™ is formed from synthetic HA and has been structurally manipulated to form granules that can maintain their structural integrity when placed into a wound (Coathup et al., 2012). The similarity of synthetic HA ($Ca_{10}(PO_4)_6(OH)_2$) to natural bone minerals has led to its extensive use within bone grafting material for hard tissue implants (Von Doenrberg et al., 2006). The combination of the pure-phase HA and strut/macro-porous structure in ApaPore™ has shown to be osteoconductive and encourages ingrowth, support bone formation and can lead to remodelling of natural bone (Podaropoulous et al., 2009; Harding et al., 2005). ApaPore™ structure has a similar trabecular structure to the cancellous bone and allows for the diffusion of growth factors, absorption of blood and bone marrow as well as attracting osteogenic proteins (Von Doenrberg et al., 2006; Hing et al., 2005).

### 1.10.2 Actifuse™

Actifuse™ (ApaTech, Foxborough, UK) is a synthetic silicate-substituted porous HA. In Actifuse™ silicate ions were incorporated into the HA lattice structure and were developed to improve osteoinduction and osseointegration (Bohner, 2009). The incorporation of 0.8% of silicon into HA occurs through aqueous precipitation method using $Ca_2(OH)_2$ and $H_3PO_4$ and then sintered at 1200$^{o}$C. The Ca/(P+Si) ratio of Actifuse™ is kept constant at 1.67, leading to the stoichiometric HA and final substitution of silicon ions into phosphorous sites (McNamara et al., 2010; Von Doenrberg et al., 2006). Actifuse™ has a granule size, which ranges between 2-5 mm and a reported porosity size marketed as 60% but there have been reports that the true total porosity ranges between 60-67% (McNarmara et al., 2010). The same company that supplies Apapore™ supplies Actifuse™. Both BGS have similar topography but Actifuse™ contains 0.8% silicon.

### 1.10.3 Inductigraft™

Inductigraft™ is a silicate-substituted HA material developed in the same manner as Actifuse™ however, with increased strut porosity (Mangano et al., 2008). The increased porosity creates a greater surface area that allows for higher amounts of proteins to bind to its surface (Gibson et al., 2009). The increase strut porosity has been described to

influence osteoinduction and osteointegration when compared to similar materials with lower porosity (Coathup et al., 2012; Nakata et al., 2016; Yka-Soininmaki et al., 2013).

### 1.10.4 β -TCP™

Tricalcium phosphate (TCP) is a calcium salt of phosphoric acid, whose chemical formula is $Ca_3(PO_4)_2$. TCP is more soluble than HA, with a greater rate of bioresorption (Rouahi et al., 2006). TCP has two allotropic forms: Alpha-TCP (α –TCP (α -$Ca_3(PO_4)^2$)), and Beta-TCP (β –TCP (β -$Ca_3(PO_4)_2$)). α-TCP is stable between 1180$^o$C and 1400$^o$C, whereas β -TCP is stable below 1180$^o$C and both have a chemistry that is similar to the inorganic phase of natural bone. Commercially β -TCP™ is supplied commercially, whereas α -TCP is mainly found as fine powder in CaP cement (Botelho et al., 2006). β-TCP™ has a stoichiometry similar to amorphous biologic precursors of bone mineral and displays a Ca-to-P molar ratio of 1.516.

### 1.10.5 Orthoss®

Orthoss® is a bio-derived BGS developed from highly purified bovine natural HA and is available as granules or blocks forms that have various sizes (Dorati et al., 2013). During processing Orthoss®, any organic components are removed and leave the decellularised and deproteinised matrix (Dorati et al., 2013; Garin et al., 2016). Orthoss® has shown to cause a reduced local inflammation reaction while being highly osteoinductive (Garin et al., 2016; Kouroupis et al., 2012). Orthoss® has similar topography as human bone (Dorati et al., 2013; Kouroupis et al., 2013).

## 1.11 *In vivo* studies using these BGS's.

Below is a brief description of some of the published *in vivo* studies involving the BGS investigated.

### 1.11.1 Apapore™

The 2017 Kumar et al. study, retrospectively investigated the impact of graft revision in total hip replacement of 21 patients. The patients received allograft, synthetic graft or allograft alone. Eight patients received a 50/50 allograft and ApaPore™ mixture, while seven patients just received allograft. Six patients died from unrelated causes. Bone loss was classified using Paprosky classification with an average follow-up for 10 years. The results indicated Apapore™ was a viable and possible safer option compared to the allograft. While McNamara et al. (2010) investigated 50 consecutive acetabular reconstructions retrospectively. A 1:1 mixture of frozen, ground irradiated bone and ApaPore™60 was used in 48 patients, and they showed comparable results to frozen, irradiated bone alone over their 60-month follow-up period.

The *in vivo* study by Coathup et al., (2008), in 12 female sheep investigated impaction of allografting over 6 months. The first group was 50:50 mixture of ApaPore™ and allograft

group while the second group was 90:10 ApaPore™ and allograft mixture. There was no significant difference between both groups meaning the results for both were comparable.

### 1.11.2 Actifuse™ and Inductigraft™

These studies compared different strut porosity of SiHA that represented Actifuse™ (Lower strut porosity) and Inductigraft™ (Higher strut porosity) BGSs.

Hutchens et al., (2016) investigation into SiCaP with increased strut porosity that used for ovine critical-sized metaphase defects in the distal femoral enabled a comparison to be made between SiCaP to an autologous iliac crest bone graft extender and a mixture of SiCaP with bone marrow aspirate. A strut porosity was used 39 ± 8% and evaluated at 4, 8 and 12 weeks. The results indicated that all groups had a positive response of neovascularisation, bone growth, and finally infiltration of marrow throughout the graft samples to the implants after an initial response period of mild inflammatory. However, the extender group produced higher amounts of bone formed at early time points with more desirable mechanical properties; however, this levelled out at later time points with similar amounts of bone in all samples.

Coathup et al., (2011) study investigated SiCaP that had 80% macroporosity with a 30% strut porosity. These were implanted ectopically into ovine for 12 weeks. Significant bone formation occurred compared to the control of stoichiometric calcium phosphate. They concluded that SiCaP samples had significantly higher amounts of bone formed within and on its surface of the samples.

Harshavardhana et al. (2015) used Actifuse™ in 35 patients who have adolescent idiopathic scoliosis. SiCaP was added to locally harvested bone at 60:40 ratios. 6 weeks post-operation; they observed osteointegration using radiographic fusion, and the granules were fully integrated into bone as solid fusion mass by 24 months. These results indicated that Actifuse™ had increased neovascularisation, bone apposition formation, and standard trabecular architecture when compared to controls.

#### 1.11.2.1 Comparison of different strut porosities.

These studies compared SiHA BGS with different in their strut porosities. The 2012 study by Coathup et al., compared increased the strut porosity of both CaP and SiCaP BGS. They were again implanted ectopically in ovine in the right paraspinal muscle. The strut porosity of the samples was 10, 20 and 30%. After 12 weeks, they showed increased levels of osteoinduction in the 30% SiCaP, and this was higher than the matching 30% CaP. They were unable to see any bone growth in the 10% strut porosity samples.

In their 2016 study, Coathup et al., (2016) compared SiCaP with microporosity of 22.5% and 36%. These were surgically placed into ovine poster lateral spinal fusion. They aimed to investigated bone apposition, bone formation, bone-implant contact and the levels of resorption of the graft at three-time points post-surgery, 8 12, and 24 weeks. They noted

no significant difference between the two materials in bone apposition, formation, and bone-implant contact. However, at 8 weeks there was a significantly higher CT score obtained in the 36% group (0.83 ± 0.17) with significantly fewer scaffolds remaining at 12 weeks. Both formulations showed augmented bone formation. Increased strut porosity did not produce any significant increase in bone formation; however, at 8 weeks did promote increased mineralised bone formation and significantly higher CT scores which they believed caused more mature bone tissue formation.

Chan et al., (2012) comparison included placing SiCaP ectopically with strut porosities of 22.5%, 32% and 46% into ovine paraspinal muscles. They investigate bone area; implant area and bone-implant contact at 8, 12 and 24 weeks. No significant difference between the grafts at 8 weeks, but there was at 12 weeks in 46% sample compared to 22.5%. At 24 weeks, this showed a 75-fold increase in the 46% samples. This indicated that increased strut porosity leads to higher bone formation and implant contact.

### 1.11.3 β -TCP™

During the Galois et al., (2002) they investigated 110 patients who required β-TCP™ for a range of bone-related issued including non-unions, benign tumours, and hip revisions. In 86 cases β-TCP™ was used alone, 22 cases were used in combination with corticocancellous autografts bone, and the final 2 patients were in combination with allograft bone. In 30 cases, there was excellent that incorporation of ceramic, 51 cases had good incorporation, and the final 26 had fair incorporation. They indicated that 75% had a rating of good or above. Three cases had the graft removed due to infection. They concluded that β -TCP™ is an excellent choice for medium-sized defects.

In 2017 Hernigou et al., study retrospectively investigated the outcome of 50 patients who had orthopaedic surgery with 25 of them had β-TCP™ and 25 with autografts. There were 54 surgeries for bone defects with 34 open-wedge high tibial osteotomies, and 20 osteonecrosis treatments with core decompression. Their results indicated a 100% fusion rate of the osteotomies β-TCP™ group compared to 94% of the autografts group. For the 20 caviar defects found that both groups had 100% presences of osseous bridging. One-year post-surgery the β-TCP™ group showed less pain and improved safety. However, they noted that the β-TCP™ group had established a clinical parameter that it could be used alone and could successfully support osteogenic processes.

### 1.11.4 Orthoss®

Piattello et al., (2010) retrospectively investigated Bio-Oss® (Another name for Orthoss®) used during sinus augmentation procedures over a long period in 20 patients. They aim to investigate the rapid replacement of host bone as other researchers noted that Bio-Oss® has slow resorption or no resorption post insertion of 6 months to 4 years in some patients. Piattello et al. noted the granules were surrounded by mature compact bone with small

capillaries, with both MSC's and osteoblasts in conjunction with new bone with some semblance of granules resorption by osteoblasts. Their results led them to believe that Bio-Oss® can be biocompatible, osteoconductive, however, with a slow resorption rate.
While Garin et al., (2016) performed another retrospective analysis of Orthoss® in the presents and absents of bone marrow aspirate in 47 young patients with spinal fusion including scoliosis, degenerative spine, lumbosacral transitional anomalies, and spine drama. The patients had a 1:1 ratio of autologous bone to Orthoss® granules with follow-ups at three, six, twelve and twenty months. They noted a functional recovery in the majority of patients within three months and progressive bone formation with evidence of bone fusion in the majority of patients within six months with no fusion failure seen in any of the patients.

### 1.12 Identification of the Absorbed Protein

Absorbed proteins that attach to biomaterials can influence a phenotypic response and in turn, can initiate osteoinduction via an intracellular signalling cascade (Chen et al., 2008; Shelton et al., 1988; Allen et al., 2006). There have been numerous studies that have described how optimising protein attachment influences cellular attachment and proliferation, while also being able to promote increased levels of osteoinduction (Guth et al., 2011; Shelton et al., 1988). This optimisation could lead to the development of BGS with a more successful clinical outcome.
Guth et al., (2010) described that the addition of Si to HA could attract proteins in higher amounts; they noted that this included both fibronectin and vitronectin proteins when the compared to HA alone. The effect of the molecular weight of proteins on the kinetics is very complex and different from its role in the equilibrium adsorption isotherms (Fang et al., 2005). It is noted that increased strut-porosity can expand the surface area and in succession, this should cause an increased quantity and possible variation in proteins attachment (Coathup et al., 2010; Hing et al., 2005).

#### 1.12.1 SDS-PAGE Gel

A standard method of protein separation is by electrophoresis. One mode of electrophoresis uses a combination of discontinuous polyacrylamide gel (PAGE) as a support medium and anionic sodium dodecyl sulfate (SDS) which denatures the proteins also known as SDS-PAGE.
The SDS detergent causes a negatively charged complex; the amount of SDS that binds to the protein cause a change in the charge. SDS causes the protein to be denatured and solubilised, causing the complex to form into a rod/ellipsoid shape that proportional to the proteins molecular weight. The negatively charged protein complex is then separated based on the difference in the size and charge when the electrophoresis is run, and the

polyacrylamide gel acts as a sieving matrix. It enables the more mobile proteins to move further through the matrix leading to the separation of the different proteins out.
The identification and characterisation of the proteins is the main aim of the proteomic analysis, to identify these proteins requires the extraction of them from the SDS-PAGE gel (Huynh et al., 2009). The proteins within the gel required processing which included removal of the protein stain, reduction, and alkylation of the proteins, before digestion and extraction of the peptides from the gel (Huynh et al., 2009). The extracted proteins could be analysed by mass spectrometry (MS).

### 1.12.2 Spin Column Cut Off

Spin columns were used to separate proteins and produced batches of proteins within specific size ranges (Zang et al., 2006). These proteins are then digested by trypsin prior before submitted for MS analysis.

### 1.12.3 Tandem Mass Tags™

detached proteins before the MS analysis, enabling the proteins to be more easily identified (Rauniyar et al., 2014). The addition of stable isotope labelling strategies is commonly used to profile targeted protein quantity (Gevaert et al., 2008).
Isobaric tandem mass tags (TMTs) are used for quantitative proteomics. TMTs that are attached to proteins before MS/MS to detect proteins while being high sensitivity and reduces the noise. TMT labelling enables qualitative and quantitative proteome analysis (Thompson et al., 2003). The tags allow peptides from different samples to be both identify and measured with accuracy that could not be matched by other methods (Thompson et al., 2003). TMT is isobaric tags that enable the simultaneous identification of the peptides and the relative quantity (Thompson et al., 2003). The TMT tags consist of a reporter group, a mass-balancing group, a cleavable linker and a peptide-reactive group, and could be used to perform at the MS/MS level where the signals already intensified (Liang et al., 2015).
Multiplexing is the ability to simultaneously identifying and quantifying signals from different sources run within the same experiment, allowing for a relative quantity of proteins to be calculated over several time points (Liang et al., 2015). TMT tagging is done by covalently attaching a molecule to the N-terminus of the peptides and during the MS/MS analysis the reporter ion breaks at the cleavable linker site and can be detected (Olshina et al., 2016). The peptide-reactive group for the amine-reactive TMT tags bind covalently to the N-terminal α-amino groups and ε-amino groups of lysine residues of the peptides and proteins using the N-hydroxysuccinimide ester (Liang et al., 2015). This isotope labelling can be performed by the addition of combinatorial heavy isotopologues of C, H, N, and O by either metabolic or chemical derivatisation processes (Rauniyar et al., 2014).

After TMT tagging the samples are fractionated by OFFGEL fractionation. OFFGEL fractionation electrophoresis allows for the separation of the proteins by their isoelectric points that can be recovered in a liquid phase. The isoelectric point is the pH at which the particular protein carries.

MS/MS fragmentation leads to fragments ions peaks observed at higher mass to charge (m/z) ratios and is used to sequence amino acids that help to identify the peptides (Rauniyar et al., 2014). The peptide spectrum is assigned to proteins. The peptides tagged with the TMT isotopic appear as a single composite peak at the same m/z value in the mass spectrometer scan and these are identical liquid chromatography (LC) retention time (Rauniyar et al., 2014). Two forms of product ions, (1) reporter ion peaks and (2) peptide fragment ions peaks can be identified (Rauniyar et al., 2014). The quantity of the peptides can be measured by directly comparing the relationship between the reporter ions to the peptide selection.

### 1.12.4 Mass Spectrometry

Mass spectrometry (MS) is an essential tool used to characterise proteins leading to protein identification. A mass spectrometer will ionise a sample and measure the m/z ratio of the resulting ions (Finehout and Lee, 2003). MS can produce qualitative and quantitative information about proteins that can be used to identify them. This requires ionisation of the proteins. Ionisation is the process that involves either atoms or molecules acquiring either a positive or a negative charge. This change in charge occurs due to the gain or loss of electrons, making the molecules become an ion. There are multiple types of ionisation methods for mass spectrometry techniques. These methods include Electron Impact (EI), Chemical Ionisation (CI), Electrospray Ionisation (ESI), Atmospheric Pressure Chemical Ionisation (APCI) and Matrix-Assisted Laser Desorption Ionisation (MALDI). ESI time of flight (TOF) MS was used for the experiments performed in this thesis.

Liquid chromatography (LC) physically separate the proteins before ESI-MS. LC and ESI-MS is commonly used in conjugation with each other (Pitt, 2009). LC is an analytical chromatography technique that separates different ions or molecules within a solvent. In the column liquid chromatography, the liquid mobile phase passes through the column, where the proteins within the liquid phase interacts with the solid stationary phase. The rate of the elution of the proteins from the liquid column depends on their physicochemical interactions between the stationary and mobile phases.

LC-MS combines the physical separation of LC with the analytical ability of MS. LC-MS/MS is a tandem mass spectrometry, involves two attached mass spectrometers, where the samples are first ionised by either electrospray ionisation (ESI), MADLI or EI that generates the mixture of ions and these are separated based on their mass to charge ratio (m/z). Fragmentation of these ions occurs in a second mass spectrometer; these can then be used to generate the ions, which are then detected.

ESI-MS is a critical clinical technique due to its reliability and sensitivity. The ESI that uses electrical energy to transfer ions from a solvent solution and transform them into a gaseous phase that increases the MS sensitivity. This transfer from the solvent solution to the gas phase occurs in three steps, according to Ho et al., (2003). The liquid is then dispersed into a fine spray of charged droplets, and the solvent evaporates. The ions are then ejected from the charged droplets, which are then released from a high voltage tube into the main chamber and form a mist of charged droplets with the same polarity as the capillary voltage, nebulised gas such as nitrogen shears the eluted sample solution that increases the samples flow rate. These charged droplets exit the electrospray tip and move down the pressure gradient moving towards the analysers region of the mass spectrometer (Ho et al., 2003). The ions pass through the TOF chambers at an accelerated pace through a high voltage (Pitt, 2009). The length of time it takes for the ions to travel through a gas medium to a detector form a spectrum that can be used to identify the proteins.

### 1.12.5 Mass Spectrum Proteomic Analysis

The online software Mascot (Matrix Science, USA) used to analyse the MS produced peak lists. Mascot is a probabilistic scoring algorithm that identifies proteins using an adapted MOWSE algorithm. MOWSE is a method of identifying proteins based on the peptide's molecular weights (Pappin et al., 1993).

Some of the proteins identified by this method can mediate cellular recruitment and regulate their responses to the graft (Amini et al., 2013; Hing et al., 2004). The proteins identified will be prioritised based on their potential to increase osteoinduction and associated pathways; however, the role that many of the proteins play in osteoinduction is still poorly understood (Li et al., 2010). Proteins will also be prioritised based on the current knowledge available from several online databases. This method is outlined in the Methods section of Chapter 6.

## 1.13 Protein Coating of Bone Graft Substitutes

Proteins coated onto the surface of the BGS have shown to be pivotal in the subsequent cellular interactions and the success or failure of the BGS. Identifying the correct proteins to coat onto the BGS before implantation could cause increased cellular adhesion and osteoinduction (Simon et al., 2003). Other studies have shown the addition of fibronectin (FINC) to tissue culture polystyrene can increase cell adhesion and osteoblastic differentiation (Wilson et al., 2005; Steele et al., 1993; Stephansson et al., 2002). Some studies select sequences from various proteins, rather than using whole proteins. Several investigations of HA which were coated in RGD peptides before implantation has shown the ability to increase MSC's attachment and spreading compared to non-coated materials (Lee et al., 2014; Sawyer et al., 2005).

# Chapter 2

# The Effect of Different Bone Graft Materials on the Growth and Differentiation of Ovine Stem Cells.

## 2.1 Introduction

In recent years, the market for BGS has been flooded with new products, meaning there are more available now than ever before. Bone grafts are used during surgical procedures that can aid in restoring the bone to its original state in terms of both structural and mechanical integrity after it's been damaged. To obtain this crucial goal of bone repair requires the graft to be able to aid in the promotion of osteointegration, osteoinduction, osteoconduction, and osteogenesis while maintaining structural support.

It is critical to identify what was required from the BGS and selects the graft from all different types available that meet these requirements for the clinical situation and specific properties required (Moore et al., 2003).

Ovine cells were selected for these experiments because the ovine model have been used regularly as an orthopaedic animal model for translational research due to their similar size, joint structure, bone/cartilage regenerative and weight when compared to humans while also being valuable for evaluating the biocapacity of BGS's and other orthopaedics (Sartorette et al, 2016; Mccarty et al., 2009). They also can have 12 samples placed within one animal. Their volume of small tissues and blood volume is comparable to humans while having the ability to be used for investigation into regeneration and repair for critical-sized defects. The use of Ovine cells also enable comparison against previously published *in vivo* and *in vitro* experiments that have investigated the same BGS before. These studies include but not limited to the ones outlined here, Apapore™ studies by Coathup et al., 2006 and 2008. While for the SiHA formed BGS studies also by Coathup et al., in 2010, 2011 and 2016. For β-TCP™, there was studies by Sanjurjo-Rodriguez et al., (2017) and Koepp et al., (2004) who used Ovine models. While for the Orthoss® Herten et al., 2019, an Ovine model was used. Ovine cells will further enable a comparison of any future *in vivo* experiments that would take place in an ovine model.

## 2.2 Aims and Hypothesis

### 2.2.1 Aims

The first part of the study aimed to characterise the ovine MSC population through differentiation along the adipogenic, chondrogenic and osteogenic pathway. The second part of this study aimed to investigate the effect macroporous, microporous structure and graft chemistry of the five commercially available BGSs on MSC attachment, proliferation, viability, and osteogenic differentiation.

### 2.2.2 Hypothesis

Scaffold porosity, topography, and chemistry differs in each BGS, and therefore I hypothesised a difference in the attachment, proliferation, viability and differentiation of stem cells when cultured on the commercially available granular porous BGS investigated.

### 2.2.3 Objective

Five BGS scaffolds were investigated, and the objectives were:

1. To qualitatively investigate macro- and microporous (strut) structure of the BGS after they have been embedded into resin.
2. To quantify and compare cell metabolic activity using AlamarBlue® over 21 days.
3. To quantify and compare osteogenic differentiation using an ALP assay over 14 days using externally expressed ALP levels.
4. To investigate cell viability using a live assay on day 21 post cell seeding.
5. To investigate cell attachment to the BGS surfaces using Scanning Electron Microscopy (SEM).

## 2.3 Materials and Methods

### 2.3.1 Study design

Bone marrow-derived ovine MSCs (*n*=9) were characterised and cultured on five different commercially available granular BGS's materials. The BGS's investigated have been discussed in more detail in Chapter 1. An *n*=9 was used throughout this chapter unless stated. Three different sources of cells with three repeats.

### 2.3.2 Isolation of MSCs from Bone Marrow Aspirate.

Bone marrow was isolated from the iliac crest of skeletally mature female commercially available crossbred sheep. Using aseptic techniques, a Jamshedi needle was inserted through a stab incision into the iliac crest and approximately 5mls of marrow collected into a syringe containing 1000IU of heparin. The needle was retracted and re-positioned and a further 5mls collected from a separate adjacent bony location. Two mls of aspirate was placed into a T75 flask containing 10mls of DMEM+ containing 10% foetal calf serum (FCS) (First Link, UK) and 1% penicillin and streptomycin (P/S, Gibco, UK).

The mixture of bone aspirate and DMEM+ was placed into an incubator at 37$^{o}$C, and 5% CO2 and the media changed every 3-5 days until cells were 80-90% confluent. Cells were then passaged where the DMEM+ was removed and discarded and cells washed with phosphate-buffered saline (PBS). Cells were immersed in a solution of 10% trypsin (Gibco, UK) in PBS for 3 minutes at 37$^{o}$C and following detachment, the cells and trypsin solution were removed from the flask and placed in a universal tube. The solution and cells were then centrifuged at 2000rpm to form a pellet. The pellet was re-suspended in fresh DMEM+ in a T75 flask, and 50µl was removed to determine cell viability and cell density. The pellet was then diluted 1:10 in trypan blue (Sigma-Aldrich, UK), and a small amount was pipetted under a coverslip on a haemocytometer viewed using a phase-contrast light microscope (CKX31, Olympus, Japan).

For cell storage, DMEM+ containing cells were centrifuged, and the DMEM+ was removed before adding freezing media (10% DMSO (Sigma-Aldrich, UK) in 1ml of FCS). One ml of the freezing media with the cells was taken and placed into cryovials, which were frozen slowly to a minimum temperature of -80oC over 8 hours. The cryovials were then transferred to liquid nitrogen and stored until required.

#### 2.3.2.1 Cell Resuscitation

When required, cells were thawed in 10mls of DMEM+ before placing them into T75 flasks (Corning, USA). Cells were allowed to adhere for 24 hours before the media was changed and then allowed to grow, changing the media every 3 days until the culture reached 80-90% confluence. At this point, the cells were passaged.

### 2.3.3 Characterisation of Stem Cells

These methods were performed previously by previous members of my laboratory group and have been published in Sanghani-Keri, (2017) and Samizadeh, (2010). However, they performed them with rats and human MSC cells, respectively. There have been several published methods on Ovine MSCs similar to the one performed in this thesis. One such publication is Sanjurjo-Rodriguez et al.,(2017), presented data that shows that ovine MSCs will present morphology, surface markers and the ability to be multipotent in a similar to those in human MSCs. Using a similar method to isolate and culture the ovine cells, they investigated cells that were between 2-8 passages using morphological, phenotypical and functional culture studies. Flow cytometry was used for the phenotypic characterisation on passages 3, 4 and 8. The antibodies markers used were specific for both mesenchymal and hematopoietic cells. The molecular analysis technique of RT-PCR was used to investigate differentiation by the expression of typical genes for both differentiation and multipotency. Finally, they performed both cytological and histological analysis using the staining techniques of Alizarin red, Oil Red O and Alcian blue, among other stains. Immunohistochemistry was used for further confirmation of osteogenic and chondrogenic differentiation. Their results indicated that the ovine cells had similar morphologic and plastic adherence as human-sourced cells. The immunophenotypic analysis was done to show the expression of mesenchymal and hematopoietic markers in the cells. They used antibodies from both human and rat as there are limited antibodies available for sheep. They used human CD29, CD34, CD45, CD69, CD73, CD90, CD105, CD106, CD166, CD271, SSEA4 and STRO1 and rat CD45 and CD90. Most antibodies didn't work but CD29 (87.58%±11.70% positivity), CD166 (66.85%±8.79% positivity), SSEA4 (11.67%±11.31% positivity), anti-sheep CD44 (81.08%±16.68% positivity) (Sanjurjo-Rodriguez et al.,2017),. The cells were also negative for CD45; however, it showed positive in ovine blood. They noted that these results indicated no contamination with cells of hematopoietic origin.

Sanjurjo-Rodriguez et al.,(2017), demonstrated differentiation staining showed all three cell types differentiated with appropriate staining compared to no staining in the controls. They used RT-PCR to demonstrated that the majority of genes that were investigating had increased relative expression in genes that were relative to the differentiate lineages ($n$=3). For Osteogenic differentiation (OP and OCN), adipogenic differentiation (LPL and FABP4) and chondrogenic differentiation (COL II and AGG). They also investigated expression levels of multipotency genes (VIM and SOX2) were the expression levels in the majority of cases were down by day 21 compared to day 0. It is noted that in the adipogenic cells, 2 samples have similar SOX2 gene expression at day 21. While in chondrogenic differentiation, the SOX2 gene expression was increased in 2 samples.

Sanjurjo-Rodriguez et al. (2017), conclude that they demonstrated that ovine MSCs could effectively be from bone marrow aspirates. These cells show similar properties as human MSCs concerning morphological, phenotypically and functional.

### 2.3.4 Characterisation (Tri-differentiation) of MSCs: Osteogenic differentiation

Osteogenic differentiation was performed on 1 x 104 P3 cells (*n*=9). MSCs were cultured in osteogenic conditions for 21 days, and Alizarin Red S staining used to confirm calcium deposition by the cells. The control group comprised of cells cultured in normal media without the addition of osteogenic supplements. In all groups, the media was changed every 3-4 days.

**Table 2.1** Reagents for Osteogenic media.

| Regents | Supplier | Amount |
|---|---|---|
| Ascorbic acid | Thermo Fisher Scientific, USA | 0.2mM |
| β-glycerol phosphate | Thermo Fisher Scientific, USA | 10mM |
| Dexamethasone | Sigma Aldrich, UK | 0.1µM |

#### 2.3.4.1 Alizarin Red Staining Protocol

Cells were washed with PBS, fixed in 10% formalin for 30 minutes and then washed again with PBS. Alizarin Red solution was made with 1g of Alizarin Red powder (Sigma-Aldrich, UK) was dissolved in 100ml of distilled water, filtered and the pH adjusted to 4.1 - 4.3 using ammonium hydroxide. Cells were then stained for 5 minutes, the staining solution removed, the cells washed with distilled water before observation using phase-contrast microscopy.

### 2.3.5 Adipogenic Differentiation

Adipogenic differentiation was performed on 1 x 104 P3 cells (*n*=9). MSCs were cultured in adipogenic conditions for 21 days, and Oil Red O staining used to confirm the presence of lipid droplets, indicating differentiation into adipocytes. The control group consisted of cells cultured in normal media and without the addition of adipogenic supplements. The media was changed every 3-4 days.

**Table 2.2** Reagents for Adipogenic media.

| Regents | Supplier | Amounts |
|---|---|---|
| Isobultyl-1-methylxanthine | Sigma Aldrich, UK | 0.5mM |
| Dexamethasone | Thermo Fisher Scientific, USA | 1 µM |
| Insulin | Sigma Aldrich, UK | 10 µg/ml |

#### 2.3.5.1 Oil Red O Staining Protocol

Cells were washed in PBS followed by immersion in 2mls of 10% formalin and incubated for 30 minutes before being washed in distilled water. Once fixed, 2mls of 60% isopropanol was added, and cells incubated for 5 minutes. The stock solution was prepared by adding 100ml of 99% isopropanol with 300mg of Oil Red O powder (Sigma-Aldrich, UK).
The isopropanol was removed, and 2mls of the Oil Red O working solution was added, followed by incubation for 10 minutes at room temperature. The sample was then rinsed with water to remove the stain. Two mls of haematoxylin stain was added to the culture and allowed to incubate for 1 minute at room temperature before rinsing. Two mls of water was added before viewing under phase-contrast microscopy.

### 2.3.6 Chondrogenic Differentiation

Chondrogenic differentiation was carried out in a 3D environment using a pellet culture containing 3 x 104 MSCs (*n*=9). Cells were placed in a universal tube and centrifuged to form a pellet. Cells within the floating pellet were then grown over 21-days in chondrogenic media.The alcian blue will stain the proteoglycans produced by chondrocytes a dark blue, which can be used to confirm chondrogenic differentiation has occurred. The control group consisted of cells cultured in standard media without chondrogenic supplements, where the media was changed every 3-4 days.

Table 2.3 Chondrogenic media reagents.

| Reagents | Supplier | Amount |
|---|---|---|
| Dexamethasone | Thermo Fisher Scientific, USA | 100mM |
| Sodium Pyruvate | Sigma Aldrich, UK | 1mM |
| Proline | Sigma Aldrich, UK | 40µg/ml |
| Transforming Growth Factor β1 | Sigma Aldrich, UK | 10ng/ml |
| Insulin-Transferrin-Selenium-1 | Thermo Fisher Scientific, USA | 6.25µg/ml |

#### 2.3.6.1 Alcian Blue Dye Staining Protocol

The Alcian Blue staining protocol occurred in two parts, (i) staining and (ii) destaining:

**(i) Staining**

The Alcian blue solution created by adding 60mls of ethanol with 40mls of acetic acid. 10mg of Alcian Blue 8 Gx (Sigma-Aldrich, UK) was then dissolved in the ethanol/acetic acid solution. The micromass of cells was washed with PBS before immersion in a 10% formalin solution. The sample was incubated at room temperature for 60 minutes before the micromass was washed with distilled water and the Alcian stain added. Samples were stained for 20 minutes before destaining.

#### (ii) Destaining

The destaining solution created by mixing 120mls of ethanol with 80mls of acetic acid. The solution was aspirated and the micromass washed in the destaining solution for 20 minutes. The destaining solution was then removed and replaced with PBS. The micromass of cartilage spheroids were then visually analysed for a blue colour change that represented the presence of chondrogenic cells.

### 2.3.7 Characterisation of Scaffolds

#### 2.3.7.1 Acrylic Resin Impregnation and Casting

To observe the different scaffolds structures, SEM was used. 0.5g of the BGS was placed into moulding containers, immersed within LR White™ hard resin (London Resin Company Ltd.) and placed under vacuum pressure for 1 hour to allow for impregnation of the resin within the granules. The polymerisation of the resin was performed by placing one drop of the catalyst regent into 10mls of the LR White™ hard resin (London Resin Company Ltd.). The samples were allowed to set slowly. Embedded samples were longitudinally sectioned using an EXAKT cutting saw (EXAKT, Germany), and the surfaces were polished using the Motopol 2000 machine (Buehler, UK). Before undergoing SEM analysis, the samples were sputter-coated with a thin layer of gold-palladium (K550, EmiTech Ltd, Ashford, UK). The SEM was then used to visually analyse and compare the BGS structures (JEOL JSM 5500 LV; Tokyo, Japan).

### 2.3.8 MSCs Growth on Porous BGS Granules

0.08g of each BGS was used in each of the following experiments. The granules were from sterilised unopened packs and were weighted on weighing scales that were within the sterile environment of a fume hood. The cells were seeded into 12-well (4cm2 surface area) (ThermoFisher Scientific, catalogue number 150628). 10,000 ovine P3 cells were seeded onto each of the graft materials (*n*=9) and cells allowed to adhere for 1 hour at 37oC. Once adhered, 1ml of standard DMEM+ culture media was added and the granules incubated for up to 21 days at 5% CO2 at 37$^{o}$C. The DMEM+ media was changed every 3 days.

### 2.3.9 Cell Metabolic Activity

The AlamarBlue® bioassay has been used for over 50 years to assess cellular viability by measuring whether there is an increase in cellular metabolic activity (Rampersad et al., 2012). When the AlamarBlue® compound enters a cell, resazurin was reduced to resorufin, which changes the AlamarBlue® blue colour to a red depending on the viability of the cells. This change also increases the fluorescence level of the media, which can be read by the Fluoroskan Ascent machine at 510/590nm. When running over serial time points, and AlamarBlue® assay indicated the changes in cellular viability over time.

In this chapter, an AlamarBlue® assay was used to investigate MSC metabolic activity on days 1, 4, 7, 14 and 21 of culture. A 10% AlamarBlue® solution was prepared using phenol red-free media (Sigma-Aldrich, UK). One ml of the solution was added to wells containing the cell-seeded granules and cultured at 5% CO2 in a 37oC incubator for 2 hours. Following this, 100µl was taken from each sample and placed in a microwell plate were the Fluoroskan Ascent machine at 510/590nm read the absorbance levels. Two control groups, where cells were cultured on both Thermanox® discs in DMEM+ media and Osteogenic DMEM+ media.

### 2.3.10 Osteogenic Differentiation

#### 2.3.10.1 Alkaline Phosphatase (ALP) Assay

Early bone formation can be measured using an ALP assay where fluorometric changes can be quantified and compared between groups. ALP is released during the early stages of osteogenic differentiation (Stein et al., 1990) and the level of ALP activity increases as osteoblasts mature and with increased levels of mineralisation (Stein et al., 1990). Active osteoblasts release increased levels of ALP, and this has been reported to act on pyrophosphatase, which may initiate the mineralisation process. Internal ALP wasn't measured as this required lysing the cells, and this would require increased numbers of samples, but due to limited supplies of BGS, this could not be performed. External ALP levels can be used to measure the ALP levels being released from the cells into the DMEM. External ALP was measured, and the assay was performed in a 1:1 (50µl) ratio of cultured media to p-nitrophenyl phosphate (pNPP) (Sigma-Aldrich, UK). Again, control groups of cells grown on both Thermanox® discs in DMEM+ media and Thermanox® discs in Osteogenic DMEM+ media (OM) were investigated. The solution was agitated to ensure the samples were uniformly distributed before measurement using the Tecan Infinite 2000 spectrophotometer plate reader (Tecan, Switzerland).

### 2.3.11 Cell Viability

#### 2.3.11.1 Live Assay

Cell viability was assessed using a Live assay (Thermofisher, UK) on day 21 of culture. Calcein am stains live cells green. Ethidium homodimer stains dead cells red. For the Live assay, to 5mls of warmed PBS 5µl of Calcein am was added. Ethidium homodimer was used when the dead assay was performed. The samples were then placed in an incubator at 37$^{o}$C for 30 minutes. The ratio of live and dead cells was determined using a fluorescence microscope (Observer 21, Zeiss, Germany). The number of cells present on the surface in each of the experimental groups was semi-quantitatively assessed. A region was selected at random at 20x magnification and a score given based on the amount of scaffold surface covered with attached live (green) cells. The scores were limited to 10 (high), 5 and 1 (low). A high score was given when less than 75% of the surface was

covered with live cells. A sample with approximately 50% of its visible surface covered was given a score of 5 and samples with less than 25% were considered to have low cell coverage and given a score of 1.

#### 2.3.11.2 Scanning Electron Microscopy

Scanning electron microscopy (JEOL JSM 5500 LV; Tokyo, Japan) was used to investigate and compare MSC morphology, attachment, and proliferation in each of the 5 experimental groups. BGS granules seeded with cells were fixed using buffered formal saline and dehydrated through a series of alcohol washes before drops of hexamethyldisilazane (HMDS) were placed onto the sample. Samples were then air-dried before being placed in the sputter coater, where a thin layer of gold-palladium (K550, EmiTech Ltd, Ashford, UK) was applied onto the scaffold surface. Sputter coating is required to prevent the charging of the sample, which increases the secondary electrons enabling detection from the surface of the specimen while also decreasing the signal to noise ratio (Yka-soininmaki et al., 2013).

### 2.3.12 pH levels of media.

At each time point, the DMEM+ media was removed and stored at -20c until measured. pH levers were measured using Fisherbrand™ accumet™ AB15 Basic and BioBasic™ pH/mV/°C Meters (Catalogue Number: 13-636-AB15). Calibrated before use as per the manufacturer's instructions. The sensor was submerged and kept within the DMEM+ until the number on the meter had settled.

### 2.3.13 Statistical Analysis

Normality was checked using the Kolmogorov- Smirnov and Shapiro Wilkinson test. If data was normal, the comparison was made using an independent student T-test. For non-parametric data, comparison was made using the Mann Whitney U test with a Bonferroni correction. The data analysed was performed using SPSS version 24 (Chicago, USA). The figures were made using GraphPad Prism version 7.0.0 (San Diego, USA). These experiments were run in $n$=9 where there was 3 cell lines and 3 repeats of each unless stated otherwise.

## 2.4 Results

### 2.4.1 Tri-Differentiation

After 3 weeks of being cultured within the three different media solutions, each of the different cell types were then tested to see they underwent differentiation.

MSCs cultured in osteogenic media stained positively with Alizarin Red, indicating the formation of bone mineral (**Figure** 2.1). Following culture in adipogenic media, the formation of intracellular microdroplets was identified by positive Oil Red O staining, and positive chondrogenic differentiation was also observed as the 3D cell pellet stained an intense dark blue, confirming the presence of proteoglycans.

From these results, it could be concluded that the method of collecting bone marrow aspirate and subsequent culture resulted in the successful isolation and expansion of multipotent MSCs.

The controls for this experiment were cells that were not treated with any additional additive to the media that induces the cells to differentiate towards one of the differentiated cell lineages other than the FCS and penicillin/streptomycin. Previous experiments were they assessed tri-differentiation is review in the discussion

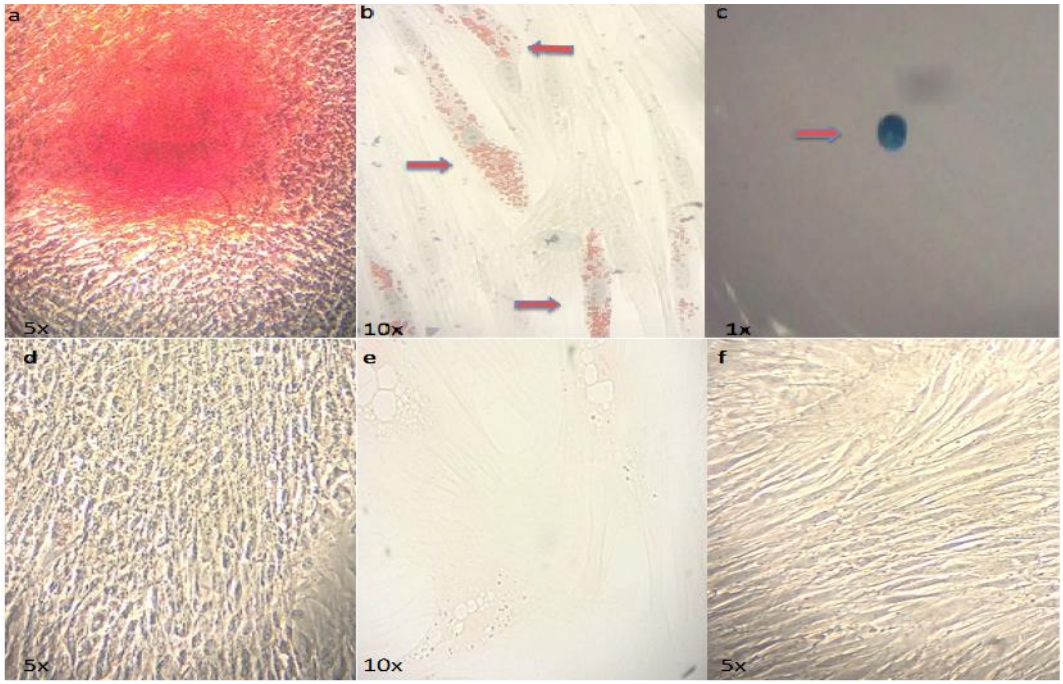


**Figure 2. 1 Trilineage differentiation of ovine MSCs.** (a) Alizarin red-stained osteoblasts, (b) Intracellular lipid droplets stained with Oil red O indicating adipogenic differentiation and (c) chondrogenic differentiated cell pellet stained positive using Alcian blue. Controls are represented in (d) osteogenic control (e) adipogenic differentiation (f) chondrogenic differentiation.

### 2.4.2 Characterisation of Scaffolds

#### 2.4.2.1 BGS Embedded in Resin

Observation using SEM enabled inspection of the scaffold structure. The internal structure of both Actifuse™ (a) and Inductigraft™ (c) appeared thinner when compared with the other BGS investigated (**Figure** 2.2). This thinner internal structure may enable increased adsorption of the BGS. In contrast, the internal structure of β-TCP™ (c) was thicker. There appeared to be higher levels of porosity seen in Actifuse™ (a), Inductigraft™ (c), and Orthoss® (e), which concurs with the porosity listed in **Table** 2.1.

Semi-quantitative calculation of the percentage area of each BGS that was taken up by pores (both macro and strut porosity) was calculated using Image J (LOCI, USA). This was performed using an *n*=3. The results of this are represented in **Table** 2.2. The outline of the graft within the resin was measured using the Image J software. Then each pore was then measured and added up to calculate the percentage of the total area they consume.

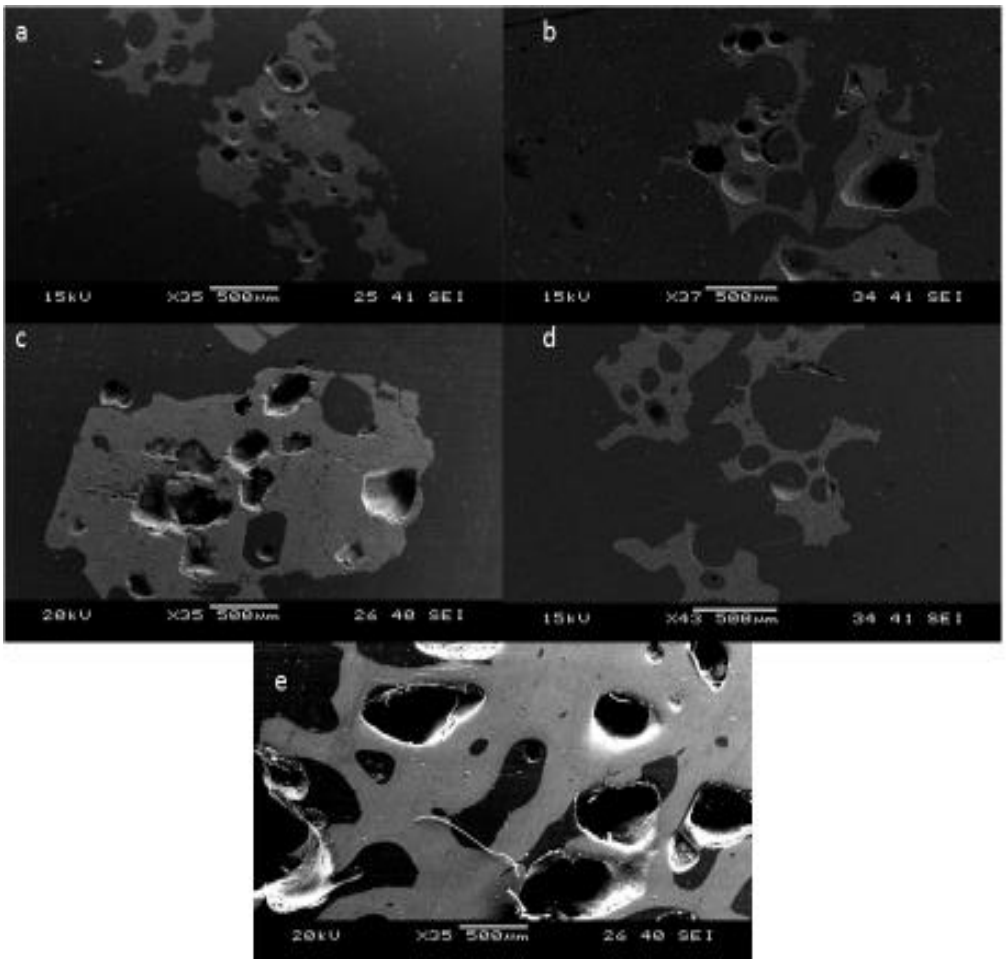


**Figure 2. 2 Scanning Electron Microscope image of BGS has embedded in resin.** a) ApaPore™, b) Actifuse™ c) β-TCP™, d) Inductigraft™ and e) Orthoss®. The images should differences in structures and porosity.

**Table 2.4 Semi-quantitative calculation of the percentage area**. The values presented are mean with standard error.

| BGS | Actifuse™ | ApaPore™ | β-TCP™ | Inductigraft™ | Orthoss® |
|---|---|---|---|---|---|
| **Percentage of porosity area** | 19.9±1.5 | 17.0±0.6 | 21.6±4.7 | 30.0±2.9 | 30.9±4.8 |

The semi-quantitative calculation included in Table 2.4 was done on an *n*=3 using the SEM images in Figure 2.2. The highest percentage area overall was Orthoss® (30.91±4.84), and the highest synthetic surface was Inductigraft™ (30.0±2.9). The lowest was the ApaPore™ surface (17.0±0.6).

### 2.4.3 Cell Viability

#### 2.4.3.1 Comparison of AlamarBlue® Metabolic Activity Assay on each surface

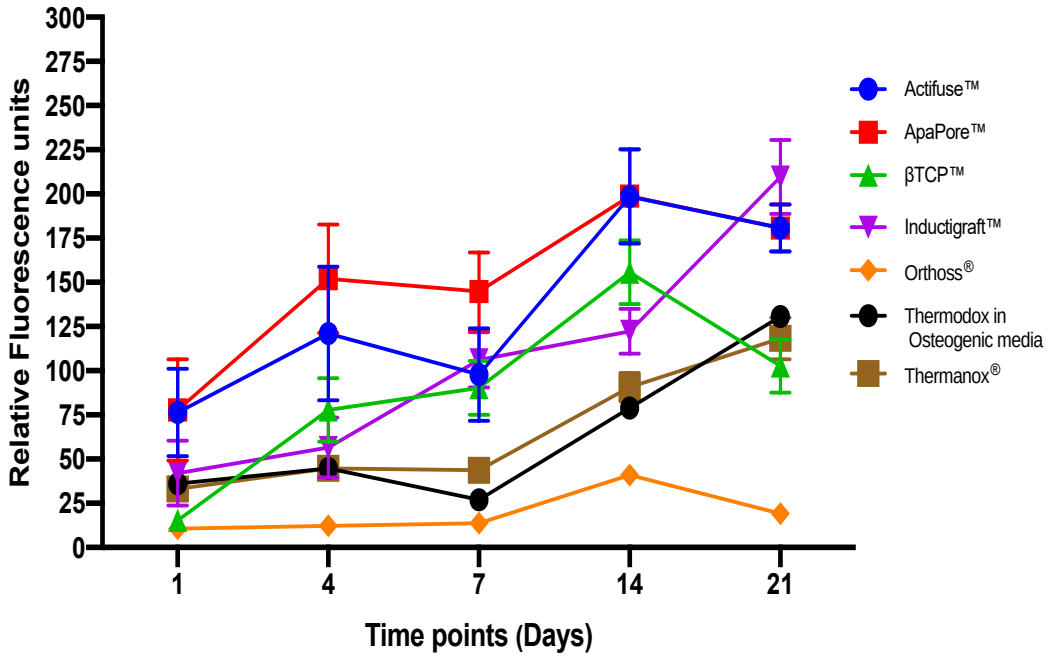


**Figure 2. 3 Metabolic activity of five BGS's over 21 days.** Measured by AlamarBlue® (*n*=9). Activity at 21 was significantly higher in Inductigraft™ compared to the lowest sample Orthoss® (*p* <0.001). Error bars represent standard error of the means.

The results are represented in **Figure** 2.3 show Inductigraft™ demonstrated highest levels of metabolic activity increased ranging from 42 (±18.3) on day 1 to 209.7 (±21.0) on day 21, which was a significant difference (*p* >0.001). This was a 399.4% percentage increase; this was the highest increase of all samples between days 1 and 21. As discussed previously, Actifuse™ and Inductigraft™ have an identical chemical composition; however, they differ in strut porosity. This difference was seen in the Actifuse™ group, where there were no significant differences seen (*p*=0.065). Orthoss® showed lower metabolic activity

compared to all other BGS investigated but still showed a significant difference seen between days 1 and 14 ($p$>0.001), and also between days 1 and day 21 ($p$=0.004).

### 2.4.3.2 Comparison of AlamarBlue® Metabolic Activity Assay at each time point

The percentage changes in metabolic activity for all BGS's between days 1 and 21 (**Figure** 2.4**)**. Inductigraft™ showed the highest significant increased percentage change (399.4%) ($p$ <0.001) in metabolic activity between the two-time points. While Orthoss® had the lowest amount percentage change (81.16%), this was also significant ($p$=0.004).

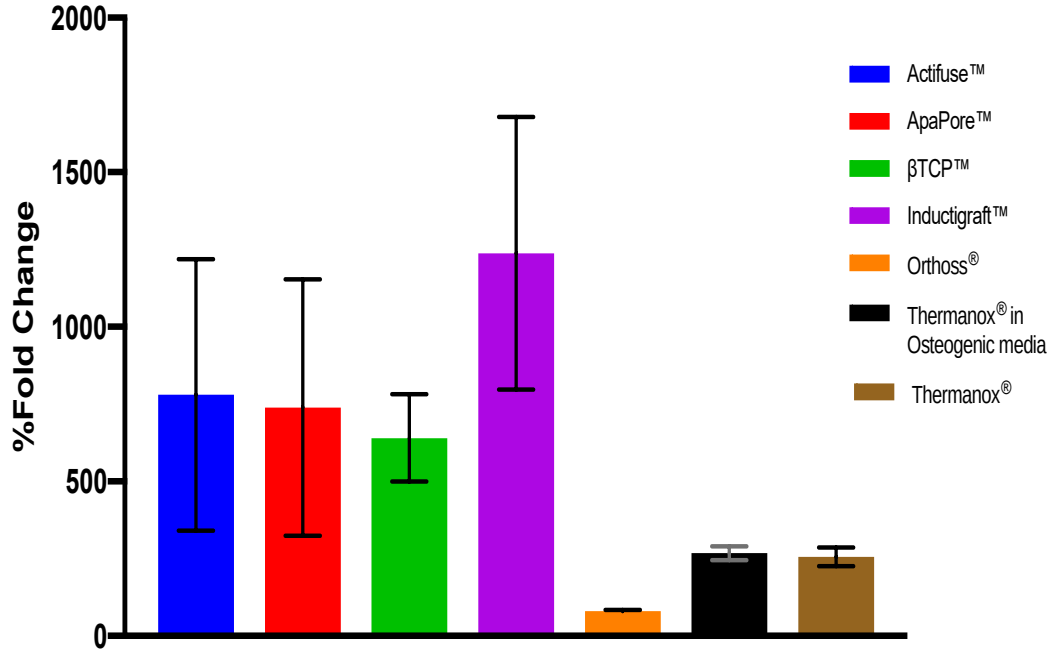


**Figure 2.4 Percentage fold change between days 1 and 21 in cellular metabolic activity.** Measured by AlamarBlue® assay ($n$=9). Highest percentage change was Inductigraft™ (399.4%) ($p$ <0.001). Lowest percentage change was Orthoss® (81.16%) ($p$=0.004). Error bars represent standard error of the means.

### 2.4.3.3 ALP Assay

The external ALP activity represented the production of ALP and released by the adhered cells was measured on days 4, 7 and 14 (**Figure** 2.5**).** It should be noted that ALP could be increased by can also be due to an expansion in cell numbers. As a control for this DNA, levels should be measured; however, due to limited BGS samples, DNA could not have been performed for these experiments.

In Actifuse™, ApaPore™, β-TCP™, Inductigraft™, and Thermanox®, there was an initial increase in ALP activity between days 4 and 7. The highest activity increase between these time points was seen in β-TCP™ of 36.74, which, however, it was not significant ($p$=0.29). Orthoss® and Thermanox® in OM both showed a decrease in activity, with the most notable decrease was Thermanox® in OM with a reduction of -25.5.

Between days 7 and 14, there was a decrease in the activity in the Actifuse™, β-TCP™, Inductigraft™ and Thermanox® in OM samples. The largest decrease was β-TCP™ (37.0±0.1), which was not significant ($p$=0.29). This appears to be due to the ALP activity reaching a peak before decreasing, which was linked stimulate the osteogenic differentiation of the adhered MSCs.

An increase in ALP activity between days 7 and 14 were seen in ApaPore™ and Thermanox®. The largest increase was in ApaPore™ (37.0±11.4); this was not significant ($p$=0.350). ApaPore™ and Thermanox® appeared not to show a peak in ALP activity, and this was linked to a slower rate of differentiation towards osteoblasts when compared to the other samples.

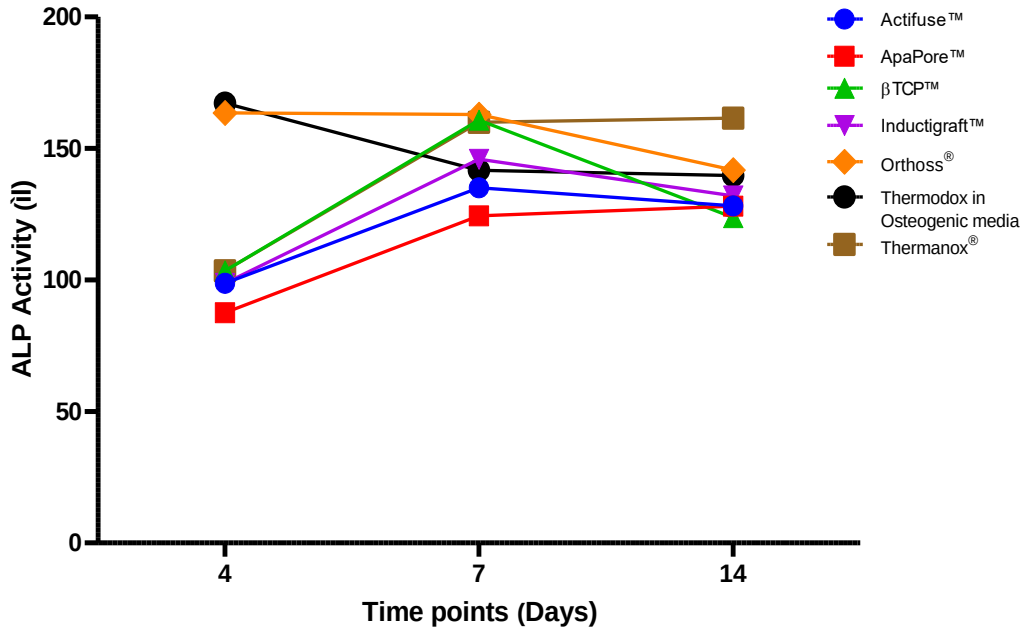


**Figure 2. 5 External released ALP activity.** Measured by spectrophotometer ($n$=9). ALP activity by Day 14 was increased in all samples other than ApaPore™ and Thermanox® control. The error bars represent the standard error of the means.

### 2.4.3.4 pH level

The pH levels of the media in which the seeded BGS was measured at days 1, 4, 7, 14 and 21 to investigate whether there were changes in the pH levels due to the presence of grafts. This is represented in **Figure** 2.6. The results showed that Orthoss® had the highest levels at every time point and has more alkaline compared to the other samples. However, this was not a significant difference when compared to any other sample ($p$=1.0). The rest of the samples had similar pH levels until day 21 when they begin to separate Inductigraft™, and Actifuse™ have lower pH levels becoming more acidic.

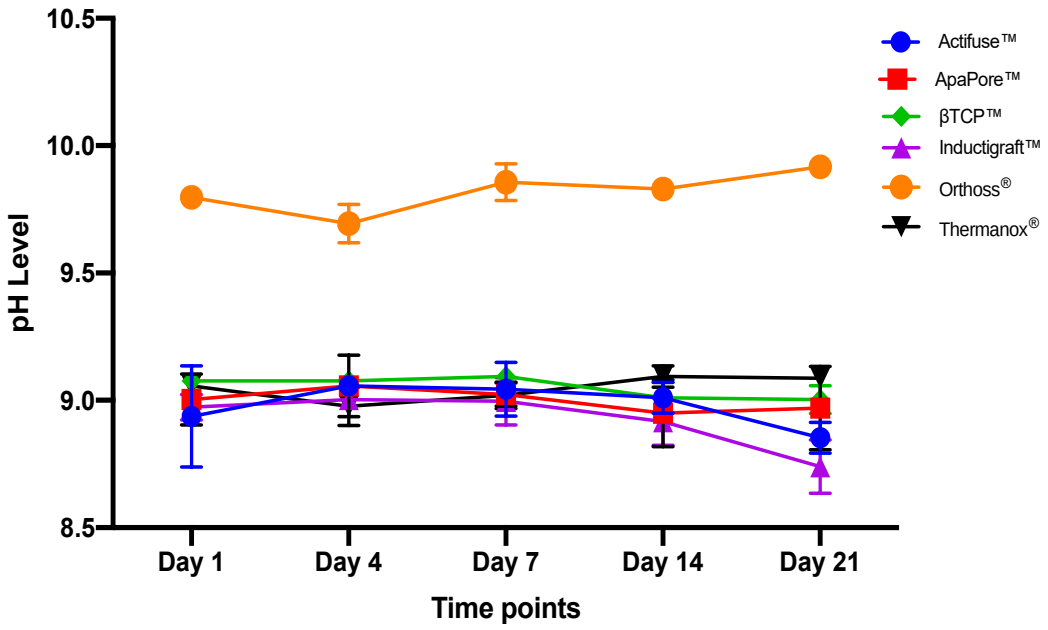


**Figure 2. 6 pH levels of DMEM+ removed from cell coated BGS.** Measured by Fisherbrand™ accumet™ AB15 Basic (*n*=9). Highest pH levels were in Orthoss® samples, which was more alkaline compared to other samples investigated. This was not significant (*p*=1.0). The error bars represent the standard error of the means.

### 2.4.4 Cell Viability Imaging

#### 2.4.4.1 Live assay

Live assay was used to assess the health of cells that were adhered to the surfaces for 21 days. Live cells could be seen on all of the different BGS groups surfaces; however, the number of cells vary on each surface (**Figure** 2.7)

A semi-quantitative analysis was used to describe the coverage of viable cells on the different BGS surfaces was described in the methods (**section** 2.3.10.1).

Four of the BGS surfaces (Actifuse™, ApaPore™, β-TCP™ and Inductigraft™), had high levels of cellular adhered and were given the highest score of 10. Orthoss® had visually had fewer cells adhered to its surface compared and was given a score of 1. It was noted that the cells that did adhere to Orthoss® appear to cluster around each other.

**Table 2.5 Semi-quantitative analysis.** This was performed using the results from the Live assay and will aid in investigating cell viability.

| Bone Graft Substitutes | Semi quantitative score |
|---|---|
| Actifuse™ | 10 |
| ApaPore™ | 10 |
| β-TCP™ | 10 |
| Inductigraft™ | 10 |
| Orthoss® | 1 |

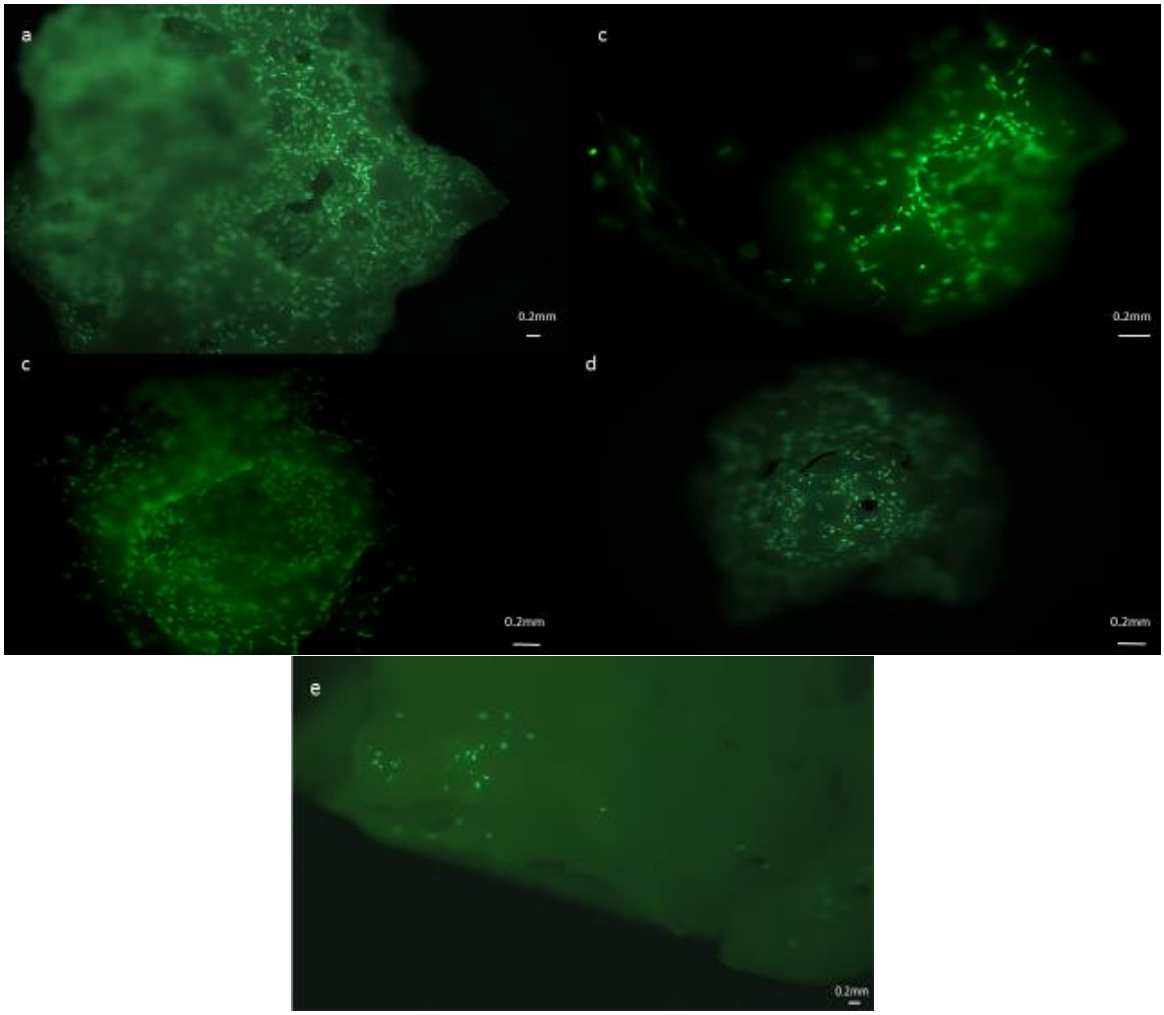


**Figure 2. 7 Live assay of cells adhered to the BGS's.** At day 21 days, post-seeding images were taken on Zeiss observer 21 fluorescence microscope (Zeiss, Germany). (**a**) Actifuse™ (**b**) ApaPore™ (**c**) β-TCP™ (**d**) Inductigraft™ and (**e**) Orthoss®). Similar amounts of Live cells (Green) were identified on all other than Orthoss®, which appeared to have low cell numbers.

#### 2.4.4.2 Scanning Electron Microscopy (SEM)

SEM was used to investigate the cellular attachment while also enabling a closer examination of both cellular attachment to the surface and any cellular structure changes that could be an indicator of cellular differentiation. These images are shown in Figure 2.8. The macroscopic level analysis showed that there were visually higher cell numbers adhered to Actifuse™, ApaPore™, and Inductigraft™ compared to the other materials investigated. The cells that were adhered to the topographical surface of the grafts appeared to be attracted to the concaved surfaces near pores; however, there was cell coating the entire surface. The cellular structure of these cells appeared to have an elongated and extended structure across the surface on these surfaces.

There were fewer cells that were adhered β-TCP™ surfaces, and these cells appeared visually to be less extended and clustered together in small, localised areas on the surface rather than being spread out across the entire surface

After a thorough search, there were no cells found on the Orthoss® surface. This may be due to low cellular adherence, which was also seen in the live assay. This low adherence may have hindered finding any adhered cell on the Orthoss® surface.

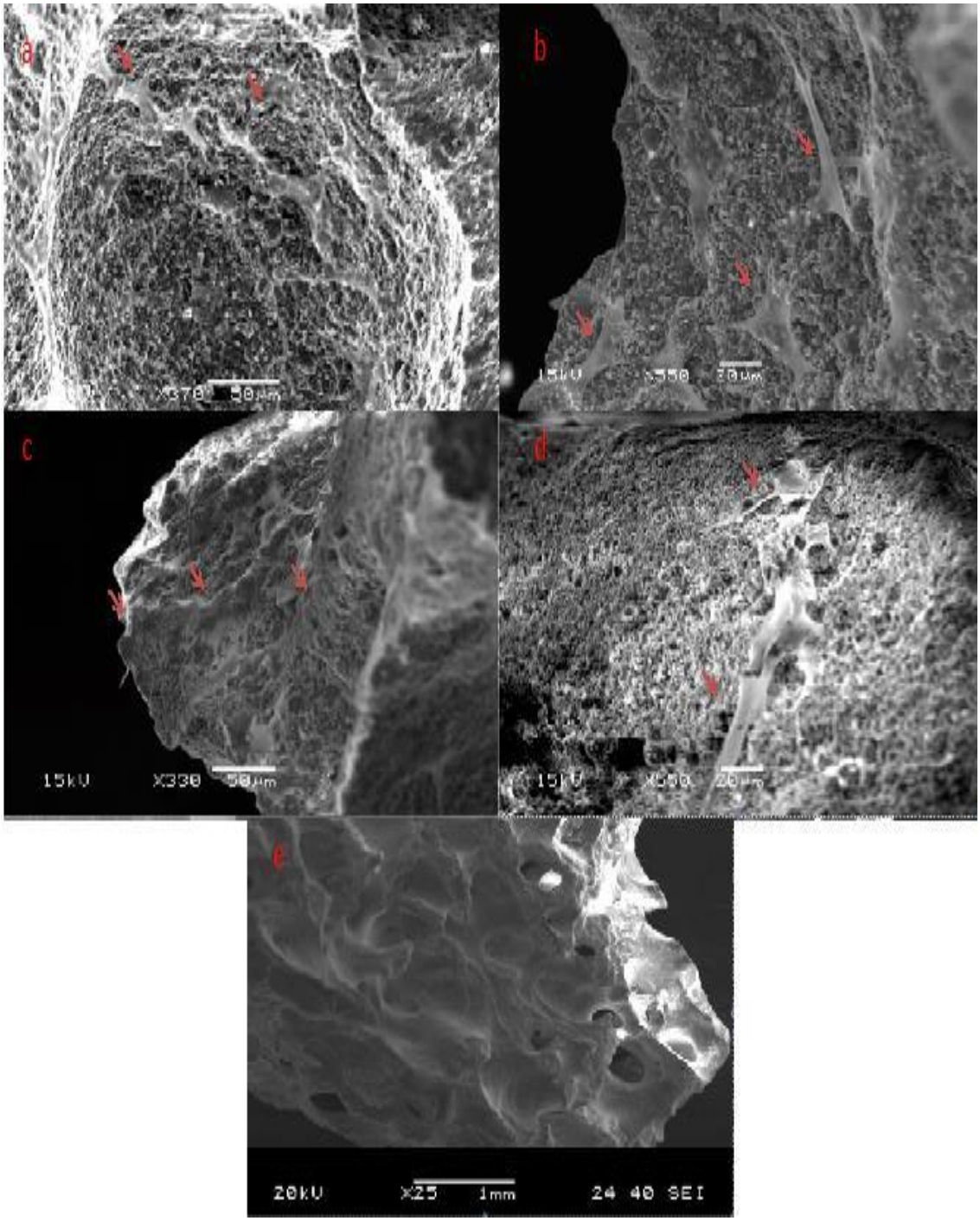


**Figure 2.8 Scanning Electron Microscopy images cells adhered to the BGS's surfaces.** 21 days post cell seeding. (**a**) Actifuse™, (**b**) ApaPore™, (**c**) β-TCP™, (**d)** Inductigraft™, and (**e**) Orthoss®. Cells were identified on all surfaces (Indicated by red arrows) other than on Orthoss®.

## 2.5 Discussion

### 2.5.1 Introduction

#### 2.5.1.1 Differentiation

The preliminary focus of this chapter was to confirm that the cells isolated from the ovine bone marrow aspirates were MSCs. MSCs are well established as excellent candidates for tissue engineering for orthopaedic tissues, as they are unspecialised cells that retain their ability of self-renewal and multipotency. Under the right conditions, these multipotent MSCs could be driven into differentiating down distinct cell lineages, including adipocytes, chondrocyte, and osteoblasts. This process can be manipulated by changing the *in vitro* conditions by adding the appropriate supplements to DMEM+. The *in vitro* MSC experiments performed in this chapter were successful in inducing MSC differentiation into adipocytes, chondrocytes, and osteoblasts.

Once cultured the appropriate straining of Oil Red O showed the presence of adipocytes cells. Adipogenic differentiation because the morphology changes to the cell types that including the formation of cell aggregate and accumulation of lipid vacuoles. For chondrocytes, the toluidine blue staining is an indicator of the differentiation of cells within the micromass culture system. There were morphology changes to the cells that included cellular projections and the development of intricate cell interactions and extracellular matrix. Alizarin red was used to confirm the MSCs had differentiation to osteoblasts. The differentiation of MSCs to osteoblasts will be investigated throughout this thesis. The combination of the three cell types differentiating from the isolated MSCs confirms the multipotency potential of the MSCs and affirms that the cell isolated were MSCs.

The tri-differentiation potential of Ovine MSC was discussed in Adamzyk et al., (2013), and they have compared two different protocols for MSC differentiation. However, they noted that there could be the donor-to-donor variation that is protocol dependent leading a highly variable difference potential of the Ovine MSCs differentiation, but they do have the potential to differentiate towards the osteoblast, adipocytes, and chondrocytes. In Herdari et al., (2013) study, they were able to demonstrate that three different sources of MSC (Bone marrow, adipose tissue, and liver). They confirmed by multilineage differentiation with the characteristics of osteoblasts, adipocytes, and chondrocytes shown under the different experimental conditions and were able to confirm this further by using mRNA expression analysis.

### 2.5.2 Characterisation of the Bone Graft Substitutes.

#### 2.5.2.1 Introduction

The second part of this study examined the ability of different commercially available BGSs to induce osteogenic differentiation of the adhered MSCs. The study also investigated and compared cellular proliferation and viability. The selected BGS materials differed on a range of features including chemistry, surface topography, macro- and strut porosity. Four of the selected BGS grafts are synthetically developed (Actifuse™, ApaPore™, β-TCP™, and Inductigraft™), whilst Orthoss® is a xenograft formed from bovine bone. It is important to note that the different structures and chemical composition of the synthetic BGSs will cause variations in their performance. Other factors can influence osteogenesis including pore interconnectivity and geometry, which has been shown to affect both the "physical" and "mechanical" pathways, which potentially increase its osteoinductive ability (Hing et al., 2005).

The ideal BGS is expected to be osteoinductive, causing the differentiation of MSCs into osteoblasts. The attachment of proteins and cells will also encourage both osteointegration and osteoconduction (Bignon et al., 2003; Coathup et al., 2012).

#### 2.5.2.2 Porosity Calculation

A semi-quantitative analysis was carried out to calculate the percentage area that was consumed by porosity (either macro or strut porosity). The samples had been placed into resin, and SEM images were taken before Image J was used to calculate the percentage area. The results showed that the highest percentage area was by Orthoss® (30.9±4.8) followed by the Inductigraft™ (30.0±2.9). The next highest was β-TCP™ (21.6±4.7) then Actifuse™ (19.9±1.5). The lowest percentage was ApaPore™ (17.0±0.6).

#### 2.5.2.3 Metabolic Activity

AlamarBlue® was used to measure the metabolic activity of the adhered cells at different time points. AlamarBlue® is a reagent used to evaluate cellular health and is an indicator of cellular viability. The results indicated that all of the synthetic BGS's and controls all had higher levels of metabolic activity when compared to the Orthoss® samples. Orthoss® appeared to have extremely low cellular viability to the extent that appears not to be reported on Orthoss® scaffolds previously.

Previous comparisons between synthetic and bovine-derived BGS have been made (Greenspan, 2013; Kouroupis et al., 2013; Kouroupis et al., 2012; Dorati et al., 2014). The majority of these studies have found that Orthoss® will encourage MSC attachment and osteoinduction (Kouroupis et al., 2013; Kouroupis et al., 2012; Dorati et al., 2014).

However, some studies noted that Orthoss® underperformed when compared to synthetic HA, but there were signs of cellular attachment to the Orthoss® (Greenspan et

al., 2013; El-Jawhari et al., 2016). Tseng et al., (2013), reported Orthoss® had that lowest cell attachment compared to the other three grafts in their studies, and they reported this was due to the formation of CaO, which was caused by the sintering process. Tseng et al. (2013) reported that the CaO formed increased the pH conditions surrounding the graft, and this turned it into a non-favourable condition for cellular activity. El-Jawhari et al, reported decreased levels of cellular attachment and proliferation on Orthoss® BGS when compared with two other materials (Orthoss®-collagen (Geistlich, Swiss) and Vitoss™ (Stryker, Malvern, PA)), however they were able to observe adhered cells using SEM (El-Jawhari et al., 2016). Kubosch et al. described a decrease in cell numbers and metabolic activity. There have been other studies have reported the osteoinductive effect of Orthoss® on stem cell behaviour (Kubosch et al., 2016, Kouroupis et al., 2012; Kouroupis et al., 2013; Garin et al., 2016).

Inductigraft™, which has the highest strut porosity of the synthetic BGS investigated, demonstrated the highest levels of cell metabolic activity throughout the 21-day *in vitro* study. It also had the highest fold change in metabolic activity between days 1 and 21 (1238.03±440.70).

Previous studies have shown that SiHA which both Inductigraft™ and Actifuse™ are formed from having the ability to attract higher numbers of MSCs to attach and proliferate when compared HA (ApaPore™) alone during *in vitro* experimentation (Cameron et al., 2012; De Godnoy et al., 2015). These studies demonstrated that the SiHA could induce osteogenesis increased amounts when compared to the HA samples, this was shown in the expression of osteoblast related genes, presence of osteogenic associated protein and mineralised matrix productions on the surfaces of the grafts. This led them to conclude that the addition of silicon increases bone production potential (Cameron et al., 2012; De Godnoy et al., 2015). Zou et al., (2009), showed that the presence of Si ions on biomaterials surfaces has the ability to the increased cellular attachment.

While other studies have described that the presence of Si ions into the HA matrix has the ability to change the matrix's surface charge leading to an increased protein adsorption to the surface-enhanced of cellular attachment (Cameron et al., 2012; Porter et al., 2006; Guth et al., 2006; Rashid et al., 2004; Anselme, 2000; Zon et al., 2009). Hing et al. (2006) discussed that the increased incorporation of silicate ions could influence surface charges and wettability.

#### 2.5.2.3.1 Metabolic Activity of samples with increased strut porosity

Coathup et al., (2011) *in vitro* study showed the addition of Si to HA does have an ability to increase the amount of bone formation to the surface of the implants when compared to HA alone. In her 2005 publication, Hing discusses that strut microstructure and pore geometry influences the entrapment of both growth factors and proteins; this can increase the graft's bioactivity while also affecting the scaffold mechanics. The increased

strut porosity that is offered by Inductigraft™ has shown that during *in vivo* studies to have the ability to increase levels of both cellular attaching and proliferation when in direct comparison to Actifuse™, which has a lower strut porosity. The increased ability to attract cellular attachment and proliferation offered by Inductigraft™ compared to Actifuse™ has been present in the metabolic activity performed in this study.

De Godnoy et al., (2015) described the increased porosity is an excellent mimic of the natural microenvironments in bone and as results will affect MSCs attachment, proliferation, and differentiation. *In vitro* studies by Campion et al., (2011) studies showed that the increased strut porosity also has the potential to encourage elevated levels of neovascularisation making nutrients more accessible along with greater surface area for both protein and cellular to attach too while also offering a larger area of mature bone tissue to create a contact with the graft.

Whereas Coathup et al. (2011), described that there was not a significant amount of bone been formed; instead, they saw earlier mineralised bone tissue formation. Gao et al., (2016), described β-TCP™ granules as an aid in inducing MSCs to differentiate towards osteoblast and saw increased expressed osteogenic genes and related proteins. They used β-TCP™ because of the limitation, they saw with HA. These limitations included low degradation and absorption rates, which could lead to hindering the bone's ability to remodelling and form. Gao et al., (2016), used glucose consumption to access metabolic activity and they noted rapidly increased activity during the initial first 7 days before slowing. This was not noted in my AlamarBlue®, which saw an increased growth but decreases by day 21, this decrease is due to a drop in viability cells. Uchida et al., (2008), described significantly higher cell numbers at day 7 compared to the day 0 using MTT assay, which was different to what was seen in my stuff day 1 and 7 which wasn't significant difference in Alamar activity, however it there was significant difference between day 1 and 21.

#### 2.5.2.4 Alkaline Phosphate Assay

ALP assay activity is an indicator of early osteoblastic activity and is widely accepted as a biochemical marker of their activity (Sabokbar et al., 1994). ALP plays a critical role in bone mineralisation, and this occurs through the initiation and/or in the promotion of the HA crystals in the matrix vesicle of the osteoblasts (An et al., 2015; Orimo and Shimada, 2008).

The differentiation of MSCs towards osteogenic lineage occurs in three stages; this occurs in three stages days 1-4 where the highest number of cells appears; during days 5-14 the transcription and proteins expressions of ALP and then the ALP levels will decline (Huang et al., 2007; Aubin, 2001). The final stage involves the expressions of osteocalcin and osteopontin, with the deposition of calcium and phosphate (Hoemann et al., 2009; Huang et al., 2007).

The ALP measured in this chapter was external released by the adhered cells and measured on days 4, 7 and 14. The control of Thermanox® in OM had initially high levels of ALP activity, which appear to decrease over time. This is thought to be due to an early peak in ALP activity. The low levels of Orthoss® cellular activity appear to be due to the lack of cellular adhered to its surfaces. Orthoss® initial high levels ALP; however, this could be due to its formation from natural bone.

In the synthetic materials, Actifuse™, β-TCP™ and, Inductigraft™ all have a peak in activity at day 7 before the second stage where there ALP levels begin to decline by day 14. This would indicate that the adhered cells are moving towards the osteogenic lineages. Both ApaPore™ and the control Thermanox® appear not to have peaked by day 14 due to increased ALP activity from day 7; this demonstrates that these cells have not moved towards the osteogenic lineage. This may mean that ApaPore™ takes longer to differentiate, and the Thermanox® control was expected not to cause the cells to differentiate. The Orthoss® samples appeared to encourage limited ALP activity; however, this could be due to the lower than expected cellular adhesion and metabolic activity. *In vitro* studies indicated that the SiHA BGS could increase, the osteoinductive activity of the BGS investigated (Coathup et al., 2013).

#### 2.5.2.4.1 Alkaline Phosphate Assay in BGSs with the addition of Si.

The early ALP activity up-regulation has been previously reported in studies using Inductigraft™ due to the differentiation of the stem cells compared to the HA (De Godoy et al., 2015). Osteoblast activity such as ALP expression and activity was directly affected by Si ions release by the grafts (Guth et al., 2006). The osteogenic differentiation occurs in three phases of principal biological periods, which include cellular proliferation, cellular maturation and matrix mineralisation (Sodek and Cheifetz, 2001).

During the initial proliferation time points osteoblasts will synthesise and secrete type I collagen and there will be biosynthesis of the extracellular matrix being produced, while ALP is expressed post proliferation when the extracellular matrix is maturating. In the final stage, there is the mineralisation of the extracellular matrix mineralisation, during which the osteopontin, osteocalcin, and bone sialoprotein will be expressed (Sodek and Cheifetz, 2001). Guth et al.,(2006) suggested that the Si ions can affect osteoblast-like cell biology by interactions with both collagen I and ALP expression. This is critical to bone development and mineralisation.

Si presences, concentration, and location are required for bone formation, and their hypothesis agrees with other studies that have shown that SiHA up-regulates bone mineralisation and apposition *in vivo*. *In vitro* studies performed by Gibson *et al.,* demonstrated that the incorporation of Si into a phase-pure HA could stimulate osteoblast-like cell activity when compared against stoichiometric HA (Gibson et al., 2002). Gibson et al., (*In-vitro*) and Patel et al., (*In vivo*), also demonstrated enhanced

osteoblast cell activity following substitution of silicate ions for phosphate ions in the HA lattice compared to phase pure.

#### 2.5.2.5 Scanning Electron Microscopy

In this chapter, the SEM confirmed cellular attachment and enabled visual comparison to the number of cells attached to the different BGS's. It was, however clear that a high number of cells were associated with all the BGS scaffolds except Orthoss®. These results were similar to those obtained using the Live assay.

The other BGS have rougher surface topography that should enhance cellular attachment, differentiation and spread (Sammons et al., 2005; Ayobian-Markazi et al., 2012). The topography of the BGS materials made it difficult to observe whether the morphology of the cells had changed and differentiated into osteoblasts. Ayobian-Markazi et al. reported to be able to find a monolayer of rounds cells adhered to the Orthoss® surfaces; however, they were using Human osteoblast-like cells (SaOS-2) (Ayobian-Markazi et al., 2012).

A high number of cells can be seen in both SEM and Live assay images adhered to Actifuse™, ApaPore™, β-TCP™, and Inductigraft™. The cells appear to attach around the concaved surfaces close to the pores of Actifuse™, ApaPore™, and Inductigraft™. The cell morphology appears to be elongated and extended; previous studies observed osteoblasts having a flattened morphology with extended filopodia that attach closely to the pores within the graft (Annaz et al., 2004). SEM results in this chapter showed that cells adhered to the BGS after 21 days caused the seeded MSCs to change in structure from an elongated spindle shape to become more cuboidal and osteoblasts-like. The SEM images showed that the manufactured BGSs appeared to have less formal and sporadic pore structure when compared to the natural forming Orthoss®. β-TCP™ was the largest granules investigated with large pores evident. However, some granules appeared not to have any pores at all, and this may be due to the manufacturing process.

The results from the SiHA BGS (Actifuse™ and Inductigraft™) appear to have the ability to increase osteoinduction activity and cellular activity compared to the other BGSs investigated (Vallet-Regi et al., 2005; Patel et al., 2005). The additions of Si ions to the HA matrix, such as in the SiHA examined here was 0.8wt%. This will increase both protein and osteoblastic adherence to the BGS surfaces while it affects their subsequent proliferation (Campion et al., 2010; Guth et al., 2010). The BGS's structure and chemistry can influence the interactions between the graft and the surrounding fluids. This influence can affect how the ions are released from the surface of the grafts. While also affecting protein absorption to the surface, their conformation and the subsequent biochemical cascades that can influence cellular activities (Vogler, 1998; Xu et al., 2007).

#### 2.5.2.6 pH levels

The pH levels of the DMEM+ were affected; however, there was no colour change in the DMEM+ red pH indicator. However, as Tseng et al., (2013), reported that the pH levels changed by an increase of 0.5 towards a more alkaline pH, which was higher than normal bodily fluid pH levels. It is possible that Orthoss® may be leaching CaO and that it is still affecting cellular activity. This leaching of CaO could be due to the deproteinising process and may not be affected in other studies due to the more considerable amount of fluids that could be removing the toxicity.

The presence of CaO as reported by Tseng et al., (2013) would have the ability to cause the media's pH to become more alkaline, as calcium oxide reacts with water in DMEM+, forming calcium hydroxide that can increase the alkalinity of the DMEM+. The presence of a more alkaline media solution cannot only affect the local biological microenvironment it can affect cell metabolism, function, bone tissue formation and mineralisation (Monfoulet et al., 2014). Monfoulet et al., 2014 described that MSCs that are within an alkaline pH up to 8.27 were unaffected in terms of proliferation and did not note any osteogenic differentiation, however, at pH at 8.85 cells stopped proliferating and at a pH of 9.37 the cells died. As this was an exploratory investigating, there were time constraints, and there was a limited ability to investigate the release of ions and the pH levels.

#### 2.5.2.7 Further points

The BGS scaffold porosity has shown to promote both cellular and vascular ingrowth into the graft, enabling mechanical fixation of the graft to the bone. This will contribute to increasing bioactivity interactions while promoting accelerated osteoinduction (Campion et al., 2010; Coathup et al., 2012; Hing et al., 2006; Patel et al., 2005). The increased strut porosity (Inductigraft™) has the potential to increase the osteogenic potential of the graft, surface area and interconnectivity of the BGS and further regeneration of bone sites (Campion et al., 2010; Hing, 2005; Coathup et al., 2012).

A combination of SiHA with an increased strut porosity, as found in Inductigraft™ could potentially lead to the highest osteoinductive compared to other BGS investigated The osteoinductive behaviour of the BGS is manipulated through the interactions with cells via the soluble ions being released from its surfaces (Hing et al., 2005). The results from this chapter show that differences in the different BGSs in terms of macro/strut porosity, topography and chemistry can affect the rate of proliferation, viability, and bioactivity of seeded MSC's.

#### 2.5.2.8 Limitations

Limitations of this study include the low sample size number. Repeating the study using primary cells from more sheep would improve the power of the study. It would have been

interesting to investigate human MSCs and measure their response to the different BGS's.

Further to the ALP analysis, it would have been good to get more positive confirmation of osteoblastic differentiation occurred. To do this requires an investigating the gene expression of osteoblastic related genes using QPCR or using FACS analysis with the correct CD markers. There is a limited availability of Ovine CD markers.

Due to the process in retrieving MSC's, there can be a mixed population of cells been extracted, including hematopoietic stem cells and blood cells (Khatri et al., 2009). There are several methods of purifying the extracted cells and leaving just MSC. The MSCs will adhere to tissue culture plastic another method is by density gradient centrifugations which a method to isolate the MSC into a layer by using ficoll to filler out cells that can be extracted before seeding on a plate (Yamamoto et al., 2015). Cell sorting is another approach that would isolate MSC from other cell types and can be done by flow cytometry (Boxall et al., 2015). Frequent changes of the DMEM+ can prevents the adherence of non-MSCs to tissue culture plastic (Soleimani et al., 2009). MSC could also be isolated directly from compact bone and more limit the amount of cross-contamination that can be seen in other methods (Guo et al., 2006; Zhu et al., 2010).

Once differentiated the osteoblasts can be stained by either von Kossa, were silver ions adhere to anions on the calcium salts (however no specific for calcium) which produced by the osteoblasts, the silver salts are reduced, and there's a colour change to dark brown or black. While the alizarin red stain binds to the calcium deposits react with calcium cation formed from chelate produced by the cells (Wang et al., 2006).To further confirm osteoblast has been differentiated Raman spectroscopy can be used to assess nodules be produced by the cells for the presence of HA and this can be done on live osteoblast cultures which beneficial over alizarin reds staining (Gough et al.,2003). Cell mineralisation can also be characterised using a field-emission scanning electron microscopy (FE-SEM), energy-dispersive X-ray spectroscopy (EDS) can be used to confirm mineralisation in carbon-coated samples (Persson et al., 2018). Transmission electron microscopy and x-ray diffraction can be used to measure the structure, composition and mineralisation of the bone tissue been formed. Chemical and physical characteristics of the mineralised nodules, which can be assessed by Fourier transform Infrared Spectroscopy (FTIR) and X-Ray Diffraction (XRD). FTIR can be used to identify biochemical changes in cells, while XRD enable phase identification of crystalline material and cell dimensions (Ishii et al., 2007).

### 2.6 Conclusions

This chapter had two aims; firstly, to identify whether MSC was isolated from Ovine bone marrow aspirates. While the second aim was the characterisation of five available

commercial BGS were investigated for their ability to induce osteoinduction by investigating metabolic and external ALP release.

The isolated MSC where capable of undergoing tri-lineage differentiation which a fundamental characterisation of MSC's. This result and the previously published studies indicating that MSCs can be isolated from Ovine MSCs leads to the conclusion that the cells extracted were MSCs and could be used for further experiments within this thesis.

The Inductigraft™ showed the greatest overall fold change in metabolic activity over a 21-day experiment (399.4%) ($p$ <0.001). This with the results of external ALP activity showing that Inductigraft™ had a high level of activity would lead to show Inductigraft had the best performance of all BGS investigate. These results align with previous studies that showed the combination of SiHA and increased strut porosity, produces a graft enables increased osteoinductive tendencies.

Orthoss® had a high level of external ALP activity but performed below expectations compared to previous studies that demonstrated that Orthoss® would encourage both MSC attachment and osteoinduction (Kouroupis et al., 2013; Kouroupis et al., 2012; Dorati et al., 2014). Changes were observed in the pH levels of Orthoss® media, which is an indicator that the pH was more alkaline. This is described as a side effect of the process in making Orthoss® which causes the formation of CaO (Tseng et al., 2013).

# Chapter 3

# Investigation into the Cellular Activity on Orthoss® Bone Grafts.

## 3.1 Introduction

This Chapter will focus on the Orthoss® BGS product produced by Geistlich (Switzerland). Throughout the experiments in Chapter 2, it became apparent that Orthoss® had a low initial cellular adherence during the *in vitro* experiments and those cells that did adhere failed to thrive and proliferate throughout the 21-day experiment.

There have been contrasting reports published about Orthoss® effectiveness. Kouroupis et al. stated Orthoss® as an "excellent natural BGS" and "bone subpopulation can rapidly migrate towards, attach and expand" however these studies were *in vivo* (Kouroupis et al., 2013).

Others have reported that Orthoss® has low levels of cellular attachment, proliferation and metabolic activity that decreased over time (El-Jawhari et al., 2016; Kubosch et al., 2016). Tseng et al., (2013), noted that the sintering process caused the formation of CaO, which affected the surrounding environment by changing the pH, making it unsuitable for the cellular seeding attachment.

Deproteination is the process of eliminating proteins from living materials. Deproteination occurs when xenogeneic bone undergoes a heat treatment process (Murugan et al., 2003). Orthoss® also known as Bio-Oss® is widely studied bovine xenograft consisting of a mineral osseous matrix obtained after the removal of organic components of medullar bovine bone during a thermal treatment at 300$^{o}$C according to the manufacturer's data (Accorsi-Mendonca et al., 2006). The standard production of xenogeneic bone occurs by cleaned of any materials before been dissected into sections and then boiled in distilled water for 12 hours before a further 12 hours in a 2% NaCl solution before washing in an acetone-ether mixture at a ratio of 3:2. The bone is then heated for 18hours, and then end product produced is a to hydroxyl carbonate apatite phase material (Murugan et al., 2003).

The novelty of this research is the comparison of the conditioned Orthoss® and Actifuse™ as neither has been compared after conditioning. Then there was also a novel experiment of taking conditioned DMEM+ (which is DMEM+ taken off the BGS that has been conditioned) and then placed onto cells to investigate the materials are leeching materials that is causing harm to the cells. Conditioning of the BGS in DMEM+, which contains FCS will enable the proteins within FCS to adhere to the surface that can change the physiochemical properties of the BGS surfaces.

## 3.2 Aims and Hypothesis

### 3.2.1 Aim

To investigate whether the issues with the Orthoss® BGS was a batch issue or was it an issue with the manufacturing and investigate whether these issues could be solved by conditioning its surfaces. Secondly, investigate if conditioning the BGS in DMEM+ which will enable proteins to adhere to the BGS surfaces and possibly increase the performance of the Orthoss® BGS in relation to cellular attachment and proliferation.

### 3.2.2 Hypothesis

1. The process of developing Orthoss® BGS, causing harm to the seeded cells during *in vitro* experiments.
2. The conditioning of Orthoss® BGS in DMEM+ media could potentially increase cellular attachment and proliferation by changing the physicochemical properties of the surface.

### 3.2.3 Objectives

1. To compare the difference between Orthoss® granules and Orthoss® blocks in metabolic activity, Live/Dead assay and cell morphology.
2. To investigate whether conditioned Orthoss® granules could increase cellular attachment and proliferation rate of the adhered cells.

### 3.3 Materials and Methods

#### 3.3.1 Study design

There are different forms of commercially available Orthoss® products. Orthoss® granules (Ref: 30870.7) have the same porosity structure and chemical composition as Orthoss® blocks (Ref: 30867.5). Both are represented in **Table** 3.1. The Orthoss® granules were previously investigated in Chapter 2. A comparison between the granule and block forms of bone graft was made to investigate whether the issues seen in the previous chapter was down to a batch issues and the difference in the material structure enabled a clear visible difference in materials.

**Table 3.1** Structural and chemical difference of two commercially Orthoss® products.

| Substrate | Size | Macro Porosity | Strut Porosity | Chemistry | Company |
|---|---|---|---|---|---|
| **Orthoss® Granules** | 1-2mm/2-4mm | 80% (100-300um) # | 10-20nm | Deproteinised bovine bone | Geistlich, Swiss |
| **Orthoss® blocks** | 10 mm x 10 mm x 8 mm. | 80%(100-300um) # | 10-20nm | Deproteinised bovine bone | Geistlich, Swiss |

# Kouroupis et al., 2013.

The *in vitro* experiments were performed over 21-days using Ovine MSCs to investigate whether the issues were on both surfaces. AlamarBlue® was used to compare metabolic activity. Cellular viability was visually assessed using a Live assay and cellular morphology using SEM. It was investigated if conditioning Orthoss® for 24 hours in DMEM+ could increase cell attachment and proliferation (Shchukarev et al., 2012).
A second experiment to investigate whether Orthoss® granules conditioned in DMEM+ before cell seeding can have improved performance. To condition the Orthoss® granules, they were submerged into a DMEM+ (this contained 10% FCS and 1% P/S). At the end of submerged time (24, 48, 96 and 168 hours); the conditioning media was removed and placed onto cells seeded cells. AlamarBlue® was monitored 72 hours post-seeding. While the 168 hours conditioned granules, were tested on 1, 4, 7 and 14 days.
Conditioning of BGS materials has been done previously using DMEM with 10% fetal bovine serum for periods of 1 and 7 days (Shchukarev et al., 2012). When compared to the non-conditioned materials, the addition of the medium showed significant increases after 1 day concerning their protein attachment, surface charge and chemical composition (Shchukarev et al., 2012). They also noted that there was a charge reversal by changing the atomic ration of Na/Cl and this was seen to aid the protein layer formation, which will have a subsequent effect on cell recognition and causing a higher level of biomineralisation (Shchukarev et al., 2012). For this reason, it was attempted to condition the surface of the Orthoss® in the hope to increase its performance due to its weak performance chapter 2.

A third investigation examined whether the Orthoss® BGS leached materials into the DMEM+, which could be affecting cells. It was hoped conditioning could remove any leeching materials from the BGS. The MSCs were seeded onto a cell culture plate (Corning® Costar®, USA) before been submerged in conditioned DMEM+ (this contained 10% FCS and 1% P/S) for 24 hours. AlamarBlue® was performed at 24 and 48 hours to investigate metabolic activity, and then a Live/Dead assay was done to assess the conditions of the cells.

### 3.3.2 Cell Seeding

0.08g of both BGS were seeded in the same manner as previously stated in **Section** 2.3.4.

### 3.3.3 Cell Metabolic Activity

AlamarBlue® assay was performed as outlined **Section** 2.3.5 and performed days 1, 4, 7 and 14.

### 3.3.4 Cell Viability

The Live assay was performed on day 21, as described in **Section** 2.3.6.1.

### 3.3.5 Scanning Electron Microscopy

The SEM experiment performed as previously outlined in **Section** 2.3.7.2.

### 3.3.6 Conditioned Granules and Media

To condition, the granules, 0.08g of Orthoss® were incubated in 2mls of media at 37ºC for 24, 48, 96 and 168 hours. The control was Actifuse™.

### 3.3.7 Seeding onto Conditioned Granules

Seeding into the conditioned granules was performed in the same manner as non-conditioned granules. The cells were allowed to adhere and proliferate for 72 hours before the performance of an AlamarBlue® assay. 72 hours was selected, as it is a time point investigated in the mass spectrometry experiments in chapter 6. The final time point for 168 hours was selected to represent a full week of conditioning. For the 168 hours conditioned granules, AlamarBlue® was performed at 1, 4, 7 and 14 days.

### 3.3.8 Conditioned DMEM+ Media

Cells were seeded as stated in **Section** 2.3.4 and allowed to proliferation for 24 hours. The Orthoss® conditioned DMEM+ was then added. The control for this experiment was Actifuse™ conditioned in DMEM+ media.
AlamarBlue® was performed at 24 hours. Fresh conditioned DMEM+ add to the cells for a further 24 hours before a second AlamarBlue® was done.

### 3.3.9 Statistical analysis

Normality was checked using the Kolmogorov- Smirnov and Shapiro Wilkinson test. If data was normal, the comparison was made using an independent student T-test. For non-parametric data, comparison was made using the Mann Whitney U test with a Bonferroni correction. The data analysed was performed using SPSS version 24 (Chicago, USA). The figures were made using GraphPad Prism version 7.0.0 (San Diego, USA). These experiments were run in $n$=9 where there was 3 cell lines and 3 repeats of each unless stated otherwise.

## 3.4 Results

### 3.4.1 Comparison of Orthoss® BGS: Cell Metabolic Activity

AlamarBlue® was performed on the Orthoss® blocks to confirm the metabolic activity results of Orthoss® granules from Chapter 2. Both are represented in **Figure** 3.1. The Orthoss® blocks had a higher metabolic activity at each time point when compared to the granules; however, these differences were not significant ($p$=0.1).

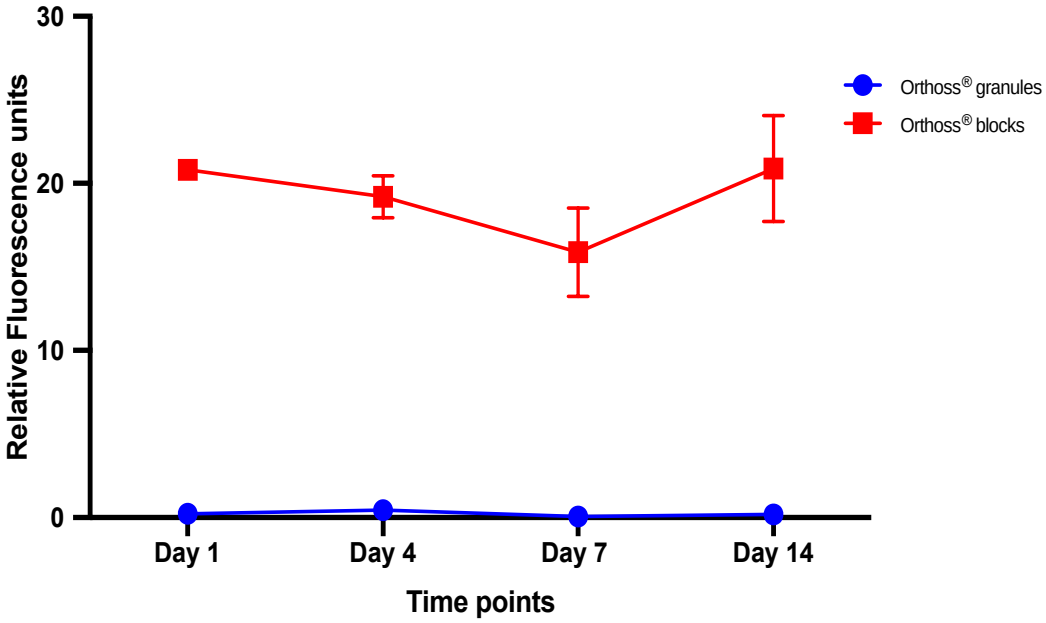


**Figure 3. 1 Comparison of Orthoss® Metabolic activity over 14days.** Measured by AlamarBlue® assay (n=9). Orthoss® blocks was not significantly increased compared to Orthoss® granules at any time point (p=0.1). The error bars represent the standard error of the mean.

### 3.4.2 Live assay

The Live assay performed at 21 days post-seeding and showed a low adherence of viable cells on both Orthoss® structures (**Figure** 3.2).

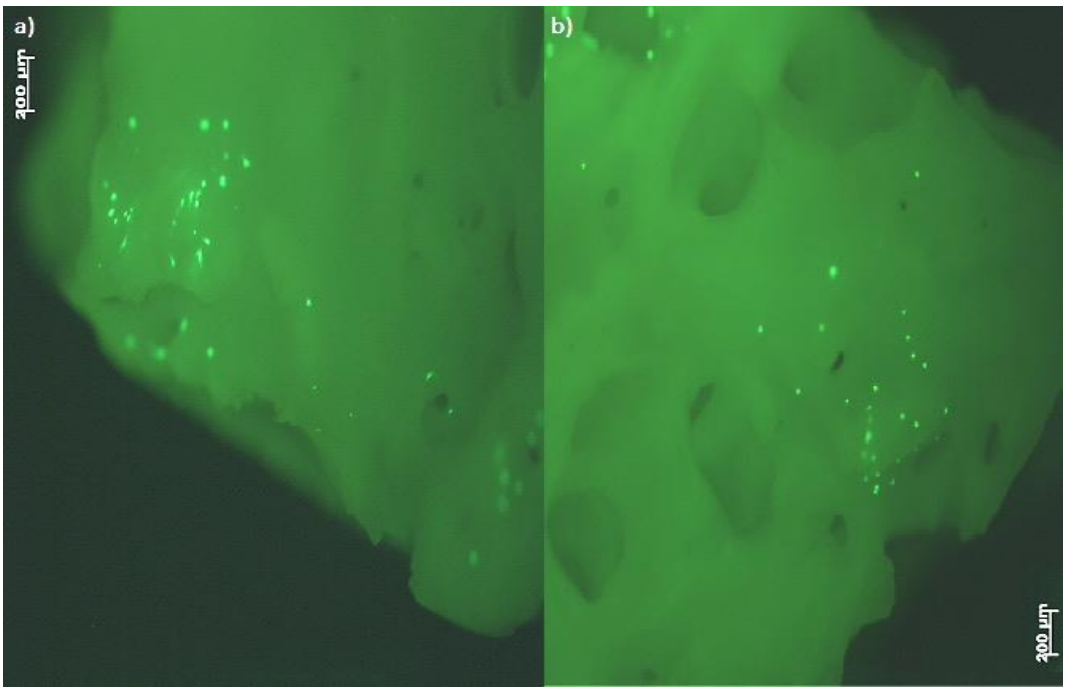


**Figure 3. 2 Live assay of Orthoss® samples 21 days post cell seeding.** (**a**) Orthoss® granules and (**b**) Orthoss® blocks. Both surfaces show similar limited cellular attachment.

### 3.4.3 Scanning Electron Microscopy

The SEM images enabled a closer investigation into cellular attachment and morphology (**Figure** 3.3). As shown previously in Chapter 2, it was difficult to find any cells adhered to either Orthoss® surfaces. The difficulty in finding any cells attached to both structures was due to the low cell numbers and low proliferation based on the results seen in both the AlamarBlue® and Live assays.

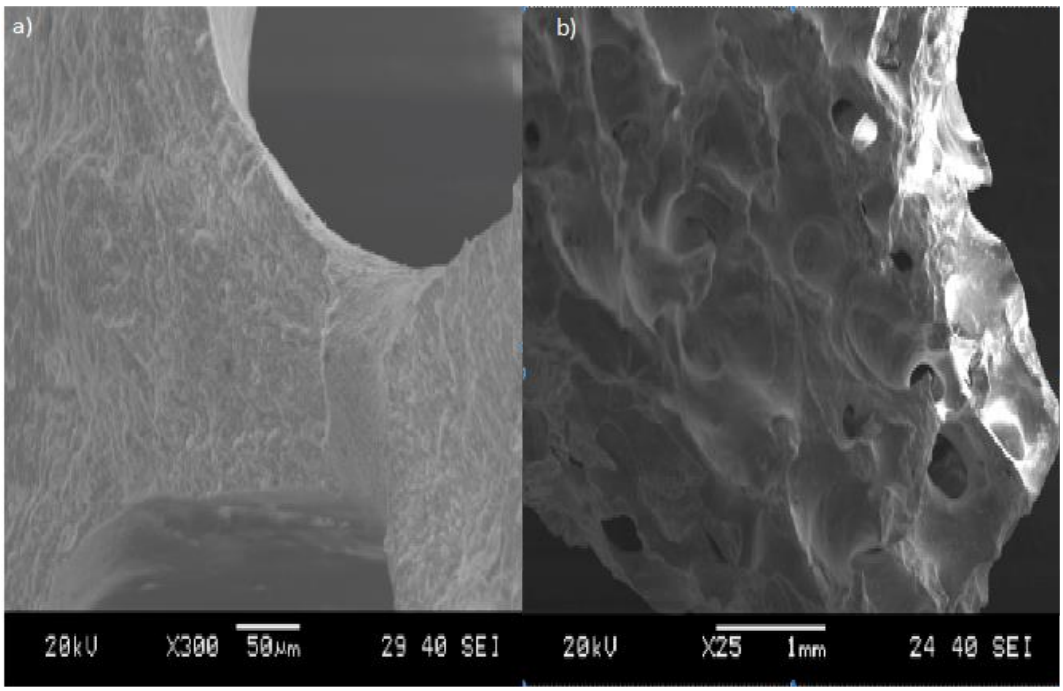


**Figure 3. 3 Scanning Electron Microscope images of Orthoss® 21 days post cell seeding.** (**a**) Orthoss® blocks and (**b**) Orthoss® granules. No adhered cells found on either surface.

### 3.4.4 Seeding Cells onto Conditioned Granules

Metabolic activity of cells on conditioned granules for either 24 or 48 hours was investigated. This was performed 72 hours post-seeding using. The control for this experiment was Actifuse™ granules that were conditioned for the same period.

The Actifuse™ outperformed Orthoss® by 2.24 (±1.4), which was not significance ($p$=1.00) (**Figure** 3.4). The Actifuse™ had higher levels of metabolic activity cells at both time points when compared to Orthoss®. There was a higher level of difference between the two samples on the 48 hours conditioned BGS 2.62, which was significant ($p$=0.0001).

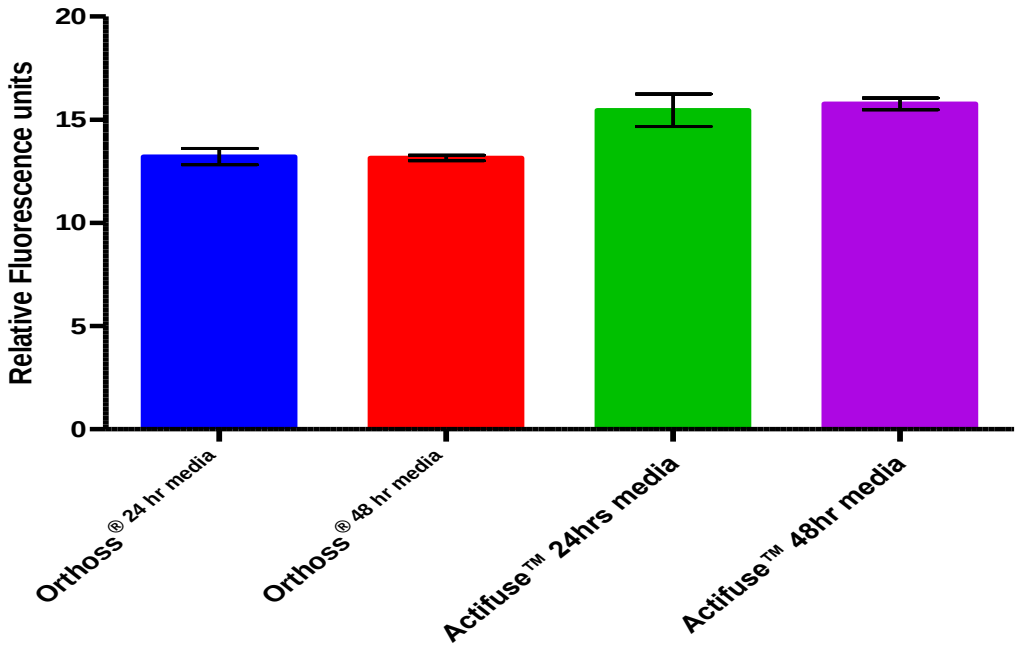


**Figure 3. 4 Metabolic activity at 24 and 48 hours post-conditioning BGS's.** Performed by AlamarBlue® assay (*n*=3). No significant difference noted between any samples (*p*=1.00). The error bars represent the standard error of the mean.

### 3.4.4.1 Extended Conditioning Period of Orthoss® Granules

An extended period of conditioning of 96hours demonstrated Actifuse™ again outperformed Orthoss® in metabolic activity by 2.5% (±-0.1) in the 24 hours conditioned samples (**Figure** 3.5). Measured via AlamarBlue® assay while the difference was 2.6% (±0.1) on the 48 hours conditioned granules.

The cell proliferation on Actifuse™ conditioned for 24 hours showed a higher significant compared to the Orthoss® sample by 6.2% (±2) (*p*=0.005). The 48 hours samples showed a more significant difference of 9.9% (±-3.3) between the materials (*p*=0.0001).

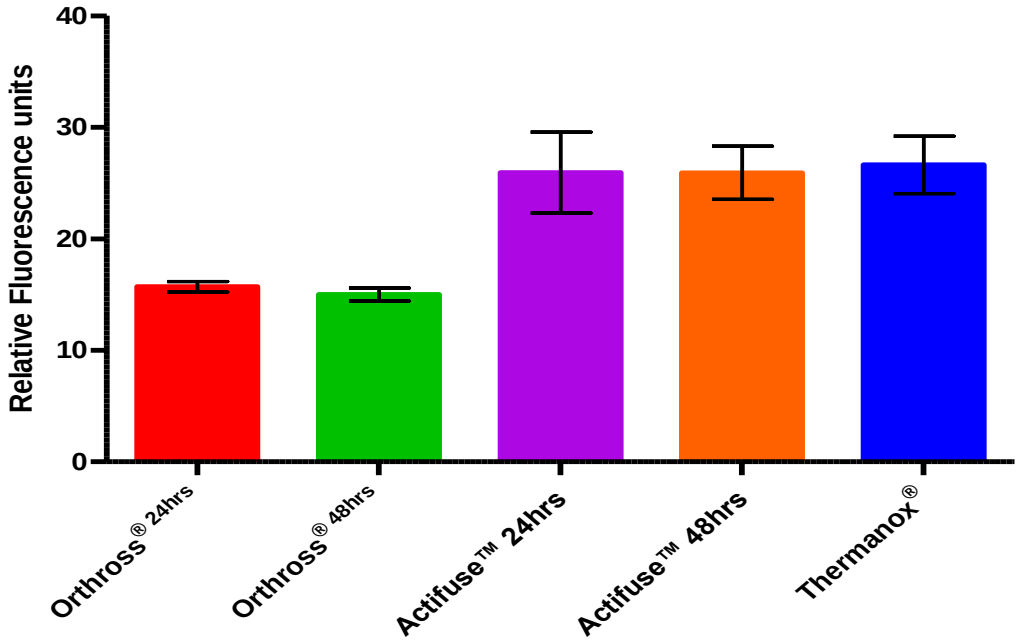


**Figure 3. 5 Metabolic activity of 96 hours conditioned BGS.** Performed by AlamarBlue® assay (*n*=3). Both Actifuse™ time points had significantly higher metabolic activity compared to counterpart Orthoss® samples (24 hours (*p*=0.05) and 48 hours (*p*=0.001)). The error bars represent the standard error of the mean.

### 3.4.5 Conditioned DMEM+ Media

Cells were seeded onto tissue culture plates in DMEM+ and allowed proliferate for 24 hours before the media was exchanged for conditioned DMEM+. 120 hours post media change the metabolic activity was assessed. Cells in the DMEM+ conditioned by Orthoss® had a lower metabolic activity compared to the Actifuse™ in both samples. This was an exploratory experiment with an *n*=3 to investigate whether condition media was potentially leaching materials that could be potential affecting cells adhering.

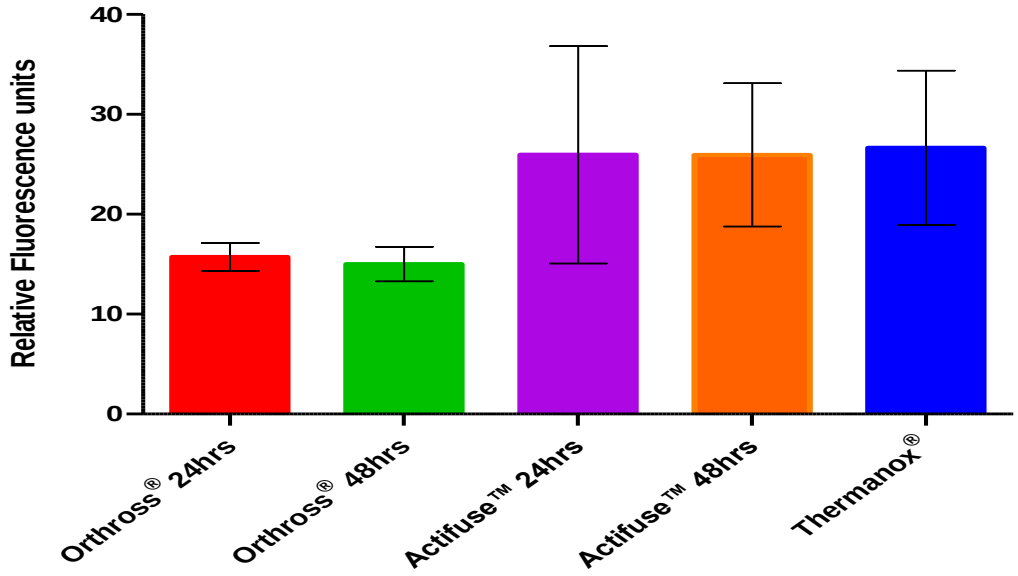


**Figure 3. 6 Metabolic activity of cells in conditioned DMEM+ media.** AlamarBlue® assay was performed 120 hours post-seeding (*n*=3). Significant Actifuse™ and Thermanox® activity compared to both Orthoss® time points (*p*=1.0). The error bars represent the standard error of the mean.

MSCs were seeded on Thermanox® disc for it, was 24 hours then the DMEM+ was removed, and Orthoss® conditioned media was added, this appeared to hurt the previously healthy cells within five minutes. The adhered MSCs began to deteriorate (**Figure** 3.7 (**a**)), and this deterioration increased with time. The deteriorating cellular membrane appeared to contract, and the cells became shrunken with blebs forming that appears to be composed of cellular components.

Light microscopy showed blebs floating in the media, as shown in **Figure** 3.7 (**a**). Cellular blebbing is associated with cells undergoing apoptosis. This issue was not apparent in the control of Actifuse™ conditioned media (**Figure** 3.7 (**b**)).

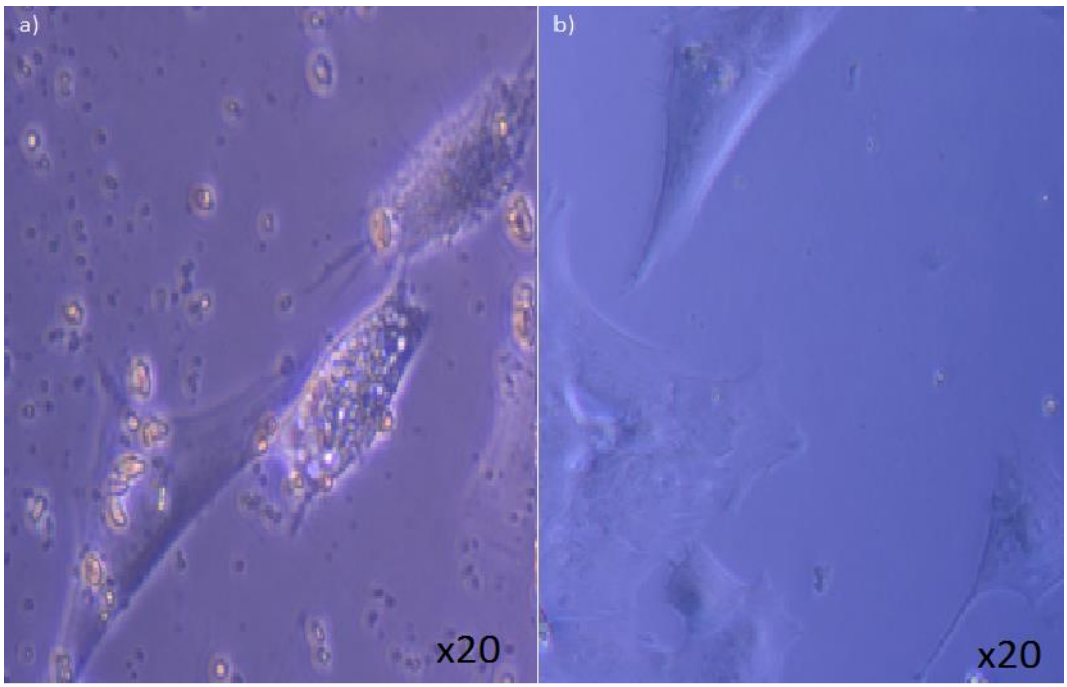


**Figure 3. 7 Cells in conditioned DMEM+ media.** Images taken on light microscopy. 1.5 hours after media was changed on seeded cells. (a) Orthoss® conditioned DMEM+ media; (b) Actifuse™ conditioned DMEM+ media. Orthoss® conditioned DMEM+ media appear to cause cells to undergo apoptosis.

On day 14 post-seeding a Live/Dead assay was performed. This showed visually there were more cells adhered to the Actifuse™ control (**Figure** 3.8). Cellular morphology between the two conditioned media differs. The cells in Actifuse™ appeared to have an elongated cellular structure, whereas the cells grown in Orthoss® conditioned media appear where shrunken and more rounded.

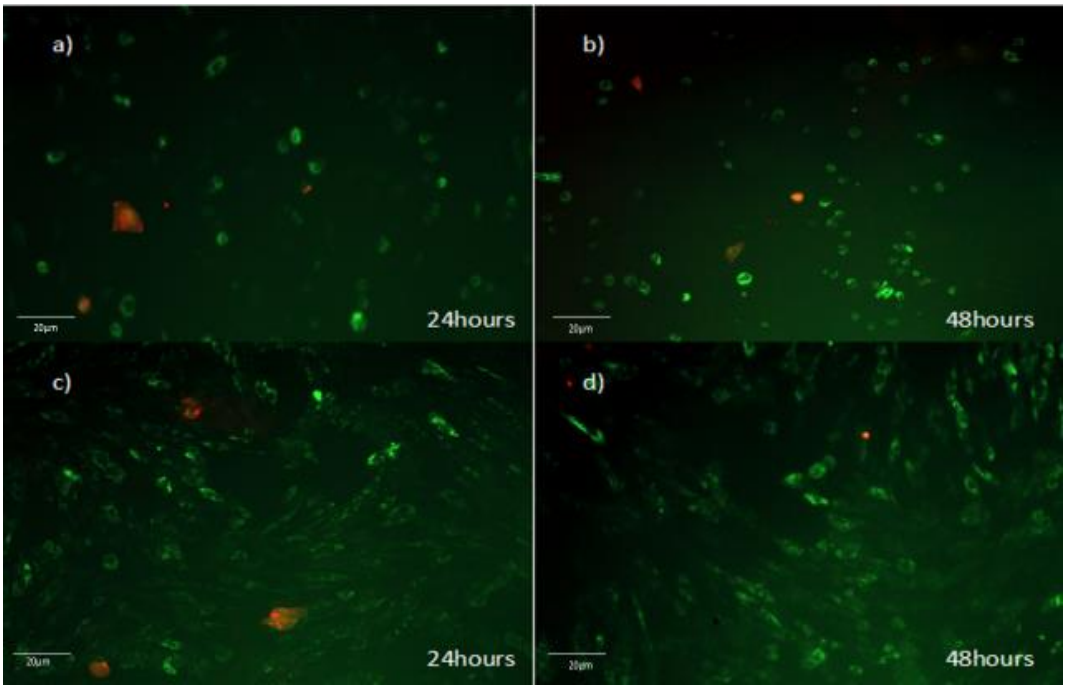


**Figure 3. 8 Live/Dead assay of cells on tissue culture plastic in conditioned media.** (**a**) Orthoss® 24 hours, (**b**) Orthoss® 48 hours, (**c**) Actifuse™ 24 hours, (**d**) Actifuse™ 48 hours. Cells in Orthoss® media appear more condensed and had lower numbers compared to the elongated and more viable cells in conditioned Actifuse™ media control.

## 3.5 Discussion

This chapter sets out to investigate why Orthoss® underperformed throughout chapter 2. The low performance of the Orthoss® had not been reported to the same extent in previous similar studies.

El-Jawhari et al. reported that Orthoss® had lower cellular attachment and proliferation rates when compared to the two other grafts in their study Orthoss-collagen® (Gieslich, Swiss) and Vitoss™ (Stryker, Malvern, PA) (El-lawhari et al., 2016) while Kubosch et al. (2016) showed that there was a tendency for cells on Orthoss® to decrease in both cell numbers and metabolic activity.

Some studies have shown Orthoss® BGS to be successful in producing a favourable response from the adhering cells. Kouroupis et al. reported that Orthoss® promotes rapid migration of MSCs, adherence, proliferation and, differentiation (Kouroupis et al., 2012; Kouroupis et al., 2013). In the 2013 study, Orthoss® granules in conjunction with a bone marrow aspirate and autografts (Kouroupis et al., 2013). They showed the Orthoss® granule's ability to attract and to be colonised by MSCs (Kouroupis et al., 2013). Dorati et al., (2013) coated the Orthoss® in a polylactide-co-glycolide (PLGA) which was shown to improve the graft's ability to stimulate growth and proliferation of adhering fibroblastic cells (Dorati et al., 2013). However, not until after 15 days of incubation was their cells adhered to non-coated Orthoss® blocks and appeared to act in the same manner as the cells on the coated Orthoss® (Dorati et al., 2013).

### 3.5.1 Metabolic Activity

The initial study in this chapter was an investigation to confirm that deproteinised bovine bone graft Orthoss® granules did not support cell proliferation and attachment, as shown throughout Chapter 2.

An *in vitro* comparison was made between Orthoss® granules (1-2mm) and blocks (1cm x 1cm x 2cm). These differences enabled a visual difference in samples. Both materials have the same internal structure but different overall structural shape. The results showed that the block form had a slight increase in cell metabolic activity on Day 14. However, this was non-significant. No cells were found visually adhered to either Orthoss® surfaces after using SEM. This is the same as Chapter 2 SEM results. Overall, the results showed that both forms of Orthoss® have limited ability to attract, attach and support the proliferation of the MSCs. This indicates that Chapter 2 results for Orthoss® granules were a true reflection of the Orthoss® BGS.

### 3.5.2 Conditioned Granules

Conditioning of the BGS in DMEM+, which contains FCS will enable the proteins within FCS to adhere to the surface that can change the physiochemical properties of the BGS

surfaces. These changes to the physiochemical properties could potentially affect cellular adherence and subsequent cellular proliferation.

Firstly, experiments were designed to condition the Orthoss® granules in DMEM+ before seeding cells. Twenty-four hours of conditioning a BGS has shown previously to increase the amount of bioactivity on the BGS (Shchukarev et al., 2012). Actifuse™ was used as the control. The conditioning of the Orthoss® was performed to allow the graft to become accustomed to the *in vitro* conditions before cell seeding and for proteins to adhere to its surface.

The conditioned granules were seeded with Ovine MSCs for 24 hours before the metabolic activity was measured by AlamarBlue® assay. In the samples conditioned for 24 hours showed Actifuse™ outperformed Orthoss® by 2.5% (±-0.1), and this increased on the 48 hours conditioned samples to 2.6% (±0.1) on samples.

However, these periods selected to allow the grafts to adjust have appeared not to cause any difference and the Orthoss® graft that again was still eclipsed by the Actifuse™ in terms of cellular attachment and metabolic activity. To evaluate whether the conditioning periods were too short, this meant an extended period of conditioning was investigated to allow more protein attachment to occur. The BGS (*n*=3) conditioned in DMEM+ for 96 hours showed, again was no significant improvement in cellular metabolic activity at 1, 4, 7, and 14 days.

### 3.5.3 Conditioned Media

To discover whether the Orthoss® BGS were created an environment that was harming the adhering cells, a conditioned media was generated. Orthoss® granules into in DMEM+ for 24 and 48-hour periods and this was placed onto MSCs adhered to tissue-cultured plastic for 24 hours.

Within five minutes of adding the Orthoss® conditioned media to the MSCs that had been seeded and allowed to proliferate on tissue culture plates, there was an apparent negative effect to the cells and began to deteriorate. A visual inspection showed that the cells had become shrunken in shape with the cell being to deteriorate, and the cells began to bleb, which is indicative of apoptosis. Cells can undergo apoptosis due to cellular processes that include cell turnover, development, immune system, hormone-dependent atrophy or chemically induced cell death (Elmore, 2007).

This was not apparent in the control of Actifuse™ conditioned media control, indicating that the Orthoss® BGS leached a material into the media that harmful to the adhering cells.

The pH levels results from Chapter 2 showed Orthoss® having a high pH at every time point. These pH readings mean the media is more alkaline compared to the other samples. Tseng et al., (2013) reported that the pH levels that changed even by an increase of 0.5 towards a more alkaline pH, which is higher than normal bodily fluid pH

levels. It is possible that Orthoss® was maybe leaching CaO, and that is affecting cellular activity. This leaching of CaO could be due to the deproteinising process and may not be causing the same effect as in other studies due to more copious amounts of surrounding fluid that could cause a smaller change if any to the pH levels of the media.
The presences of CaO as reported by Tseng et al., (2013) would have the ability to cause the media's pH to become more alkaline, as calcium oxide reacts with the water in DMEM+ causing the formation of calcium hydroxide, which in turn can increase the alkalinity of the DMEM+.
A more alkaline media, the solution cannot only affect the local biological microenvironments, but it can affect cell metabolism, function, bone tissue formation and mineralisation (Monfoulet et al., 2014). Monfoulet et al., 2014 noted that MSCs within an alkaline pH up to 8.27 were unaffected in terms of proliferation and did not note any osteogenic differentiation; however, they noted at pH at 8.85 cells stopped proliferating and at a pH of 9.37, the cells died.

### 3.5.4 Live/Dead Assay

Cell viability and morphology were investigated using a Live/Dead assay. This visually showed a clear difference in cellular morphology and viable cell numbers between the sample and control. The control cells appear to have an elongated healthier cellular structure with a higher amount of viable cells. Whereas the cells grown in the Orthoss® conditioned media appeared shrunken and with fewer viable cells present.
This appeared to be apoptosis-like cell death. Apoptosis causes shrinkage, rounding of the cell's overall structure and formation of cellular debris (Elmore et al., 2007). This issue may be neutralised in larger volumes of DMEM+ for *in vitro* experiments or, *in vivo* where the bodies' fluids may dilute and neutralise the adverse effects of CaO produced by Orthoss®. This may allow the graft to support cell attachment. Kubosch et al., (2016) believed that the decrease in viable cells that they noted overtime was due to the absence of blood that carries nutrients and growth hormones that are found in the *in vivo* but are not emulated to the same extent *in vitro*.

### 3.5.5 Limitations

However, the conditioning of BGS was not able to cause an increase in the performance of Orthoss® in terms of cellular attachment and proliferation. I was not able to identify the CaO leaching into the media that was suggested by previous studies, and this was a limitation of the study. There was no direct comparison between the conditioned and non-conditioned Orthoss® this would have helped indicated whether there was any change in the by performing conditioning.
This would have required identifying its differences compared to non-conditioned media. Mass spectrometry could have been used to investigate for the presence of CaO or any

other ions been released from the Orthoss®. An investigation into whether the cells were undergoing apoptosis would have also been appropriate to confirm apoptosis was occurring. To perform this requires one of the following methods; flow cytometry, fluorescence microscopy or commercially available apoptosis assays. It may be possible that organic material, albeit degraded in the calcining process, will be affecting.

Increasing the cell numbers seeded exponentially onto the Orthoss® may have increased its performance due to higher numbers of cells adhering; however; it could have also led to increased cell death. The failures with Orthoss® could be associated with the *in vitro* conditions, as *in vivo* investigations have shown that Orthoss® supports bone formation.

### 3.6 Conclusions

This chapter was done to access whether the below expectations of Orthoss® within chapter 2, causing cellular attachment and proliferation. These experiments were done to investigate whether this was a batch issue. Initially, a comparison was made between two different forms of Orthoss®, one was the granules used in chapter 2, and the second was a block version. Two different structures were used to ensure batch differences and give a visual difference to make comparison easier.

Both grafts had similarly poor results with cellular attachment and proliferation. These results are different from those who reported Orthoss® will encourage both MSC attachment and osteoinduction (Kouroupis et al., 2013; Kouroupis et al., 2012; Dorati et al., 2014). However, there several other publications that noted Orthoss® poor performance. El-Jawhari et al. (2016) reported lower cellular attachment and proliferation compared to other grafts. While Kubosch et al. (2016) showed that there was a tendency for decreased cell metabolic activity on Orthoss® overtime, this reduced activity may be due to the increased pH levels reported in Chapter 2 which causes the surrounding environment more alkaline.

Conditioning of the Orthoss® BGS was performed to investigate if it would improve the performance of the graft; however, conditioning the BGS didn't appear to increase the performance of the grafts.

Conditioned media was created to investigate whether the Orthoss® BGS increase alkaline media affecting the potential for cells to adhere to. Healthy cells cultured in Orthoss® conditioned media died, indicating that the alkaline solution is affecting the cells.

These issues may not be relevant during in vitro experiments as the alkaline solution may be neutralised in these situations leading to the positive results seen in many previously published studies into Orthoss®.

# Chapter 4

## Proliferation and Differentiation of Mesenchymal Stem Cells on Sintered Discs of Bone Graft Substitutes.

### 4.1 Introduction

In Chapter 2, the BGSs composed of SiHA showed the highest potential to increase bioactivity levels. The chemical composition of a graft induces bioactivity directly by releasing ionic products that will interact with cells through ion channels or affecting the local pH, which can indirectly influence the adherence of proteins, growth factors and cells (Lee et al., 2011).

The addition of 0.8wt% Si to HA has shown to stimulate collagen type 1 synthesis within osteoblast-like cells and leading to the promotion of osteoblastic differentiation (Reffitt et al., 2003). While, Patel et al., (2002) described *in vivo* studies that the addition of Si ions into the HA lattices can increase bioactivity when compared to the non-substituted HA. While Gibson et al., (1999) described *In vitro* studies of osteosarcoma cells had increased metabolic activity and again in a 2003 study by Botelho et al., demonstrated that the SiHA enhanced bioactivity, which resulted in the formation of apatite at earlier time points. While Botelho et al. (2006) studied showed that SiHA also caused increased levels of cellular adhesion.

This chapter focuses on the influence that the chemical composition of selected BGSs have on osteoinduction. Two chemical compositions where selected, (1) synthetic hydroxyapatite (HA) that represents ApaPore™ and (2) silicate-substituted hydroxyapatite (SiHA), which is used for the production of both Actifuse™ and Inductigraft™.

The powdered materials used to form the granules were compressed into a disc then sintered to produce dense discs (DD). This will control the surface topography. Sintering created the highest density disc possible and reduced grain growth (Champion, 2013).

## 4.2 Aims and Hypothesis

### 4.2.1 Aim

This study aimed was to investigate whether the combination of Si and hydroxyapatite as a BGS has the potential to influence the proliferation and differentiation of Ovine MSCs

### 4.2.2 Hypotheses

1. Increased proliferation rates will be shown on the DD formed of SiHA compared to that of HA.
2. There will be increased levels of osteogenic differentiation of Ovine MSCs seeded on the SiHA surface compared to HA alone.

### 4.2.3 Objectives

1. Create sintered DDs of both HA and SiHA.
2. Compare the differences between the HA and SiHA DDs concerning metabolic activity, ALP assay, and cellular morphology.

### 4.3 Materials and Methods

These protocols were successfully performed by a previous member of my laboratory group and published in their thesis (Samizadeh, 2010).

#### 4.3.1 Study Design

This study focuses on whether a combination of silicate and hydroxyapatite as a BGS can affect cellular attachment, differentiation and the formation of apatite. All surface topography of the BGS was removed by compressing their chemical components and sintering them into DD. This allowed for an investigated into the effect the BGSs chemistry as on the adhering MSCs.

The same fine ceramic powder that was used to create ApaPore™ formed from HA ($Ca_{10}[PO_4]_6[OH]_2$)($Ca_{10}(PO_4)_{6-x}(SiO_4)_x(OH)_{2-x}$) powder. While for SiHA ($Ca_{10}(PO_4)_{6-x}(SiO_4)_x(OH)_{2-x}$) that is also used for the production of both Actifuse™ and Inductigraft™. Depending on the BGS, the sintering temperature cycles were adjusted to ensure that the chemistry matched that of the commercial granule form. The sintered DD was used for *in vitro* experiments over 28-days. Metabolic and ALP activity was monitored on days 4, 7 and 14 after seeding the Ovine MSCs. While SEM images were used to assess cell morphology on the same days and additionally at day 28.

#### 4.3.2 Production of Dense Discs

The dry ceramic powder that was used to produce the HA DD ($(Ca_{10}[PO_4]_6[OH]_2$); Lot number: A00X0A16910) was supplied by Dr Karin Hing (Queen Mary University, London). Baxter Healthcare Ltd supplied the SiHA ceramic powder (Lot number: SOOPOO27420).

Methanol was used to clean the equipment as any debris present could cause the DD during the sintering process rendering the DD unusable. 1g of the dry ceramic powder was placed in the die mould between the upper and lower plates (**Figure** 4.1(**b**)). The assembled die was placed into the chamber of the Specac Atlas manual hydraulic press (Specac, UK) (**Figure** 4.1 (**a**)) and before being aligned, the release valves were closed. The side-lever was activated to raise the press base plate, and a 120 MPa load was applied to the die assembly and held for 1 minute. This pressure ensures that maximal powder compaction at the targeted load was achieved to create a DD, that once sintered measuring 10 mm diameter and 2 – 3 mm in thickness.

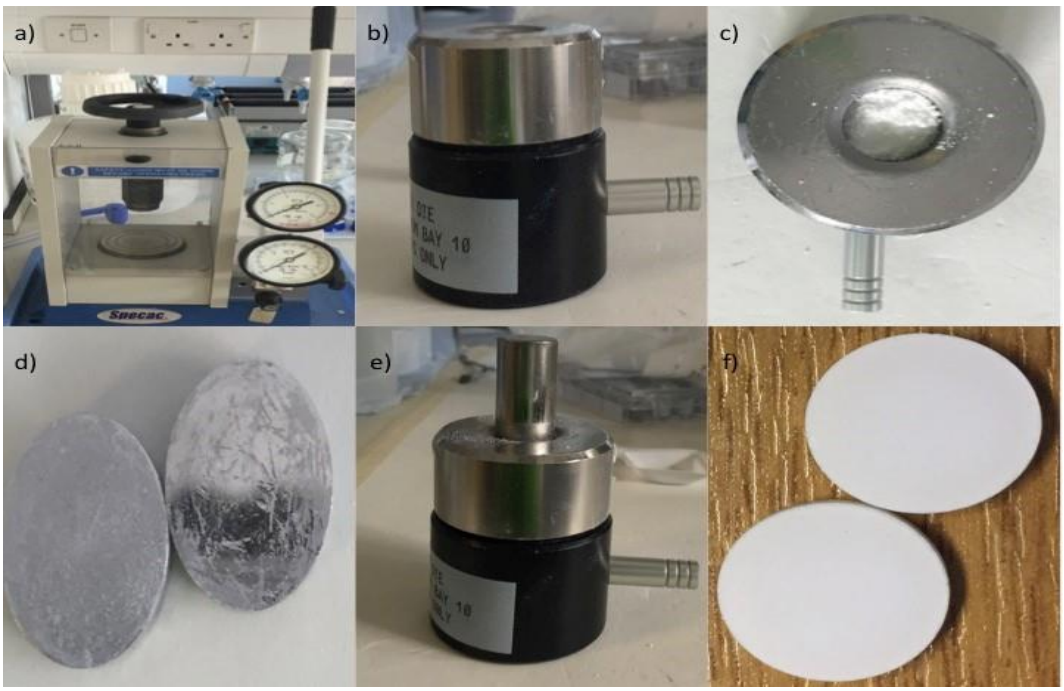


**Figure 4. 1 Equipment used for pressing dense discs.** (**a**) Manual hydraulic press, (**b**) Pressing die, (**c**) 1g of HA powder in the die, (**d**) pressing discs (**e**) Die with bolster, (**f**) sintered press disc.

### 4.3.3 Sintering of Dense Discs

The sintering temperatures for SiHA and HA were different:

**Table 4. 1 Sintering temperature of the DD.** The DD was held at their respective temperature for two hours.

| Ceramic powder | Maximum Sintering Temperature |
|---|---|
| HA | 1200$^{o}$C |
| SiHA | 1250$^{o}$C |

The temperature was slowly increased at a rate of 5$^{o}$C per minute until the sintering temperature was reached. Once reached, it was held for 2 hours before returning to room temperature at a rate of 10$^{o}$C per minute.

Once the sintered DD were cooled, the following measurements were taken to calculate the density: diameter (μm) (d), and the thickness (μm) (t). The density of DD was required to be >96%. To calculate the density **equation,** 4.1 below was used:

$$\text{Volume} = \pi r^2 \times t$$

$$= \pi (d/2)^2 \times t \text{ (units in cm (divide by 20 to get mm)).}$$

### 4.3.4 X-Ray Diffraction

X-Ray Diffraction (XRD) was used to measure the chemical composition of the sintered DD. Technical staff at Queen Mary University, London obtained the XRD spectrum and analysed it.

The spectrum was obtained using a Siemens Xperts-Pro diffractometer (Siemens, Germany). The samples were scanned continuously by a graphite detector from $20^{o}$ to $70^{o}$ 2θ, at a scanning speed of $1^{o}$/min 2θ at a minimum step size $0.02^{o}$ 2θ for a count of 2.5 seconds. The monochromatic Cu-K radiation of $Ka_1$ = 1.540598 nm and $Ka_2$ = 1.544426 nm with an intensity ratio of 0.5 was used. The three software programs used to define the crystallography parameters were:

1. Xpert HighScore Plus software and the ICDD database.
2. Pickpx2 software (Queen Mary University, UK).
3. UnitCellWin software.

### 4.3.5 Cell Seeding and sterilization of Dense Discs

The discs were sterilized by being placed into a glass container that had a loosen lid and placed within an autoclave where steam at a pressure of approximately 15psi and attaining a temperature of 121$^{o}$C. These were allowed to dry entirely before seeding with cells. It should be noted that these sterilized DD were not cleaned to remove any endotoxins that may have been adhered before cell culture experiments. Seeding was performed as previously outlined in **Section** 2.3.4.

### 4.3.6 Cell Metabolic Activity

AlamarBlue® assay was performed days 1, 4, 7 and 14 as outlined in **Section** 2.3.5.

### 4.3.7 Cell Differentiation

The ALP assay was performed as previously outlined in **Section** 2.3.6.1.

### 4.3.8 Scanning Electron Microscopy

The SEM experiment performed as previously outlined in **Section** 2.3.7.2.

### 4.3.9 Statistical analysis

Normality was checked using the Kolmogorov- Smirnov and Shapiro Wilkinson test. If data was normal, the comparison was made using an independent student T-test. Non-parametric data comparison was made using the Mann Whitney U test with a Bonferroni correction. The data analysed was performed using SPSS version 24 (Chicago, USA). Figures were made using GraphPad Prism version 7.0.0 (San Diego, USA). These experiments were run in $n$=9 where there was 3 cell lines and 3 repeats of each unless stated otherwise.

## 4.4 Results

### 4.4.1 Manufacture of Dense Discs of Bone Graft Substitute Materials

#### 4.4.1.1 Disc Density

The volume and density of the sintered DD was calculated. The density of each DD was required to be above <96%. Any of the DD that did not meet this requirement or had any chips/cracks could not be used for experiments as cracks could increase the surface area, altering the results of the experiments.

**Table 4. 2 Measurements of DD.** Average value of volume (cm), density (g/cm) and density percentage of the DD after sintering.

| | **Volume (cm)** | **Density (g/cm)** | **Density %** |
|---|---|---|---|
| HA | 0.2918 | 3.0023 | 95.09 |
| SiHA | 0.3172 | 2.9658 | 94.75 |

#### 4.4.1.2 XRD Analysis

The XRD analysis showed similar results to those presented in Samizadeh (2010), who performed the same DD sintering processes of HA and SiHA. The XRD is an analytical technique that enables a phase identification and crystallographic structure of crystalline materials. XRD was used to separate the chemical phases that were the correct formation for the DD that were required for this experiment.

The XRD data in **Figure** 4.2 presented no additional phases and that the chemistry was shown to be phase pure in both samples. High levels of crystallinity that can be noted in both spectrums as high and narrow peaks. Differences in the intensity of the spectrums were due to the presence of Silicon in the SiHA DD (**Figure** 4.2 (**b**)) (Gibson et al., 2002; Kim et al., 2003). The Ca/P ratio of the HA DD and Ca/(P+Si) ratio of SiHA found by the XRF spectrometry analysis which confirms that the presences of the silicate ion within SiHA as 0.8wt% (Jamil et al., 2018).

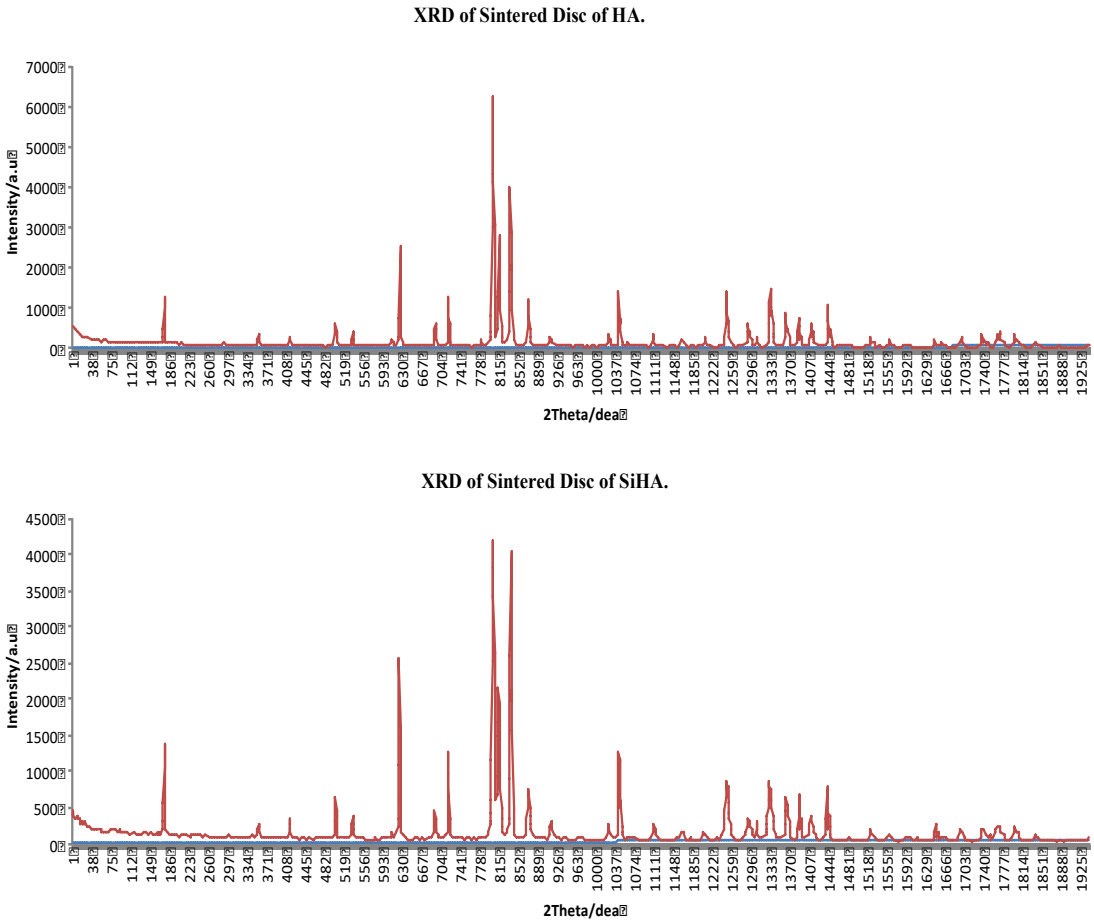


**Figure 4.2 XRD spectra of the sintered DD.** (**a**) HA and (**b**) SiHA. Performed by Queen Mary University, London technical staff. Differences in the intensity of the spectrums were due to the presence of Silicon in the SiHA.

### 4.4.2 Cellular Activity

#### 4.4.2.1 AlamarBlue® Metabolic Activity Assay

AlamarBlue® measured metabolic activity on days 4, 7 and 14. This is represented in **Figure** 4.3, while the percentage changes presented in **Figure** 4.4. Initially, the HA DD had higher activity on day 4 of 108.6 (±1.2). There was then a non-significant increase of 54% by day 7 ($p$=1.0). Between days, 7 and 14 there was a non-significant decrease of -8.58%. ($p$=1.0). Comparisons between days 4 and 14 showed a non-significant difference increase of 41.22% ($p$=1.0). There was a large variation between samples on day 14 as one of the replicates was lower than all other samples.
The SiHA DD had an initial metabolic activity of 113.9 (±2.3) on day 4 before to a 120.4% increase, which was significant by day 7 ($p$=0.03). Between days 7 and 14, there was a non-significant decrease of 2.4%, ($p$=1.0). A significant difference was noted between days 4 and 14, with an increase of 115.1% ($p$=0.04).

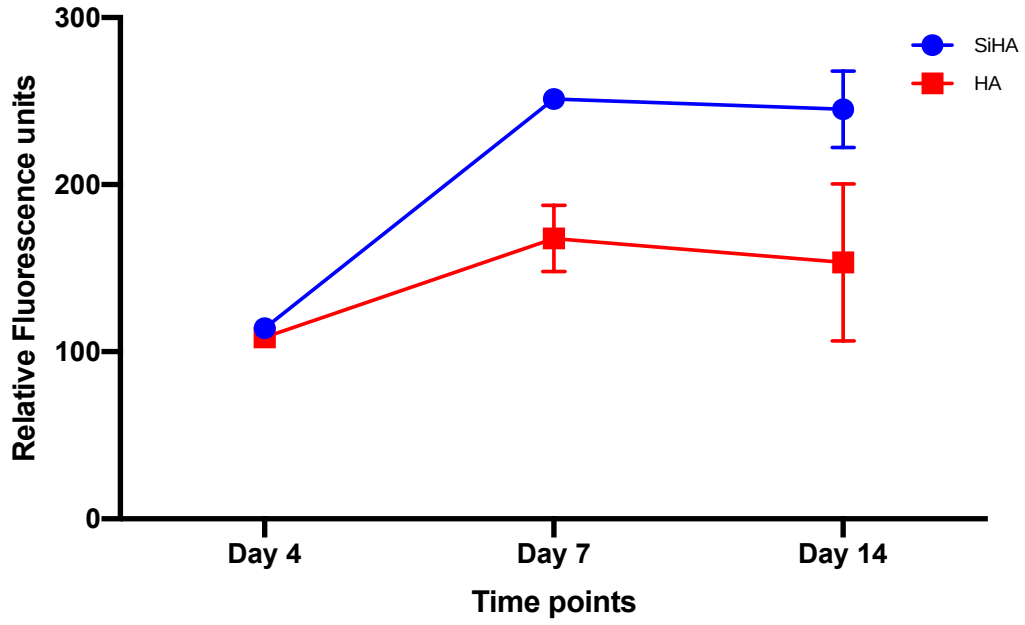


**Figure 4. 3 Metabolic activity of MSCs on sintered DD over 14 days.** AlamarBlue® measured ($n$=9). Significantly more activity on SiHA between days 1 and 14 (115.1% ($p$=0.04)). No significant between the same period on HA ($p$=1.0). The error bars represent the standard error of the mean.

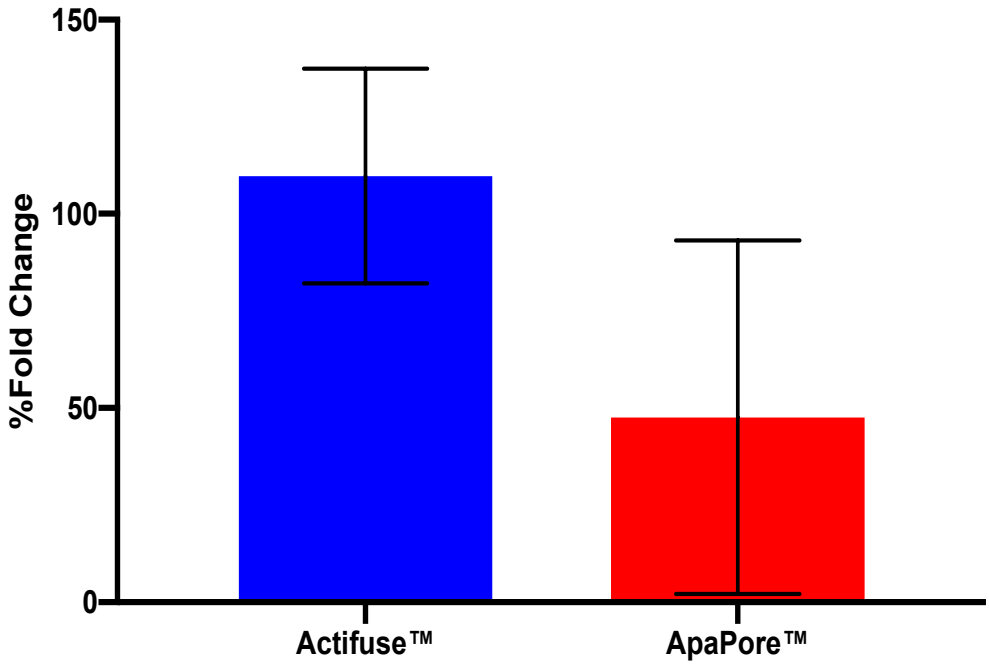


**Figure 4.4 Percentage change in metabolic activity between days 1 and 14.** Measured by AlamarBlue® assay (*n*=9). SiHA had a higher fold changed compared to HA (41.22% (*p*=1.0)). The error bars represent the standard error of the mean.

#### 4.4.2.2 Alkaline Phosphate Assay

External ALP activity was measured on days 4, 7 and 14 (**Figure** 4.5). Initially on day 4, the HA ALP activity was 158.5 (±2.9) before decreasing non-significantly by day 7 to 155.1 (±4.2) (*p*=1.0). The increase on day 14 was non-significantly (9.7 (±3.7); (*p*=0.5)). No significant change between days 4 and day 14 either (*p*=0.3).

SiHA DD ALP activity on day 4 was 158.41 (±2.9) before decreasing non-significantly by day 7 to 158.2 (±3) (*p*=0.7). A non-significant increase was noted between days 7 and 14; there was a non-significant increase of 10.5 (±1.7), (*p*=1.0). Between days 4 and day 14, there was a significant difference with an increase of 131.19 (*p*=0.04).

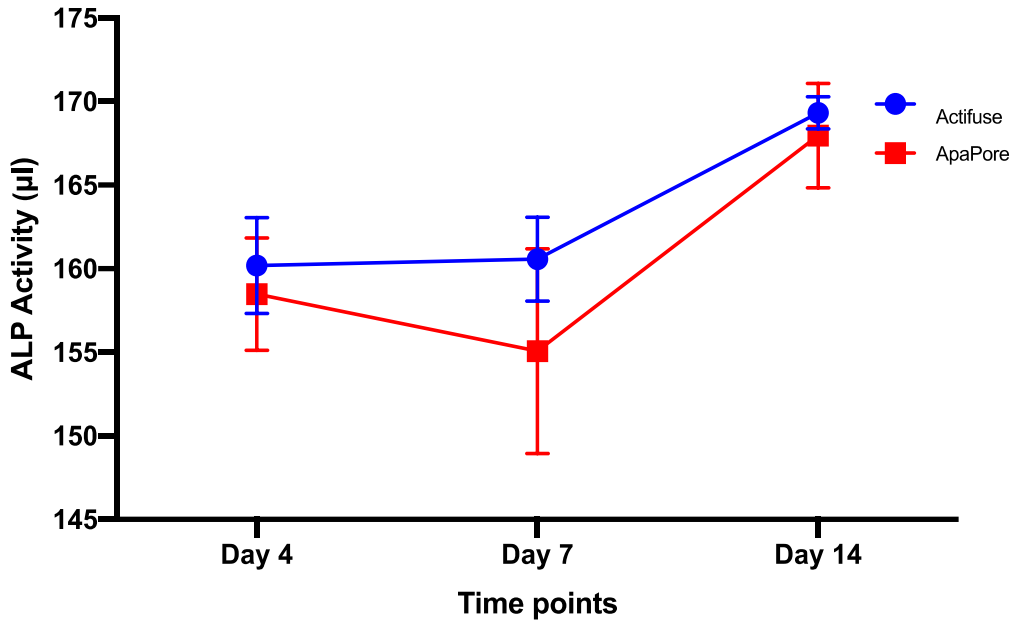


**Figure 4.5 Externally released ALP activity of the DD over 14 days.** Measured by spectrometer (*n*=9). Non-significant ALP activity noted all SiHA samples compared to HA (*p*=1.0). The error bars represent the standard error of the mean.

#### 4.4.2.3 Scanning Electron Microscopy

SEM imaging allowed for a visual assessment of cellular attachment, morphology and the presence of any extracellular matrix produced by cells (HA **Figure** 4.6; SiHA **Figure** 4.7).

There where cells adhered to both surfaces initially and the cells appeared to proliferate as the number of cells increases at the later time points. The cellular morphology of the adhered cell on day 4 appeared to be a flatter structure with long protruding extended spindles. However, by day 14, the cellular morphology changes and the cells appear to become more cuboidal in shape and similar to the structure of osteoblasts.

There were confluent layers of cells coating the entire SiHA DD surfaces by day 7 (**Figure** 4.6), but confluent layers of cells were not seen on the HA DD surfaces until day 14 (**Figure** 4.7).

Both surfaces had deposits of extracellular matrix been produced by day 7, and these increased in frequency with time. These nodules are associated with the cells that were proximity and are believed to be associated with mineralisation (Fratzi et al., 2004; Thian et al., 2006). From a visual inspection, there appeared to be a higher amount of nodules on the surface of the SiHA samples.

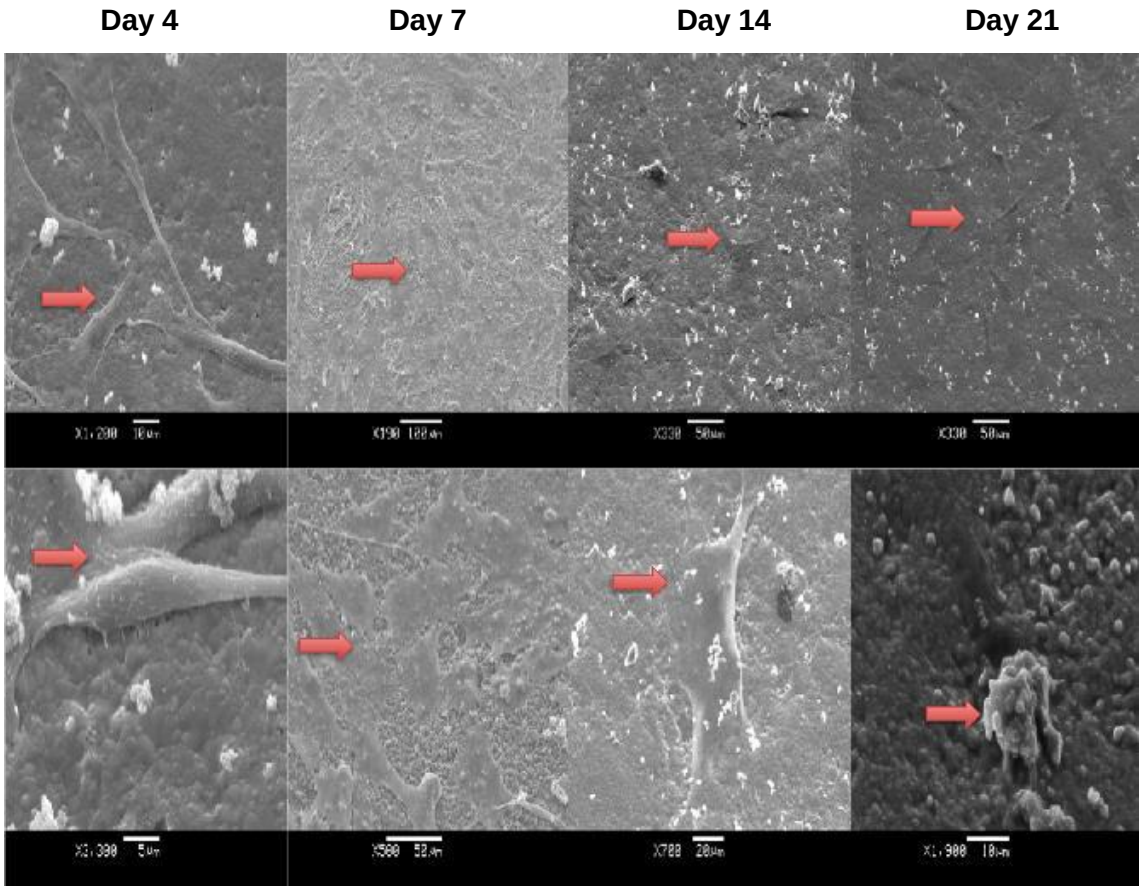


**Figure 4. 6 Scanning Electron Microscopy images of cells on HA sintered DD.** Images taken on days 4, 7, 14 and 21. Increase in cell activity with time points. Day 21 shows possible mineralisation (indicated by the arrow).

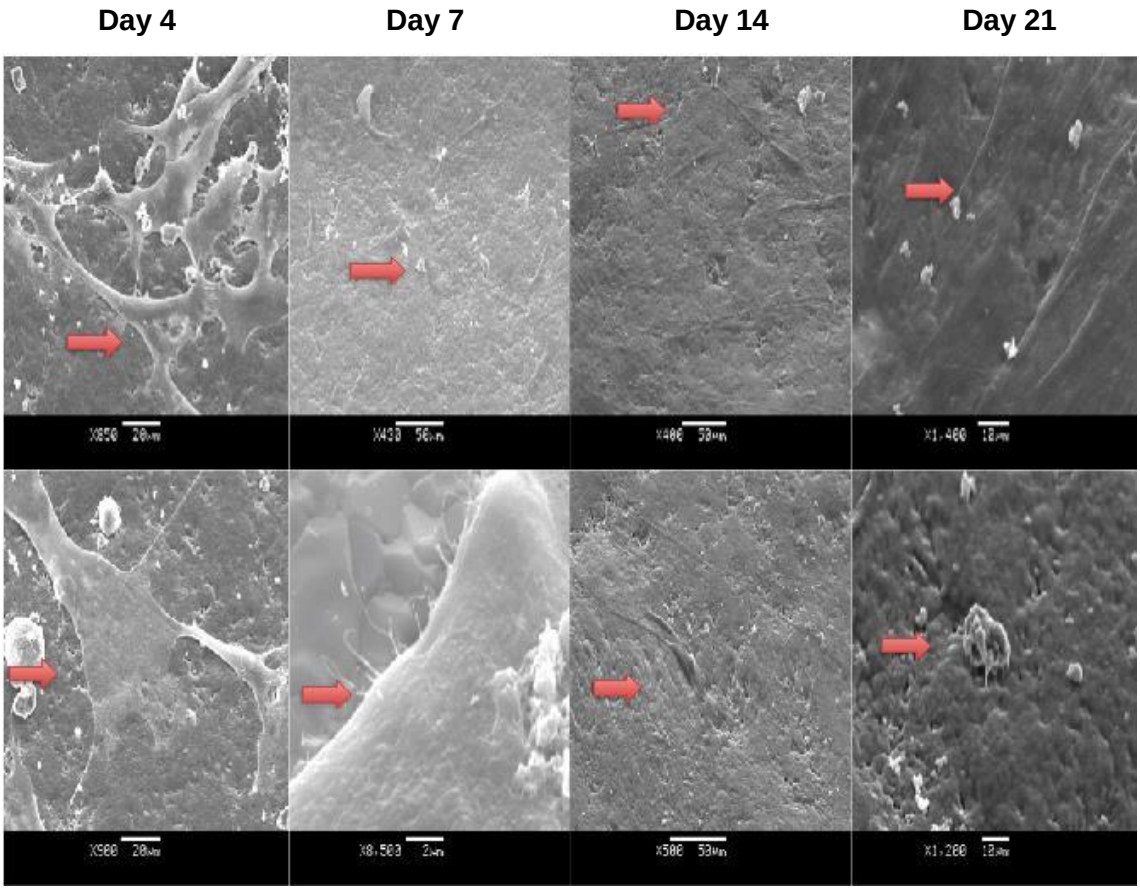


**Figure 4. 7 Scanning Electron Microscopy images of cells on SiHA sintered DD.** Images taken on days 4, 7, 14 and 21. Increase in cell activity with time points. Day 21 shows possible mineralisation (indicated by the arrow).

## 4.5 Discussion

This study investigated whether the chemical composition of selected BGSs can influence cellular viability, proliferation, and osteogenic differentiation. The BGS chemical compositions that were selected included HA ($Ca_{10}[PO_4]_6[OH]_2$) ($Ca_{10}(PO_4)_{6-x}(SiO4)_x(OH)$ 2-x) representing ApaPore™. While the SiHA ($Ca_{10}(PO_4)_{6-x}(SiO_4)_x(OH)_{2-x}$) represented both Actifuse™ and Inductigraft™. As stated before, both Actifuse™ and Inductigraft™ have the same chemical composition but differ in their strut porosity and throughout Chapter 2; strut porosity was shown to influence cell adherence and osteoinduction levels. The topographical features of certain BGS can increase their overall surface area, possibly triggering osteogenic differentiation (Habibovic et al., 2004). However, the chemical composition and surface chemistry of BGS has been known to be critical to the success of the graft and if optimized can enhance the potential to be a clinically successful outcome (Hing, 2006).

The results presented in this chapter show that the hypothesis of higher metabolic activity of the SiHA DD, when compared to the HA DD, was correct. While it was not clear whether SiHA increased the levels of osteogenic differentiation compared to the DD of HA. These results mirror those of Chapter 2, where the BGS formed from SiHA (Actifuse® and Inductigraft®) outperformed the HA (ApaPore®). This was possibly due to the addition of Si ions into the HA lattice.

### 4.5.1 X-ray diffraction

There were differences in the intensities between the HA and SiHA XRD patterns. This is due to the presence of the Si, which is known to aid in the sintering and will cause a lower crystallinity when at the same calcination temperatures than HA (Gibson et al., 2002; Kim et al., 2003).

The density of the DD was measured to show the discs had a higher density percentage of over 98%; this showed the discs lacked or had minimal porosity that would require them to be excluded from the experiments. Before 28 days *in vitro* experiment, all the sintered DD were sterilised using an autoclave, and any further work with them was performed in a cell culture hood to maintain the sterilise conditions. As noted in the methods section, these DD were not clean of any endotoxins that could have been adhered before the cultured experiments.

### 4.5.2 *In Vitro* experiments Results

The results presented in this chapter demonstrated similar outcomes to previous studies that compared the addition of Si ions to the HA. These studies have shown to increase biological activity of the adhered cells compared to HA alone in terms of the ability of the grafts to attraction, proliferation and differentiation (Pietak et al., 2007; Sun et al., 2015; Hing et al., 2005; Gibson et al., 1999; Reffitt et al., 2003). Si presence is to be essential

for the development of healthy bone and cartilage (Pietak et al., 2007). As discussed in the introduction there have been many studies that have proposed and shown that chemical composition and surface chemistry can indirectly affect many factors including; the initial absorption proteins to its surface and the subsequent attachment cells. Also, as discussed previously, SiHA has been linked to increased bioactivity when compared to non-Si substituted HA (Pietak et al., 2007).

There are several theories of how this influence occurs. One is that it occurs by an active effect whereby the Si that has been substituted (Bohner et al., 2009). The other is a passive effect; for example, involves either calcium release, change in the surface chemistry or topography (Bohner et al., 2009).

Bohner et al., (2009) analysis of Si-substituted calcium phosphate led them to believe that the BGS should be reclassified as drug delivery system as the release of ions during the resorption process should be known as a drug and the therapeutic levels that depend on the release rate and availability of the ions should be considered.

Several studies have shown that the addition of 0.8wt% silicon ion (2.6wt% silicate) has the ability to cause significant enhancements to the surface by attracting proteins to adhere and some of these proteins have been associated with increasing the bioactivity of the material (Patel et al., 2005; Hing et al., 2006; Guth et al., 2010; Campion et al., 2010). Hing (2005) described that substituting Si into HA latticed enhanced the bioactivity of the HA through either its surface chemistry and surface charge or possibly the controlled release of Si from its surface.

Several studies that demonstrate that Si substituted materials will affect the surface charge, which in turn increased bioactivity including protein adsorption, osteoblast attachment and the subsequent cellular response including ALP production and collagen I synthesis during *In vitro* studies (Hing et al., 2007). Hing et al., (2006) suggests that the introduction of Si substitution increases the dissolution rate during *in vivo* investigation. This is a synergistic mechanism with the rate of free Si being released which is a dose-dependent effect, and there is an optimal level of Si, which can stimulate an increased in bone matrix synthesis with enhanced organisation and there is no benefit to increased free Si concentrations (Hing et al., 2006).

#### 4.5.2.1 Metabolic activity

At days, 4, 7 and 14, the metabolic activity was accessed by AlamarBlue® assay. The sterilised sintered DD was seeded with Ovine MSCs cells (*n*=9). The initial results on day 4 showed that both DD had similar levels of metabolic activity (HA 108.6±1.2 and SiHA 114.0±3.8). Both showed increased metabolic activity by day 7; during this period, the SiHA sample increased by 120.4%; however, HA only increased by 54.5%. SiHA had a reduced metabolic activity at 14 days of -2.4% while HA only increased by 8.6%. This

reduced activity could be due to a lack of surface area for the cells to continue growing as cells had already consumed the entire disc surface area in the preceding time point.

There was a significant in metabolic activity increase between days 4 and 14 on SiHA with a 131.2% change ($p$=0.04). HA, however, was a non-significant increase of 41.233% ($p$=1.0) between the same time points. It was noted that on day 14 there was a large variation in metabolic activity on the HA this was due to one of the three replicates of HA exhibiting a lower than expected activity compared to the other samples.

During Gibson et al., (1999) study, they seeded cells onto tissue culture plastic and then added extra silicon ions to the DMEM. The addition of Si ions led to a significant increase in cell metabolic activity. While Hing et al., (2006) demonstrated *in vitro* investigations where Si was substitution into HA lattices assisted both bone ingrowth and repair at earlier stages within the porous structure of the scaffolds. Hing et al., (2006) believed this occurs due to physio-chemistry and metabolism of both bone formation and bone-resorbing cells releasing trace levels of bioavailable Si. They also suggested that Si presence in optimal levels within scaffolds can overcome any effects within defect sites due to mechanical stress shielding or poor host bone metabolism (Hing et al., 2006).

Higher levels of metabolic activity on SiHA may cause an increased rate of adhesion, proliferation, and differentiation of cells due to the dissolution of the Si content (Szurkowska and Kolmas, 2017). Lasgororceix et al., (2014) investigated the behaviour of SiHA during *in vitro* and *in vivo* experiments with and without insulin adsorbed to its surface. Insulin is a growth factor that is involved in many physiological processes and has to influence osteoblastic cells to proliferation, differentiation and stimulate osteocalcin production. Their results indicated that SiHA did not encourage cell adhesion and proliferation compared to HA alone. However, when they absorbed insulin onto its surface, there was an increased cellular focal contacts and RhoA activity. They believed that the addition of insulin and Si could enhance the cellular response to the grafts. The also noted a slightly higher inflammatory response to SiHA compared to the HA during the *in vivo* experiments.

Botelho et al. (2011) study showed increased levels of osteoblasts caused by the addition of the Si into the HA lattice. They state incorporation of Si leads to increased hydrophilicity of HA, and this will increase interfacial tension to the presence of unsaturated Si-O bonds leading to the formation of Si-OH in the surrounding microenvironment. They noted increased Si concentration could speed up apatite formation when compared to HA alone, which could support the mechanism of enhanced bioactivity on SiHA and leads to enhanced dissolution rate and physical-chemical properties. They also noted that SiHA is more electronegative, meaning the surface charge sites are preferential for nucleation of amorphous calcium phosphate apatite layer when compared to HA alone. This occurs via the adsorption Ca2+ ions, which can

attract phosphate groups (Botelho et al., 2011). Guth et al., (2010) suggested that this occurs due to the addition of Si affecting the surface charge, ionic interface and the resultant hydrophilicity of the surface.

The optimal amount of Si was shown to 0.8%, which can cause a higher amount of osteoblast development markers when cells were in the presence of Si (Honda et al., 2012). They suggested this was due to cell-induced to differentiation towards the osteoblastic lineage and noted that it was optimal compared to 0% or 1.6% (Honda et al., 2012). They noted that the latter percentage leads to lower levels of cellular attachment and proliferation. They believed that this occurred because the Si content has a critical effect on culture conditions (Honda et al., 2012).

In studies that have included trace amounts of Si within the structure of the graft, there was enhanced biological performance in relation to the physiological process of bone compared to those that do not, and these are associated with the Si induced changes to implants material properties (Vallet and Arcos, 2005). This enhanced bioactivity is linked to the higher levels of adsorption of cells and the release of Si into the surrounding surfaces and solution (Ducheyne et al., 1999).

#### 4.5.2.2 Alkaline Phosphate Assay

As noted previously, the ALP assay was performed on the externally released cellular ALP. ALP production often used to early indicators of preosteoblastic differentiation (Golub et al., 2007; Stein et al., 1990). There should be an early increase in ALP levels caused by the production of ALP in parallel with osteoid production (Stein et al., 1990). There then will be a subsequent decline in ALP levels, and this is due to the mineralisation of the matrix (Stein et al., 1990).

Between any time point investigated, there were non-significant change in ALP activity in either SiHA and HA. In previous studies, SiHA has demonstrated an ability to induce an earlier positive response in ALP activity when compared to other BGS compounds (DeGodoy et al., 2015). DeGodoy described SiHA samples that had increased porosity showed earlier differentiation of MSCs with an up-regulation in the ALP expression when compared positive and negative controls. They also noted that there was a trend for cellular differentiate towards the matrix producing osteoblasts with also late-stage up-regulation of osteocalcin that was produced pre-osteocytes (DeGodoy et al., 2015). Gibson et al., (1999) demonstrated that the addition of the substituted Si ions into HA could enhance osteoblasts cellular activity and increased apatite layers formation on SiHA in simulated body fluid (SBF) when compared to non-substituted HA. In the 2006 study by Guth et al., the presence of Si in a solution could affect the ALP levels, and they showed that these levels are related to the amount of Si presence, its concentration, and the localisation.

Reffet et al., (2003) indicated the concentration of Si is orthosilicic acid could stimulate the synthesis of collagen type 1 within osteoblast and claim that the Si enhanced the differentiation of osteoblastic cells. However, they note that the mechanism of how Si directly affects osteoblastic differentiation and the commitment to mineralization is unclear. However, Seaborn and Nielsen (1994) mention that Si-deficient animal experiments still report organic matrix formation but mineralization is affected, and they believe that it is the Si affecting the bone matrix synthesis indirectly.

#### 4.5.2.3 Scanning Electron Microscope

SEM imaging enables a visual investigation into both cellular morphology and extracellular matrix production on the surfaces of the discs. The sintered disc surface enabled a more accurate analysis of cellular morphology when compared to the surface topography and porosity of granule forms in Chapter 2.

It was strikingly evident that the entire surface of both samples were coated with cellular activity quickly. Notably, at each time points, there were increased numbers of cells which are an indicator proliferation was occurring. This lead to a clear confluent monolayer of cells at day 7 on SiHA however, HA was not coated fully until day 14. Cellular morphology initially appears to have a typical MSCs cellular structure with a spindle-like morphology. At later time points, the morphology changed, and the cells appear to become more cuboid-like in a structure similar to cells that have differentiated towards osteoblastic lineage.

By day 14, the images show the presence of extracellular matrix nodules formed in close approximation to cells that were adhered to the surface. Apatite formation on a BGS surface was critical for bone induction, and its formation is thought to an indicator for bioactivity formation. These nodules are typically formed from calcium hydroxyl carbonate apatite, which is equivalent in the composition and structure of the inorganic phase of natural bone and this formation of nodules (Garcia-Gareta et al., 2015). The formation of an apatite layers will be typically found in conjugation with the deposition with other organic factors that include osteogenic protein that could have the ability to induce osteogenic differentiation (Barradas et al., 2011). However, if apatite fails to deposit, osteoinduction will also fail even with the presence of osteogenic proteins to the surface (Barradas et al., 2011).

The release of Si has been shown to promote biomimetic precipitation; this will cause the increased solubility and occurs through the creation of crystalline defects with substitution that is associated charge compensation mechanism, by generating a more electronegative surface with the exchange of SiO ions that will cause the material to become a nano-crystalline material (Pietak et al., 2007).

Patel et al., (2002) described Si ions incorporated into HA could increase bioactivity during an *In vivo* experiment that resulted in bone ingrowth into both HA and SiHA

granules when in direct contact with bone. There was more significant bone growth in the SiHA sample (Patel et al., 2002). Balas et al., (2002) demonstrated increased bioactivity levels and the formation of an apatite layer on to the surface of the implant due to the presence of Si ions when compared when Si is absent. The 2003 Porter et al., study suggests that incorporation of Si ions into the HA lattice has the ability to increased rates of dissolution compared to non-substituted. The release of Ca, P and Si ions will cause subsequent diffuse through the ceramic grains to bone and the HA interface, which will be driven by a concentration gradient. An increased concentration of these ions can increase rates of biological apatite precipitation and induced bone apposition on graft surfaces (Porter et al., 2003). This is also associated with the accelerated results seen when the Si ions increases in the bioactivity of HA samples (Porter et al., 2003).

### 4.5.3 Limitations

The study could be made more robust by increasing the “n” number. Ovine MSCs were used for this study; however, human MSCs would have allowed for a better comparison with other similar studies. Zon et al., (2008), showed different cell populations would respond differently to the addition of silicate to a BGS. Even if roughness analyses were not performed, the topography of the disc surface should have been measured to confirm the entire disc surface was uniform. The protocol performed under the guidance and within the used Dr Hing lab at Queen Mary University. Unfortunately, this was not accessed and meant that the results couldn’t be confidently called control. This was performed as the method in the Castagna(2016) and Samizadeh, (2010). These studies were performed in an *in vitro* setting, and could not match the complex mechanisms that occur during differentiation *in vivo* due to a limited ability to mimic the *in vivo* environment.

## 4.6 Conclusions

The chemical composition of a graft induces bioactivity directly by releasing ionic products that will interact with cells. This chapter focuses on the influence that the chemical composition of selected BGSs have on osteoinduction. This study aimed was to investigate whether the combination of Si and hydroxyapatite as a BGS has the potential to influence the proliferation and differentiation of Ovine MSCs. Compressed into a compact disc to control the surface topography so that chemistry is just investigated.

The metabolic activity experiment indicated that SiHA appeared to promote increased levels of both cellular adherence and proliferation when compared to HA throughout the 28-day *in vitro* experiments. SiHA had a non-significant higher fold changed compared to HA (41.22% ($p$=1.0)). Both materials showed similar amounts of ALP activity levels

between the two graft materials. In SEM images, both materials showed visually cellular proliferation and mineralisation production by day 28.

The results showed that SiHA could increase cellular attachment and proliferation which within keeping with previous studies that have shown that the addition of silicon ions to HA is a cost-effective method of boosting cellular adherence and proliferation levels while increasing the grafts osteoinductive potential (Zuo et al., 2008).

# Chapter 5

## Protein Attachment to Bone Graft Materials

### 5.1 Introduction.

Protein attachment occurs within seconds of placing BGS granules into biological fluid, and proteins will be attracted to it and begin to interact with its surface. These protein interactions are critical for the successful integration of the implant and the formation of bone tissue (Guth et al., 2010; McFarland 2000; Green et al., 1999; Rouahi et al., 2006; Kilpadi et al., 2001; Rouahi et al., 2006). Protein adsorption has been shown to influence subsequent biological events that lead to cellular recruitment, attachment and mobility (Wang et al., 2012; Chatakun et al., 2014; Anselme, 2000; Lampin et al., 1997). These will have downstream effects on cell proliferation and osteoblast differentiation (Wang et al., 2012; Chatakun et al., 2014; Suzuki et al., 1997).

By the time the cells arrive, the BGS surface is generally coated in a monolayer of proteins, such that the MSCs do not directly “see” the BGS surface but instead “see” a layer of proteins to which the cells attach (Schmidt et al., 2009).

Studies have shown that the amount and type of proteins that attach to different scaffold materials will vary and this variation has been reported to be due to factors that include surface area, charge, graft chemistry, and topography (Lee et al., 2014; Mathe et al., 2013). The adherence profile of proteins will alter over time as proteins begin to adhere and then detach in a process where competitive displacement. This will result in the earlier absorbed proteins been replaced by proteins with stronger binding affinities. This process is known as the “Vroman effect” (Vilaseca et al., 2013; Hirsh et al., 2013).

The novelty within the chapter includes the experiments that investigated the variation in the amounts of proteins attaching to these five different BGS’s and how protein profile will change over the four-time points. This comparison has not been made previously using these specific BGS and over these particular time points. This chapter will also draw a comparison between different methods of protein detaching proteins from the surface of the grafts and this comparison was not found previously in publication.

## 5.2 Aims and Hypothesis

### 5.2.1 Aim

This study aimed was to investigate differences in protein adsorption of the previously investigated five different BGS (Actifuse™, ApaPore™, β-TCP™, Inductigraft™, and Orthoss®) over four time-points (30 seconds, 1 hour, 24 hours and 72 hours).

### 5.2.2 Hypothesis

The amount of protein adhered to each BGS surface will vary depending on both the BGS and the time points investigated.

### 5.2.3 Objectives

1. To quantify and compare the total amount of proteins adsorbed onto the surface of five BGS materials using a micro bicinchoninic acid (BCA) assay at 30 seconds, 1 hour, 24 hours and 72 hours.
2. To physically separate the attached proteins using SDS-PAGE gel and to quantify:
    1. Relative molecular mass.
    2. Protein distribution among fractions.
    3. Protein purity.
    4. To determine the relative abundance of proteins present on the different scaffolds at each of the time-points.

## 5.3 Materials and Methods

### 5.3.1 Study Design

Protein adsorption on the five BGS investigated throughout this thesis with uncoated Thermanox® discs used as control. Each graft was immersion in bovine FCS (Thermofisher™, UK) for investigated following 30 seconds, 1 hour, 24 hours and 72 hours to allow for proteins with the FCS to adhere to their surface.

The time point of 30 seconds was used, as it is known that proteins will adhere to the surface of a graft within seconds after being submerged in biological fluid (Ramazanoglu and Oshida, 2011). One hour was selected because it is known for being a critical time for proteins to adhere that can attract inflammatory cells (Thevenot et al., 2011). Twenty-four hours was selected, as during this period the barrier between graft and bone will be filled with a blood clot and growth factors and cytokines that function to attract both neutrophils and macrophages are released (Liu and Kerns, 2014). This includes bone morphogenic proteins, osteoinductive factors, growth, and differentiation factors, and the can mediation of inflammation, improving bone formation (Einhorn, 2005; Kuzyk and Schemitsch, 2011). Seventy-two hours was selected, as it is known to be a favourable time for cellular response in terms of spreading and proliferation (Alves and Wassall, 2009).

These experiments were performed with an *n*=3. This consisted of one FCS sample repeated three times. FCS is widely available, and frequently cell culture experiments and its proteins have been documented, however, it does contain varying amounts of these proteins depending on the individual sample (Zheng et al., 2006; Usta et al., 2014). The FCS was diluted to 10% as this the percentage used in DMEM+ during cell culture experiments.

### 5.3.2 Protein Attachment

00.5g of each of the materials investigated were immersed in 2mls of 10% FCS (Thermofisher™, UK) in a petri dish (Corning, USA) and shaken on an Orbital Oscillator (KJ-201BD) (Kangjian, China), while in a 37$^{o}$C incubator. These samples were shaken for 72 hours, 24 hours, 1 hour and 30 seconds.

### 5.3.3 Protein Detachment

Once the respective time-points had elapsed, the FCS was removed. The granules were gently washed in dH20 to remove excess FCS within the porous structure. The protein-coated BGS scaffolds were transferred to fresh well plates to eliminate any false readings due to protein attachment to the plate surface and not the granules.

Several methods of protein detachment were investigated in this study. The first method used 500µl of a 6M urea solution for 30 minutes as reported by Rashid et al., (2008).

However, this showed limited success; when these samples were run on SDS PAGE gels, only very faint bands were present, suggesting a limited amount of protein had been extracted from the material surface.

The second method investigated used a 10% SDS and water mixture (Wang et al., 2014; Rosengren et al., 2003). This technique resulted in more visible protein bands compared to the urea solution; however, after discussion with technical staff within University College London's Mass spectrometry (MS) unit, I was advised that this technique might damage the mass spectrometer.

Therefore, a third method investigated used a PBS solution prepared at pH 10. This detached the highest amount of protein samples surface compared to the other techniques. For all subsequent experiments, this method was used. The increased pH levels was done with the addition of NaOH and measured by Fisher Scientific Accumet AB15 pH mV Meter (Thermo Scientific, USA).

The protein-coated BGSs were immersed in 2 ml of PBS at pH 10 and then placed in an incubator at 37oC for 2 hours on an Orbital Oscillator (KJ-201BD) (Kangjian, China). The adhered proteins detach into solution at varying times depending on how tightly the proteins were bound (Fang et al., 2005).

The solution containing the detached proteins was used to measure total protein content, relative molecular mass, protein distribution among fractions, protein purity and the relative abundance of proteins present on the different scaffolds at each of the time-points.

### 5.3.4 Micro BCA Assay (Total Protein Content)

A micro BCA assay is a colourimetric detection and quantitation kit used to determine the total concentration of detached proteins from each BGS investigated. This experiment was repeated three times. Thermo Scientific™ Micro BCA™ Protein Assay Kit (product No, 23235) (Thermo Scientific, USA) was used. The Micro BCA assay measured protein concentration within the range of 0.5 µg/ml to 1.5 mg/ml.

#### 5.3.4.1 Preparation of Albumin Standards

Albumin (BSA) standards were prepared using the BSA standard ampule (2.0mg/ml), which was placed into an Eppendorf diluent in the sample buffer and final dilutions of 200ug/mL, 40ug/mL, 20ug/mL, 10ug/mL, 5ug/mL, 2.5ug/mL, 1ug/mL, 0.5ug/mL and 0ug/mL (Blank) were prepared. The Micro BCA working reagents were prepared by mixing 25 parts of Micro BCA regent A with 24 parts of Micro BCA reagent B with 1 part of Micro BCA reagent C. A 150µl of the sample being tested was mixed with 150µl of the working reagent in a microplate before being shaken for 30 seconds. The plate was incubated at 37oC for 2 hours before been placed into the Tecan spectrophotometer

(Tecan Trading AG, Switzerland) where it was shaken for 5 seconds before the absorbance was read at 562nm.

#### 5.3.5.1 SDS-PAGE

Protein analysis using SDS-PAGE gel electrophoresis is a standard method that elutes recovers and separates proteins (Kurien et al., 2012). The gel used allows small proteins to move through its matrix faster than larger proteins where less migration is seen. Protein structure and charge are also known to affect the mobility of proteins through the gel.

The SDS-PAGE gels were made of two components: (a) a separating gel and (b) a stacking gel. Altering the percentage of acrylamide present within the separating gel adjusted the size of pores present within the gel, which in turn controlled the physical separation of the proteins during electrophoresis. A 10% gel concentration was selected for use. Other percentage gels were investigated; however, 10% gel offered the best resolution of protein bands. **Table** 5.1 represents the reagents used.

**Table 5.1** Reagents used for 10mls of a 10% separating gel for SDS page gel.

| Regents | Supplier | Quantity |
|---|---|---|
| $H_2O$ | - | 3.8 ml |
| Acrylamide/Bis-acrylamide (30%/0.8w/v) | Bio-Rad, USA | 3.4 ml |
| 1.5 Tris (pH=8.8) | Thermo Scientific, USA | 2.6 ml |
| 10% (w/v) SDS | Thermo Scientific, USA | 0.1 ml |
| 10% (w/v) ammonium persulfate (AP) | Thermo Scientific, USA | 100ul |
| TEMED | Thermo Scientific, USA | 10ul |

A stacking gel was used to improve protein resolution before electrophoresis and concentrate the proteins before entering the separating gel. **Table** 5.2 represents the regents used for Stacking gels. Before pouring the stacking gel on top of the separating gel, a comb was placed to form the sample wells and allowed to set.

**Table 5. 2** Reagents for the 5ml of Stacking gel for SDS page gel.

| Regents | Supplier | Quantity |
|---|---|---|
| $H_2O$ | - | 2.975 ml |
| 0.5 M Tris-HC, pH 6.8 | Bio-Rad, USA | 1.25 ml |
| Acrylamide/Bis-acrylamide (30%/0.8w/v) | Thermo Scientific, USA | 0.05 ml |
| 10% (w/v) ammonium persulfate (AP) | Thermo Scientific, USA | 0.67 ml |
| 10% (w/v) SDS | Thermo Scientific, USA | 0.05 ml |
| TEMED | Thermo Scientific, USA | 0.005 ml |

15µl of each of the protein samples was combined with 5µl of loading dye (Thermo Fisher Scientific™, USA) and heated to 60ºC for 3 minutes to denature the proteins.
15µl of the denatured protein samples were then loaded into the wells. The first lane of each gel was used for the protein standard ladder (Thermo Fisher Scientific™, USA). An electrical field of 120V was used to push the proteins through the gel, which was run until the protein marker dye reached the end of the gel.

#### 5.3.5.2 SDS-PAGE Gel Staining

InstantBlue™ (Expedeon Ltd, UK), a ready-to-use Coomassie protein stain was used where staining occurring within 15 minutes without the need for fixing, washing, and destaining. Once electrophoresis was performed, the gel was then placed in 20 ml of the InstantBlue™ staining solution. The bands were visible within 15 minutes at room temperature with gentle shaking.

#### 5.3.5.3 Analysis of InstantBlue™ Stained SDS-PAGE Gels

Once stained, each gel was imaged using a ChemoDoc™ XRS+ system (Biorad, U.S.A). The images where taken and analysed using ImageLab™; (version 5.2.1 build 11; Bio-Rad, U.S.A).

### 5.3.6 Statistics Analysis

Normality was checked using the Kolmogorov- Smirnov and Shapiro Wilkinson test. If data was normal, the comparison was made using an independent student T-test. For non-parametric data, comparison was made using the Mann Whitney U test with a Bonferroni correction. Pearson correlation was calculated using GraphPad. The data analysed was performed using SPSS version 24 (Chicago, USA). Figures were made using GraphPad Prism version 7.0.0 (San Diego, USA). These experiments were run in $n$=3 where there 3 repeats of each unless stated otherwise.

## 5.4 Results

### 5.4.1 Micro Bicinchoninic Acid Assay (Micro BCA Assay)

The BCA assay results showed that Orthoss® had the highest total protein concentration at all time-points investigated (**Figure** 5.1).

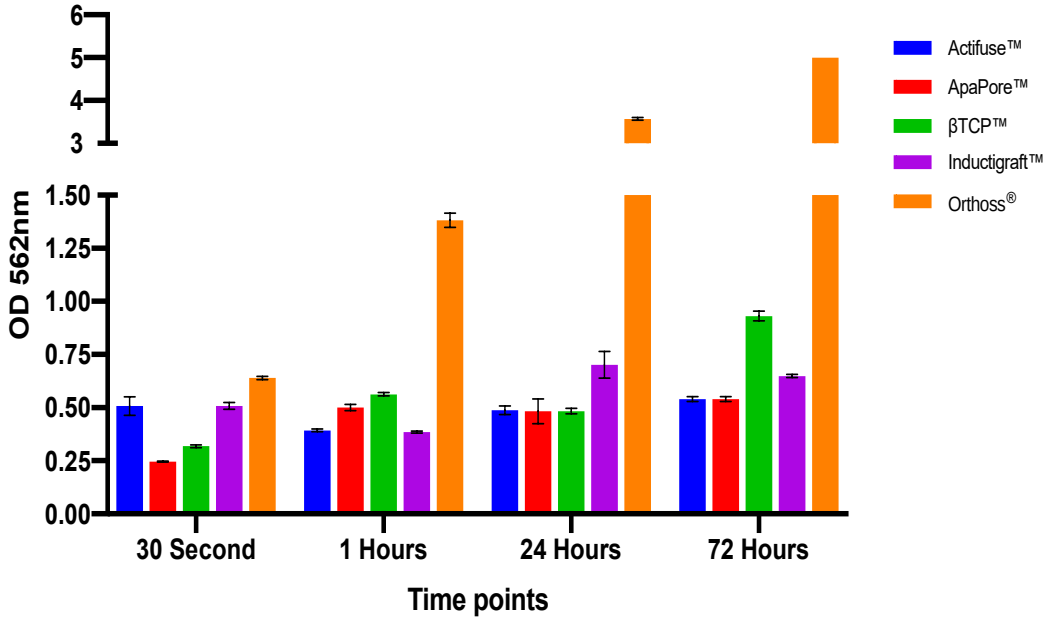


**Figure 5.1 Comparison of protein concentration removed from BGS surfaces.** Measured by BCA assays results (*n*=3). Orthoss® at 72 hours had the highest protein levels while the lowest was 30 seconds, in ApaPore™. The error bars represent the standard error of the mean.

At the 30 seconds, the highest amount of total protein measured was Orthoss® (0.63 µg/ml (±0.008)) with significantly more protein when compared with all other samples investigated ($p < 0.001$ in all cases) (**Figure** 5.1). Both Actifuse™ and Inductigraft™ had similar protein levels with no significant differences between them. There were significantly lower protein levels on ApaPore™ (0.25 µg/ml (±0.030)) when compared to all other groups except for β-TCP ($p = 0.495$).

At 1 hour, Orthoss® showed a significantly increased protein levels compared to 30 seconds of 117.46% ($p < 0.001$). β-TCP™ also had a significant increase of 75% to 0.56 (±0.024) ($p < 0.001$). There was a significantly decrease in proteins levels on Inductigraft™ group compared with all other groups except Actifuse™ (ApaPore™ $p = 0.008$; β-TCP™ $p < 0.001$; Orthoss® $p < 0.001$).

At 24 hours, Orthoss® had a significant increase of 158.39% ($p < 0.001$). Inductigraft™ had significantly higher ($p<0.001$) protein levels compared to β-TCP™ (219 µg/ml (±0.060)) and ApaPore™ (0.218 µg/ml (±0.060)). However, Inductigraft™ was not

significantly higher compared to Actifuse™ ($p$=0.052) with a difference of 0.214 µg/ml (±0.060).

Again, at 72hours Orthoss® had significantly higher protein levels when compared to all other grafts ($p$ < 0.001). The levels of proteins detached from Orthoss® reached the maximum optical density reading on the Tecan spectrophotometer (Tecan Trading AG, Switzerland) of 5ug/ml. Inductigraft™ had a significant decrease in protein levels of 7.15% but remained significantly higher than Actifuse™ ($p$=0.01), with different protein levels of 0.108µg/ml.

### 5.4.2 Comparison of proteins overtime on each surface

The comparison of protein adsorption onto the Actifuse™ surface showed an initial decrease in protein adsorption, which was not significant between 30 seconds and 1 hour ($p$ = 0.068). By 24 hours, there was a non-significant increase in protein levels ($p$ = 1.0). A further non-significant increase was noted at 72 hours ($p$ = 1.0). There was a significant change measured between 30 seconds and 72 hours ($p$ = 0.001).

ApaPore™ showed a significant increase after 1 hour, compared to the initial 30 seconds time point ($p$ = 0.02). 24 hours post-immersion, there was a non-significant decrease in amounts ($p$=1.0). Then a non-significant increase was noted between 24 hours and 72hours ($p$=1.0). There was a significant change measured between 30 seconds and 72 hours ($p$ = 0.001).

A significant increase between 30 seconds and 1 hour was noted on β-TCP™ ($p$ = 0.0001). By 24 hours there was a significantly decreased in protein levels from the 1-hour ($p$ = 0.023); however, levels significantly increased to its highest amount at 72 hours post-immersion ($p$=0.001). There was a significant change measured between 30 seconds and 72 hours ($p$ = 0.001).

Inductigraft™ results indicated a non-significant decrease in protein levels between 30 seconds and 1 hour ($p$=0.165). Followed by a significant increase in protein levels at 24 hours to 0.70 µg/ml (p=0.01), (0.317 (± 0.046)). There was a non-significant decrease by 72 hours ($p$ = 1.0). There was a significant change measured between 30 seconds and 72 hours ($p$ = 0.001).

The Orthoss® group demonstrated, significantly increased protein levels at each of the time points investigated. The results showed that protein levels doubled between 30 seconds and 1 hour (p=0.001). This trend continued at 24 hours (p=0.001) and 72 hours (p < 0.001).

### 5.4.3 SDS PAGE Gel

#### 5.4.3.1 SDS PAGE Gel: Actifuse™

Bands of proteins can be observed between 55kDa and 150kDa (**Figure** 5.2). A smearing of protein was present in the 30 seconds, 24 hours and 72 hours time points. A band was present at approximately 55kDa in all samples; however; it was less prominent at the 1-hour time-point. There are two visual protein bands at between 55kDa and 70kDa in the 30 seconds, 24 hours and 72 hours lanes. There is also a single band between 70kDa and 100kDa in 30 seconds, 24 hours and 72 hours. There are also several other fainter bands present of lower molecular mass identified in the 30-second lane.

There is an apparent visual decrease of bands presented between 30 seconds and 1 hour before rising again by 24 hours. A predominately-thick band is possibly the well-characterised serum albumin at 66kDa. (The band showed slightly below the 55kDa marker; this was due to the alignment of the molecular weight ladder and lanes of samples that appears to be slightly off).

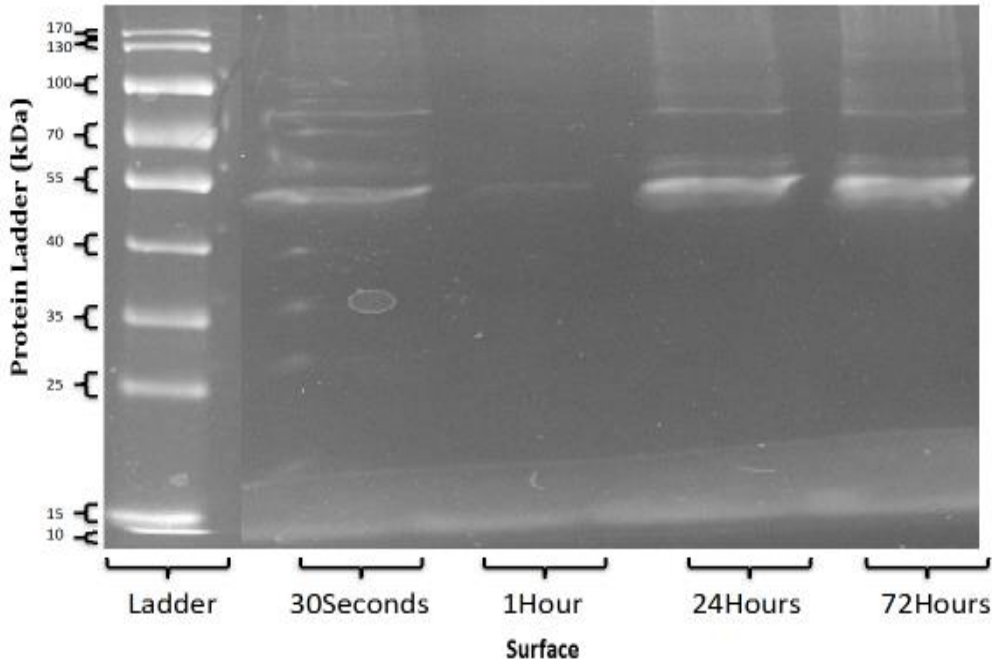


**Figure 5.2 SDS-PAGE gel of protein isolated from Actifuse™.** FCS proteins detached from the BGS surface after submersion for 30 seconds; 1 hour; 24 hours and 72 hours. Proteins stained using InstantBlue™ (Expedeon, U.S.A). Imaging performed using ChemoDoc™ XRS+ system (Biorad, U.S.A). The molecular weights ladder is shown on the left.

### 5.4.3.2 SDS PAGE Gel: ApaPore™

This SDS-PAGE gel (**Figure** 5.3) showed smearing of bands particularly at the 1, 24 and 72-hour time points and between 170kDa and 130kDa. Distinct protein bands are not identified at the 30-second time point in this group. There is no visible band where a band is expected to represent serum albumin. This should be at 66kDa. Samples in this group produced the lowest amount of visible protein bands compared to all other BGS's. There are a few possible reasons for this, including the amount of protein may be of a concentration that is too low to form a band. Another possibility could be due to the degradation of the proteins before running on the gel. However, the low levels of proteins do correlate with the results was seen in the BCA assay that also showed ApaPore™ having low levels of proteins.

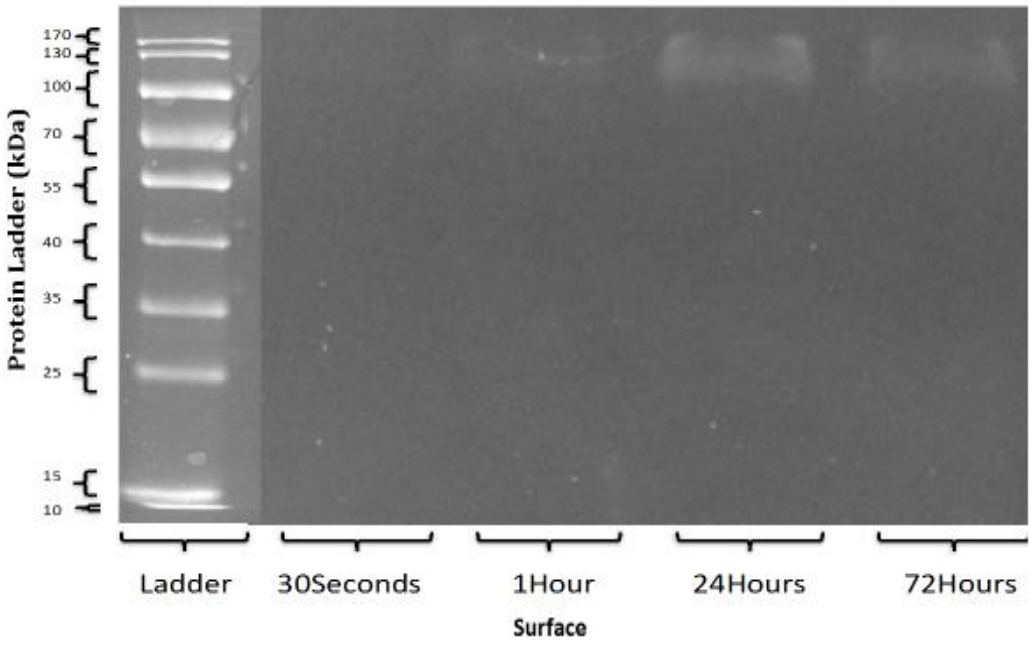


**Figure 5.3 SDS-PAGE gel of protein isolated from ApaPore™.** FCS proteins detached from the BGS surface after submersion for 30 seconds; 1 hour; 24 hours and 72 hours. Proteins stained using InstantBlue™ (Expedeon, U.S.A). Imaging performed using ChemoDoc™ XRS+ system (Biorad, U.S.A). The molecular weights ladder is shown on the left.

### 5.4.3.3 SDS PAGE Gel: β-TCP™

The β-TCP™ gel showed intensely stained bands at the 72-hour time point (**Figure** 5.4). These bands began above the top of the ladder, and their increased intensity indicated an increased quantity of proteins when compared to other time-points. At each of the time points investigated except for the 30-second lane, a smearing of proteins was seen at approximately 55kDa indicating high amounts of protein present. The dominant thick band at 66kDa could be serum albumin and is well resolved. This band at 72 hours is brighter than the other times as it may have the highest levels of serum albumin. At 30seconds, there was a very faint band representing a low amount of serum albumin present. Defined protein bands were also observed at the 100kDa and 130kDa markers.

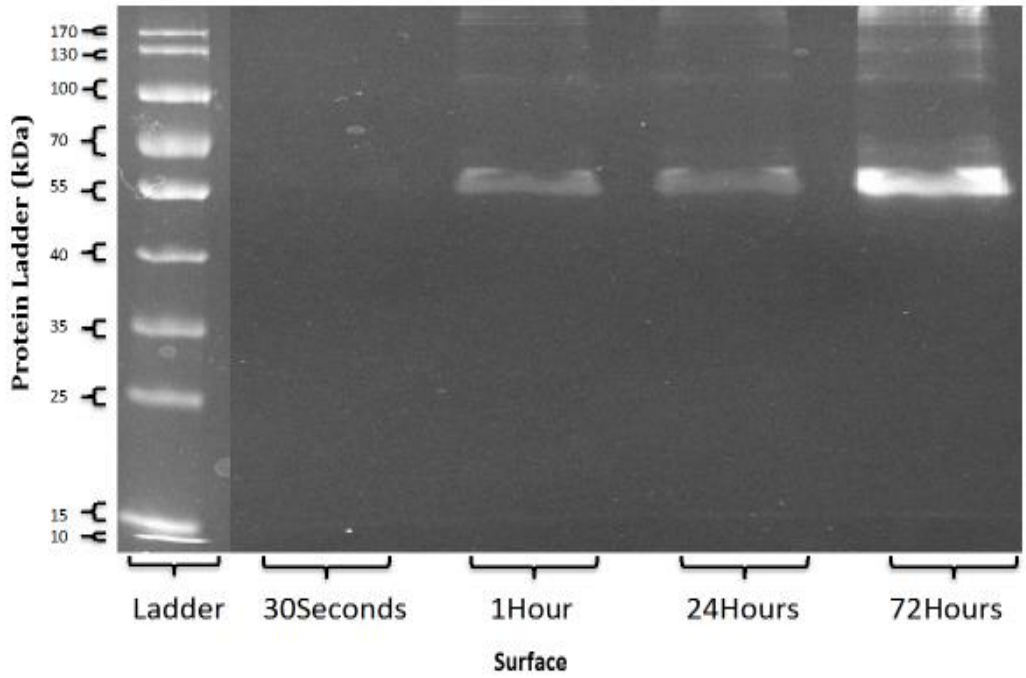


**Figure 5.4 SDS-PAGE gel of protein isolated from β-TCP™.** FCS proteins detached from the BGS surface after submersion for 30 seconds; 1 hour; 24 hours and 72 hours. Proteins stained using InstantBlue™ (Expedeon, U.S.A). Imaging performed using ChemoDoc™ XRS+ system (Biorad, U.S.A). The molecular weights ladder is shown on the left.

#### 5.4.3.4 SDS PAGE Gel: Inductigraft™

Inductigraft™ appeared to have the most amounts of visual protein bands when compared to other BGS's (**Figure** 5.5). Four bands can be seen between 55kDa and 100kDa and at all-time points, and these bands increased in intensity with time. As time increased, the presence of more faint bands became apparent between 55kDa to 170kDa and with bands that appeared above the 170kDa ladder. A thick band represents the serum albumin at 66kDa; however, the band is shown slightly below the 55kDa marker, this is due to the alignment of the molecular weight ladder to the sample lanes was slightly off similar to the Actifuse™ SDS PAGE gel. The amount of serum albumin appears to increase at each time point; this was identified by the growing intensity of the bands at the later time points.

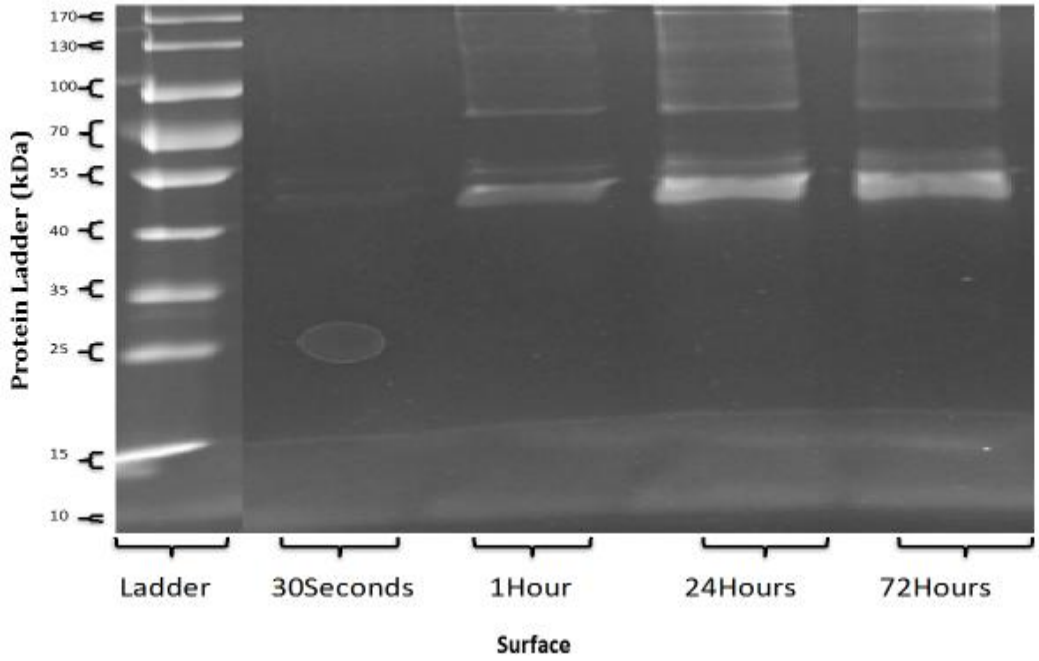


**Figure 5.5 SDS-PAGE gel of protein isolated from Inductigraft™.** FCS proteins detached from the BGS surface after submersion for 30 seconds; 1 hour; 24 hours and 72 hours. Proteins stained using InstantBlue™ (Expedeon, U.S.A). Imaging performed using ChemoDoc™ XRS+ system (Biorad, U.S.A). The molecular weights ladder is shown on the left.

### 5.4.3.5 SDS PAGE Gel: Orthoss®

In this group, as time increased, the number of protein bands increased in amount and their intensity (**Figure** 5.6). The majority of the proteins present were between 55kDa and 170kDa. However, at 24 and 72 hours, several bands that represented proteins of lower molecular mass had appeared, and these were not evident at 30 seconds and 1 hour. Fourteen visible bands were present at 72 hours, representing more protein bands compared to other BGSs investigated. The amount of serum albumin (66kDa) increased with time and 72 hours having the highest amount of all time points; while the lowest band intensity was noted at 30 seconds. This correlates with the BCA assay, which showed it had the highest amount of protein at each time point.

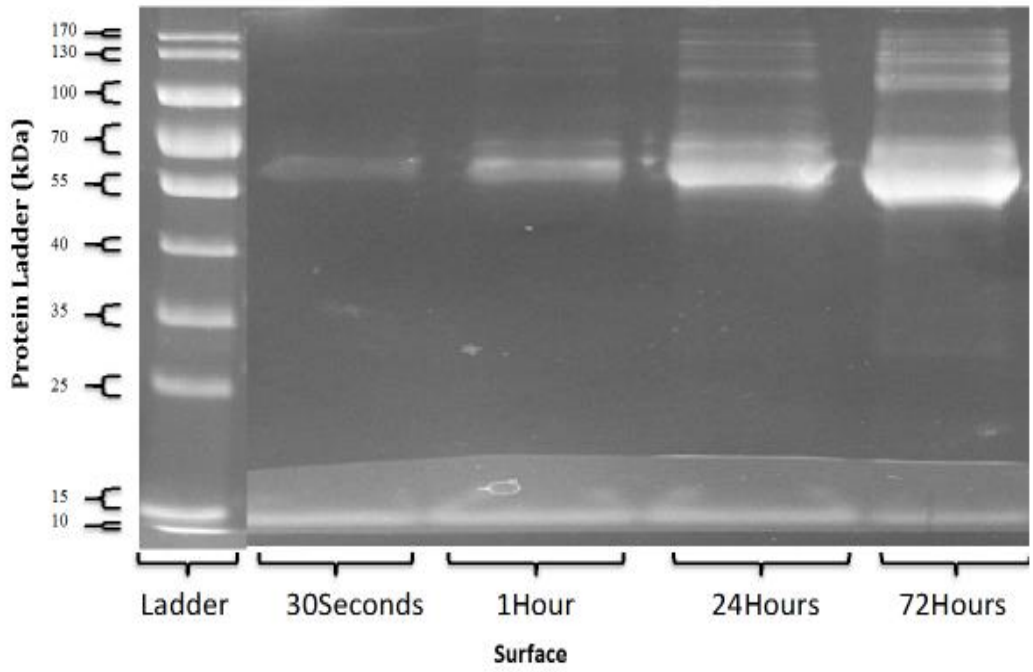


**Figure 5.6. SDS-PAGE gel of protein isolated from Orthoss®.** FCS proteins detached from the BGS surface after submersion for 30 seconds; 1 hour; 24 hours and 72 hours. Proteins stained using InstantBlue™ (Expedeon, U.S.A). Imaging performed using ChemoDoc™ XRS+ system (Biorad, U.S.A). The molecular weights ladder is shown on the left.

## 5.5 Discussion

The adsorption of proteins to the BGS surface is considered to be one of the primary factors in influencing the amount and type of cellular interaction that will occur between the implant and host (Hayes et al., 2012; Botelho et al., 2006; Deligianni et al., 2000; Anderson et al., 2008; Keselwsky et al., 2005). Deligianni et al., (2000) suggested protein and cellular responses to the implant are reliant on the composition of both physical and chemical characteristics of the BGS, particularly the chemical composition. Within seconds of submerging an implant into biological fluid, proteins will absorb to the implant surfaces. This is the first critical step within the sequential biological events that will occur, and this is why it may play a significant role in affecting the microenvironment surrounding the BGS. Differences in BGS surfaces can affect the interactions with proteins, and it is this interaction, which can control cellular functions and their subsequent functions (Alves et al., 2010). Surface engineering of BGSs aims to mimic the natural bone topography, and as a result, the molecular mechanisms that cause the adsorption of proteins onto the graft surface (Nath et al., 2004). By regulating the proteins that adhere to a scaffold surface, it may be possible to influence the different cellular interactions and subsequent bone formation (Norde et al., 1992; Combes et al., 2002). Nath et al. (2004) suggests the surface could potentially be engineered to resist unwanted protein attachment and tailor the implant to control interactions and increase biocompatibility.

In 1969, Brash and Lysman were able to demonstrate that the amount of protein adsorption to a surface correlates in direct proportion to the concentration of proteins in the solution. The cell integrin receptors react to the adsorbed proteins and are the mechanisms responsible for the bioactivity (Horbett, 2004). These proteins are continually being interchanged with proteins in a solution. This process is known as the “Vroman effect” (Vroman and Adams, 1986; Botelho et al., 2011). This effect is how proteins naturally compete to attract to a surface and is believed to be one of the underlying mechanisms that can trigger molecular cascades (Wang et al., 2012). Proteins with lower molecular affinity will adhere to the surface first before being replaced by higher molecular weight proteins (Wang et al., 2012).

The protein adsorption kinetics are time-dependent, this means that the first responding adhering proteins interact with the surface and the proteins which arrive later are influenced by the proteins that have already adhered to the surface (Fang et al., 2005). Hing et al., (2005) suggested that this competitive manner of protein adhesion to a BGS surface could be influenced by the quantity of proteins being adsorbed or by variation in the proteins that adhere and in their conformation.

By the time the cells arrive, the BGS surface is coated in a monolayer of proteins, and these cells do not directly “see” the BGS surface but instead “see” a layer of proteins to

which the cells attach (Schmidt et al., 2009). There have been a number of studies that have shown that the proteins which adhere to the surface of the implant has the ability to influence a response the subsequent adhering phenotypic cells and this influence may have the ability to initiate osteoinduction via an intracellular signalling cascade (Allen et al., 2006; Sawyer et al., 2014).

The different surface characteristics of the five BGSs investigated in this chapter is one of many factors known to be responsible for influencing the diversity of proteins that adhere to. These BGSs were submersed into FCS, and then the quantity of protein absorbance was assessed by micro BCA, SDS-PAGE gel electrophoresis was used to analyse distribution, purity and relative abundance of proteins.

### 5.5.1 Current knowledge of protein interaction with BGS.

The BGS surface interactions with proteins will be affected by both the physical and chemical properties of the grafts, which can be critical in influencing the response of the proteins in terms of quantity and diversity (Rosengren et al., 2002).

The chemical formula and surface topography of the BGS's and the amount of proteins in the surrounding fluid and tissues are all critical in determining the amount of proteins that will adhere to the implant (Guth et al., 2010; Fang et al., 2005: Thevenot et al., 2011).

Wang et al., (2012) proposed hydrophobicity, ions and surface charge will also influence protein absorbance and these levels of protein adsorption were affected by the release of ions into the surrounding area, which has been reported to be controlled by the BGS surface charge.

Bajpai et al., (2007) discussed how the majority of studies that investigations into protein and implant surface interactions in terms of electrostatic and van der Waals interactions will focus on surface charge, protein size and solution ionic strength. However, there is a correlation between protein adsorption and the concentration of proteins in the solution should take into consideration adsorption isotherm and Langmuir equations due to the lower complexity and broader applicability to the different adsorption data (Baipai et al., 2007).

The addition of silicate to the HA lattice will influence a combination of the above factors (Guth et al., 2010). They showed that the cellular adhesion is sensitive to the protein layer that develops on the discs and that there is a difference in the protein layers of HA and SiHA with enhanced cellular attachment on the latter. They believe this is because of the presence of Si on the apatite surface; however, they suggest it is more likely related to a presence of a counterbalancing ions associated with a difference in a surface charged with increased hydrophilicity. In further studies, they commented on significantly higher levels of co-localization actin and integrin in cells that were adhered to SA discs and not on HA discs. They believe that this occurs on SiHA via a separate mechanism

to HA and the higher levels of integrin may cause higher levels of enhanced osteoblastic cellular attachment and development.

During protein adherence studies, the competitive manner that this occurs in have shown that surface topographies negate any effect physicochemistry has on this matter, but both micro and nano topographies could be more influential (Hing et al., 2005; Guth et al., 2010). Rashid et al., (2008), the study used discs of SiHA and HA-coated in proteins using a 10% FCS for 10 minutes, 2, 4, 8, 12 and 24 hours then removed the attached proteins using a 6M Urea. They demonstrated increased the level of protein adherence to SiHA during compared to an HA BGS and during *in vitro* studies, this lead to increased cellular attachment, proliferation, and differentiation.

### 5.5.2 Attaching and Detaching Proteins off BGS surfaces

Once the granules reached their respective time points, the adhered proteins needed to be detached from the surface. Several different methods were assessed, including a 10% SDS solution, Urea, and pH10 PBS solution. After discussions with MS technical staff, they felt confident that the PBS solution would not damage the MS machines.

### 5.5.3 BCA assay

The colourimetric changes of the micro BCA assay showed visual colour changes in each of the groups and indicated low protein (Green) and high protein amounts (dark purple). Once the micro BCA analysis was performed, it showed that at 30 seconds and 1 hour, both Actifuse™ and Inductigraft™ had similar protein levels, and both showed significantly higher levels when compared with ApaPore™ and β-TCP™. These results are similar to those of Guth et al., (2010), who reported that silicate-substituted HA (as in Actifuse™ and Inductigraft™) have the potential to attract proteins in a combination of factors associated with the addition of silicate, that includes on its surface and the ionic charges at the interface. Guth et al. (2010) removed all topographical features similar to the experiments in chapter 4 and to investigate whether the chemistry alone could affect protein absorbance. They do note that total protein adsorption at early time points is not found to be a good indicator of the graft's potential overall performance (Guth et al., 2010).

Protein levels of both ApaPore™ and β-TCP™ increased at the latter two-time points compared to the levels on the silicate-substituted HA BGS and at 72 hours, the β-TCP™ had the second-highest protein levels behind Orthoss®.

Orthoss® had significant ($p$=0.0001) higher levels compared to all other BGS at all time-points. At 72 hours, Inductigraft™ had higher protein compared to Actifuse™. This increased protein levels on Inductigraft™ BGS could be due to the increased strut porosity that leads to higher surface area, in turn, enabling more proteins to adhere to its surface (Coathup et al., 2012).

A Pearson correlation test of the surface area of the BGS explored in Chapter 2 was then compared to the results of the BCA assay at 72 hours gave a Pearson R = 0.6414. This means that there is a positive correlation between the surface area available and the amount of protein adhering.

### 5.5.4 Increased amounts of proteins on Orthoss®

Orthoss® had the highest protein levels at each time-point. In Tseng et al., (2013) study, one of their aims was to investigate the adsorption of proteins to BGS's of which Orthoss® was one. They measured the influence that extracellular matrix (ECM) proteins have on the adhesion of osteogenic cells by measuring the viability of the adhering cells. Extra ECM proteins (fibronectin, vitronectin, and type I collagen) were added to the FCS solution, and the BGS was a condition in for 12 hours before cell seeding. They measured cell viability using water-soluble tetrazolium salt-1 dye (Tseng et al., 2013). Their results indicated that coating BGS in ECM proteins would increase cell attachment *in vitro* (Tseng et al., 2013). This appears not to be the same in my study as my results indicated that Orthoss® had the highest concentration of protein attachment at each of the time points investigated. This could be related to the surface area calculation discussed in Chapter 2 of which Orthoss® had the highest percentage area of all five grafts. This is also noted in the Pearson correlation discussed in the above section.

### 5.5.5 SDS page

Noh et al., (2006) states that the standard method to measure multi-protein adsorption is by using SDS-PAGE gel as it an excellent for both separation and quantification of proteins. They were able to observe adsorption behaviours of proteins and the effects this adsorption has on proteins kinetics. They also observed the Vroman effect believing it not to occur due to biochemistry or protein adsorption kinetics but actually due to a physical process.

The proteins were separated using SDS-PAGE gel, enabling the relative abundance and the purity of those proteins detached. The SDS-PAGE gels allowed for a comparison to the BCA assays results. In all the SDS-PAGE gels, there may be proteins presents; however; the amount of protein was too low in quantity to form a visible band and could be identified using mass spectrometry. The higher BCA assay results corresponded to increased numbers of protein bands and higher intensities in the SDS-PAGE gels. The serum albumin protein was used as an example of a well-characterised protein and one of the most abundant proteins, which causes a thick band at approximately 66kDa. Serum albumin functions include transport of hormones, fatty acids, and various compounds through the bloodstream.

ApaPore™ sample that had the lowest overall micro BCA assay levels also had the lowest amount of visible bands in its SDS-PAGE gel. This was evident with the lack of serum albumin bands, which appeared in all other samples. The lack of these serum albumin bands could be due to the possible degrading of the band or the low quantity of this protein to form the visible band.

In comparison, the Orthoss® SDS-PAGE gel had the highest BCA assays readings and had the highest levels of visible protein bands in its gel and the most intense band represented by serum albumin at 72 hours.

The results of this chapter showed that proteins are adhering to all surfaces. Variation in proteins depends on the graft being investigated and how the length of time it was submerged in FCS. The next chapter hopes to identify which proteins are adhering to the different materials and their relative amounts.

### 5.5.6 Limitations

A limitation of this study is that *in vivo* environments will attract different proteins that are not fully comparable to the *in vitro* environment. Different serum concentrations may give a different protein profile. There are also issues about protein conservation between two different species. FCS was used because this serum is most commonly used in cell culture experiments and previous studies investigating BGS, and ovine cells used it as a component of DMEM media (Samizadeh, 2010).

## 5.6 Conclusions

This chapter investigated the protein levels of the five BGS at four-time points. The adherence of proteins to an implant is one of the first events to occur once it is submerged into biological fluids. These proteins can influence the success of the graft, and the profile of these adhered proteins will change over time may be due to the influence of the Vroman effect. This was demonstrated by the amount of protein attached to each of the BGS measured by micro BCA assay and physically separate the attached proteins using SDS-PAGE gel. The results indicated that the highest levels of proteins were on the Orthoss® BGS, which was not expected based on its performance in both Chapters 2 and 3. However, the Pearson correlation between the surface area available and the amount of protein adhering to the BGS surface showed a positive correlation.

Previous studies have shown that BGS that have been developed by HA will attract lower proteins amounts compared to graft developed from SiHA. This was demonstrated here with ApaPore™ an HA material having lower protein adherence compared to both SiHA materials Actifuse™ and Inductigraft™.

The surface area is also an essential factor and Actifuse™, which has a lower strut porosity/surface area, had lower protein amounts compared to Inductigraft™, especially at 24 hours. The combination of surface area and chemistry, leading to increased protein

amount adhered could potentially be why there is a higher cellular response from Inductigraft™ during the *in vivo* experiments in Chapter 2.

# Chapter 6

# The Identification of Proteins Detached from the Bone Graft Materials Surfaces by Mass Spectrometry.

## 6.1 Introduction

It has been long accepted that proteins mediate the biological response to the implants and affect the behaviour of cells (Amini et al., 2013; Schmidt et al., 2009). The proteins that adhered may potentially promote bone healing by mediating cellular recruitment, attachment performance and differentiation (Hing et al., 2004; Guth et al., 2010).

This chapter focus on the identification of the proteins detached from the surfaces of the graft during Chapter 5. The relative quantity of the detached proteins was assessed at four time-points. Different methods of protein isolation and Mass Spectrometry (MS) was compared, and the final experiments were conducted using Tandem Mass Tags™ (TMT™) (Thermo Fisher Scientific Inc., UK) and LC-MS/MS. The proteins identified were subsequently ranked on their potential to influence a multitude of factors, including cellular attachment and osteoinduction. The top five ranking proteins were further investigated to find which had the potential to increase the bioactivity of BGS when coated onto the surface before cell seeding *in vitro*.

## 6.2 Aims and Hypothesis

### 6.2.1 Aims

The main aim of this study was to identify the proteins that were detached from the surfaces of the five different BGS materials in Chapter 5. This required optimising the method of isolating proteins using MSCs. The relative amounts of proteins adhering to the grafts over time will be investigated to show the dynamic interchange of proteins. This will illustrate the attachment and detachment of proteins from the surface over time, showing a possible Vroman effect.

Once the proteins are identified, they will be investigated for their potential to impact cellular attachment and osteoinduction of MSCs. The top five ranking proteins will be investigated further, with the two proteins judged to have the potential to increase the BGS performance selected for *In vitro* experiments in Chapter 7.

### 6.2.2 Hypothesis

There will be differences in the proteins and their relative quantities that adhere to different surfaces. The highest number of proteins found on the Si substituted BGS.

### 6.2.3 Objectives

1. Evaluate different methods of protein isolation for MS analysis.
2. Identify the detached proteins using M/S analysis.
3. Rank the identified proteins by their potential to affect cells grown on the BGS surface.
4. Demonstrate that the profile of absorbed proteins changes over time, illustrating the Vroman effect.

## 6.3 Materials and Methods

### 6.3.1 Study Design

This study was designed to identify the proteins that were detached from the five different BGS investigated in previous chapters, after the grafts were submerged in FCS for 30 seconds, 1, 24 and 72 hours. Proteins were isolated for identification; three different techniques were compared using MS (*n*=1).

The optimal MS technique selected to measure protein was Tandem Mass Tags™ (TMT™) paired with liquid chromatography (LC-MS/MS; *n*=2). The MS identified proteins were then ranked using different online resources that calculate the protein's influence on cellular attachment and osteoinduction.

### 6.3.2 Protein attachment to and detachment from the BGS surfaces,

Protein attachment to the BGS was performed as in **Section** 5.3.2. Detachment was performed as in **Section** 5.3.3

### 6.3.3 SDS-PAGE Gels.

The SDS-PAGE Gels made, run and stained as performed **Sections** 5.3.5.1 and 5.3.5.3.

### 6.3.4 In-Gel Tryptic Digestion and Mass Spectrometry.

The extraction of the separated proteins from the SDS-PAGE gels was completed using an In-gel tryptic digestion kit (89871) (Thermo Fisher Scientific Inc., UK). The first step included excising the protein bands from the gel, and it was reduced in size, before then being placed into an alkylation buffer before been shrunk again by acetonitrile. The shrunken sample was placed into 37$^{o}$C-activated Trypsin (10µl) to digest the protein into peptides overnight. Then it was placed into a 1% formic acid solution for 5 minutes to extract the peptides before digestion buffer was added to stop the enzymatic reaction.

This sample was transferred to UCL's School of Pharmacy where MS technical staff used a Thermo LCQ Duo Mass Spectrometer coupled with an LC system to produce raw data, which was submitted to the online Mascot database (www.matrixscience.com; Matrix Science Ltd, UK) to identify the proteins. The search terms used can be found in **Table** 6.1.

**Table 6. 1** Search terms used for In-Gel Tryptic Digestion.

| Field | Selected |
|---|---|
| Taxonomy Filter | Mammals |
| Enzyme | Trypsin |
| Quantitation method | None |
| Variable Modifications | Carbamidomethyl (C), Oxidation (M) |
| Peptide Mass Tolerance | 1.2 |
| Peptide Mass Tolerance Units | Da |
| Fragment Mass Tolerance | 0.6 |
| Fragment Mass Tolerance Units | Da |
| Mass values | Monoisotopic |
| Instrument type | ESI-QUAD-TOF |
| Isotope error mode | 0 |

### 6.3.5 In-Solution Digestion

A new protocol was developed involving in-solution separation and digestion of the detached proteins based on previous work by Zheng et al., (2006). Sized spin columns separated and produced batches of proteins within a specific size for MS. This involved placing the detach protein solution into Spin-X columns (with a Cut-off 10kDa) (Sigma-Aldrich, UK) and centrifuged for 30 minutes at 4ºC (13000xg). A 100µl of protein mixture (>10KDa) was added to 500µl Dithriothreitol (4mM) and incubated for a further 30 minutes at 60ºC. Then 500µl Iodoacetamide (20mM) was added and allowed to react at room temperature for 1 hour. Protein precipitation was performed using 1000µl of 100% ethanol for 20 hours at 4ºC before being centrifuged for another 30 minutes at 13000xg, at 4ºC. Over 3-hours, SpeedVac removed any remaining liquid. The proteins were broken down into peptides by incubating them in 1000µl Ammonium Bicarbonate buffer (0.1 M, pH 8.2) containing 0.2mg trypsin incubated for 37ºC for 24 hours before a final SpeedVac evaporation for a further 3 hours.

These samples were again sent for LC/MS at Mass Spectrometry Laboratory at UCL School of Pharmacy, where the technical staff executed the same MS experiment as completed in **section** 6.3.4. However, after one run of this MS experiment, the MS machine used above became unusable due to a mechanical issue, placing the machine beyond repair.

### 6.3.6 Tandem Mass Tags™ (TMT™) and LC-MS/MS

For these experiments, Tandem Mass Tags™ (TMT™) paired with liquid chromatography-tandem mass spectrometry (LC-MS/MS) was used. The CEMS Proteomics Facility, at Kings College London, Denmark Hill, was used.

#### 6.3.6.1 Sample Preparation of Tandem Mass Tagged Proteins

Once the proteins were detached from the BGS, the protein solution was stored at -20$^{o}$C and transferred to the CEMS Proteomics Facility. The technical staff preformed the Tandem Mass Tagging proteins as per the protocol. TMT10plex™ Isobaric Label Reagent Set (Catalogue number: 90110; Thermo Fisher Scientific Inc., UK) was used. 1ml of each of the protein solution sample was reduced to 200µl. Then the proteins were precipitated, washed and formed into a pellet before being solubilised in a dissolution buffer (1M triethylammonium bicarbonate) for TMT labelling.

#### 6.3.6.2 Enzymatic Digestion and Peptide Labelling

The newly solubilised proteins were modified and digested as follows. Tris (2-carboxyethyl) phosphine was used to reduce the Cysteine residues. This was then derivative-using iodoacetamide to create a stable form of Carbamidomethyl derivatives before the solution was digested by Trypsin overnight at 37$^{o}$C. The peptides were labelled with the appropriate TMT labels. The labelled peptides from each time-point from the same BGS were combined. The labelled peptides were purified and excess labels removed by solid-phase extraction, and the remaining purified labels were lyophilised.

#### 6.4.6.3 OFF-GEL Fractionation

The lyophilised peptides were reconstituted in an isoelectric focusing buffer, and the peptides were then resolved using isoelectric point on immobilised pH3-10 gradient strip. This generated five fractions for each of the BGS. A portion of each fraction was purified using both Ziptips (Merck, German) and lyophilised.

### 6.4.8 LC-MS/MS

The fractionated peptides were each reconstituted using ammonium bicarbonate and then loaded into LC-MS/MS analysis. The chromatographic separations were performed using the EASY NanoLC system (Thermo Fisher Scientific, UK). The peptides were resolved by reversed-phase chromatography on a 75µm C18 PepMap column. A three-step linear gradient of acetonitrile in 0.1% formic acid was used and added to the eluted protein at a flow rate of 300nL/min over 120 minutes.

The eluted solution was ionised by electrospray ionisation using the Orbitrap Velos Pro (Thermo Fisher Scientific Inc., UK) that was operated under Xcalibur v2.2 software (Thermo Fisher Scientific Inc., UK). The instrument was run in an automated data-

dependent switching mode, selecting precursor ions based on their intensity for sequencing by higher energy collision-induced fragmentation using a Top 10 method. MS/MS analyses were performed using the collision energy profiles, chosen based on the mass-to-charge ratio (m/z) and the charge state of the peptide. There were two separate runs performed at different times for each of the BGS materials, giving a total of *n*=2.

### 6.4.9 Database Searching

The raw data produced by the MS/MS was used to produced lists of proteins isolated from the BGS surfaces at different time points; two different databases were used. These were:

1. Proteome Discoverer Daemon (Thermo Fisher Scientific Inc., UK).
2. Proteome Discoverer 1.4 (Thermo Fisher Scientific Inc., UK).

Then the Mascot search algorithm version 2.2.06 (www.matrixscience.com) was used to search a 'Bos Taurus' protein database (6870 reviewed entries for 'Bos Taurus'; www.uniprot.com). A full list of the database setting is in **Table** 6.2.

**Table 6. 2** The setting used for the Mascot search database TMT.

| Field | Selected |
|---|---|
| Precursor Ion Mass Tolerance | 20ppm |
| Fragment Ion Mass Tolerance | 0.8Da |
| Digestion Enzyme | Trypsin |
| Allowance of Missed Cleavages. | 3 |
| Variable Modification | 3 missed cleavages |
| Fixed Modifications | Carbamidomethyl (Cysteine) |
| TMT | Lysine and N-terminus |

### 6.4.10 Ranking of Identified Proteins

The logic behind ranking the identified proteins came from different online databases. The proteins were given a score based on the potential influence they could have on MSCs. The basis for the score for each database can be found in the different tables below. All of the scores were combined for each protein and ranked from highest to lowest.

#### 6.4.10.1 Uniprot

Uniprot (www.uniprot.org) is a database that contains information derived from research literature. The scoring system represented in **Table** 6.3.

**Table 6. 3** Uniprot: The scoring system is associated with the Uniprot database**.**

| Option | Score |
|---|---|
| Yes | 10 |
| No | 0 |

#### 6.4.10.2 PathCards: Pathway unification Database

PathCards (www.pathcards.genecards.org) is a database of human biological pathways and their annotations. The scoring system represented in **Table** 6.4

**Table 6. 4** Pathway of interest using PathCards database.

| Option | Score |
|---|---|
| Yes | 10 |
| Possibly | 5 |
| No | 0 |

#### 6.4.10.3 OsteoChondroGene DB

OsteoChondroDB (www.itb.cnr.it/osteochondrogene/php/search_physio.php) is a database that facilitates the mining of mechanisms involved in bone tissues and cellular differentiation. The scoring was given depending on whether the protein is present in a pathway of interest; the scoring represented **Table** 6.5.

**Table 6. 5** Present of the gene using OsteoChondroGene DB.

| Option | Score |
|---|---|
| Yes | 10 |
| Possibly | 5 |
| No | 0 |

#### 6.4.10.4 Human Protein Atlas

Human Protein Atlas (www.proteinatlas.org) is an online database that will show the spatial distribution of proteins in human tissue. The scoring represented in **Table** 6.6.

**Table 6. 6** Human Protein Atlas scoring**.**

| Option | Score |
|---|---|
| High | 10 |
| Medium | 7 |
| Low | 3 |
| No result | 0 |

#### 6.4.10.5 Biograph.be

Biograph.be is a data mining database that will offer prioritisation of functional hypotheses where the lower the percentage, the more close the linkage to the function. This required investigating the proteins associated genes. Represented in **Table 6.7**, while the scoring system represented in **Table 6.8.**

**Table 6. 7** The functions investigated on Biograph.be

| Function |
|---|
| Osteoblast differentiation |
| Osteoblast proliferation |
| Regulation of cell differentiation |
| Cellular differentiation process |
| Prostheses and implant |
| Cell Adhesion |
| Bone Development |
| Response to protein stimulus |
| Osteoblast development |
| Positive regulation of cell-substrate adhesion |
| Positive regulation of cell differentiation |

**Table 6. 8** The scoring associated with Biograph.be database.

| Ranking | Score |
|---|---|
| ≤ 1% | 10 |
| 1≥2% | 7 |
| 2≥3% | 5 |
| 3≥5% | 3 |
| ≥5% | 0 |

#### 6.4.11 Heat maps

Heat maps were created using the Xlstat (Addinsoft, France) software. This was done using the relative percentage amounts of the proteins.

## 6.5 Results

### 6.5.1 Comparison of the Different Protein Sample Preparation and Mass Spectrometry

This experiment used the Orthoss® 72 hours (**Table** 6.9). The lowest amount of proteins identified was on the in-gel tryptic digestion method, which identified 8 proteins. In-Solution digestion was able to identify more proteins (30); however, there were 106 proteins identified using TMT.

**Table 6. 9** The number of proteins identified by the different protein samples preparation and the MS techniques.

| Mass Spectrometry Techniques | Number of Proteins Identified |
|---|---|
| In Gel Tryptic Digestion | 8 |
| In Solution Digestion | 30 |
| Tandem Mass Tags™ | 106 |

### 6.5.2 Relative Amount of Protein at Four Timepoints.

The TMTs were adhered to the proteins before MS/MS to detect proteins; this will produce high sensitivity and reduces the signalling noise. TMT labelling enabled quantitative and quantitative proteome analysis (Thompson et al., 2003).

The relative amount of each protein was calculated by comparing the peptide amount between the samples. **Figure 6.1** shows two separate runs were combined, and an average calculated.

The per cent fold change for all samples is represented in **Figure** 6.7. The fold change of each sample was calculated relative to the time point, which preceded it. This method was used for all subsequent analysis of proteins detached from the surfaces of BGS.

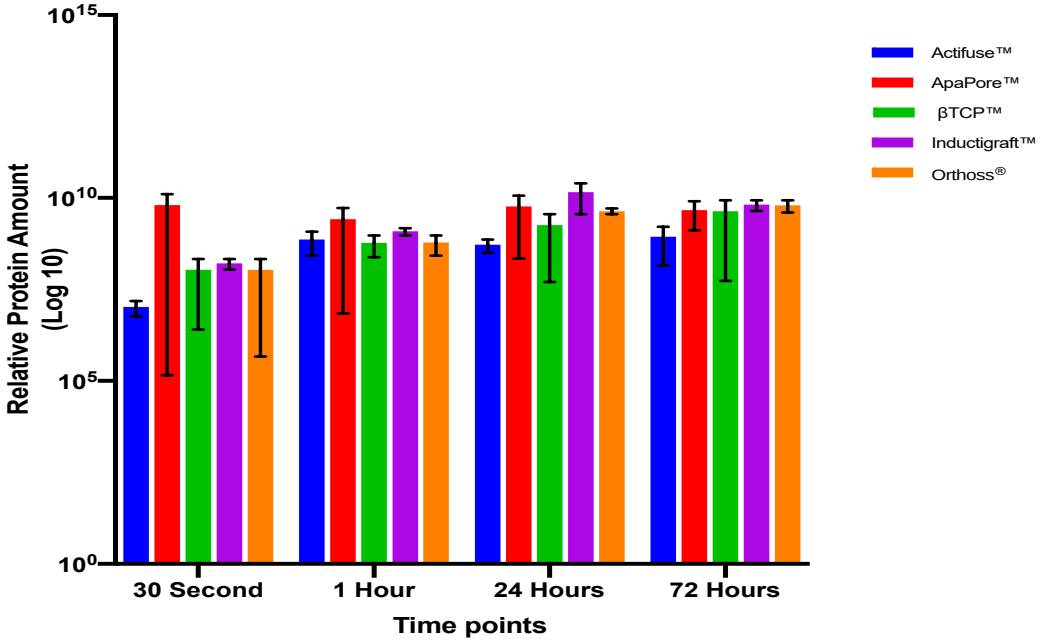


**Figure 6. 1 Relative protein amounts removed from BGS.** Performed by MS TMT labelling with LC/MS at four-time points (*n*=2). Relative protein amounts represented as Log10. Inductigraft™ at 24 hours the highest relative amount of protein. The lowest amount of protein was Actifuse™ (30seconds). The error bar represents the standard error of the mean.

### 6.5.2.1 Relative Amount of Proteins on Actifuse™ at Each Time Point.

The relative protein amount on Actifuse™ over the four-time points is represented in **Figur**e 6.2. Initially, at 30 seconds, the number of proteins was lowest before increasing by 6850.38% after 1 hour. There was a decrease at 24 hours (-27.87%) before rising again at 72 hours of 67.48%. The percentage increased for protein between 30 seconds and 72 hours was 8296%.

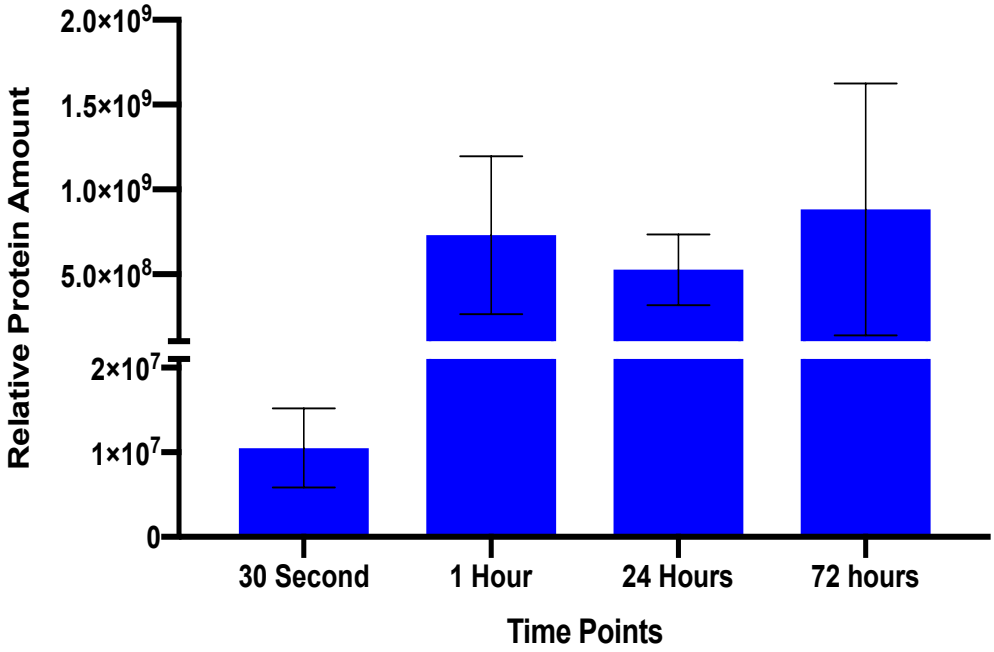


**Figure 6. 2 Relative protein amount on Actifuse™.** Four-time points were measured using TMT labelling with LC/MS (*n*=2). 72 hours had the highest relative amount while the lowest was at 30 seconds. The error bars represent standard error of the mean.

### 6.5.2.2 Relative Amount of Proteins on ApaPore™ at Each Time Point.

The relative protein amounts on ApaPore™ over the four-time points are shown in **Figure** 6.3. There was a decreasing of -58.38% by 1 hour from 30 seconds. There was then an increase at 24 hours of 122.28% before decreasing at 72 hours by -20.25%. There was a decreased in the protein levels between 30 seconds and 72 hours was -26.22%.

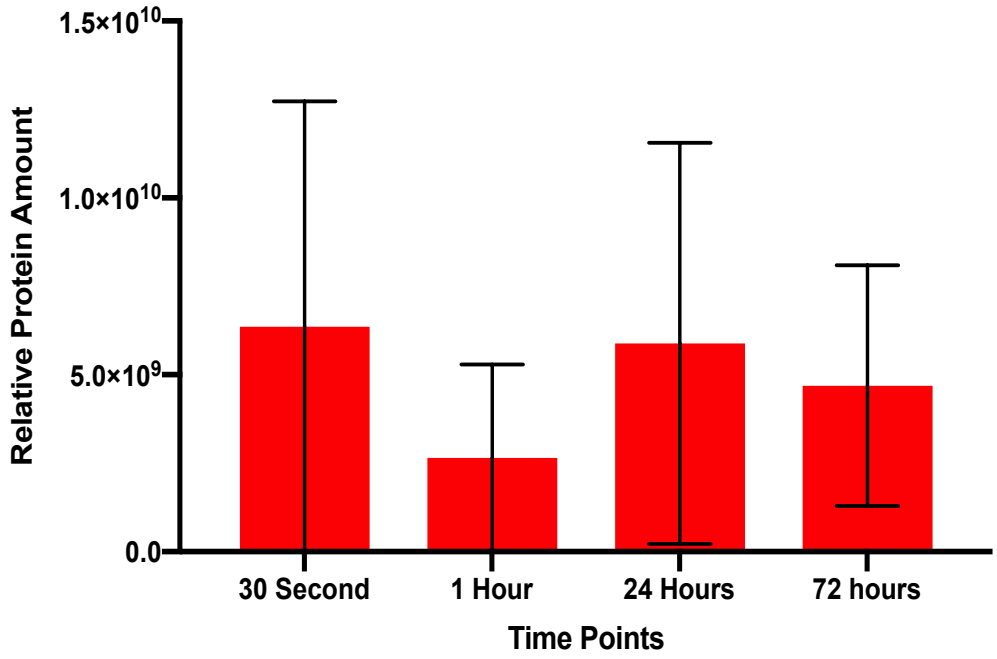


**Figure 6.3 Relative protein amount on ApaPore™.** Four-time points were measured using TMT labelling with LC/MS (*n*=2). 30 seconds had the highest relative amount while the lowest was at 1 hour. The error bars represent standard error of the mean.

### 6.5.2.3 Relative Amount of Proteins on β-TCP™.

The relative protein amounts on β-TCP™ over the four-time points are shown in **Figure** 6.4. There was an increase of 444.32% by 1 hour from the low 30-second level. The amount of protein then decreased by 24 hours by 206.87% before rising again at 72 hours by 139.1%. There was a percentage fold decreases between 30 seconds and 72 hours by 26.2%.

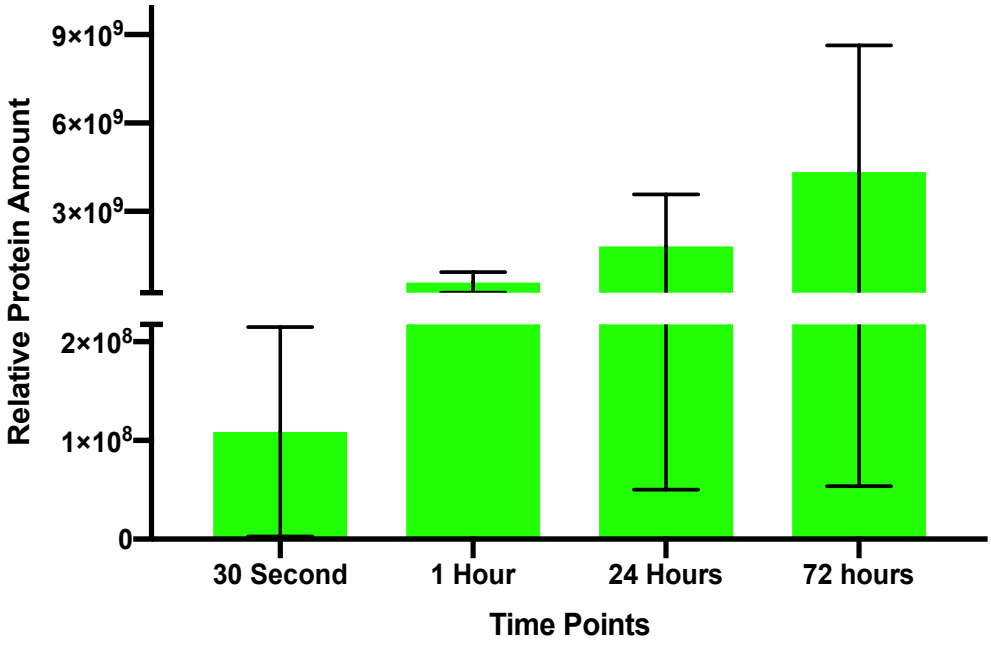


**Figure 6. 4 Relative protein amount on β-TCP™.** Four-time points were measured using TMT labelling with LC/MS (n=2). 72 hours had the highest relative amount while the lowest was at 30 seconds. The error bars represent standard error of the mean.

### 6.5.2.4 Relative Amount of Proteins on Inductigraft™,

The relative protein amounts on Inductigraft™ over the four-time points are shown in **Figure** 6.5. 30 seconds was the lowest level before increasing by 648.35% by 1 hour, further increased by 1077.03% at 24 hours before decreasing at 72 hours by -54.53%. The percentage fold increases for proteins between 30 seconds and 72 hours was 3893.54%.

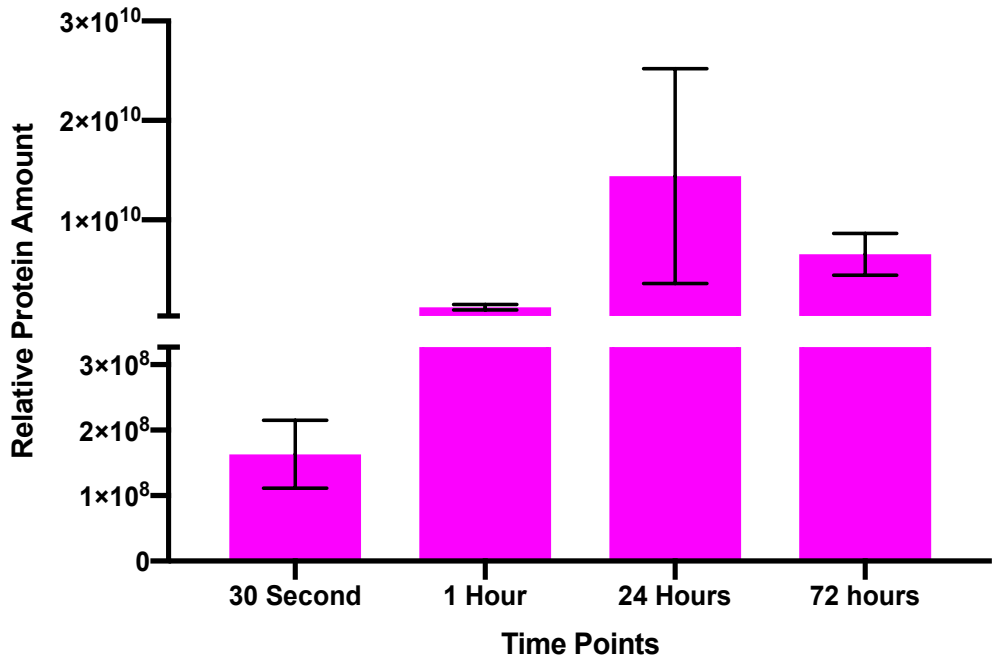


**Figure 6.5 Relative protein amount on Inductigraft ™.** Four-time points were measured using TMT labelling with LC/MS (*n*=2). 24 hours had the highest relative amount while the lowest was at 30 seconds. The error bars represent standard error of the mean.

### 6.5.2.5 Relative Amount of Proteins on Orthoss®.

The relative protein amounts on Orthoss® over the four-time points is shown in **Figure** 6.6. The protein levels at 30 seconds was the lowest of all time points before increasing by 648.3% at 1 hour. There was a further increase at 24 hours of 1077.03%. Again 72 hours there was a to 54.53% increase. The total percentage fold increase between 30 seconds and 72 hours was 3904.78%.

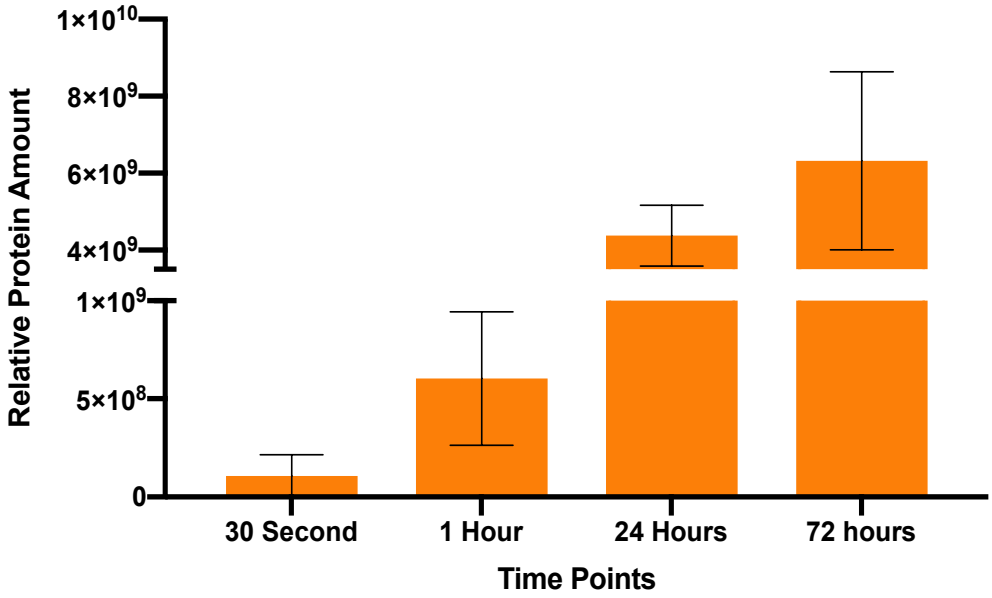


**Figure 6.6 Relative protein amount on Orthoss®**. Four-time points were measured using TMT labelling with LC/MS (*n*=2).72 hours had the highest relative amount, while the lowest was at 30 seconds. The error bars represent standard error of the mean.

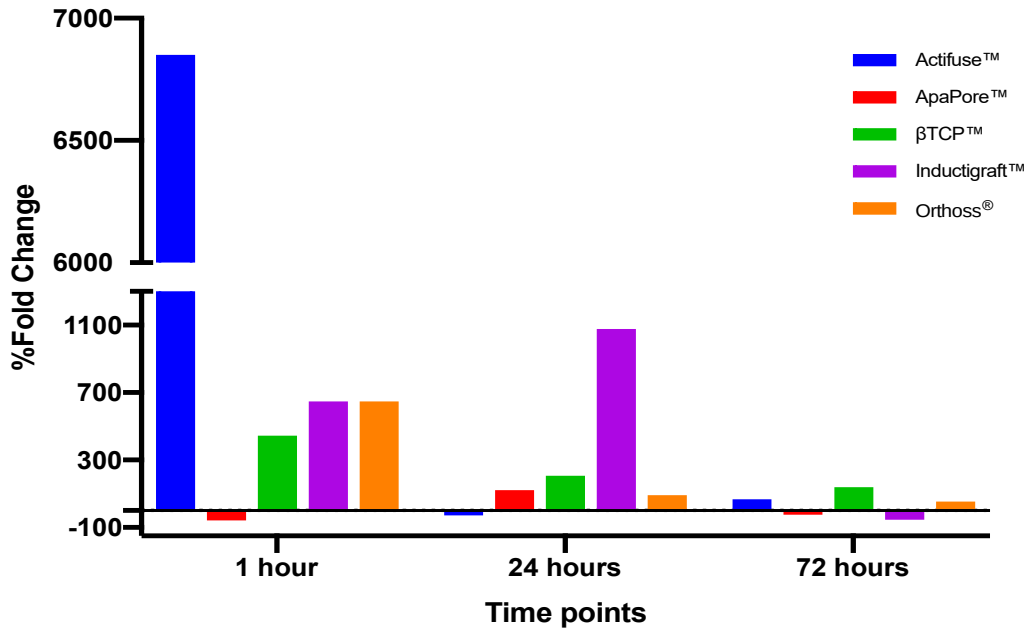


**Figure 6.7 Percentage fold change of relative protein amount**. It was measured using TMT labelling with LC/MS (n=2). The fold change was calculated on the time point before it. The highest increase was on Actifuse™ between 30 seconds and 1 hour. The largest decrease was on ApaPore™ between 30 seconds and 1 hour.

### 6.5.3 Similarities of Protein Identified on the Different Surface

31 proteins were common to all surfaces (**Figure** 6.8). The highest amount of proteins was found on Inductigraft™, with 37 proteins that were not found on any other surface. The only graft without any unique proteins adhering to its surface was β-TCP™.

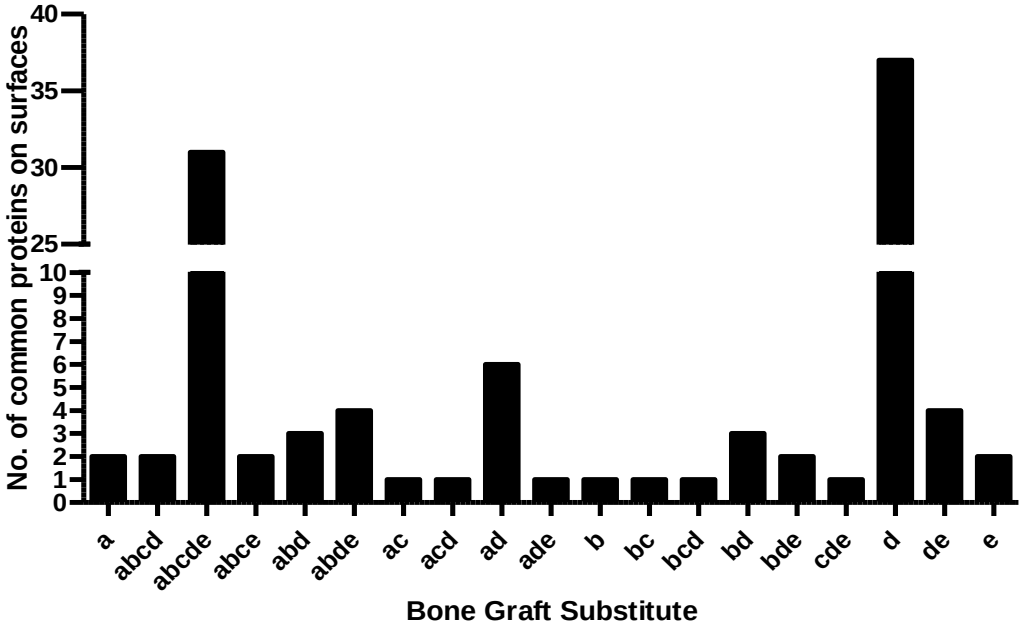


**Figure 6.8 Similarity of proteins on each surface.** Measured using TMT labelling with LC/MS (*n*=2). (**a**) Actifuse™, (**b**) ApaPore™, (**c**) β-TCP™, (**d**) Inductigraft™ and (**e**) Orthoss®. 31 proteins found adhered to all surfaces. Highest amount of proteins only on a single surface was Inductigraft™ (37).

### 6.5.4 Heat maps

Heat maps enable a visual representation of the proteomic data, showing quantitative patterns across time points. The data represents the specific amount of the different proteins, expressed in a variety of colour in the heat maps below.

The relative amount of proteins levels is expressed in colour intensity on the heat map in a red-green colour scheme. The red represents the highest protein amount identified at that particular time, while green is an indicator of low protein amounts.

The different BGS were separated into individual heat maps that have separated into four columns representing the four-time points. The heat maps below show that the interactions of proteins with the different surfaces and change with time points. Some proteins attach in relatively large quantities at early time points before being overtaken by other proteins, while others start low and increase with time. This shows the changing protein profiles of the different BGS surfaces.


**Figure 6. 9 Heat map of relative amounts of protein identified from Actifuse™.** Measured using TMT labelling with LC/MS (n=2). Images formed using Xlstat (Addinsoft, France) software. Red represents the highest protein amounts. Green represents low proteins amounts. Black represents no protein found.

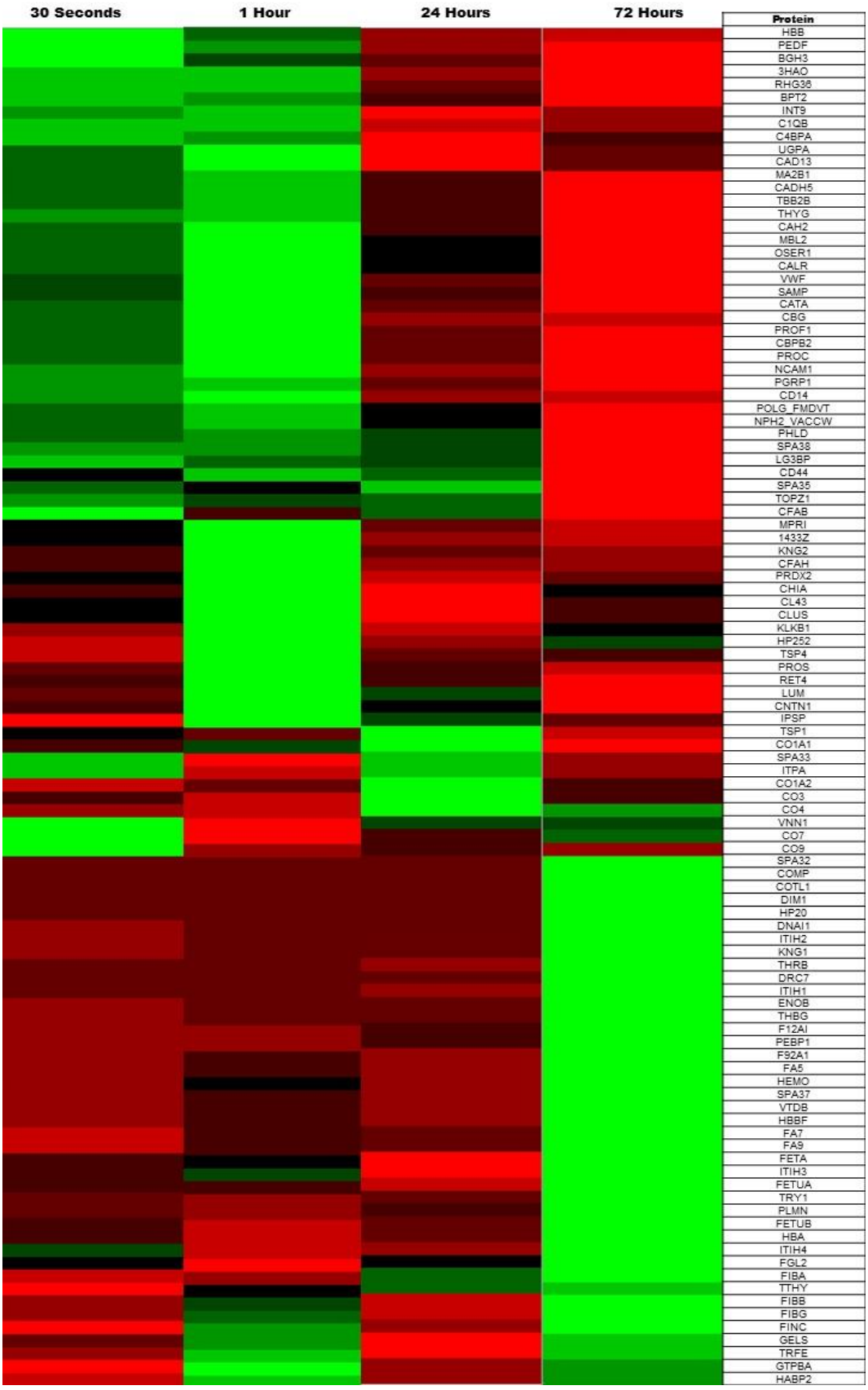


**Figure 6. 10 Heat map of relative amounts of protein identified from ApaPore™.** Measured using TMT labelling with LC/MS (n=2). Images formed using Xlstat (Addinsoft, France) software. Red represents the highest protein amounts. Green represents low proteins amounts. Black represents no protein found.

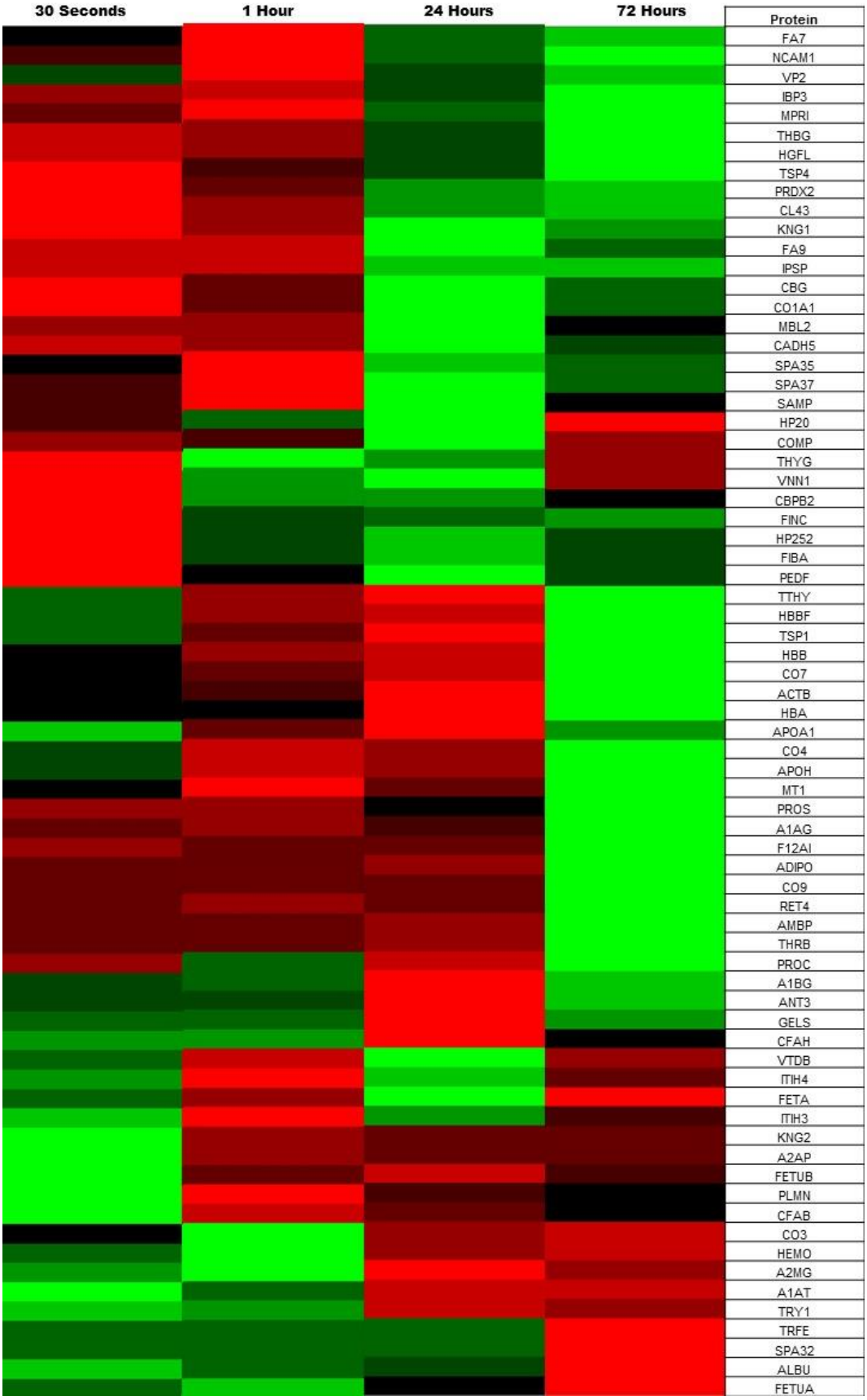


**Figure 6. 11 Heat map of relative amounts of protein identified from β-TCP™.** Measured using TMT labelling with LC/MS (n=2). Images formed using Xlstat (Addinsoft, France) software. Red represents the highest protein amounts. Green represents low proteins amounts. Black represents no protein found.

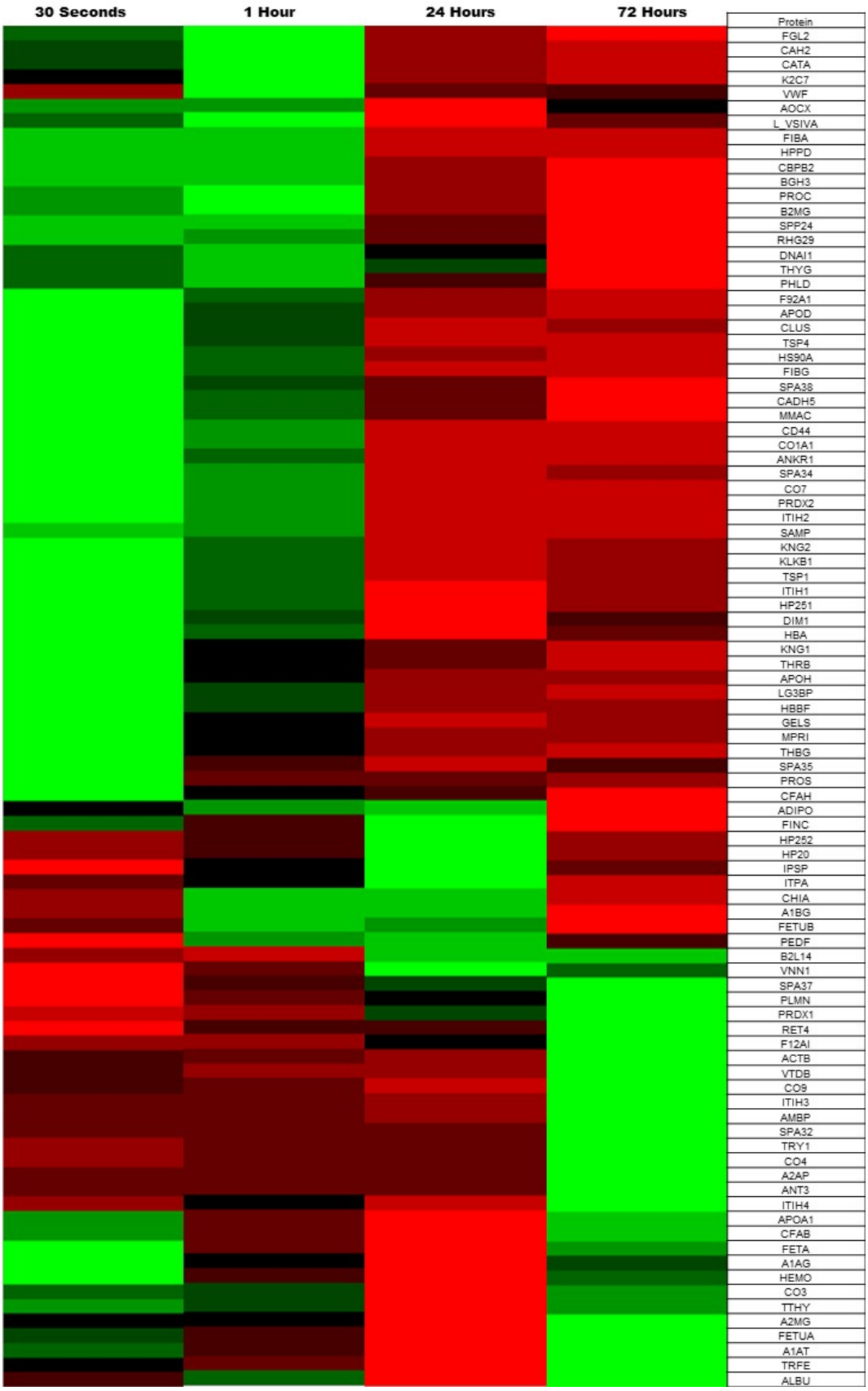


**Figure 6. 12 Heat map of relative amounts of protein identified from Inductigraft™.** Measured using TMT labelling with LC/MS (n=2). Images formed using Xlstat (Addinsoft, France) software. Red represents the highest protein amounts. Green represents low proteins amounts. Black represents no protein found.

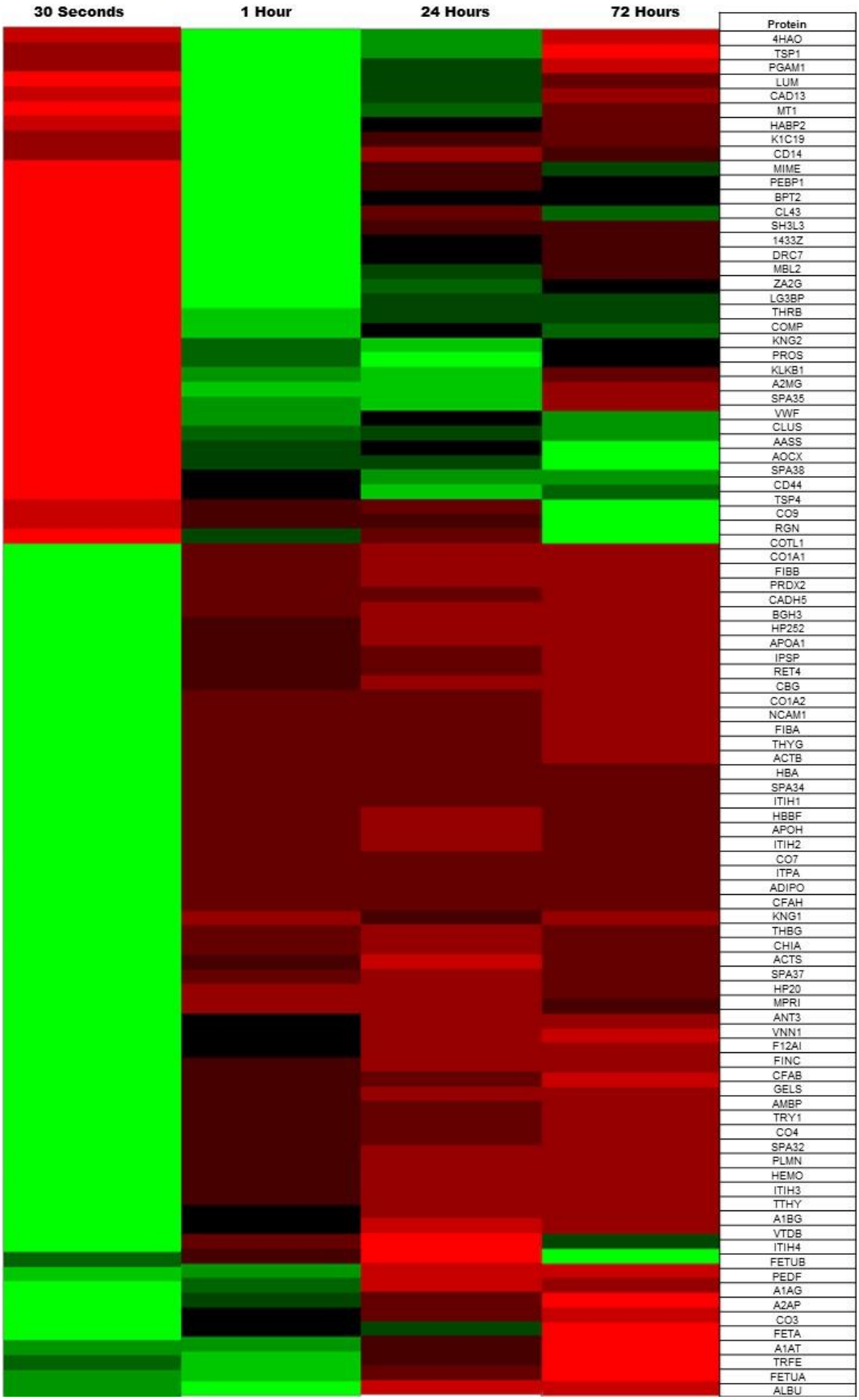


**Figure 6. 13 Heat map of relative amounts of protein identified from Orthoss®.** Measured using TMT labelling with LC/MS (n=2). Images formed using Xlstat (Addinsoft, France) software. Red represents the highest protein amounts. Green represents low proteins amounts. Black represents no protein found.

### 6.5.5 Top 5 ranked proteins

The highest-ranking protein was Fibronectin (FINC) and can be found on all surfaces. Collagen alpha-1(I) chain (COL1A1) found on all surfaces and was the second-highest ranked protein. The CD44 protein was the third-highest ranked protein and was only found on four surfaces (Actifuse™, ApaPore™, Inductigraft™ and Orthoss®). Collagen alpha-2(I) chain (COL1A2), the fourth-highest protein, only found on four surfaces (Actifuse™, ApaPore™, β-TCP™ and Orthoss®). The fifth-ranked protein was Thyroid hormone receptor beta (THRB) and was found on all of the surfaces. The top 5 ranked proteins identified are presented in **Table** 6.10 with their score and which surface they adhered too.

**Table 6. 10** The top five ranked proteins identified by MS.

| Protein | Score | Surface |
|---|---|---|
| **FINC** | 99 | All |
| **COL1A1** | 95 | All |
| **CD44** | 76 | Actifuse™, ApaPore™, Inductigraft™ and Orthoss®. |
| **COL1A2** | 63 | Actifuse™, ApaPore™, β-TCP™ and Orthoss®. |
| **THRB** | 54 | All |

## 6.6 Discussion

### 6.6.1 Background

The absorbed protein layer on a BGS occurs within seconds of being submerged in a biological fluid and mediate the subsequent cellular responses (Guth et al., 2010). The composition of the BGS influences the proteins that absorb and the amounts that attach, while the attached proteins mediate cell recruitment and regulate the cellular response through their molecular receptors.

Currently, the role that surface adhered proteins play in osteoinduction is still poorly understood (Li et al., 2011). Understanding the critical roles that these proteins play in orchestrating the signalling cascade could lead to engineering BGS that enhance protein attachment and could potentially increase differentiation of osteoblasts (Li et al., 2011).

El-Ghannam et al. (2009) showed there were significantly higher numbers of serum proteins attached to HA when compared to bioactive glass and surface-modified porous bioactive glasses. However, they noted increased protein concentrations did not increase cell adhesion to its surface (Ghannam et al., 2009). As discussed previously, the composition of the protein layer can influence the cellular response, and this has been shown with HA and SiHA surface where the can form a protein layer that has caused enhanced levels of cellular attachment (Guth et al., 2010). It's also clear that variations in strut porosity, higher strut levels will increased surface area, affects the amount of proteins as there is more surface for proteins to adhere too (Coathup et al., 2012).

Although processing the proteins after detachment from the graft surfaces is time-consuming, the data produced can increase the understanding of how BGS promote bone healing and integration into bone (Lv et al., 2013). Hakkinen (2009), states that performing proteome analysis produces large quantities of valuable data. Proteomics analysis enables the identification of proteins that are involved in the pathways of interest, including cell signal transduction that could regulate and control cell differentiation (Ji-Hyun Lee, 2014). Proteins that have the ability to effects the adhesion of MSCs to the surfaces and the cell recruitment through the interaction with cell surface receptors (El-Ghannam et al., 1999; Guth et al., 2010). According to the 2017 review by Tang et al., several different molecules can regulate the orchestration of MSCs towards the osteogenic differentiation; these can include hormones, cytokines, morphogens, growth factors, matrix proteins, transcription factors and their co-regulatory proteins. As mentioned before, signalling pathways can also be affected, and these pathways include; Hh, notch, Wnt, and FGF signalling.

Using LC-MS/MS-based quantitative methods in conjugation with TMT labelling, it enabled the identification of the proteins and their relative amounts over time can be elucidated. This enables a comparison of the relative amount of each protein across

each time point on a single graft. Unfortunately, this technique does not allow a comparison of the relative amounts of specific proteins on different grafts at each time point.

### 6.6.2 Mass Spectrometry Techniques

Chapter 5 demonstrated that the amount of protein detached from the BGS surfaces varies depending on the grafts chemistry, topography and surface area. The first method attempted to identify the detached proteins used to isolate the protein bands from SDS PAGE gels before in-gel tryptic digesting and LC/MS. The results returned were a lower number than expected, with only 8 proteins were identified. The issue with this technique was a limited amount of protein solution that could be run on SDS PAGE gels, resulting in limited the amount of protein extracted from the gel leading to a further limited amount of protein identified by LC/MS.

The second method investigated used an in-solution separation based on previous work by Zheng et al. (2006). This involved separating the proteins by their mass using spin columns that would separate proteins by size before digesting them. This method has no limit on the amount of protein that could be isolated from the protein solution; meaning larger volumes could be used in MS analysis. This technique had led to 30 proteins being identified. However, this method did not enable the relative amount of proteins to be calculated.

Tandem mass tags (TMTs) enabled the relative amount of proteins to be calculated. TMT tags were used to identify the proteins at each time point. Then all four-time points from each BGS were then combined into one solution before LC/MS. This method was able to identify 106 proteins.

The ability to quantify the protein levels at each time point showed attachment and detachment of specific proteins over time, an effect that generally referred to as the Vroman effect. The heat maps show a visual change of the overall amount of proteins and give a visual representation of the changes in relative amounts of each protein over the four-time points.

### 6.6.3 Analysis of the Mass Spectrometry Results.

While 106 proteins were identified, it was imperative to find which proteins had the potential to increase the bioactivity of the BGS. A scoring system was developed to rank the proteins against each other and isolation proteins of interest. This system unitises previously known information on proteins involved in bone formation that was produced by the databases and these were assigned a score. If the output was positive, the score was high, but if there was a negative or no output, the score was lower.

Below is an example of the scoring system using FINC (the highest scoring protein). On the human protein atlas, which showed FINC having low expression levels in bone,

meant it was given a score of 3. It was then given a score of 10 for being present on the OsteoChondroGene database. The results from all the different databases were combined, and the total score was determined. The top five proteins were investigated in more detail through literature searches. It was also assessed whether the protein was freely available to purchase at a high enough quantity to make it cost-effective to pre-adhere them to the surface of the graft.

### 6.6.4 Top Five Proteins

The top five proteins selected for further investigation included: (There is further information on FINC and COL1A1 in the below section 6.6.5).

1. FINC (Fibronectin): It has been well established that FINC is involved in cellular adhesion, migration and processes that include wound healing, bone formation, blood coagulation and host defence (Steffens et al., 2012).
2. COL1A1 (Collagen alpha-1(I) chain): Type 1 collagen is found in abundance of bone and tendons.
3. CD44 (CD44 antigen): CD44 is a cell surface glycoprotein involved in cell interaction, cell adhesion and migration. CD44 mediates cell-cell and cell-matrix interaction, including interaction with osteopontin, which is essential in bone remodelling (Senbanjo et al., 2017; Goodison et al., 1999; Weber et al., 1996). CD44 plays a significant physiological roll in organ and tissue structures and regulates lymphocyte activation (Goodison et al., 1999).
4. COL1A2 (Collagen alpha-2 (I) chain): COL1A2 is associated with COL1A1 and found in high amounts in connective tissue such as bone and tendons. COL1A2 has been demonstrated to regulate osteoblast and osteocyte differentiation (Guo et al., 2016).
5. THRB (Thyroid hormone receptor beta): Involved in osteoinductive pathway and the highest-ranking protein on all surfaces. It is also involved in controlling bone development and maintenance within osteoblasts (Bassett et al., 2016). THRB has been shown to increase skeletal development due to advanced endochondral and intramembranous ossification and increased bone mineral deposition during the development stage in mice (O'Shea et al., 2012).

### 6.6.5 Noted Other Proteins

Other proteins of interest included; Alpha-2-HS-glycoprotein (FETUA) (7th ranked) is known to influence the promotion of the mineral phase of bone tissue, found during bone growth were it's suggested that it is involved in endochondral ossification (Uniprot.com; Schinke et al., 1996; Yang et al., 1991). Albumin (12th ranked) found on all surfaces and Weszl et al., (2012) has reported that the absorbing Albumin onto allograft with MSCs before freeze-drying would improve the bone formation. They also noted that this would

significantly increase the MSCs proliferation; however, it was shown to only affect on human bone surfaces and not on hydroxyapatite or bovine bone scaffolds (Weszl et al., 2012). TRFE, also known as Serotransferrin (16th) may have a role in stimulating cell proliferation and studies have shown that growing cells in its presence increased proliferation of osteoblasts progenitor cells although it also suppressed ALP activity of osteoblasts, which has been shown to be a marker of osteoblast differentiation (Uniprot.com; Yang et al., 2011).

### 6.6.6 Top Two Proteins

The top two proteins FINC and COL1A1 were selected for further research. Both of which have been used to coat the surface of tissue culture plastic to increase cell-seeding efficiency (Weszl et al., 2012; Athanassiou et al., 2001). Both FINC and COL1A1 proteins indirectly interact through their Arginylglycylaspartic acid peptide motif with other proteins and integrin leading to enhance cellular attachment (Parenteau-Bareil et al., 2010).

#### 6.6.5.1 Fibronectin

FINC is one of the most critical proteins the from serum that when adsorb to the surface of implants has shown to be responsible for enhanced osteoblastic adhesion and the interactions between cellular attachment and implant in terms of cell adhesion, proliferation and migration (Pierschbacher et al., 1984; Kennedy et al., 2006).

FINC is associated with increased cellular adhesion, migration, proliferation and osteoblastic differentiation (Chatakun et al., 2014). Chatakun et al., (2014) concluded that there using FINC to pre-treat biomaterial improves the osteogenic differentiation on both titanium and polymer surfaces. Athanassiou et al., (2001) noted that FINC could also aid in increasing the adhesion strength to 107% of MSCs compared to known coated. Deligianni et al., (2006) explained HA-coated with FINC had shown increased cellular adhesion strength when interacted with osteoblasts on smooth surfaces during *in vitro* conditions. They also showed that when the surfaces are rough, increasing cellular attachment. Chatakun et al., (2014) demonstrated this further with *in vitro,* experiments where FINC was absorbed to HA surface leading to significant increases in cell adhesion; this increased by 40% (Smooth) and 62 % (Rough).

Pierschbacher et al., (1984) results showed that cellular attachment is aided by the cells recognition of arginine, glycine and aspartic acid residues. Kennedy et al. (2006) study suggested that FINC causing quicker proliferation of hydrophobic regions with increased surface energy. Osteoblasts secrete FINC when undergoing differentiation has led the researcher to believe that it participates in the formation of bones and Moursi et al., (1996) demonstrated that osteoblasts that have interacted with the central cell-binding domain of the endogenously produced FINC during early stages of differentiation and this leads to both normal morphogenesis and gene expression.

A layer of FINC adsorbed onto CaP has been shown to improve proliferation, while promoting MSCs towards early differentiation osteoblasts (Cairns et al., 2010). FINC has also shown to enhance vascular calcification by promoting the osteoblastic differentiation of vascular smooth muscle cells via the ERK signalling pathway (Chatakun et al., 2014; Ding et al., 2006).

In studies, FINC has shown to promote the binding and differentiation of the adhering osteogenic cells when absorbed to either SiHA and HA, and other studies have shown that the absorption of FINC can have a positive effect on the cellular morphology and actin formation in osteoblasts *in vivo* (Castagna et al., 2012). Rico et al. (2009) suggests that there is a correlation between FINC absorption and osteoblast adhesion through morphology and actin cytoskeleton formation.

However, some *in vivo* studies have shown less profound effects of FINC (Schonmeyr et al., 2008). Schonmeyr et al., (2008) results showed that the addition of FINC to HA was capable of significantly increasing cellular attachment and proliferation when investigating *in vitro; however*, they note it is not a profound difference, and these results were replicated during *in vivo* conditions. Also, Tseng et al., study showed that the attached FINC to BGS would increase cellular attachment but only on specific BGS, as in Orthoss®. They noted that FINC hurt cellular attachment compared to a non-coated surface (Tseng et al., 2013). Jae-Jo et al., (2011) stated that when FINC is pre-absorbed to a surface, it could affect the competitive adsorption and desorption of the other serum proteins.

#### 6.6.5.2 COL1A1

Collagen is regarded as the most beneficial biomaterials (Lee et al., 2001). An essential structural protein can aid both the formation and mineralisation of bone (Boskey et al., 1999; Robey et al., 1996). Collagen is one of the most abundant proteins within the body and COL1A1 accounts for 90% of the total body's collagen (Strover et al., 2010). Very few people are known to have an immune reaction to collagen, which is beneficial for when it is coated onto implant (Parenteau-Bareil et al., 2010).

COL1A1 has the potential to influence the BGS surface; it is also used as an early indicator of osteoblast differentiation and is expressed in newly formed bone by osteoblasts and osteocytes (Walsh et al., 2017; Suzuki et al., 2001). COL1A1 has been shown to contribute to increased growth rates of bone and decreased fractures (Speed et al., 2016).

Composite bone substitutes, which are composed of porous inorganic calcium phosphate and collagen, can be osteoconductive and have excellent bone formation properties (Erbe et al., 2005). Collagen is commonly used is tissue engineering applications, and studies of the collagen/HA combination have shown the potential to mimic skeletal bones (Parenteau-Bareil et al., 2010). Reyes-Sanchez et al., (2017) noted

that in conjugation with polyvinylpyrrolidone and autografts, COL1A1 can cause an enhanced response in bone consolidation process when placed rabbit model. Another study has noted that collagen-coated PLGA/HA, scaffold caused an increase in mechanical strength and hydrophilic properties, which can aid both cellular adhesion and proliferation (Bi et al., 2018). They also developed a scaffold+Col+DGEA that can to promote osteogenesis (Bi et al., 2018). MSCs, when cultured in the presence of COL1A1, have shown increased levels of ALP activity and increased osteoblastic differentiation, forming mineralised tissue more rapidly (Mizuno et al., 2000).

It has also been stated that COL1A1 can independently induce the expression of osteogenic differentiation markers (Viale-Bouroncle et al., 2014). This includes both ALP and OPN that occurs through the FaK and ERK pathways (Viale-Bouroncle et al., 2014). The FaK pathway is involved in promoting cellular turnover with the extracellular matrix and can promote cellular migration while being critical for the osteogenic differentiation of MSCs. While the ERK pathway is involved in different pathway that including growth factors including osteoblast differentiation and skeletal development.

### 6.6.6 Limitations

There was limitation, including time and budget to work with a mass spectrometry machine if it was possible could have increased the “n” number to strengthen the statistical significance of the study. The relative amount calculated the amount of each protein, and it is possible that if there were a different source of serum, it would have produced a different protein profile. To classify which proteins were the most interesting to investigate further different online databases were used to investigate their potential to induce an osteogenic effect, it may have been interesting to investigate other proteins identified however this would have taken an extended period.

A was limitation included proteins that were expected to be present, such as bone morphogenic proteins (BMP’s), were not identified. This may be due to the proteins not being attached, or they may have possibly been washed off or degraded during the detachment process or in the MS analysis.

## 6.7 Conclusions

This study was performed to identify the proteins detached from five different BGS materials in the previous chapter and identify which two proteins could potentially increase cellular attachment and differentiation towards the osteogenic lineage.

This required optimising the method of isolating proteins using MSCs. The proteins were identified and measured their relative amounts using TMT labelling with LC/MS. Once the proteins are identified, they will be investigated for their potential to impact cellular attachment and osteoinduction of MSCs and the top five ranking proteins were

investigated further, and the top two proteins were selected based on their potential to increase the BGS performance.

The relative amounts of proteins adhering to the grafts over time show the dynamic interchange of proteins. This illustrated the attachment and detachment of proteins from the surface over time, showing a possible Vroman effect.

106 different proteins were identified with 36 unique proteins identified adhered to Inductigraft$^{TM}$ that were not found adhered to any other surface. Vroman effect was evident with heat maps which shows the protein levels were fluctuating over time. Not all the proteins could be investigated further due to both a limited amount of budget and time. The proteins were ranked based on the information from different online databases about their ability to affect osteoinductivity and bone repair. The highest-ranking proteins were FINC and COL1A1. Previous studies have shown they have the potential to affect cellular adhesion, osteoinduction, and proliferation.

# Chapter 7

## The Effect of Selected Proteins Adsorbed onto HA on Cell Activity

### 7.1 Introduction

After ranking the proteins identified in Chapter 6 identified the top two proteins as Fibronectin (FINC) and Collagen type I, alpha-1(I) Chain (COL1A1).

As discussed previously, FINC has multiple effects on cellular interactions, including cellular adhesion, migration, growth and differentiation of cells (Pankov et al., 2002). Cowles et al. (1998) noted that FINC is the earliest bone matrix proteins synthesized by osteoblast. It then proceeded by the synthesis of collagen in the development of bone (Cowles et al., 1998). Lee et al., (2014) showed coating an implant with FINC caused increased contact osteogenesis during early bone healing stages.

COL1A1 is crucial in terms of strength and support of tissues such as cartilage, bone, tendon and skin. COL1A1 is known to be an early marker of osteoprogenitor cells (Jikko et al., 1999). Mizuno et al., (2000) have shown COL1A1 can influence cellular behaviour, induce the osteoblastic differentiation and cause a four-fold increase in ALP activity compared to control after only 6 days compared to controls. They also noted that it caused the production of calcium nodules after 12 days of culturing (Mizumo et al., 2000).

Both proteins where coated independently onto the surface of different sintered discs the HA investigated in Chapter 4. By coating the disc with the proteins, it is hoped that it could enhance cellular attachment and the osteoconductive when compared to the non-coated HA surfaces.

## 7.2 Aims and hypothesis

### 7.2.1 Aims

The main aim for these experiments was to investigate whether the highest-ranked proteins identified in the previous chapter (FINC or COL1A1) have the potential to induce higher levels of cellular attachment or subsequent osteoinduction of MSCs that were seeded to sintered discs of HA compared to non-coated HA.

### 7.2.2 Hypothesis

The addition of either FINC or COL1A1 will increase the number of cells that adhere to the surface of the sintered HA discs and cause an increased cellular attachment or rate of osteoinduction compared to the non-coated HA.

### 7.2.3 Objectives

1. Coat sintered dense disc of HA with either FINC or COL1A1 proteins before cell seeding.
2. Investigate whether the addition of these proteins will increase either cellular attachment, proliferation or boost the level of ALP production when compared to non-coated sintered discs.

## 7.3 Materials and methods

### 7.3.1 Study Design

This study investigated whether the coating, with either FINC or COL1A1, could potentially increase the performance of sintered discs of HA. The proteins were allowed to adhere to the surface of the sintered discs before seeding with MSCs. Once adhered MSCs were seeded.

On days, 4, 7 and 14 AlamarBlue® assessed the metabolic activity, and the ALP assay will indicate early bone formation. On day 21 post, cellular seeding SEM will be used to investigate cellular attachment and structure.

These experiments were performed with an *n*=9 with control of non-protein coated sintered HA discs. The experiment will be considered successful if osteoinductive activity increased when compared to the non-coated discs.

### 7.3.2 Production of Sintered Dense Discs

Performed as outlined in **Section's** 4.3.2 and 4.3.3.

### 7.3.3 Absorbance of proteins

A concentration of 0.1mg/ml of each of the proteins was made in DMEM without any other additives. A pipette was used to drop 0.1µl/mg onto the top surface of the sintered disc and allowed to adhere for 1 hour in an incubator at $37^0$C at 5% CO2. Millipore (Millipore Limited, UK) supplied the FINC (Ref: 341631-1MG), while Abcam (Abcam plc. UK) supplied the COL1A1 (Ref: ab7526).

### 7.3.4 Cell Seeding

Performed as previously outlined in **Section** 2.3.4.

### 7.3.5 Cell Metabolic Activity, Alkaline Phosphatase assay and Scanning Electron Microscopy Analysis.

AlamarBlue® assay performed as in **Section** 2.3.5. The ALP assay performed as previously outlined in **Section** 2.3.6.1. While the method for the SEM experiment performed as it was in **Section** 2.3.7.2.

### 7.3.8 Statistical analysis

Normality was checked using the Kolmogorov- Smirnov and Shapiro Wilkinson test. If data was normal, the comparison was made using independent student T-test. For non-parametric data, comparison was made using the Mann Whitney U test with a Bonferroni correction. The data analysed was performed using SPSS version 24 (Chicago, USA). The figures were made using GraphPad Prism version 7.0.0 (San Diego, USA). These

experiments were run in *n*=9 where there was 3 cell lines and 3 repeats of each unless stated otherwise.

### 7.4 Results

#### 7.4.1 Cell Metabolic Activity

A significant difference on day 4 between FINC and COL1A1 of 16.2 (±3.4) ($p$=0.012). There was also a significant difference between FINC and the non-coated control of 30.6 (±4.5) ($p$>0.001). However, no significant difference noted between COL1A1 and non-coated control ($p$=0.052).

On day 7, no significant difference reported between COL1A1 and FINC of 5.5 (±8.5) ($p$=1.000), but COL1A1 was slightly higher activity. No significant difference between either of the samples and the control ($p$=1.000).

The final time point Day 14 again showed no significant difference in metabolic activity between FINC and COL1A1 of 17.0 (±12.8) ($p$=1.000); however, there was a significant difference between the protein-coated samples and the controls (FINC ($p$=0.001) and COL1A1 ($p$=0.003)). These comparisons are represented in **Figure** 7.1.

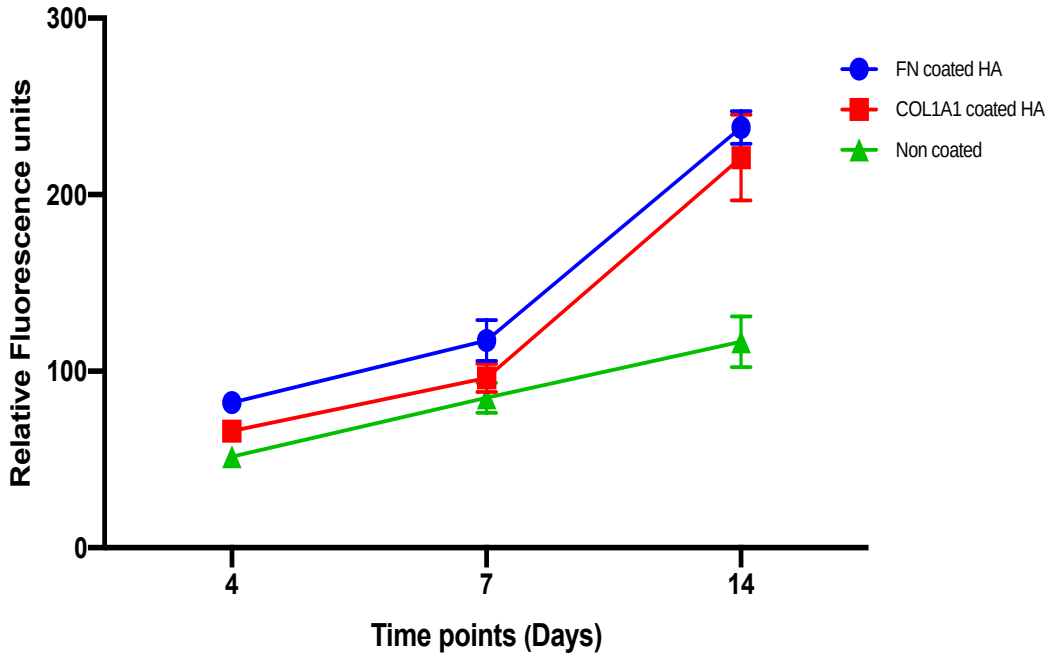


**Figure 7. 1 Cell metabolic activity of protein-coated DD over 14days.** Measured by AlamarBlue® assay. Significant difference on day 14 between coated surfaces and the non-coated control (FINC (p=0.001) and COL1A1 (p=0.003)). The error bars represent standard error of the mean.

In **Figure 7.2,** the results represent the percentage fold increase in metabolic activity between day 4 and 14 that showed there was significant in all samples tested ($p$=0.001).

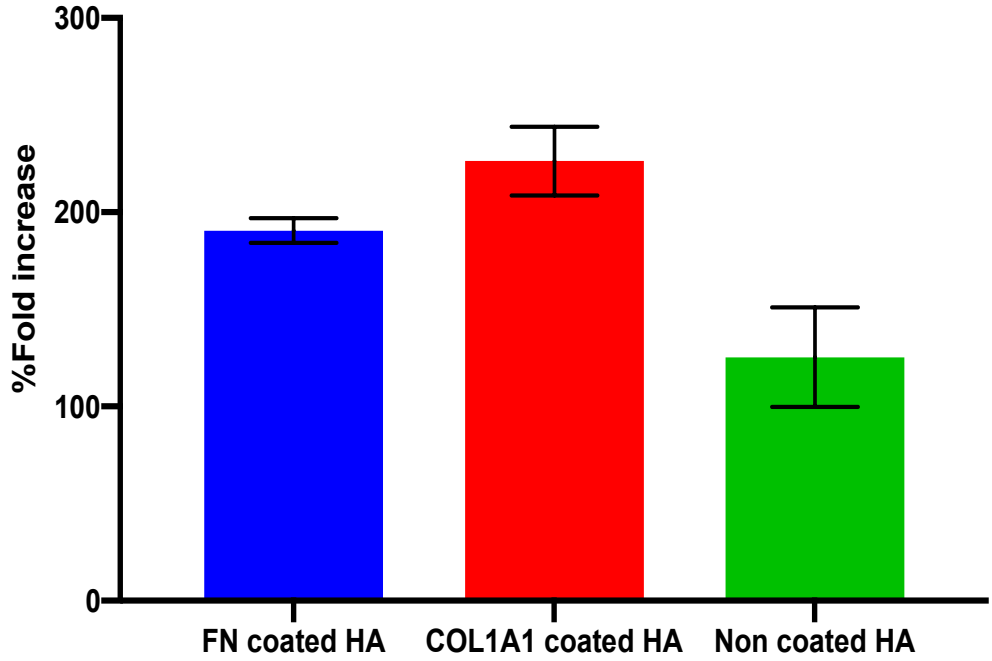


**Figure 7. 2 Percentage fold change in metabolic activity of protein-coated DD.** Measured by AlamarBlue® assay ($n$=9). Significant differences in all samples and control between days 1 and 14($p$=0.001). The error bars represent standard error of the mean.

### 7.4.2 Alkaline Phosphatase Assay

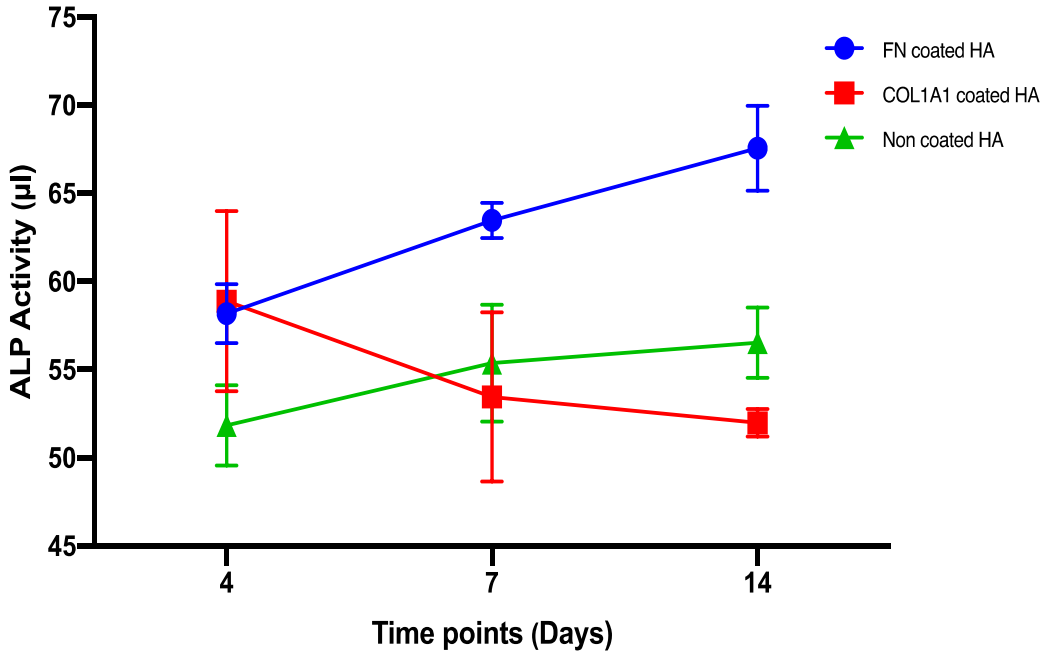


**Figure 7. 3 External ALP activity of protein-coated DD over 14days.** Measured by spectrometer ($n$=9). Significant ALP levels on FN on day 14 compared to other samples (COL1A1 ($p$=0.000) and control ($p$=0.016)). The error bars represent standard error of the mean.

ALP levels (**Figure** 7.3) were initially higher on COL1A1 compared to the other two surfaces, but this was not significant ($p$=1.000). At day 7 FINC ALP levels are higher than the two other surfaces, and this trend continues into day 14. FINC ALP activity was significantly higher than the other two surfaces at day 14 (COL1A1 ($p$=0.000) and control ($p$=0.016)). The ALP activity of COL1A1 dropped below that of the control, however, not significantly ($p$=0.0016).

### 7.4.3 Scanning Electron Microscopy

The SEM imaging allowed for the assessment of cellular attachment, morphology and to assess whether there were any presents of extracellular matrix being produced (FINC coated HA sintered dense discs **Figure** 7.4, COL1A1 coated HA sintered dense discs **Figure** 7.5 and non-coated HA sintered dense discs **Figure** 7.6).

There appears to be cells attached and growing on all surfaces, with an appearance of increasing numbers of cells at each time point indicating the cells were proliferating. From a visual assessment suggested that higher numbers of cellular attachment can seem on the FINC coated HA sintered dense discs at each time point.

The cells on the protein-coated surfaces appear to coat the entire discs by day 7 and begin to form layers of cells by day 14. The cells on the control surface appear to colonise the surface at a slower rated compared to the coated surface.

On day 21, the surfaces appear to higher levels of extracellular granules believed to be associated with mineralisation with the highest amount found on FINC coated surface compared to the COL1A1 and with little to no mineralisation production on the control surfaces.

As for cellular morphology, the normal MSCs morphology is for cells to be flat and have long protruding extended spindles. This shape of cells can be seen on the early time points. However, at the later time points, the cells appear to change their cellular morphology becoming more cuboidal in shape, which is typically associated with osteoblasts morphologies.

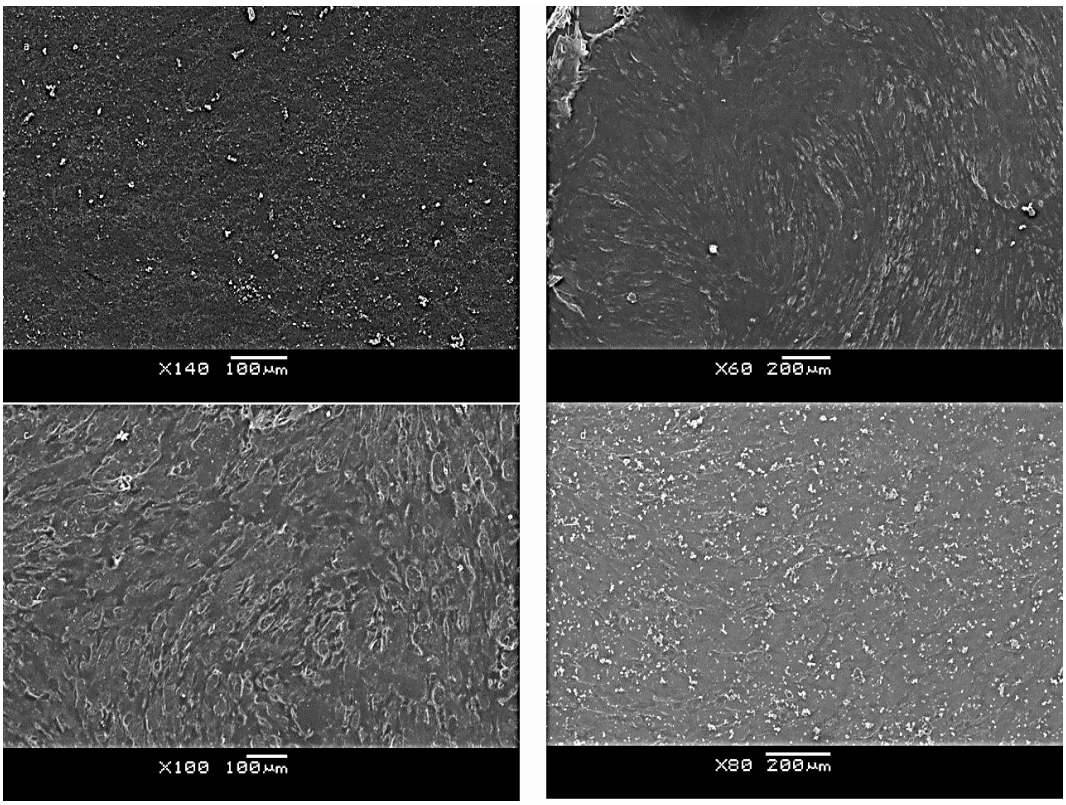


**Figure 7. 4 SEM images of cells adhered to FINC coated on sintered DD of HA.** (**a**) Day 4, (**b**) Day 7, (**c**) Day 14 and (**d)** Day 21. Cell numbers appear to increase in number with time.

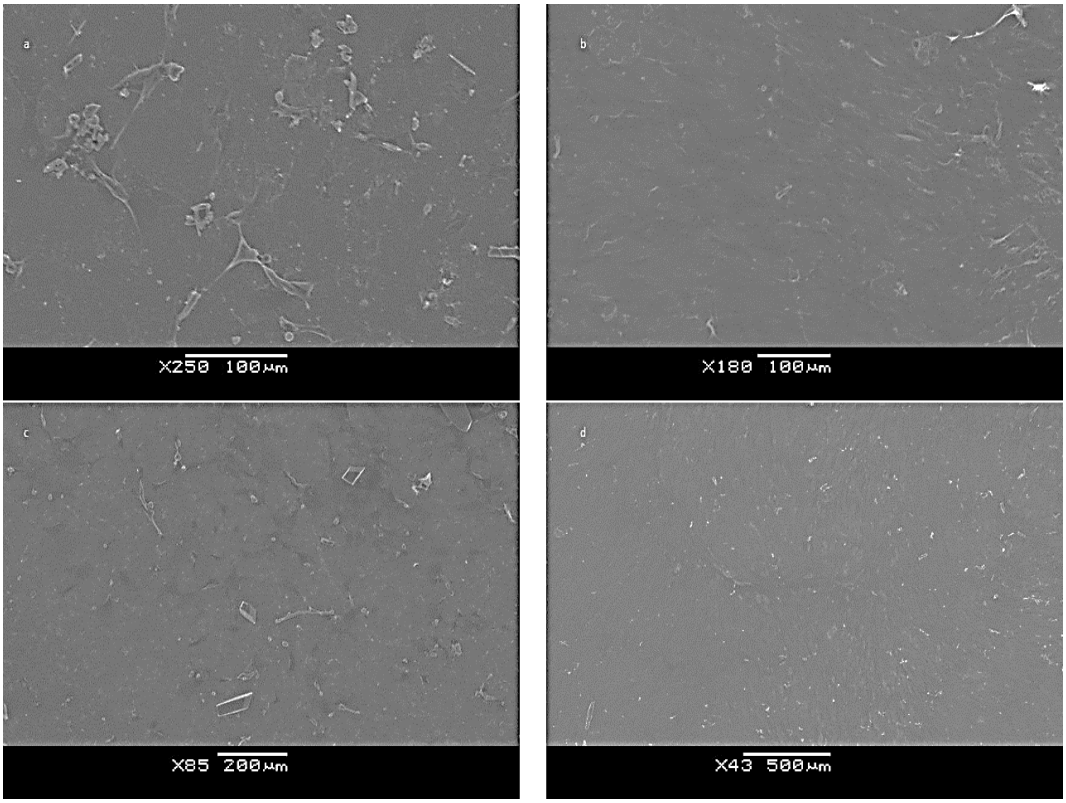


**Figure 7. 5 SEM images of cell adhered to COL1A1 coated on sintered DD of HA.** (**a**) Day 4, (**b**) Day 7, (**c**) Day 14 and (**d**) Day 21. Cell numbers appear to increase in number with time.

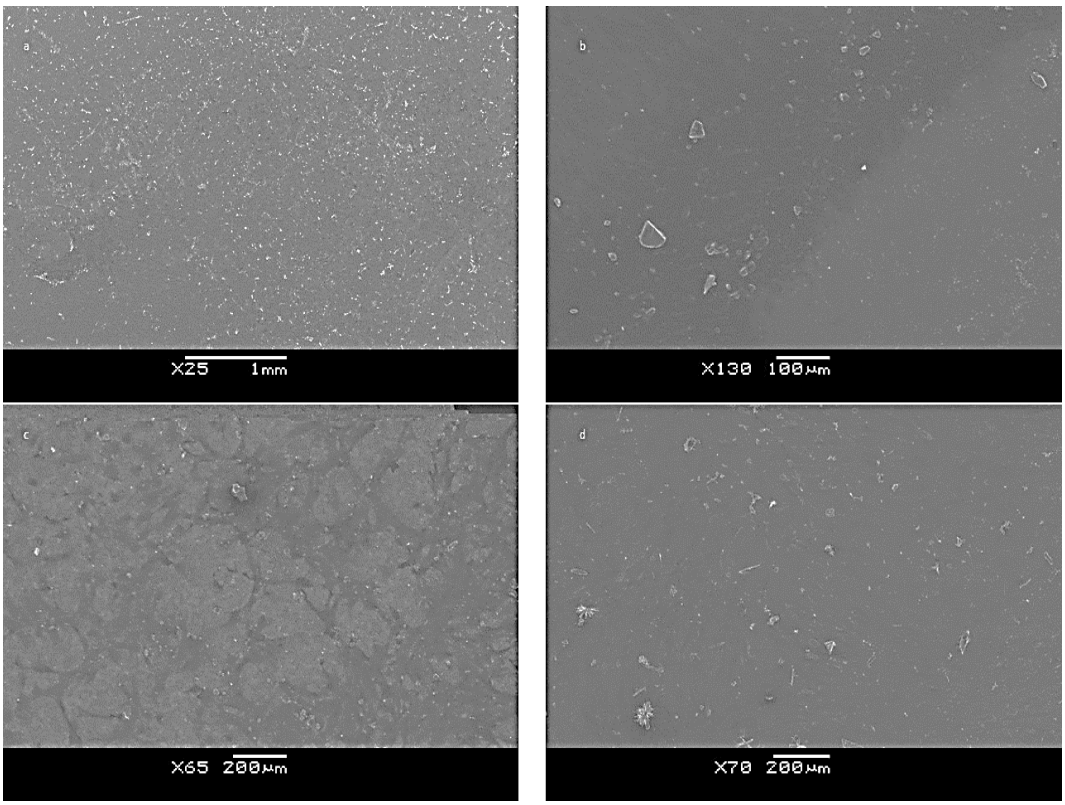


**Figure 7. 6 SEM images of cells on non-coated control of sintered DD of HA.** (**a**) Day 4, (**b**) Day 7, (**c**) Day 14 and (**d**) Day 21. Cell numbers appear to increase in number with time but visually less cells compared to other surfaces investigated.

## 7.5 Discussion

### 7.5.1 Introduction

Understanding the influences that proteins have on the molecular biology of a cell, can and could lead to potentially increasing the levels osteoinduction. Guth et al. (2010) reported that cellular adhesion on calcium phosphate was associated with adsorbed proteins rather than the substrate itself.

During Chapter 6, the top two proteins, FINC and COL1A1, were selected. It should be noted that other candidate proteins that could be important; however, due to time and monetary constraints; other less abundantly attached proteins with potential to influence MSC differentiation was not investigated.

By coating the HA discs with either of the selected proteins, it was hoped they could potentially increase the performance concerning of the HA. This approach may have the ability to increase the performance of the other grafts. The combinations of these proteins with different BGS have previously been investigated. FINC has long been established as an excellent protein that increased cell adherence to surfaces (Pierschbacher et al., 1984) and can be found in high levels during osteogenesis at the early stages of bone healing and binds to osteoblasts and to other ECM proteins to aid in osteoblastic adhesion, differentiation and matrix mineralization (Tseng et al., 2013). Lee et al., (2014) showed that coating an implant with FINC showed increased contact osteogenesis during early bone healing stages.

COL1A1 is, therefore, a candidate to combine with a BGS (Parenteau-Bareil et al., 2010). An immune reaction to COL1A1 is rare (Parenteau-Bareil et al., 2010). The absorption of COL1A1 to surfaces has previously shown to promote both osteoblastic differentiation and their activity (Sogo et al., 2007). MSCs, when cultured in the presence of COL1A1 have shown increased ALP activity and mineralisation inducing osteoblastic differentiation (Mizuno et al., 2000). These increases are due to the amino acid sequence within the protein and integrin's that can affect cell adhesion (Sogo et al., 2007).

However, as discussed in the previous chapter Orthoss® when pre-coated with FINC proteins reduced cell attachment and harm its bioactivity, however, when Orthoss® is coated with COL1A1 proteins it had a positive impact causing enhanced cell adhesion (Tseng et al., 2013).

### 7.5.2 Metabolic activity

The AlamarBlue® assay performed here was used to assess the metabolic activity of the cells that have adhered to the discs on days 4, 7 and 14. In the previous experiments in Chapter 4, cell proliferation on HA was reduced in comparison to the SiHA DD all time points. The results presented in this chapter showed that addition of the FINC and COL1A1 appears to increase the performance compared to the non-coated HA. FINC

coated discs initially had significantly higher metabolic activity when compared COL1A1 and the control ($p$=0.012; $p$=0.000). COL1A1 coating induced higher metabolic activity compared to the non-coated surface; however, this was not significant ($p$=0.052).

There was a substantial percentage fold increase in metabolic activity of the protein-coated surfaces with FINC had 121.3% activity over the control ($p$=0.001), and COL1A1 had a slighter lower difference of 104.3%, which was also significant ($p$=0.003).

The day 4 results are comparable with previous studies that showed that the FINC protein increased cellular attachment initially, but COL1A1 has also shown to increase the initial adhesion (Deligianni et al., 2006; Somaiah et al., 2015). Deligianni et al., (2006) noted that FINC preabsorption onto HA surface resulted in enhanced osteoblastic adhesion to the graft surface. They noted that there was increased osteoblast attachment on smooth HA surfaces (165%) compared to on rough HA surfaces (73%) when performed under *in vitro* conditions. Kilpadi et al., (2001) also suggests that FINC enhances the HA performances in relations to stimulated increased cellular attachment on rough surfaces compared to the smooth metal surfaces. El-Ghannam et al., (1999) suggested that FINC coating onto a CaP layer which was on bioactivity glass could increase osteoblast cellular adhesion.

Several other studies that mirror the results presented in my study, which show increases in proliferation growth compared to non-coated controls (Somaiah et al., 2015; Linsley et al., 2013). While Kilpadi et al., (2001) also suggests that FINC enhances the HA performances in relations to stimulated increased cellular attachment on rough surfaces compared to the smooth metal surfaces.

Jae Jo et al., (2011) reported initial results that appeared to confirm a positive response of cellular attachment in the present of FINC, but they noted that this response faded leading to the conclusion there were no benefits to coating with FINC. These results are different from the results shown here.

Somaiah et al., (2015), results demonstrated that collagen can increase cellular migration, adhesion, proliferation under stressful conditions and increased osteogenic differentiation. However, their results, showed similar results to my study that FINC out preformed both COL1A1 and controls, with increases in metabolic activity and proliferation when compared to the control sample (Somaiah et al., 2015).

### 7.5.3 Alkaline Phosphate Assay

ALP activity is an indicator of osteoblastic activity and widely accepted as a biochemical marker of early mineralisation (Sabokbar et al., 1994). The results presented here indicate that COL1A1 protein may induce earlier osteoblastic differentiation. Which is in contrast to those reported in Somaiah et al., (2015). They who believes that COL1A1 induces osteoinduction even in the absence of other osteoinductive factors.

The high levels of ALP activity on the FINC coated HA compares with Lee et al., (2015) and Ogura et al., (2004) whose studies showed that cells adhered to FINC coated tissue culture plastic, caused an increase in ALP activity compared to cells grown in the absence of FINC. Carins et al., (2010) noted there was an enhanced response in osteoblast-like cellular differentiation and proliferation to the coating FINC onto HA at earlier time points. They noted their results indicated that the addition of FINC on top of the microstructure and roughness, causing increased attachment and enhanced cellular differentiation (Carins et al., 2010).

### 7.5.4 Scanning Electron Microscopy

SEM was used to study the morphology of the cells that have adhered to the BGS surface. By day 7, the surface of the entire disc was colonised with cells, which formed layers. These layers made it challenging to assess the morphology of cells directly attached to the disc surface; however, the fact that cell layers had formed at this time point indicates the high proliferation rate of cells on these surfaces.

Both protein-coated surfaces showed a high amount of mineralisation production by day 28 compared to the control surfaces, where there was limited extracellular matrix nodules formations. However, FINC visually had a higher number of extracellular matrix nodules formation compared to COL1A1.

These nodules were associated with the cells nearby and were often associated with bone formation (Thian et al., 2006). Thian et al., (2006) also noted that the SiHA coated surfaces they investigated could form a carbonate-containing apatite nanocrystalline structure faster than the non-SiHA coated controls when submerged in simulated body fluids. Osteoblast create these nanocomposite structure of bone that was released by ECM, where apatite crystals formed, however precise role that they have in bone formation is mostly unknown (Boonrungsiman et al., 2012). Once formed, these crystallites can grow spontaneously and transform into bone-like apatite the surface of the implant.

### 7.5.5 Limitations

There were limitations to these studies, including pre-coating proteins onto a sintered DD may be different to coating on granules. By creating a sintered DD, it allowed for a comparison of the protein coating but did not allow for an understanding of how vital the graft architecture is for protein binding (Sant et al., 2008). Changes to either the micro/macro architecture or chemistry influence how the proteins interact with the graft (Hutmacher, 2001). It should also be noted that a complex matrix of proteins possibly have a greater impact on cell proliferation and osteoinduction than individual proteins.

## 7.6 Conclusions

The main aim for these experiments was to investigate whether FINC or COL1A1 that have been coated onto sintered discs of HA could induce an increased level of cellular attachment or subsequent osteoinduction of MSCs compared to non-coated HA.

The results demonstrated that the proteins coated HA surfaces could increase metabolic activity compared to the control of non-coated HA surfaces. The FINC appears to have a significantly higher level of ALP compared to COL1A1 and non-coated discs by day 14 ($p$=0.001). FINC protein also appeared visually to cause an increase in the production of extracellular mineralisation nodules compared to other surfaces.

The overall results would indicate that FINC protein-coated HA can enhance the performance of the material compared to COL1A1 control and a non-coated surface.

# Chapter 8

# General Discussion, Contribution to Scientific Research and Proposals for Future Work

## 8.1 Introduction and background

The main aim of this thesis was to investigate the proteins that adhere to different BGS's surfaces and identify which of these proteins have the potential to increase cellular attachment and osteoinduction levels of selected BGS's. The novelty of this thesis included:

1. A comparison was made at a cellular level five commercially available BGS's that have not been previously grouped before.
2. The identification of proteins that adhere to the five different BGS surfaces after being submerged in FCS.
3. New techniques to identify the proteins required the development of new methods to remove the proteins that adhered to the BGS before MS.
4. 106 adhered proteins, which were identified by these techniques. Ranking these proteins could potentially lead to identifying the best proteins that could potentially lead to increasing both cellular attachment and osteogenesis.
5. The final part involved coated a selection of these identified protein onto a BGS to investigate whether it would cause increased cellular attachment and osteogenesis compared to a non-coated control.

The initial experiment for the thesis was to confirm that the cells isolated from ovine bone marrow aspirate were MSCs. This was confirmed via tri-lineage differentiation staining.

## 8.2 Chapter 2 conclusions

The five BGS's investigated had variations in physio-chemical, surface topography, micro- and macro-porosity. These differences were laid out in detail in Table 1.1. The ideal BGS can attract cellular adherence, then proliferate before inducing differentiation of MSCs towards the osteoblasts lineage. The 21-day experiment was designed to enable a comparison between the BGS about cellular metabolic activity, ALP activity, live assay and cellular attachment with SEM.

The analysis of all the results from these experiments indicated that Inductigraft™ showed the top ability to attract the most amount of cells to attach initially and had the highest possible increased metabolic rate and ALP activity when compared with the other four materials and controls.

Inductigraft™ increased activity is due to the combination of SiHA chemical composition and increased strut porosity. The addition of Si ions into the HA lattice has been shown to influence cellular proliferation, differentiation and osteoinduction levels (Gibson et al., 1999; Botelho et al., 2006). Si is essential for life, and Si deficiency has shown to lead to

a decrease in collagen formation in bone (Seaborn and Nielson, 2002). HA materials are enhanced by incorporating silicon into the HA structure, concerning increases bioactivity, enhances bone formation and osteoblast cell activity (Polo-Corrales et al., 2014). Regi and Acros (2004) showed that SiHA had increased bioactivity both during *in vitro* and *in vivo* situations leading to increased interactions between bone and implant, which causes improved osteointegration and the long-term success of the implant.

It has also been demonstrated that the incorporation of Si ions into a phase-pure HA can stimulate osteoblast-like cell activity when compared to stoichiometric HA. This directly affected the biomineralisation processes, cellular differentiation, proliferation, collagen synthesis and calcification during early bone development (Gibson et al., 1999; Lee et al., 2014; Patel et al., 2002). Si has shown to cause higher rates of electronegative surface, and this can aid in effect bone formation, osteoblastic differentiation, and proliferation (Price et al., 2013; Lerner and Liljenqvist, 2013). Coathup et al., (2011) placed increased strut porosity SiCaP into ectopically, lead to significant bone formation compared CaP. They concluded that both are osteoinductive; however, the SiCaP samples had significantly higher amounts of bone formed within the sample and on its surface.

Actifuse™ developed from the same chemical composition as Inductigraft™ but differed in having lower strut porosity. This increased strut porosity has shown to increase bone growth within the graft and earlier neovascularization while being able to maintain structural strength (Campion et al., 2010). Other have shown that increasing the strut porosity will cause surge in osteoinduction and osteointegration levels compared to similar materials with lower porosity (Coathup et al., 2012; Coathup et al., 2012; Nakata et al., 2016; Yka-Soininmaki et al., 2013). Hutchens et al., (2015) study showed that increased strut porosity in SiCaP BGS, that was then placed into ovine distal femoral within critical-sized metaphase defects caused the production of higher amounts of bone formation at early time points.

Coathup et al., (2012) investigated whether increasing the strut porosity of both CaP and SiCaP BGS, and the results showed increased levels of osteoinduction and bone formation in the SiCaP with strut porosity of 30% that were higher than the CaP with matching strut porosity. Again Chan et al., (2012) compared the osteoinductivity of SiCaP biomaterials with porosities of 22.5%, 32% and 46% at 8, 12 and 24 weeks. At 8 weeks showed non-significant differences but at 12 weeks, 46% strut porosity had significantly increased. Finally, at 24 weeks there was a 75-fold increase in the 46% samples compared the rest. Their results indicated that by increasing strut porosity, it could lead to both increased bone formation and bone-implant contact. The results I have shown in in vitro show comparably that increased strut porosity and chemical structure of SiHA can cause these effects at a cellular level.

### 8.3 Chapter 3 conclusions.

Throughout the comparison of the five BGS experiments of chapter 2, it became apparent that there were issues with Orthoss®. This deficiency included failure for cells to adhere to the surface and thrive. Literature reviewing showed conflicting with reports about Orthoss® capabilities. Kouroupis et al., (2013) studies have reported that it is an "excellent natural BGS" which "bone subpopulation can rapidly migrate towards, attach and expand" but negate this with low levels of cellular attachment, proliferation and metabolic activity which will deteriorate over time (El-Jawhari et al., 2016; Kubosch et al., 2016). Tseng et al., (2012) that the sintering process of Orthoss® produces CaO formation, which increases the alkaline pH, and this change hurt cellular survival.

To investigate this matter, two forms of commercially available Orthoss® were selected (block and granules). Both were identical in chemistry and porosity but differed on their overall structure. Again, the results were poor concerning to cellular adhesion and metabolic activity for both forms of Orthoss®. These results are consistent with the reports by El-Jawhari et al., who reported Orthoss® had decreased cellular attachment and proliferation rates compared to the other grafts within their study (El-Jawhari et al., 2016). Kubosch et al. (2016) showed Orthoss® metabolic activity to decrease over time due to the occurrence of cellular death.

To try to explain why the cells were failing to thrive, conditioned media was created using the Orthoss® to explore whether the granules was leaching materials which may have been affecting the potential for cells to adhere. This indicated in the pH reading in chapter 2 that showed DMEM+ removed from Orthoss® had the highest readings. When healthy cells were adhered to tissue culture surface and then Orthoss® conditioned media placed onto these cells, the cells began to go towards apoptosis and eventually died. This lead to the belief that the Orthoss® BGS were producing substances could affect the cells in a negative manner which would correspond with Tseng et al., (2012) result that Orthoss® is releasing CaO that would kill cells.

### 8.4 Chapter 4 conclusions

The initial experiments and previously published studies have indicated that the chemical composition of the BGSs is critical to quality of the bone repair by affecting attachment and osteoinductive potential of the adhering cells (Hing et al., 2007). To investigate the role chemical composition has on inducting osteoinduction two chemical compositions were selected and representing three of the commercially BGS's granules (Synthetic hydroxyapatite (HA) represented ApaPore™, while silicate-substitute hydroxyapatite (SiHA) represented both Actifuse™ and Inductigraft™).

The results of these experiments indicated the sintered SiHA DD promoted higher cellular adherence and metabolic activity when seeded with Ovine MSCs *in vitro*. These

results are in line with the results from chapter 2 into the BGS's and published literature. The results in chapter 2 showed that SiHA materials outperformed HA materials in every experiment. Previous studies have shown that increased bioactivity can be demonstrated with the addition of silicon ions into the HA lattice. These increases apply to cellular adherence, proliferation and osteoinductive potential (Zuo et al., 2008).

### 8.5 Chapter 5 conclusions

The profiles of the protein adherence to the different BGS's is continuously changing as proteins adhere and detach overtime. Different methods to detach proteins from the graft surface and PBS at pH 10 was selected based on a comparison SDS-Page gel that indicated it detached the highest amount. The BCA assay results indicated that the highest protein detachment levels from any surface were those from Orthoss®. These results were unexpected based on the poor performances about the earlier experiments.

Previous studies note that HA attracted fewer proteins to adhere to when compared to SiHA BGS (Guth et al., 2010). The results from both BCA assay and SDS-Page performed in this chapter confirm as the HA material (ApaPore™) had lower protein adherence compared to both grafts composed from SiHA (Actifuse™ and Inductigraft™).

Another result showed that the increased strut porosity of Inductigraft™ meant there was a larger surface area for protein to adhere when compare to Actifuse™. This produced higher protein numbers seen at both 24 hours and 72 hours. These results could also be linked to the increased activity on Inductigraft™ during the *in vitro* experiments of Chapter 2. As reported before proteins can increase the levels of bioactivity and osteoinduction (Guth et al., 2010; Campion et al., 2010). The attachment of proteins to BGS is a critical event, as the approaching cells are attracted to the adhered proteins rather than the graft surfaces (Vroman, 2009; Mager et al., 2011).

### 8.6 Chapter 6 conclusions

Identification of the adhered proteins is critical in mediating further protein attachment, cellular recruitment and the regulation the cellular response to the BGS (Hing et al., 2004; Guth et al., 2010). Proteins detached from the BGS surfaces were identified by TMT™ combined with LC-MS/MS, and through this technique, 106 different proteins were identified as well as their relative amounts on the five different BGS over four time-points. With this data, it was possible to identify the Vroman effect occurring using the relative amount of proteins, which appear to increase and decrease over time, showing an interchange of protein attached to the surface.

After ranking the 106 proteins, the top two candidate proteins identified were FINC and COL1A1. Both these proteins have previously linked to indirectly enhanced cell attachment (Parenteau-Bareil et al., 2010). FINC is well established for its involvement

in cellular adhesion, migration and processes that include wound healing, bone formation, blood coagulation and host defence (Steffens et al., 2012). Coating biomaterials with FINC has been shown to improve the osteogenic differentiation on both titanium and polymer surfaces leading to increased adhesion, cellular differentiation and morphology changes (Chatakun et al., 2014; Lee et al., 2015).

COL1A1 is found in abundance in bone, tendons and commonly used in tissue engineering applications. It is crucial in terms of strength and support of tissues such as cartilage, bone, tendon and skin. Studies show collagen/HA; combination has the ability to potential mimic skeletal bones (Parenteau-Bareil et al., 2010). MSCs, when cultured in the presence of COL1A1, have shown increased levels of ALP activity, osteoblastic differentiation and formed mineralised tissue more quickly (Mizuno et al., 2000).

### 8.7 Chapter 7 conclusions

The top two proteins independently were coated onto the surface sintered discs of HA. These were then compared to control of non-coated HA DD to investigate the proteins influence on their performance concerning osteoconductivity.

FINC coated discs showed significantly higher metabolic activity when compared to both COL1A1 and non-coated control. As discussed, other studies have shown similar results to these (Somaiah et al., 2015; Linsley et al., 2013; Jae Jo et al., 2011; El-Ghannam et al., 1999). Somaiah et al., (2015) showed FINC outperformed both COL1A1 and their controls when they also investigated metabolic activity and proliferation. While El-Ghannam et al., (1999) suggested when bioactive glass are coated in FINC; could form a calcium phosphate layer on the surface of the glass, leading to increased osteoblast cellular adhesion to its surface. The results from Jae Jo et al., (2011) study, showed initial positive response with cellular attachment in the presence of FINC; however, they noted that these initial positive results began to fade with time and the protein-coated samples eventually had similar results to the control.

Concerning ALP activity, the FINC coated DD showed an ability to cause significantly increased ALP levels when compared to both COL1A1 and the non-coated discs by day 14. The ALP levels of the FINC samples compare with Lee et al., (2015) and Ogura et al., (2004) studies, demonstrated that cells adhered to FINC coated tissue culture plastic, had increased ALP activity compared to cells grown in the absence of FINC.

Carins et al., (2010) also noted enhanced response in osteoblast-like cellular differentiation and proliferation to the coating FINC onto HA at earlier time points. The addition of FINC on top of the microstructure and roughness caused an increased attachment and enhanced cellular differentiation when compared to controls. However, my results contrasted those previously performed study by Somaiah et al., (2015), who believes that COL1A1 induces osteoinduction even in the absence of other

osteoinductive factors. These results could indicate that COL1A1 protein may induce earlier osteoblastic differentiation.

### 8.8 Further extension to experiment performed

These include the development of a technique that would enable sintered dense discs, of the other BGS mentioned in this thesis, to be created. This would enable for investigation into all four different chemical composition of the five different BGS investigated in this thesis. This would enable an investigation into the influences their chemistry has at a cellular activity.

The development of a porous bag, with pores that were small enough to enable proteins to only to adhere to the BGS inside the bag, could be used *in vivo*. This would enable an MS investigation of proteins that interact with the BGS with the *in vivo* environment. These proteins could potentially be different from those identified in the *in vitro* studies.

Only two proteins were selected from the investigation of the proteins identified during MS analysis. There is a potential possibility that other proteins identified could lead to a higher positive cellular activity than the ones investigated in this study when adhered to DD. There is also the possibility that a combination of proteins identified could also lead to better results.

At a molecular level, QPCR could be used to look further into the genes responsible for osteogenic differentiation. These genes could potentially have increased expression levels when stimulated by the protein-coated DD.

A critical investigation for the future would be an analysis of the protein-coating to identify the optimal level of protein to adhere to the DD and to identify how long these proteins remained attached to the sintered surfaces.

A long-term prospect would be to investigate placing a protein-coated BGS into an actual fracture site *in vivo* and to measure the potential increase of bone healing compared to the controls. This would lead to further investigations into where freeze-drying the adhered protein-coated surface would enable it to be stored “shelf-ready” and could be “brought back to life” before implantation into patients during surgery.

### 8.9 Conclusion

In conclusion, proteins are critical to the success of BGS. Proteins adherence to a BGS is just as crucial as the physio-chemical, surface topography, micro- and macroporosity of the grafts. These adhering proteins can influence how the cells interact with the graft. They are critical in aiding the healing of bone repair and increasing the ideal BGS, ability to attract cells to adhere to its surface.

**Bibliography**


Aarden, E.M., Nijweide, P.J. and Burger, E.H., 1994. Function of osteocytes in bone. *Journal of cellular biochemistry*, *55*(3), pp.287-299.

Abagnale, G., Steger, M., Nguyen, V.H., Hersch, N., Sechi, A., Joussen, S., Denecke, B., Merkel, R., Hoffmann, B., Dreser, A. and Schnakenberg, U., 2015. Surface topography enhances differentiation of mesenchymal stem cells towards osteogenic and adipogenic lineages. *Biomaterials*, *61*, pp.316-326.

Abhay, S. and Haines, S.J., 1997. Repairing holes in the head: a history of cranioplasty. *Neurosurgery*, *40*(3), pp.588-603

Absolom, D.R., Zingg, W. and Neumann, A.W., 1987. Protein adsorption to polymer particles: role of surface properties. *Journal of biomedical materials research*, *21*(2), pp.161-171.

Accorsi-Mendonça, T., Conz, M.B., Barros, T.C., Sena, de Soares, L.Á., Almeida,G. & Granjeiro, J.M. (2008). Physicochemical characterization of two deproteinized bovine xenografts. *Brazilian Oral Research*, *22*(1), 5-10.

Adamzyk, C., Emonds, T., Falkenstein, J., Tolba, R., Jahnen-Dechent, W., Lethaus, B. and Neuss, S., 2013. Different culture media affect proliferation, surface epitope expression, and differentiation of ovine MSC. *Stem cells international*, *2013*.

Albrektsson, T. and Johansson, C., 2001. Osteoinduction, osteoconduction and osseointegration. *European spine journal*, *10*(2), pp.S96-S101.

Alford, A.I., Terkhorn, S.P., Reddy, A.B. and Hankenson, K.D., 2010. Thrombospondin-2 regulates matrix mineralization in MC3T3-E1 pre-osteoblasts. *Bone*, *46*(2), pp.464-471.

Allen, M. R., Iwata, K., Phipps, R., & Burr, D. B. (2006). Alterations in canine vertebral bone turnover, microdamage accumulation, and biomechanical properties following 1-year treatment with clinical treatment doses of risedronate or alendronate. *Bone*. 39(4): 872-879.

Allen, M.R., Iwata, K., Phipps, R. and Burr, D.B., 2006. Alterations in canine vertebral bone turnover, microdamage accumulation, and biomechanical properties following 1-year treatment with clinical treatment doses of risedronate or alendronate. *Bone*, *39*(4), pp.872-879.

Amini, A.R., Laurencin, C.T. and Nukavarapu, S.P., 2012. Bone tissue engineering: recent advances and challenges. *Critical Reviews™ in Biomedical Engineering*, *40*(5).

Amini, A.A. and Nair, L.S., 2013. Evaluation of the bioactivity of recombinant human lactoferrins toward murine osteoblast-like cells for bone tissue engineering. *Tissue Engineering Part A*, *19*(9-10), pp.1047-1055.

Anderson, J.M. and Jones, J.A., 2007. Phenotypic dichotomies in the foreign body reaction. *Biomaterials*, *28*(34), pp.5114-5120.

Anh, D.J., Dimai, H.P., Hall, S.L. and Farley, J.R., 1998. Skeletal alkaline phosphatase activity is primarily released from human osteoblasts in an insoluble form, and the net release is inhibited by calcium and skeletal growth factors. *Calcified tissue international*, *62*(4), pp.332-340.

Annaz, B., Hing, K.A., Kayser, M., Buckland, T. and Silvio, L.D., 2004. Porosity variation in hydroxyapatite and osteoblast morphology: a scanning electron microscopy study. *Journal of Microscopy*, *215*(1), pp.100-110.

Anselme, K. and Bigerelle, M., 2011. Role of materials surface topography on mammalian cell response. *International Materials Reviews*, *56*(4), pp.243-266.

Anselme, K., 2000. Osteoblast adhesion on biomaterials. *Biomaterials*, *21*(7), pp.667-681.

Arcos, D., Sanchez-Salcedo, S., Izquierdo-Barba, I., Ruiz, L., Gonzalez-Calbet, J. and Vallet-Regí, M., 2006. Crystallochemistry, textural properties, and in vitro biocompatibility of different silicon-doped calcium phosphates. *Journal of Biomedical Materials Research Part A: An Official Journal of The Society for Biomaterials, The Japanese Society for Biomaterials, and The Australian Society for Biomaterials and the Korean Society for Biomaterials*, *78*(4), pp.762-771.

Ashman, O. and Phillips, A.M., 2013. Treatment of non-unions with bone defects: which option and why?. *Injury*, *44*, pp.S43-S45.
Athanassiou, G. and Deligianni, D., 2001. Adhesion strength of individual human bone marrow cells to fibronectin. Integrin β 1-mediated adhesion. *Journal of Materials Science: Materials in Medicine*, *12*(10-12), pp.965-970.
Aubin, J.E., 2001. Regulation of osteoblast formation and function. *Reviews in Endocrine and Metabolic Disorders*, *2*(1), pp.81-94.
Augat, P. and Schorlemmer, S., 2006. The role of cortical bone and its microstructure in bone strength. *Age and ageing*, *35*(suppl_2), pp.ii27-ii31.
Augello, A. and De Bari, C., 2010. The regulation of differentiation in mesenchymal stem cells. *Human gene therapy*, *21*(10), pp.1226-1238.
Ayobian-Markazi, N., Fourootan, T. and Kharazifar, M.J., 2012. Comparison of cell viability and morphology of a human osteoblast-like cell line (SaOS-2) seeded on various bone substitute materials: An in vitro study. *Dental research journal*, *9*(1), p.86.
Babaie, E., Lin, B. and Bhaduri, S.B., 2017. A new method to produce macroporous Mg-phosphate bone growth substitutes. *Materials Science and Engineering: C*, *75*, pp.602-609.
Babiker, H., 2013. Bone graft materials in fixation of orthopaedic implants in sheep. *Danish medical journal*, *60*(7), pp.B4680-B4680.
Bagher, Z., Rajaei, F., and Shokrgozar, M., 2012. Comparative Study of Bone Repair Using Porous Hydroxyapatite/ β-Tricalcium Phosphate and Xenograft Scaffold in Rabbits with Tibia Defect. Iran Biomed Journal, 16(1), pp.18-24.
Bajpai, A.K., 2007. Blood protein adsorption onto macroporous semi-interpenetrating polymer networks (IPNs) of poly (ethylene glycol) (PEG) and poly (2-hydroxyethyl methacrylate) (PHEMA) and assessment of in vitro blood compatibility. *Polymer International*, *56*(2), pp.231-244.
Bandyopadhyay-Ghosh, S., 2008. Bone as a collagen-hydroxyapatite composite and its repair. *Trends Biomaterial Artif Organs*, *22*(2), pp.116-124.
Barradas, A.M., Yuan, H., van Blitterswijk, C.A. and Habibovic, P., 2011. Osteoinductive biomaterials: current knowledge of properties, experimental models and biological mechanisms. *Eur Cell Mater*, *21*(407), p.29.
Bauer, T.W. and Muschler, G.F., 2000. Bone graft materials: an overview of the basic science. *Clinical Orthopaedics and Related Research®*, *371*, pp.10-27.
Best, S., Sim, B., Kayser, M. and Downes, S., 1997. The dependence of osteoblastic response on variations in the chemical composition and physical properties of hydroxyapatite. *Journal of Materials Science: Materials in Medicine*, *8*(2), pp.97-103.
Bi, M., Han, H., Dong, S., Zhang, Y., Xu, W., Zhu, B., Wang, J., Zhou, Y. and Ding, J., 2018. Collagen-coated poly (lactide-co-glycolide)/hydroxyapatite scaffold incorporated with DGEA peptide for synergistic repair of skull defect. *Polymers*, *10*(2), p.109.
Bignon, A., Chouteau, J., Chevalier, J., Fantozzi, G., Carret, J.P., Chavassieux, P., Boivin, G., Melin, M. and Hartmann, D., 2003. Effect of micro-and macroporosity of bone substitutes on their mechanical properties and cellular response. *Journal of Materials Science: Materials in Medicine*, *14*(12), pp.1089-1097.
Billström, G.H., Blom, A.W., Larsson, S. and Beswick, A.D., 2013. Application of scaffolds for bone regeneration strategies: current trends and future directions. *Injury*, *44*, pp.S28-S33.
Blair, H.C., Larrouture, Q.C., Li, Y., Lin, H., Beer-Stoltz, D., Liu, L., Tuan, R.S., Robinson, L.J., Schlesinger, P.H. and Nelson, D.J., 2017. Osteoblast differentiation and bone matrix formation in vivo and in vitro. *Tissue Engineering Part B: Reviews*, *23*(3), pp.268-280.
Blair, H.C., 1998. How the osteoclast degrades bone. *Bioessays*, *20*(10), pp.837-846.
Blokhuis, T.J. and Arts, J.C., 2011. Bioactive and osteoinductive bone graft substitutes definitions, facts and myths. *Injury*, *42*, pp.S26-S29.

Bohner, M., 2009. Silicon-substituted calcium phosphates–a critical view. *Biomaterials*, *30*(32), pp.6403-6406.
Bonewald, L.F., 2007. Osteocytes as dynamic multifunctional cells. *Annals of the New York Academy of Sciences*, *1116*(1), pp.281-290.
Boonrungsiman, S., Gentleman, E., Carzaniga, R., Evans, N.D., McComb, D.W., Porter, A.E. and Stevens, M.M., 2012. The role of intracellular calcium phosphate in osteoblast-mediated bone apatite formation. *Proceedings of the National Academy of Sciences*, *109*(35), pp.14170-14175.
Boskey, A.L. and Paschalis, E., 2000. Matrix proteins and biomineralization. *Bone engineering. Toronto: em squared*, pp.44-61.
Boskey, A.L., Spevak, L., Paschalis, E., Doty, S.B. and McKee, M.D., 2002. Osteopontin deficiency increases mineral content and mineral crystallinity in mouse bone. *Calcified tissue international*, *71*(2), pp.145-154.
Boskey, A.L., 2013. Bone composition: relationship to bone fragility and antiosteoporotic drug effects. *BoneKEy reports*, *2*.
Botelho, C.M., Brooks, R.A., Best, S.M., Lopes, M.A., Santos, J.D., Rushton, N. and Bonfield, W., 2006. Human osteoblast response to silicon-substituted hydroxyapatite. *Journal of Biomedical Materials Research Part A: An Official Journal of The Society for Biomaterials, The Japanese Society for Biomaterials, and The Australian Society for Biomaterials and the Korean Society for Biomaterials*, *79*(3), pp.723-730.
Boyce, B.F. and Xing, L., 2008. Functions of RANKL/RANK/OPG in bone modeling and remodeling. *Archives of biochemistry and biophysics*, *473*(2), pp.139-146.
Boyce, B., Yao, Z. and Xing, L., 2009. Osteoclasts have multiple roles in bone in addition to bone resorption. *Critical Reviews™ in Eukaryotic Gene Expression*, *19*(3).
Boxall S., Jones E. (2015) The Use of Multiparameter Flow Cytometry and Cell Sorting to Characterize Native Human Bone Marrow Mesenchymal Stem Cells (MSC). In: Rich I. (eds) Stem Cell Protocols. *Methods in Molecular Biology (Methods and Protocols*), vol 1235. Humana Press, New York, NY
Brandoff, J.F., Silber, J.S. and Vaccaro, A.R., 2008. Contemporary alternatives to synthetic bone grafts for spine surgery. *American journal of orthopedics (Belle Mead, NJ)*, *37*(8), pp.410-414.
Brash, J.L. and Lyman, D.J., 1969. Adsorption of plasma proteins in solution to uncharged, hydrophobic polymer surfaces. *Journal of biomedical materials research*, *3*(1), pp.175-189.
Brown, J.M., Archer, A.J., Pfau, J.C. and Holian, A., 2003. Silica accelerated systemic autoimmune disease in lupus-prone New Zealand mixed mice. *Clinical & Experimental Immunology*, *131*(3), pp.415-421.
Buckwalter, J.A., Glimcher, M.J., Cooper, R.R. and Recker, R., 1996. Bone biology. I: Structure, blood supply, cells, matrix, and mineralization. *Instructional course lectures*, *45*, p.371.
Cairns, M.L., Meenan, B.J., Burke, G.A. and Boyd, A.R., 2010. Influence of surface topography on osteoblast response to fibronectin-coated calcium phosphate thin films. *Colloids and Surfaces B: Biointerfaces*, *78*(2), pp.283-290.
Cairns, M.L., Meenan, B.J., Burke, G.A. and Boyd, A.R., 2008. Effect of nanoscale topography on fibronectin adsorption to sputter-deposited calcium phosphate thin films. *International Journal of Nano and Biomaterials*, *1*(3), pp.280-298.
Campana, V., Milano, G., Pagano, E., Barba, M., Cicione, C., Salonna, G., Lattanzi, W. and Logroscino, G., 2014. Bone substitutes in orthopaedic surgery: from basic science to clinical practice. *Journal of Materials Science: Materials in Medicine*, *25*(10), pp.2445-2461.
Campbell, A.A., 2003. Bioceramics for implant coatings. *Materials today*, *6*(11), pp.26-30.
Canillas, M., Pena, P., Antonio, H. and Rodríguez, M.A., 2017. Calcium phosphates for biomedical applications. *Boletín de la Sociedad Española de Cerámica y Vidrio*, *56*(3), pp.91-112.

Caplan, A.I., 1991. Mesenchymal stem cells. *Journal of orthopaedic research*, *9*(5), pp.641-650.
Carlisle, E.M., 2008. Silicon as an essential trace element in animal nutrition. *Silicon biochemistry*, *703*, p.123.
Carlisle, E.M., 1980. A silicon requirement for normal skull formation in chicks. *The Journal of nutrition*, *110*(2), pp.352-359.
Carlisle, E.M., 1980. Biochemical and morphological changes associated with long bone abnormalities in silicon deficiency. *The Journal of nutrition*, *110*(5), pp.1046-1056.
Carsons, S.E., Santiago-Schwarz, F. and Diola, C., 2000. Detection and quantitation of stem cell factor (kit ligand) in the synovial fluid of patients with rheumatic disease. *The Journal of rheumatology*, *27*(12), pp.2798-2800.
Castagna, V., 2014. Doctoral thesis, Queen Mary University of London.
Castagna, V., Sullivan A., Hing K. (2012) Environmental Sensitivity of Fibronectin Adsorption to Stoichiometric and Silicate Substituted Hydroxyapatite Bone Graft Substitutes, ORS Conference.
Castano-Izquierdo, H., Álvarez-Barreto, J., Dolder, J.V.D., Jansen, J.A., Mikos, A.G. and Sikavitsas, V.I., 2007. Pre-culture period of mesenchymal stem cells in osteogenic media influences their in vivo bone forming potential. *Journal of biomedical materials research Part A*, *82*(1), pp.129-138.
Champion, E., 2013. Sintering of calcium phosphate bioceramics. *Acta biomaterialia*, *9*(4), pp.5855-5875.
Chan, O., Coathup, M.J., Nesbitt, A., Ho, C.Y., Hing, K.A., Buckland, T., Campion, C. and Blunn, G.W., 2012. The effects of microporosity on osteoinduction of calcium phosphate bone graft substitute biomaterials. *Acta biomaterialia*, *8*(7), pp.2788-2794.
Charriere, G., Bejot, M., Schnitzler, L., Ville, G. and Hartmann, D.J., 1989. Reactions to a bovine collagen implant: Clinical and immunologic study in 705 patients. *Journal of the American Academy of Dermatology*, *21*(6), pp.1203-1208.
Chatakun, P., Núñez-Toldrà, R., López, E.D., Gil-Recio, C., Martínez-Sarrà, E., Hernández-Alfaro, F., Ferrés-Padró, E., Giner-Tarrida, L. and Atari, M., 2014. The effect of five proteins on stem cells used for osteoblast differentiation and proliferation: a current review of the literature. *Cellular and Molecular Life Sciences*, *71*(1), pp.113-142.
Chen, Z.F., Darvell, B.W. and Leung, V.H., 2004. Hydroxyapatite solubility in simple inorganic solutions. *Archives of oral biology*, *49*(5), pp.359-367.
Chou, L.B., Mann, R.A., Coughlin, M.J., III, W.T.M. and Mizel, M.S., 2007. Stress fracture as a complication of autogenous bone graft harvest from the distal tibia. *Foot & ankle international*, *28*(2), pp.199-201.
Clarke, B., 2008. Normal bone anatomy and physiology. *Clinical journal of the American Society of Nephrology*, *3*(Supplement 3), pp.S131-S139.
Coathup, M.J., Cai, Q., Campion, C., Buckland, T. and Blunn, G.W., 2013. The effect of particle size on the osteointegration of injectable silicate-substituted calcium phosphate bone substitute materials. *Journal of Biomedical Materials Research Part B: Applied Biomaterials*, *101*(6), pp.902-910.
Coathup, M.J., Hing, K.A., Samizadeh, S., Chan, O., Fang, Y.S., Campion, C., Buckland, T. and Blunn, G.W., 2012. Effect of increased strut porosity of calcium phosphate bone graft substitute biomaterials on osteoinduction. *Journal of Biomedical Materials Research Part A*, *100*(6), pp.1550-1555.
Colnot, C., 2011. Cell sources for bone tissue engineering: insights from basic science. *Tissue Engineering Part B: Reviews*, *17*(6), pp.449-457.
Combes, C. and Rey, C., 2002. Adsorption of proteins and calcium phosphate materials bioactivity. *Biomaterials*, *23*(13), pp.2817-2823.
Combes, C., Cazalbou, S. and Rey, C., 2016. Apatite biominerals. *Minerals*, *6*(2), p.34.
Compston, J.E., 2002. Bone marrow and bone: a functional unit. *Journal of Endocrinology*, *173*(3), pp.387-394.
Costa, A.G., Walker, M.D., Zhang, C.A., Cremers, S., Dworakowski, E., McMahon, D.J., Liu, G. and Bilezikian, J.P., 2013. Circulating sclerostin levels and markers of bone

turnover in Chinese-American and white women. *The Journal of Clinical Endocrinology & Metabolism*, *98*(12), pp.4736-4743.
Daculsi, G., Fellah, B.H., Miramond, T. and Durand, M., 2013. Osteoconduction, Osteogenicity, Osteoinduction, what are the fundamental properties for a smart bone substitutes. *Irbm*, *34*(4-5), pp.346-348.
Damien, E., Hing, K., Saeed, S. and Revell, P.A., 2003. A preliminary study on the enhancement of the osteointegration of a novel synthetic hydroxyapatite scaffold in vivo. *Journal of Biomedical Materials Research Part A: An Official Journal of The Society for Biomaterials, The Japanese Society for Biomaterials, and The Australian Society for Biomaterials and the Korean Society for Biomaterials*, *66*(2), pp.241-246.
De Godoy, R.F., Hutchens, S., Campion, C. and Blunn, G., 2015. Silicate-substituted calcium phosphate with enhanced strut porosity stimulates osteogenic differentiation of human mesenchymal stem cells. *Journal of Materials Science: Materials in Medicine*, *26*(1), p.54.
Dee, K.C., Puleo, D.A. and Bizios, R., 2002. Protein-surface interactions. *An introduction to tissue-biomaterial interactions. John Wiley*, pp.37-52.
Deligianni, D.D., Katsala, N.D., Koutsoukos, P.G. and Missirlis, Y.F., 2000. Effect of surface roughness of hydroxyapatite on human bone marrow cell adhesion, proliferation, differentiation and detachment strength. *Biomaterials*, *22*(1), pp.87-96.
Delloye, C., Cornu, O., Druez, V. and Barbier, O., 2007. Bone allografts: what they can offer and what they cannot. *The Journal of bone and joint surgery. British volume*, *89*(5), pp.574-580.
Dimitriou, R., Jones, E., McGonagle, D. and Giannoudis, P.V., 2011. Bone regeneration: current concepts and future directions. *BMC medicine*, *9*(1), p.66.
Ding, K.H., Wang, Z.Z., Hamrick, M.W., Deng, Z.B., Zhou, L., Kang, B., Yan, S.L., She, J.X., Stern, D.M., Isales, C.M. and Mi, Q.S., 2006. Disordered osteoclast formation in RAGE-deficient mouse establishes an essential role for RAGE in diabetes related bone loss. *Biochemical and biophysical research communications*, *340*(4), pp.1091-1097.
Ding, K.H., Wang, Z.Z., Hamrick, M.W., Deng, Z.B., Zhou, L., Kang, B., Yan, S.L., She, J.X., Stern, D.M., Isales, C.M. and Mi, Q.S., 2006. Disordered osteoclast formation in RAGE-deficient mouse establishes an essential role for RAGE in diabetes related bone loss. *Biochemical and biophysical research communications*, *340*(4), pp.1091-1097.
Dorati, R., Colonna, C., Genta, I., Bruni, G., Visai, L. and Conti, B., 2014. Preparation and characterization of an advanced medical device for bone regeneration. *AAPS PharmSciTech*, *15*(1), pp.75-82.
Dorati, R., DeTrizio, A., Modena, T., Conti, B., Benazzo, F., Gastaldi, G. and Genta, I., 2017. Biodegradable scaffolds for bone regeneration combined with drug-delivery systems in osteomyelitis therapy. *Pharmaceuticals*, *10*(4), p.96.
Dorozhkin, S.V., 2010. Calcium orthophosphates as bioceramics: state of the art. *Journal of functional biomaterials*, *1*(1), pp.22-107.
Dowling, P. and Clynes, M. (2011), Conditioned media from cell lines: A complementary model to clinical specimens for the discovery of disease-specific biomarkers. *Proteomics, 11*, pp.794-804.
Ducheyne, P. and Qiu, Q., 1999. Bioactive ceramics: the effect of surface reactivity on bone formation and bone cell function. *Biomaterials*, *20*(23-24), pp.2287-2303.
Ducheyne, P., Mauck, R.L. and Smith, D.H., 2012. Biomaterials in the repair of sports injuries. *Nature materials*, *11*(8), p.652.
Erbe E, Clineff T, Bagga C, Nagvajara G, Koblish A and Brown S, 2005. Bone graft substitute. U.S. Patent WO2005074614, 2005.
El-Ghannam, A., Ducheyne, P. and Shapiro, I.M., 1999. Effect of serum proteins on osteoblast adhesion to surface-modified bioactive glass and hydroxyapatite. *Journal of Orthopaedic Research*, *17*(3), pp.340-345.

El-Jawhari, J.J., Sanjurjo-Rodríguez, C., Jones, E. and Giannoudis, P.V., 2016. Collagen-containing scaffolds enhance attachment and proliferation of non-cultured bone marrow multipotential stromal cells. *Journal of Orthopaedic Research*, *34*(4), pp.597-606.

Fang, F., Satulovsky, J. and Szleifer, I., 2005. Kinetics of protein adsorption and desorption on surfaces with grafted polymers. *Biophysical journal*, *89*(3), pp.1516-1533.

Faour, O., Dimitriou, R., Cousin, C.A. and Giannoudis, P.V. 2011.The use of bone graft substitutes in large cancellous void: any specific needs?. Injury. Sep (42), Suppl 2: S87-90.

Fernandez de Grado G, Keller L, Idoux-Gillet Y, Wagner Q, Musset AM, Benkirane-Jessel N, Bornert F, and Offner D., 2018. Bone substitutes: a review of their characteristics, clinical use, and perspectives for large bone defects management. *J Tissue Eng*, 9 (1-18).

Finehout, E.J. and Lee, K.H., 2003. Comparison of automated in-gel digest methods for femtomole level samples. *Electrophoresis*, *24*(19-20), pp.3508-3516.

Florencio-Silva, R., Sasso, G.R.D.S., Sasso-Cerri, E., Simões, M.J. and Cerri, P.S., 2015. Biology of bone tissue: structure, function, and factors that influence bone cells. *BioMed research international*, *2015*.

Franceschi, R.T., 1999. The developmental control of osteoblast-specific gene expression: role of specific transcription factors and the extracellular matrix environment. *Critical Reviews in Oral Biology & Medicine*, *10*(1), pp.40-57.

Fratzl, P., Gupta, H.S., Paschalis, E.P. and Roschger, P., 2004. Structure and mechanical quality of the collagen–mineral nano-composite in bone. *Journal of materials chemistry*, *14*(14), pp.2115-2123.

Friedenstein, A.J., Chailakhjan, R.K. and Lalykina, K.S., 1970. The development of fibroblast colonies in monolayer cultures of guinea-pig bone marrow and spleen cells. *Cell Proliferation*, *3*(4), pp.393-403.

Gadaleta, S.J., Paschalis, E.P., Betts, F., Mendelsohn, R. and Boskey, A.L., 1996. Fourier transform infrared spectroscopy of the solution-mediated conversion of amorphous calcium phosphate to hydroxyapatite: new correlations between X-ray diffraction and infrared data. *Calcified tissue international*, *58*(1), pp.9-16.

Gao, P., Zhang, H., Liu, Y., Fan, B., Li, X., Xiao, X., Lan, P., Li, M., Geng, L., Liu, D. and Yuan, Y., 2016. Beta-tricalcium phosphate granules improve osteogenesis in vitro and establish innovative osteo-regenerators for bone tissue engineering in vivo. *Scientific reports*, *6*, p.23367.

Garcia, R., Raad, I., Abi-Said, D., Bodey, G., Champlin, R., Tarrand, J., Hill, L.A., Umphrey, J., Neumann, J., Englund, J. and Whimbey, E., 1997. Nosocomial Respiratory Syncytial Virus Infections Prevention and Control in Bone Marrow Transplant Patients. *Infection Control & Hospital Epidemiology*, *18*(6), pp.412-416.

Garcia-Castro, J., Trigueros, C., Madrenas, J., Perez-Simon, J.A., Rodriguez, R. and Menendez, P., 2008. Mesenchymal stem cells and their use as cell replacement therapy and disease modelling tool. *Journal of cellular and molecular medicine*, *12*(6b), pp.2552-2565.

Garg, P., Mazur, M.M., Buck, A.C., Wandtke, M.E., Liu, J. and Ebraheim, N.A., 2017. Prospective review of mesenchymal stem cells differentiation into osteoblasts. *Orthopaedic surgery*, *9*(1), pp.13-19.

Garin, C. and Boutrand, S., 2016. Natural hydroxyapatite as a bone graft extender for posterolateral spine arthrodesis. *International orthopaedics*, *40*(9), pp.1875-1882.

Gaston, M.S. and Simpson, A.H.R.W., 2007. Inhibition of fracture healing. *The Journal of bone and joint surgery. British volume*, *89*(12), pp.1553-1560.

Gerstenfeld, L.C., Cullinane, D.M., Barnes, G.L., Graves, D.T. and Einhorn, T.A., 2003. Fracture healing as a post-natal developmental process: molecular, spatial, and temporal aspects of its regulation. *Journal of cellular biochemistry*, *88*(5), pp.873-884.

Gevaert, K., Impens, F., Ghesquière, B., Van Damme, P., Lambrechts, A. and Vandekerckhove, J., 2008. Stable isotopic labeling in proteomics. *Proteomics*, *8*(23-24), pp.4873-4885.

Giannoudis, P.V. and Pountos, I., 2005. Tissue regeneration: the past, the present and the future. *Injury*, *36*(4), pp.S2-S5.

Giannoudis, P.V., Dinopoulos, H. and Tsiridis, E., 2005. Bone substitutes: an update. *Injury*, *36*(3), pp.S20-S27.

Gibson, I.R., Best, S.M. and Bonfield, W., 2002. Effect of silicon substitution on the sintering and microstructure of hydroxyapatite. *Journal of the American Ceramic Society*, *85*(11), pp.2771-2777.

Gibson, I.R., Best, S.M. and Bonfield, W., 1999. Chemical characterization of silicon-substituted hydroxyapatite. *Journal of Biomedical Materials Research: An Official Journal of The Society for Biomaterials, The Japanese Society for Biomaterials, and The Australian Society for Biomaterials*, *44*(4), pp.422-428.

Gibson, I.R., Rehman, I., Best, S.M. and Bonfield, W., 2000. Characterization of the transformation from calcium-deficient apatite to β-tricalcium phosphate. *Journal of materials science: materials in medicine*, *11*(9), pp.533-539.

Gilbert, S.F., 2000. Osteogenesis: the development of bones. *Developmental biology*, *6*.

Goldring, S.R., 2015. The osteocyte: key player in regulating bone turnover. *RMD open*, *1*(Suppl 1), p.e000049.

Golub, E.E. and Boesze-Battaglia, K., 2007. The role of alkaline phosphatase in mineralization. *Current Opinion in Orthopaedics*, *18*(5), pp.444-448.

Goodison, S., Urquidi, V. and Tarin, D., 1999. CD44 cell adhesion molecules. *Molecular Pathology*, *52*(4), p.189.

Goodman, P.A., Li, H., Gao, Y., Lu, Y.F., Stenger-Smith, J.D. and Redepenning, J., 2013. Preparation and characterization of high surface area, high porosity carbon monoliths from pyrolyzed bovine bone and their performance as supercapacitor electrodes. *Carbon*, *55*, pp.291-298.

Goodman, S.B., Yao, Z., Keeney, M. and Yang, F., 2013. The future of biologic coatings for orthopaedic implants. *Biomaterials*, *34*(13), pp.3174-3183.

Gough, J. E., Notingher, I., & Hench, L. L. (2004). Osteoblast attachment and mineralized nodule formation on rough and smooth 45S5 bioactive glass monoliths. *Journal of Biomedical Materials Research Part A*, *68*(4), 640-650.

Grabowski, G. and Cornett, C.A., 2013. Bone graft and bone graft substitutes in spine surgery: current concepts and controversies. *JAAOS-Journal of the American Academy of Orthopaedic Surgeons*, *21*(1), pp.51-60.

Graham, J.M., Ayati, B.P., Holstein, S.A. and Martin, J.A., 2013. The role of osteocytes in targeted bone remodeling: a mathematical model. *PloS one*, *8*(5), p.e63884.

Green, J.R., Nemzek, J.A., Arnoczky, S.P., Johnson, L.L. and Balas, M.S., 1999. The effect of bone compaction on early fixation of porous-coated implants. *The Journal of arthroplasty*, *14*(1), pp.91-97.

Greenspan, D.C., 2012. Comparison of a synthetic and bovine derived hydroxyapatite bone graft substitute. *Zimmer Dental Inc*, pp.1-4.

Greenwald, A., Boden, S., Goldberg, V., Khan, Y., Laurencin, C. and Rosier, R. Bone-Graft Substitutes: Facts, Fictions, and Applications. *The Journal of Bone and Joint Surgery-American Volume.* 83(): pp.98-103.

Guth, K., Campion, C., Buckland, T. and Hing, K.A., 2011. Effects of serum protein on ionic exchange between culture medium and microporous hydroxyapatite and silicate-substituted hydroxyapatite. *Journal of Materials Science: Materials in Medicine*, *22*(10), p.2155.

Guth, K., Campion, C., Buckland, T. and Hing, K.A., 2010. Surface physiochemistry affects protein adsorption to stoichiometric and silicate-substituted microporous hydroxyapatites. *Advanced Engineering Materials*, *12*(4), pp.B113-B121.

Guo, Z., Li, H., Li, X., Yu, X., Wang, H., Tang, P., et al. (2006). *In vitro* characteristics and *in vivo* immunosuppressive activity of compact bone-derived murine mesenchymal progenitor cells. *Stem Cells* 24, 992–1000.

Habibovic, P., Van der Valk, C.M., Van Blitterswijk, C.A., De Groot, K. and Meijer, G., 2004. Influence of octacalcium phosphate coating on osteoinductive properties of biomaterials. *Journal of Materials Science: Materials in Medicine*, *15*(4), pp.373-380.

Habibovic, P., Bassett, D.C., Doillon, C.J., Gerard, C., McKee, M.D. and Barralet, J.E., 2010. Collagen biomineralization in vivo by sustained release of inorganic phosphate ions. *Advanced materials*, *22*(16), pp.1858-1862.

Habibovic, P., Juhl, M.V., Clyens, S., Martinetti, R., Dolcini, L., Theilgaard, N. and Van Blitterswijk, C.A., 2010. Comparison of two carbonated apatite ceramics in vivo. *Acta biomaterialia*, *6*(6), pp.2219-2226.

Habraken, W., Habibovic, P., Epple, M. and Bohner, M., 2016. Calcium phosphates in biomedical applications: materials for the future?. *Materials Today*, *19*(2), pp.69-87.

Häkkinen, J., Vincic, G., Månsson, O., Wårell, K. and Levander, F., 2009. The proteios software environment: an extensible multiuser platform for management and analysis of proteomics data. *Journal of proteome research*, *8*(6), pp.3037-3043.

Harding, I.S., Rashid, N. and Hing, K.A., 2005. Surface charge and the effect of excess calcium ions on the hydroxyapatite surface. *Biomaterials*, *26*(34), pp.6818-6826.

Hayes, A.R., Brungs, D. and Pavlakis, N., 2018. Osteoclast inhibitors to prevent bone metastases in men with high-risk, non-metastatic prostate cancer: A systematic review and meta-analysis. *PloS one*, *13*(1), p.e0191455.

Heaney, R.P. and Layman, D.K., 2008. Amount and type of protein influences bone health. *The American journal of clinical nutrition*, *87*(5), pp.1567S-1570S.

Hedges, R.E. and Van Klinken, G.J., 1992. A review of current approaches in the pretreatment of bone for radiocarbon dating by AMS. *Radiocarbon*, *34*(3), pp.279-291.

Heidari, B., Shirazi, A., Akhondi, M.M., Hassanpour, H., Behzadi, B., Naderi, M.M., Sarvari, A. and Borjian, S., 2013. Comparison of proliferative and multilineage differentiation potential of sheep mesenchymal stem cells derived from bone marrow, liver, and adipose tissue. *Avicenna journal of medical biotechnology*, *5*(2), p.104.

Hench L.L., 1998. Biomaterials: a forecast for the future. *Biomaterials*, 19 (16), p. 1419-1423.

Hench, L.L. and Polak, J.M., 2002. Third-generation biomedical materials. *Science*, *295*(5557), pp.1014-1017.

Henkel, J., Woodruff, M.A., Epari, D.R., Steck, R., Glatt, V., Dickinson, I.C., Choong, P.F., Schuetz, M.A. and Hutmacher, D.W., 2013. Bone regeneration based on tissue engineering conceptions—a 21st century perspective. *Bone research*, *1*, p.216.

Henriksen, S.S., Ding, M., Juhl, M.V., Theilgaard, N. and Overgaard, S., 2011. Mechanical strength of ceramic scaffolds reinforced with biopolymers is comparable to that of human bone. *Journal of Materials Science: Materials in Medicine*, *22*(5), p.1111.

Hing, K.A., 2004. Bone repair in the twenty–first century: biology, chemistry or engineering?. *Philosophical Transactions of the Royal Society of London. Series A: Mathematical, Physical and Engineering Sciences*, *362*(1825), pp.2821-2850.

Hing, K.A., Annaz, B., Saeed, S., Revell, P.A. and Buckland, T., 2005. Microporosity enhances bioactivity of synthetic bone graft substitutes. *Journal of Materials Science: Materials in Medicine*, *16*(5), pp.467-475.

Hing, K.A., Wilson, L.F. and Buckland, T., 2007. Comparative performance of three ceramic bone graft substitutes. *The Spine Journal*, *7*(4), pp.475-490.

Hing, K.A., 2005. Bioceramic bone graft substitutes influence of porosity and chemistry. *International journal of applied ceramic technology*, *2*(3), pp.184-199.

Hing, K.A., Revell, P.A., Smith, N. and Buckland, T., 2006. Effect of silicon level on rate, quality and progression of bone healing within silicate-substituted porous hydroxyapatite scaffolds. *Biomaterials*, *27*(29), pp.5014-5026.

Hing, K.A., Best, S.M., Tanner, K.E., Bonfield, W. and Revell, P.A., 2004. Mediation of bone ingrowth in porous hydroxyapatite bone graft substitutes. *Journal of*

*Biomedical Materials Research Part A: An Official Journal of The Society for Biomaterials, The Japanese Society for Biomaterials, and The Australian Society for Biomaterials and the Korean Society for Biomaterials*, *68*(1), pp.187-200.

Hirsh, S.L., McKenzie, D.R., Nosworthy, N.J., Denman, J.A., Sezerman, O.U. and Bilek, M.M., 2013. The Vroman effect: competitive protein exchange with dynamic multilayer protein aggregates. *Colloids and Surfaces B: Biointerfaces*, *103*, pp.395-404.

Ho, C.S., Lam, C.W.K., Chan, M.H.M., Cheung, R.C.K., Law, L.K., Lit, L.C.W., Ng, K.F., Suen, M.W.M. and Tai, H.L., 2003. Electrospray ionisation mass spectrometry: principles and clinical applications. *The Clinical Biochemist Reviews*, *24*(1), p.3.

Hojo, H., Ohba, S. and Chung, U.I., 2015. Signaling pathways regulating the specification and differentiation of the osteoblast lineage. *Regenerative Therapy*, *1*, pp.57-62.

Horbett, T.A., 2004. The role of adsorbed proteins in tissue response to biomaterials. *Biomaterials science: an introduction to materials in medicine*, *2*, pp.237-246.

V Hogan, M., N Irvine, J., Ma, R., James, R., F El-Amin, S. and Cui, Q., 2012. Recent patents in bone graft substitute for bone, tendon, and ligament reconstruction. *Recent Patents on Biomedical Engineering*, *5*(2), pp.142-147.

Hoemann, C.D., El-Gabalawy, H. and McKee, M.D., 2009. In vitro osteogenesis assays: influence of the primary cell source on alkaline phosphatase activity and mineralization. *Pathologie Biologie*, *57*(4), pp.318-323.

Honda, M., Kikushima, K., Kawanobe, Y., Konishi, T., Mizumoto, M. and Aizawa, M., 2012. Enhanced early osteogenic differentiation by silicon-substituted hydroxyapatite ceramics fabricated via ultrasonic spray pyrolysis route. *Journal of Materials Science: Materials in Medicine*, *23*(12), pp.2923-2932.

Huang, Z., Nelson, E.R., Smith, R.L. and Goodman, S.B., 2007. The sequential expression profiles of growth factors from osteroprogenitors to osteoblasts in vitro. *Tissue engineering*, *13*(9), pp.2311-2320.

Humphries, M.J., Obara, M., Olden, K. and Yamada, K.M., 1989. Role of fibronectin in adhesion, migration, and metastasis. *Cancer investigation*, *7*(4), pp.373-393.

Hutmacher, D.W., 2001. Scaffold design and fabrication technologies for engineering tissues—state of the art and future perspectives. *Journal of Biomaterials Science, Polymer Edition*, *12*(1), pp.107-124.

Huynh-Ba, G., Pjetursson, B.E., Sanz, M., Cecchinato, D., Ferrus, J., Lindhe, J. and Lang, N.P., 2010. Analysis of the socket bone wall dimensions in the upper maxilla in relation to immediate implant placement. *Clinical oral implants research*, *21*(1), pp.37-42.

Hynes, R.O., 1986. Fibronectins. *Scientific American*, *254*(6), pp.42-51.

Ishii, K., Kimura, A., Kushibiki, T., & Awazu, K. (2007). Fourier transform infrared spectroscopic analysis of cell differentiation. In *Optics in Tissue Engineering and Regenerative Medicine*, 6439, pp. 64390I.

Jahangir, A.A., Nunley, R.M., Mehta, S. and Sharan, A., 2008. Bone-graft substitutes in orthopaedic surgery. *AAos now*, *2*(1), pp.35-37.

Jamil, M., Elouatli, B., Khallok, H., Elouahli, A., Gourri, E., Ezzahmouly, M., Abida, F. and Hatim, Z., 2018. Silicon substituted hydroxyapatite: Preparation with Solid-State Reaction, Characterization and Dissolution Properties.

Jikko, A., Harris, S.E., Chen, D., Mendrick, D.L. and Damsky, C.H., 1999. Collagen integrin receptors regulate early osteoblast differentiation induced by BMP-2. *Journal of bone and mineral research*, *14*(7), pp.1075-1083.

Jo, Y.J., Kim, K.H., Koo, K.T., Kim, T.I., Seol, Y.J., Lee, Y.M., Ku, Y., Chung, C.P. and Rhyu, I.C., 2011. Initial adhesion of bone marrow stromal cells to various bone graft substitutes. *Journal of periodontal & implant science*, *41*(2), pp.67-72.

Kang, S.M., You, I., Cho, W.K., Shon, H.K., Lee, T.G., Choi, I.S., Karp, J.M. and Lee, H., 2010. One-step modification of superhydrophobic surfaces by a mussel-inspired polymer coating. *Angewandte Chemie International Edition*, *49*(49), pp.9401-9404.

Kanis, J.A. and World Health Organization Scientific Group, 2007. WHO technical report. *University of Sheffield, UK*, *66*.

Khatri, M., O'Brien, T. D., Sharma, J. M., 2009. Isolation and differentiation of chicken mesenchymal stem cells from bone marrow. *Stem Cells Dev. 18*, pp.1485–1492.

Keller, J.C., Collins, J.G., Niederauer, G.G. and McGee, T.D., 1997. In vitro attachment of osteoblast-like cells to osteoceramic materials. *Dental Materials*, *13*(1), pp.62-68.

Kennedy, S.B., Washburn, N.R., Simon Jr, C.G. and Amis, E.J., 2006. Combinatorial screen of the effect of surface energy on fibronectin-mediated osteoblast adhesion, spreading and proliferation. *Biomaterials*, *27*(20), pp.3817-3824.

Keselowsky, B.G., Collard, D.M. and García, A.J., 2005. Integrin binding specificity regulates biomaterial surface chemistry effects on cell differentiation. *Proceedings of the National Academy of Sciences*, *102*(17), pp.5953-5957.

Kilpadi, K.L., Chang, P.L. and Bellis, S.L., 2001. Hydroxylapatite binds more serum proteins, purified integrins, and osteoblast precursor cells than titanium or steel. *Journal of Biomedical Materials Research: An Official Journal of The Society for Biomaterials, The Japanese Society for Biomaterials, and The Australian Society for Biomaterials and the Korean Society for Biomaterials*, *57*(2), pp.258-267.

Kim, E.J., Bu, S.Y., Sung, M.K. and Choi, M.K., 2013. Effects of silicon on osteoblast activity and bone mineralization of MC3T3-E1 cells. *Biological trace element research*, *152*(1), pp.105-112.

Ko, C.L., Chen, J.C., Tien, Y.C., Hung, C.C., Wang, J.C. and Chen, W.C., 2015. Osteoregenerative capacities of dicalcium phosphate-rich calcium phosphate bone cement. *Journal of Biomedical Materials Research Part A*, *103*(1), pp.203-210.

Komori, T., 2006. Regulation of osteoblast differentiation by transcription factors. *Journal of cellular biochemistry*, *99*(5), pp.1233-1239.

Kouroupis, D., Baboolal, T.G., Jones, E. and Giannoudis, P.V., 2013. Native multipotential stromal cell colonization and graft expander potential of a bovine natural bone scaffold. *Journal of Orthopaedic Research*, *31*(12), pp.1950-1958.

Kouroupis, D., Jones, E., Baboolal, T. and Giannoudis, P.V., 2013, April. Bone marrow multipotential stromal cell colonisation of natural bone substitute Orthoss® - Osteoconductivity, osteoinductivity and graft expander potential. In *Orthopaedic Proceedings* (Vol. 95, No. SUPP_16, pp. 25-25). The British Editorial Society of Bone & Joint Surgery.

Kübler, A., Neugebauer, J., Oh, J.H., Scheer, M. and Zöller, J.E., 2004. Growth and proliferation of human osteoblasts on different bone graft substitutes an in vitro study. *Implant Dentistry*, *13*(2), pp.171-179.

Kubosch, E.J., Bernstein, A., Wolf, L., Fretwurst, T., Nelson, K. and Schmal, H., 2016. Clinical trial and in-vitro study comparing the efficacy of treating bony lesions with allografts versus synthetic or highly-processed xenogeneic bone grafts. *BMC musculoskeletal disorders*, *17*(1), p.77.

Kuzyk, P.R. and Schemitsch, E.H., 2011. The basic science of peri-implant bone healing. *Indian journal of orthopaedics*, *45*(2), p.108.

Lampin, M., Warocquier-Clérout, R., Legris, C., Degrange, M. and Sigot-Luizard, M.F., 1997. Correlation between substratum roughness and wettability, cell adhesion, and cell migration. *Journal of Biomedical Materials Research: An Official Journal of The Society for Biomaterials and The Japanese Society for Biomaterials*, *36*(1), pp.99-108.

Langstaff, S., Sayer, M., Smith, T.J.N., Pugh, S.M., Hesp, S.A.M. and Thompson, W.T., 1999. Resorbable bioceramics based on stabilized calcium phosphates. Part I: rational design, sample preparation and material characterization. *Biomaterials*, *20*(18), pp.1727-1741.

Lasgorceix, M., Costa, A.M., Mavropoulos, E., Sader, M., Calasans, M., Tanaka, M.N., Rossi, A., Damia, C., Chotard-Ghodsnia, R. and Champion, E., 2014. In vitro and in vivo evaluation of silicated hydroxyapatite and impact of insulin adsorption. *Journal of Materials Science: Materials in Medicine*, *25*(10), pp.2383-2393.

Laskus, A. and Kolmas, J., 2017. Ionic substitutions in non-apatitic calcium phosphates. *International journal of molecular sciences*, *18*(12), p.2542.
Lee, C.H., Singla, A. and Lee, Y., 2001. Biomedical applications of collagen. *International journal of pharmaceutics*, *221*(1-2), pp.1-22.
Lee, C.S., Szczesny, S.E. and Soslowsky, L.J., 2011. Remodeling and repair of orthopaedic tissue: role of mechanical loading and biologics: part II: cartilage and bone. *American journal of orthopedics (Belle Mead, NJ)*, *40*(3), pp.122-128.
Lee, J.H. and Cho, J.Y., 2014. Proteomics approaches for the studies of bone metabolism. *BMB reports*, *47*(3), p.141.
Lee, J.S., Yang, J.H., Hong, J.Y., Jung, U.W., Yang, H.C., Lee, I.S. and Choi, S.H., 2014. Early bone healing onto implant surface treated by fibronectin/oxysterol for cell adhesion/osteogenic differentiation: in vivo experimental study in dogs. *Journal of periodontal & implant science*, *44*(5), pp.242-250.
Lee, S.J., Suh, C.W., Lee, S.I., Kim, W.S., Lee, W.S., Kim, H.J., Choi, C.W., Kim, J.S. and Shin, H.J., 2014. Clinical characteristics, pathological distribution, and prognostic factors in non-Hodgkin lymphoma of Waldeyer's ring: nationwide Korean study. *The Korean journal of internal medicine*, *29*(3), p.352.
Lee, S., Lee, D.S., Choi, I., Pham, L. and Jang, J.H., 2015. Design of an osteoinductive extracellular fibronectin matrix protein for bone tissue engineering. *International journal of molecular sciences*, *16*(4), pp.7672-7681.
Lee, W.H., Loo, C.Y. and Rohanizadeh, R., 2014. A review of chemical surface modification of bioceramics: effects on protein adsorption and cellular response. *Colloids and Surfaces B: Biointerfaces*, *122*, pp.823-834.
Leung, K.S., Fung, K.P., Sher, A.H., Li, C.K. and Lee, K.M., 1993. Plasma bone-specific alkaline phosphatase as an indicator of osteoblastic activity. *The Journal of bone and joint surgery. British volume*, *75*(2), pp.288-292.
Li, J., Zhang, F. and Chen, J.Y., 2011. An integrated proteomics analysis of bone tissues in response to mechanical stimulation. *BMC systems biology*, *5*(3), p.S7.
Liang, C., Guo, B., Wu, H., Shao, N., Li, D., Liu, J., Dang, L., Wang, C., Li, H., Li, S. and Lau, W.K., 2015. Aptamer-functionalized lipid nanoparticles targeting osteoblasts as a novel RNA interference–based bone anabolic strategy. *Nature medicine*, *21*(3), p.288.
Linsley, C., Wu, B. and Tawil, B., 2013. The effect of fibrinogen, collagen type I, and fibronectin on mesenchymal stem cell growth and differentiation into osteoblasts. *Tissue Engineering Part A*, *19*(11-12), pp.1416-1423.
Liu, J. and Kerns, D.G., 2014. Suppl 1: Mechanisms of Guided Bone Regeneration: A Review. *The open dentistry journal*, *8*, p.56.
Logan, C.Y. and Nusse, R., 2004. The Wnt signaling pathway in development and disease. *Annu. Rev. Cell Dev. Biol.*, *20*, pp.781-810.
Logeart-Avramoglou, D., Anagnostou, F., Bizios, R. and Petite, H., 2005. Engineering bone: challenges and obstacles. *Journal of cellular and molecular medicine*, *9*(1), pp.72-84.
Long, F. and Ornitz, D.M., *Development of the endochondral skeleton. Cold Spring Harb Perspect Biol. 2013; 5 (1): a008334*. Epub 2013/01/04. doi: 10.1101/cshperspect. a008334 PMID: 23284041.
Lord, M.S., Cousins, B.G., Doherty, P.J., Whitelock, J.M., Simmons, A., Williams, R.L. and Milthorpe, B.K., 2006. The effect of silica nanoparticulate coatings on serum protein adsorption and cellular response. *Biomaterials*, *27*(28), pp.4856-4862.
Ludwig, S.C., Kowalski, J.M. and Boden, S.D., 2000. Osteoinductive bone graft substitutes. *European Spine Journal*, *9*(1), pp.S119-S125.
Lv, Y., Tan, T. and Svec, F., 2013. Molecular imprinting of proteins in polymers attached to the surface of nanomaterials for selective recognition of biomacromolecules. *Biotechnology advances*, *31*(8), pp.1172-1186.
Mackie, E., Ahmed, Y.A., Tatarczuch, L., Chen, K.S. and Mirams, M., 2008. Endochondral ossification: how cartilage is converted into bone in the developing skeleton. *The international journal of biochemistry & cell biology*, *40*(1), pp.46-62.

Mager, M.D., LaPointe, V. and Stevens, M.M., 2011. Exploring and exploiting chemistry at the cell surface. *Nature chemistry*, *3*(8), p.582.

Malaval, L., Liu, F., Roche, P. and Aubin, J.E., 1999. Kinetics of osteoprogenitor proliferation and osteoblast differentiation in vitro. *Journal of cellular biochemistry*, *74*(4), pp.616-627.

Mangano, C., Perrotti, V., Iezzi, G., Scarano, A., Mangano, F. and Piattelli, A., 2008. Bone Response to New Modified Titanium Surface Implants in Nonhuman Primates (Papio ursinus) and Humans: Histological Evaluation. *Journal of Oral Implantology*, *34*(1), pp.17-24.

Matassi, F., Botti, A., Sirleo, L., Carulli, C., & Innocenti, M. (2013). Porous metal for orthopedics implants. *Clinical Cases in Mineral and Bone Metabolism*. http://doi.org/10.11138/ccmbm/2013.10.2.111

Mathé, C., Devineau, S., Aude, J.C., Lagniel, G., Chédin, S., Legros, V., Mathon, M.H., Renault, J.P., Pin, S., Boulard, Y. and Labarre, J., 2013. Structural determinants for protein adsorption/non-adsorption to silica surface. *PloS one*, *8*(11), p.e81346.

Mavrogenis, A.F., Dimitriou, R., Parvizi, J. and Babis, G.C., 2009. Biology of implant osseointegration. *J Musculoskelet Neuronal Interact*, *9*(2), pp.61-71.

Meyer, H., 1966. Studies of the Response Speed of Silicon Surface Barrier Detectors, When Irradiated with Different Particles. *IEEE Transactions on Nuclear Science*, *13*(3), pp.180-188.

McComb, R.B., Bowers, G.N. and Posen, S., 1979. Clinical utilization of alkaline phosphatase measurements. In *Alkaline phosphatase* (pp. 525-786). Springer, Boston, MA.

McFarland, C.D., Thomas, C.H., DeFilippis, C., Steele, J.G. and Healy, K.E., 2000. Protein adsorption and cell attachment to patterned surfaces. *Journal of Biomedical Materials Research: An Official Journal of The Society for Biomaterials and The Japanese Society for Biomaterials*, *49*(2), pp.200-210.

McNamara, I., Deshpande, S. and Porteous, M.J.L.P., 2010. Impaction grafting of the acetabulum with a mixture of frozen, ground irradiated bone graft and porous synthetic bone substitute (Apapore 60). *The Journal of bone and joint surgery. British volume*, *92*(5), pp.617-623.

Millán, J.L., 2006. Alkaline phosphatases. *Purinergic signalling*, *2*(2), p.335.

Minguell, J.J., Erices, A. and Conget, P., 2001. Mesenchymal stem cells. *Experimental biology and medicine*, *226*(6), pp.507-520.

Mizuno, M., Fujisawa, R. and Kuboki, Y., 2000. Type I collagen-induced osteoblastic differentiation of bone-marrow cells mediated by collagen-α2β1 integrin interaction. *Journal of cellular physiology*, *184*(2), pp.207-213.

Mohamed, A.M., 2008. An overview of bone cells and their regulating factors of differentiation. *The Malaysian journal of medical sciences: MJMS*, *15*(1), p.4.

Monfoulet, L.E., Becquart, P., Marchat, D., Vandamme, K., Bourguignon, M., Pacard, E., Viateau, V., Petite, H. and Logeart-Avramoglou, D., 2014. The pH in the microenvironment of human mesenchymal stem cells is a critical factor for optimal osteogenesis in tissue-engineered constructs. *Tissue Engineering Part A*, *20*(13-14), pp.1827-1840.

Moore, W.R., Graves, S.E. and Bain, G.I., 2001. Synthetic bone graft substitutes. *ANZ journal of surgery*, *71*(6), pp.354-361.

Morra, M., 2000. On the molecular basis of fouling resistance. *Journal of Biomaterials Science, Polymer Edition*, *11*(6), pp.547-569.

Mosher, D. F. (1989). "Fibronectin." Academic Press, New York.

Moursi, A.M., Damsky, C.H., Lull, J., Zimmerman, D., Doty, S.B., Aota, S.I. and Globus, R.K., 1996. Fibronectin regulates calvarial osteoblast differentiation. *Journal of cell science*, *109*(6), pp.1369-1380.

Moursi, A.M., Globus, R.K. and Damsky, C.H., 1997. Interactions between integrin receptors and fibronectin are required for calvarial osteoblast differentiation in vitro. *Journal of cell science*, *110*(18), pp.2187-2196.

Mravic, M., Péault, B. and James, A.W., 2014. Current trends in bone tissue engineering. *BioMed research international*, *2014*.

Murugan, R., Rao, K.P. and Kumar, T.S.S., 2003. Heat-deproteinated xenogeneic bone from slaughterhouse waste: Physico-chemical properties. *Bulletin of Materials Science, 26* (5), pp.523-528.

Nair, A.K., Gautieri, A., Chang, S.W. and Buehler, M.J., 2013. Molecular mechanics of mineralized collagen fibrils in bone. *Nature communications*, *4*, p.1724.

Nakata, H., Kuroda, S., Tachikawa, N., Okada, E., Akatsuka, M., Kasugai, S. and Kondo, H., 2016. Histological and micro-computed tomographic observations after maxillary sinus augmentation with porous hydroxyapatite alloplasts: a clinical case series. *Springerplus*, *5*(1), p.260.

Nandi, S.K., Roy, S., Mukherjee, P., Kundu, B., De, D.K. and Basu, D., 2010. Orthopaedic applications of bone graft & graft substitutes: a review. *Indian Journal of Medical Reseach*, *132*(1), pp.15-30.

Nath, N., Hyun, J., Ma, H. and Chilkoti, A., 2004. Surface engineering strategies for control of protein and cell interactions. *Surface science*, *570*(1-2), pp.98-110.

Nath, S., Basu, B. and Sinha, A., 2006. A comparative study of conventional sintering with microwave sintering of hydroxyapatite synthesized by chemical route. *Trends in Biomaterials & Artificial Organs*, *19*(2), pp.93-98.

Navarro, M., Michiardi, A., Castano, O. and Planell, J.A., 2008. Biomaterials in orthopaedics. *Journal of the royal society interface*, *5*(27), pp.1137-1158.

Noh, H. and Vogler, E.A., 2006. Volumetric interpretation of protein adsorption: mass and energy balance for albumin adsorption to particulate adsorbents with incrementally increasing hydrophilicity. *Biomaterials*, *27*(34), pp.5801-5812.

Norde, W. and Favier, J.P., 1992. Structure of adsorbed and desorbed proteins. *Colloids and surfaces*, *64*(1), pp.87-93.

O'brien, F.J., 2011. Biomaterials & scaffolds for tissue engineering. *Materials today*, *14*(3), pp.88-95.

O'Shea, P.J., Kim, D.W., Logan, J.G., Davis, S., Walker, R.L., Meltzer, P.S., Cheng, S.Y. and Williams, G.R., 2012. Advanced bone formation in mice with a dominant-negative mutation in the thyroid hormone receptor β gene due to activation of Wnt/β-catenin protein signaling. *Journal of Biological Chemistry*, *287*(21), pp.17812-17822.

Ogura, N., Kawada, M., Chang, W.J., Zhang, Q., Lee, S.Y., Kondoh, T. and Abiko, Y., 2004. Differentiation of the human mesenchymal stem cells derived from bone marrow and enhancement of cell attachment by fibronectin. *Journal of oral science*, *46*(4), pp.207-213.

Olshina, M.A. and Sharon, M., 2016. Mass spectrometry: a technique of many faces. *Quarterly reviews of biophysics*, *49*.

Pagliari, D., Ciro Tamburrelli, F., Zirio, G., Newton, E.E. and Cianci, R., 2015. The role of “bone immunological niche” for a new pathogenetic paradigm of osteoporosis. *Analytical Cellular Pathology*, *2015*.

Parenteau-Bareil, R., Gauvin, R. and Berthod, F., 2010. Collagen-based biomaterials for tissue engineering applications. *Materials*, *3*(3), pp.1863-1887.

Pappin, D.J., Hojrup, P. and Bleasby, A.J., 1993. Rapid identification of proteins by peptide-mass fingerprinting. *Current biology*, *3*(6), pp.327-332.

Patel, N., Brooks, R.A., Clarke, M.T., Lee, P.M.T., Rushton, N., Gibson, I.R., Best, S.M. and Bonfield, W., 2005. In vivo assessment of hydroxyapatite and silicate-substituted hydroxyapatite granules using an ovine defect model. *Journal of materials science: materials in medicine*, *16*(5), pp.429-440.

Patel, M.S. and Karsenty, G., 2002. Regulation of bone formation and vision by LRP5.

Perry, C.R., 1999. Bone repair techniques, bone graft, and bone graft substitutes. *Clinical Orthopaedics and Related Research®*, *360*, pp.71-86.

Person, J., Helgason, B., Enggvist, H., Ferguson, S., and Persson, C., 2018. Stiffness and strength of cranioplastic implant systems in comparison to cranial bone. *Journal of Cranio-Maxillofacial Surgery, 46*(3), pp.418-423.

Petrochenko, P. and Narayan, R.J., 2010. Novel approaches to bone grafting: porosity, bone morphogenetic proteins, stem cells, and the periosteum. *Journal of long-term effects of medical implants*, *20*(4).

Pierschbacher, M.D. and Ruoslahti, E., 1984. Variants of the cell recognition site of fibronectin that retain attachment-promoting activity. *Proceedings of the National Academy of Sciences*, *81*(19), pp.5985-5988.

Pietak, A.M., Reid, J.W., Stott, M.J. and Sayer, M., 2007. Silicon substitution in the calcium phosphate bioceramics. *Biomaterials*, *28*(28), pp.4023-4032.

Pitt, J.J., 2009. Principles and applications of liquid chromatography-mass spectrometry in clinical biochemistry. *The Clinical Biochemist Reviews*, *30*(1), p.19.

Porter, A.E., Patel, N., Skepper, J.N., Best, S.M. and Bonfield, W., 2004. Effect of sintered silicate-substituted hydroxyapatite on remodelling processes at the bone–implant interface. *Biomaterials*, *25*(16), pp.3303-3314.

Rabe, M., Verdes, D. and Seeger, S., 2011. Understanding protein adsorption phenomena at solid surfaces. *Advances in colloid and interface science*, *162*(1-2), pp.87-106.

Ramazanoglu, M. and Oshida, Y., 2011. Osseointegration and bioscience of implant surfaces-current concepts at bone-implant interface. In *Implant Dentistry-A Rapidly Evolving Practice*. InTech.

Rashid, N., Harding, I.S., Buckland, T. and Hing, K.A., 2008. Nano-scale manipulation of silicate-substituted apatite chemistry impacts surface charge, hydrophilicity, protein adsorption and cell attachment. *International Journal of Nano And Biomaterials*, *1*(3), pp.299-319.

Rauniyar, N. and Yates III, J.R., 2014. Isobaric labeling-based relative quantification in shotgun proteomics. *Journal of proteome research*, *13*(12), pp.5293-5309.

Reffitt, D.M., Ogston, N., Jugdaohsingh, R., Cheung, H.F.J., Evans, B.A.J., Thompson, R.P.H., Powell, J.J. and Hampson, G.N., 2003. Orthosilicic acid stimulates collagen type 1 synthesis and osteoblastic differentiation in human osteoblast-like cells in vitro. *Bone*, *32*(2), pp.127-135.

Regan, J. and Long, F., 2013. Notch signaling and bone remodeling. *Current osteoporosis reports*, *11*(2), pp.126-129.

Reyes-Sánchez, A., Reyes-Tarrago, F., García-Ramos, C., Zárate-Kalfópulos, B., Estrada-Villaseñor, E. and Alpizar-Aguirre, A., 2017. Lumbar fusion with collagen type I and polyvinylpyrrolidone in combination with autograft. An experimental study in New Zealand rabbits. *Acta ortopedica mexicana*, *31*(4), pp.165-170.

Rico, P., Hernández, J.C.R., Moratal, D., Altankov, G., Pradas, M.M. and Salmerón-Sánchez, M., 2009. Substrate-induced assembly of fibronectin into networks: influence of surface chemistry and effect on osteoblast adhesion. *Tissue Engineering Part A*, *15*(11), pp.3271-3281.

Robey, P.G., 1996. Vertebrate mineralized matrix proteins: structure and function. *Connective tissue research*, *35*(1-4), pp.131-136.

Rosenberg, N., Rosenberg, O. and Soudry, M., 2012. Osteoblasts in bone physiology—Mini review. *Rambam Maimonides medical journal*, *3*(2).

Rosengren, Å., Pavlovic, E., Oscarsson, S., Krajewski, A., Ravaglioli, A. and Piancastelli, A., 2002. Plasma protein adsorption pattern on characterized ceramic biomaterials. *Biomaterials*, *23*(4), pp.1237-1247.

Rosengren, K.J., Daly, N.L., Plan, M.R., Waine, C. and Craik, D.J., 2003. Twists, knots, and rings in proteins structural definition of the cyclotide framework. *Journal of Biological Chemistry*, *278*(10), pp.8606-8616.

Rouahi, M., Gallet, O., Champion, E., Dentzer, J., Hardouin, P. and Anselme, K., 2006. Influence of hydroxyapatite microstructure on human bone cell response. *Journal of Biomedical Materials Research Part A: An Official Journal of The Society for Biomaterials, The Japanese Society for Biomaterials, and The Australian Society for Biomaterials and the Korean Society for Biomaterials*, *78*(2), pp.222-235.

Rousselle, A.V. and Heymann, D., 2002. Osteoclastic acidification pathways during bone resorption. *Bone*, *30*(4), pp.533-540.

Rubin, J., Rubin, C. and Jacobs, C.R., 2006. Molecular pathways mediating mechanical signaling in bone. *Gene*, *367*, pp.1-16.

Ruoslahti, E., 1984. Fibronectin in cell adhesion and invasion. *Cancer and Metastasis Reviews*, *3*(1), pp.43-51.

Rutkovskiy, A., Stensløkken, K.O. and Vaage, I.J., 2016. Osteoblast differentiation at a glance. *Medical science monitor basic research*, *22*, p.95.

Sabokbar, A., Millett, P.J., Myer, B. and Rushton, N., 1994. A rapid, quantitative assay for measuring alkaline phosphatase activity in osteoblastic cells in vitro. *Bone and mineral*, *27*(1), pp.57-67.

Sanjurjo-Rodríguez, C., Castro-Viñuelas, R., Hermida-Gómez, T., Fernández-Vázquez, T., Fuentes-Boquete, I. M., de Toro-Santos, F. J., Blanco-García, F. J. (2017). Ovine Mesenchymal Stromal Cells: Morphologic, Phenotypic and Functional Characterization for Osteochondral Tissue Engineering. *PloS one*, *12*(1).

Samizadeh, S.; (2010) Bone formation on calcium phosphate bone substitute materials. Doctoral thesis, UCL (University College London).

Sammons, R.L., Lumbikanonda, N., Gross, M. and Cantzler, P., 2005. Comparison of osteoblast spreading on microstructured dental implant surfaces and cell behaviour in an explant model of osseointegration: a scanning electron microscopic study. *Clinical oral implants research*, *16*(6), pp.657-666.

Sanghani-Kerai, A., 2017. Do Stem Cells Transfected with CXCR4 Enhance Bone Formation in Osteoporosis? Doctoral thesis, UCL (University College London).

Sant, S., Poulin, S. and Hildgen, P., 2008. Effect of polymer architecture on surface properties, plasma protein adsorption, and cellular interactions of pegylated nanoparticles. *Journal of Biomedical Materials Research Part A: An Official Journal of The Society for Biomaterials, The Japanese Society for Biomaterials, and The Australian Society for Biomaterials and the Korean Society for Biomaterials*, *87*(4), pp.885-895.

Sawyer, A.A., Hennessy, K.M. and Bellis, S.L., 2005. Regulation of mesenchymal stem cell attachment and spreading on hydroxyapatite by RGD peptides and adsorbed serum proteins. *Biomaterials*, *26*(13), pp.1467-1475.

Sawyer, A.A., Hennessy, K.M. and Bellis, S.L., 2007. The effect of adsorbed serum proteins, RGD and proteoglycan-binding peptides on the adhesion of mesenchymal stem cells to hydroxyapatite. *Biomaterials*, *28*(3), pp.383-392.

Schmidt, A., Forne, I. and Imhof, A., 2014. Bioinformatic analysis of proteomics data. *BMC systems biology*, *8*(2), p.S3.

Schönmeyr, B.H., Wong, A.K., Li, S., Gewalli, F., Cordiero, P.G. and Mehrara, B.J., 2008. Treatment of hydroxyapatite scaffolds with fibronectin and fetal calf serum increases osteoblast adhesion and proliferation in vitro. *Plastic and reconstructive surgery*, *121*(3), pp.751-762.

Schwartz, Z., Weesner, T., Van Dijk, S., Cochran, D.L., Mellonig, J.T., Lohmann, C.H., Carnes, D.L., Goldstein, M., Dean, D.D. and Boyan, B.D., 2000. Ability of deproteinized cancellous bovine bone to induce new bone formation. *Journal of periodontology*, *71*(8), pp.1258-1269.

Schwartz, Z. and Boyan, B.D., 1994. Underlying mechanisms at the bone–biomaterial interface. *Journal of cellular biochemistry*, *56*(3), pp.340-347.

Schwarz, G., Trapp, M., Schimko, R., Butzke, G. and Rogge, K., 1973. Concentration profiles of implanted boron ions in silicon from measurements with the ion microprobe. *physica status solidi (a)*, *17*(2), pp.653-658.

Schwarz, K., 1973. A bound form of silicon in glycosaminoglycans and polyuronides. *Proceedings of the National Academy of Sciences*, *70*(5), pp.1608-1612.

Seaborn, C.D. and Nielsen, F.H., 2002. Silicon deprivation decreases collagen formation in wounds and bone and ornithine transaminase enzyme activity in liver. *Biological trace element research*, *89*(3), pp.251-261.

Seaborn, C.D. and Nielsen, F.H., 2002. Dietary silicon and arginine affect mineral element composition of rat femur and vertebra. *Biological trace element research*, *89*(3), pp.239-250.

Senbanjo, L.T. and Chellaiah, M.A., 2017. CD44: a multifunctional cell surface adhesion receptor is a regulator of progression and metastasis of cancer cells. *Frontiers in cell and developmental biology*, *5*, p.18.

Sharma, U., Pal, D. and Prasad, R., 2014. Alkaline phosphatase: an overview. *Indian Journal of Clinical Biochemistry*, *29*(3), pp.269-278.

Shchukarev, A., Mladenovic, Z. and Ransjö, M., 2012. Surface characterization of bone graft substitute materials conditioned in cell culture medium. 2. Protein adsorption. *Surface and Interface Analysis*, *44*(8), pp.919-923.

Shelton, R.M., Rasmussen, A.C. and Davies, J.E., 1988. Protein adsorption at the interface between charged polymer substrata and migrating osteoblasts. *Biomaterials*, *9*(1), pp.24-29.

Simon, A., Cohen-Bouhacina, T., Porte, M.C., Aime, J.P., Amedee, J., Bareille, R. and Baquey, C., 2003. Characterization of dynamic cellular adhesion of osteoblasts using atomic force microscopy. *Cytometry Part A: the journal of the International Society for Analytical Cytology*, *54*(1), pp.36-47.

Sogo, Y., Ito, A., Onoguchi, M., Oyane, A., Tsurushima, H. and Ichinose, N., 2007. Formation of a FGF-2 and calcium phosphate composite layer on a hydroxyapatite ceramic for promoting bone formation. *Biomedical Materials*, *2*(3), p.S175.

Soleimani, M., Nadri, S, 2009. A protocol for isolation and culture of mesenchymal stem cells from mouse bone marrow. *Nat Protoc,* 4, 102–106.

Somaiah, C., Kumar, A., Mawrie, D., Sharma, A., Patil, S.D., Bhattacharyya, J., Swaminathan, R. and Jaganathan, B.G., 2015. Collagen promotes higher adhesion, survival and proliferation of mesenchymal stem cells. *PLoS One*, *10*(12), p.e0145068.

Šponer, P., Kučera, T., Diaz-Garcia, D. and Filip, S., 2014. The role of mesenchymal stem cells in bone repair and regeneration. *European Journal of Orthopaedic Surgery & Traumatology*, *24*(3), pp.257-262.

Gray, H. and Standring, S., 2008. *Gray's anatomy* (pp. 1429-63). Arcturus Publishing.

Steele, J.G., McFarland, C., Dalton, B.A., Johnson, G., Evans, M.D., Rolfe Howlett, C. and Underwood, P.A., 1994. Attachment of human bone cells to tissue culture polystyrene and to unmodified polystyrene: the effect of surface chemistry upon initial cell attachment. *Journal of Biomaterials Science, Polymer Edition*, *5*(3), pp.245-257.

Steffens, S., Schrader, A.J., Vetter, G., Eggers, H., Blasig, H., Becker, J., Kuczyk, M.A. and Serth, J., 2012. Fibronectin 1 protein expression in clear cell renal cell carcinoma. *Oncology letters*, *3*(4), pp.787-790.

Stein, G.S., Lian, J.B. and Owen, T.A., 1990. Bone cell differentiation: a functionally coupled relationship between expression of cell-growth-and tissue-specific genes. *Current opinion in cell biology*, *2*(6), pp.1018-1027.

Stephansson, S.N., Byers, B.A. and García, A.J., 2002. Enhanced expression of the osteoblastic phenotype on substrates that modulate fibronectin conformation and integrin receptor binding. *Biomaterials*, *23*(12), pp.2527-2534.

Studer, D., Millan, C., Ozturk, E., Maniura-Weber, K. and Zenobi-Wong, M., 2012. Molecular and biophysical mechanisms regulating hypertrophic differentiation in chondrocytes and mesenchymal stem cells. *Eur Cell Mater*, *24*(24), pp.118-135.

Sun, C., Tian, Y., Xu, W., Zhou, C., Xie, H. and Wang, X., 2015. Development and performance analysis of Si-CaP/fine particulate bone powder combined grafts for bone regeneration. *Biomedical engineering online*, *14*(1), p.47.

Suzuki, K., Aoki, K. and Ohya, K., 1997. Effects of surface roughness of titanium implants on bone remodeling activity of femur in rabbits. *Bone*, *21*(6), pp.507-514.

Szurkowska, K. and Kolmas, J., 2017. Hydroxyapatites enriched in silicon–Bioceramic materials for biomedical and pharmaceutical applications. *Progress in Natural Science: Materials International*, *27*(4), pp.401-409.

Tang, Y., Liu, L., Wang, P., Chen, D., Wu, Z. and Tang, C., 2017. Periostin promotes migration and osteogenic differentiation of human periodontal ligament mesenchymal stem cells via the Jun amino-terminal kinases (JNK) pathway under inflammatory conditions. *Cell proliferation*, *50*(6), p.e12369.

Tang, Z., Li, X., Tan, Y., Fan, H. and Zhang, X., 2017. The material and biological characteristics of osteoinductive calcium phosphate ceramics. *Regenerative biomaterials*, *5*(1), pp.43-59.

Tang, L., Thevenot, P. and Hu, W., 2008. Surface chemistry influences implant biocompatibility. *Current topics in medicinal chemistry*, *8*(4), pp.270-280.

Thian, E.S., Huang, J., Best, S.M., Barber, Z.H. and Bonfield, W., 2006. Novel silicon-doped hydroxyapatite (Si-HA) for biomedical coatings: An in vitro study using acellular simulated body fluid. *Journal of Biomedical Materials Research Part B: Applied Biomaterials: An Official Journal of The Society for Biomaterials, The Japanese Society for Biomaterials, and The Australian Society for Biomaterials and the Korean Society for Biomaterials*, *76*(2), pp.326-333.

Thian, E.S., Huang, J., Best, S.M., Barber, Z.H. and Bonfield, W., 2006. Silicon-substituted hydroxyapatite thin films: Effect of annealing temperature on coating stability and bioactivity. *Journal of Biomedical Materials Research Part A: An Official Journal of The Society for Biomaterials, The Japanese Society for Biomaterials, and The Australian Society for Biomaterials and the Korean Society for Biomaterials*, *78*(1), pp.121-128.

Thian, E.S, Huang, J., Best, S.M., Barber, Z.H., Brooks, R.A., Rushton, N. and Bonfield, W., 2006. The response of osteoblasts to nanocrystalline silicon-substituted hydroxyapatite thin films. *Biomaterials*, *27*(13), pp.2692-2698.

Thompson, A., Schäfer, J., Kuhn, K., Kienle, S., Schwarz, J., Schmidt, G., Neumann, T. and Hamon, C., 2003. Tandem mass tags: a novel quantification strategy for comparative analysis of complex protein mixtures by MS/MS. *Analytical chemistry*, *75*(8), pp.1895-1904.

Tseng, L.L., Ho, C.M., Liang, W.Z., Hsieh, Y.D. and Jan, C.R., 2013. Comparison of efficacies of different bone substitutes adhered to osteoblasts with and without extracellular matrix proteins. *Journal of Dental Sciences*, *8*(4), pp.399-404.

Ullah, I., Subbarao, R.B. and Rho, G.J., 2015. Human mesenchymal stem cells-current trends and future prospective. *Bioscience reports*, *35*(2), p.e00191.

Usta, M. and Urganci, N., 2014. Does gluten-free diet protect children with celiac disease from low bone density?. *Iranian journal of pediatrics*, *24*(4), p.429.

Arcos, D., Sanchez-Salcedo, S., Izquierdo-Barba, I., Ruiz, L., Gonzalez-Calbet, J. and Vallet-Regí, M., 2006. Crystallochemistry, textural properties, and in vitro biocompatibility of different silicon-doped calcium phosphates. *Journal of Biomedical Materials Research Part A: An Official Journal of The Society for Biomaterials, The Japanese Society for Biomaterials, and The Australian Society for Biomaterials and the Korean Society for Biomaterials*, *78*(4), pp.762-771.

Vallet-Regí, M. and Arcos, D., 2005. Silicon substituted hydroxyapatites. A method to upgrade calcium phosphate based implants. *Journal of Materials chemistry*, *15*(15), pp.1509-1516.

Viale-Bouroncle, S., Gosau, M. and Morsczeck, C., 2014. Collagen I induces the expression of alkaline phosphatase and osteopontin via independent activations of FAK and ERK signalling pathways. *Archives of oral biology*, *59*(12), pp.1249-1255.

Viguet-Carrin, S., Garnero, P. and Delmas, P.D., 2006. The role of collagen in bone strength. *Osteoporosis international*, *17*(3), pp.319-336.

Vilaseca, P., Dawson, K.A. and Franzese, G., 2013. Understanding and modulating the competitive surface-adsorption of proteins through coarse-grained molecular dynamics simulations. *Soft Matter*, *9*(29), pp.6978-6985.

von Doernberg, M.C., von Rechenberg, B., Bohner, M., Grünenfelder, S., van Lenthe, G.H., Müller, R., Gasser, B., Mathys, R., Baroud, G. and Auer, J., 2006. In vivo behavior of calcium phosphate scaffolds with four different pore sizes. *Biomaterials*, *27*(30), pp.5186-5198.

Voronkov, A.V., Kopylov, V.M. and PARSONS, I.W., 1997. Furan-containing modified organosilicon polymers: Preparation, properties and some applications. *European polymer journal*, *33*(7), pp.979-990.

Vroman, L., 2009. When blood is touched. *Materials*, *2*(4), pp.1547-1557.

Vroman, L. and Adams, A.L., 1987, January. Why plasma-proteins interact at interfaces. In *Acs Symposium Series* (Vol. 343, pp. 154-164). 1155 16TH ST, NW, WASHINGTON, DC 20036: AMER CHEMICAL SOC.

Walsh, M.C. and Choi, Y., 2014. Biology of the RANKL–RANK–OPG system in immunity, bone, and beyond. *Frontiers in immunology*, *5*, p.511.
Walsh, W.R., Oliver, R.A., Christou, C., Lovric, V., Walsh, E.R., Prado, G.R. and Haider, T., 2017. Critical size bone defect healing using collagen–calcium phosphate bone graft materials. *PloS one*, *12*(1), p.e0168883.
Wang, K., Zhou, C., Hong, Y. and Zhang, X., 2012. A review of protein adsorption on bioceramics. *Interface focus*, *2*(3), pp.259-277.
Wang, P., Zhao, L., Chen, W., Liu, X., Weir, M.D. and Xu, H.H.K., 2014. Stem cells and calcium phosphate cement scaffolds for bone regeneration. *Journal of dental research*, *93*(7), pp.618-625.
Wang, W. and Yeung, K.W., 2017. Bone grafts and biomaterials substitutes for bone defect repair: A review. *Bioactive Materials*, *2*(4), pp.224-247.
Wang, Y. H., Liu, Y., Maye, P., & Rowe, D. W., 2006. Examination of mineralized nodule formation in living osteoblastic cultures using fluorescent dyes. *Biotechnology progress*, *22*(6), 1697-1701.
Watabe, T. and Miyazono, K., 2009. Roles of TGF-β family signaling in stem cell renewal and differentiation. *Cell research*, *19*(1), p.103.
Weber, G.F., Ashkar, S., Glimcher, M.J. and Cantor, H., 1996. Receptor-ligand interaction between CD44 and osteopontin (Eta-1). *Science*, *271*(5248), pp.509-512.
Weiss, R.E. and Reddi, A.H., 1981. Appearance of fibronectin during the differentiation of cartilage, bone, and bone marrow. *The Journal of cell biology*, *88*(3), pp.630-636.
Weszl, M., Skaliczki, G., Cselenyák, A., Kiss, L., Major, T., Schandl, K., Bognár, E., Stadler, G., Peterbauer, A., Csönge, L. and Lacza, Z., 2012. Freeze-dried human serum albumin improves the adherence and proliferation of mesenchymal stem cells on mineralized human bone allografts. *Journal of Orthopaedic Research*, *30*(3), pp.489-496.
Wilson, C.J., Clegg, R.E., Leavesley, D.I. and Pearcy, M.J., 2005. Mediation of biomaterial–cell interactions by adsorbed proteins: a review. *Tissue engineering*, *11*(1-2), pp.1-18.
Wu, M., Chen, G. and Li, Y.P., 2016. TGF-β and BMP signaling in osteoblast, skeletal development, and bone formation, homeostasis and disease. *Bone research*, *4*, p.16009.
Wuthier, R.E., Rice, G.S., Wallace, J.E., Weaver, R.L., LeGeros, R.Z. and Eanes, E.D., 1985. In vitro precipitation of calcium phosphate under intracellular conditions: formation of brushite from an amorphous precursor in the absence of ATP. *Calcified tissue international*, *37*(4), pp.401-410.
Yamada, K.M. and Clark, R.A., 1988. Provisional matrix. In *The molecular and cellular biology of wound repair* (pp. 51-93). Springer, Boston, MA.
Yamada, M. and Egusa, H., 2018. Current bone substitutes for implant dentistry. *Journal of Prosthodontic Research*. 62 (2), pp 152-161.
Yamamoto, K., Kishida, T., Sato, Y., Nishioka, K., Ejima, A., Fujiwara, H., Kubo, T., Yamamoto, T., Kanamura, N. and Mazda, O., 2015. Direct conversion of human fibroblasts into functional osteoblasts by defined factors. *Proceedings of the National Academy of Sciences*, *112*(19), pp.6152-6157.
Yang, F., Yang, D., Tu, J., Zheng, Q., Cai, L. and Wang, L., 2011. Strontium enhances osteogenic differentiation of mesenchymal stem cells and in vivo bone formation by activating Wnt/catenin signaling. *Stem cells*, *29*(6), pp.981-991.
Yang, X. and Karsenty, G., 2002. Transcription factors in bone: developmental and pathological aspects. *Trends in molecular medicine*, *8*(7), pp.340-345.
Ylä-Soininmäki, A., Moritz, N., Turco, G., Paoletti, S. and Aro, H.T., 2013. Quantitative characterization of porous commercial and experimental bone graft substitutes with microcomputed tomography. *Journal of Biomedical Materials Research Part B: Applied Biomaterials*, *101*(8), pp.1538-1548.
Yuan, H., Fernandes, H., Habibovic, P., de Boer, J., Barradas, A.M., de Ruiter, A., Walsh, W.R., van Blitterswijk, C.A. and de Bruijn, J.D., 2010. Osteoinductive ceramics as

a synthetic alternative to autologous bone grafting. *Proceedings of the National Academy of Sciences*, *107*(31), pp.13614-13619.

Zang, H., Liu, Y., Chen, J. and Wang, K., 2006. An experimental research on different temperature sintered bone as carrier of bone morphogenetic protein. *Journal of biomedical engineering*, *23*(2), pp.366-369.

Zambonin, G. and Grano, M., 1995. Biomaterials in orthopaedic surgery: effects of different hydroxyapatites and demineralized bone matrix on proliferation rate and bone matrix synthesis by human osteoblasts. *Biomaterials*, *16*(5), pp.397-402.

Zivko, M., Sahlin-Platt, A., Andersson, B. and Johnsson, A., 2013. *In vitro* study of the biological interface of Bio-Oss: implications of the experimental setup. *Clinical Oral Implants Research.* 24(3), pp.329-335.

Zhang, B., Myers, D., Wallace, G., Brandt, M. and Choong, P., 2014. Bioactive coatings for orthopaedic implants—recent trends in development of implant coatings. *International Journal of Molecular Sciences*, *15*(7), pp.11878-11921.

Zhao, B. and Ivashkiv, L.B., 2011. Negative regulation of osteoclastogenesis and bone resorption by cytokines and transcriptional repressors. *Arthritis research & therapy*, *13*(4), p.234.

Zhen, G. and Cao, X., 2014. Targeting TGFβ signaling in subchondral bone and articular cartilage homeostasis. *Trends in pharmacological sciences*, *35*(5), pp.227-236.

Zheng, X., Baker, H., Hancock, W.S., Fawaz, F., McCaman, M. and Pungor Jr, E., 2006. Proteomic analysis for the assessment of different lots of fetal bovine serum as a raw material for cell culture. Part IV. Application of proteomics to the manufacture of biological drugs. *Biotechnology progress*, *22*(5), pp.1294-1300.

Zhu, Heng, Zi-Kuan Guo, Xiao-Xia Jiang, Hong Li, Xiao-Yan Wang, Hui-Yu Yao, Yi Zhang, and Ning Mao. "A protocol for isolation and culture of mesenchymal stem cells from mouse compact bone." *Nature protocols* 5, no. 3 (2010): 550.

Zou, S., Ireland, D., Brooks, R.A., Rushton, N. and Best, S., 2009. The effects of silicate ions on human osteoblast adhesion, proliferation, and differentiation. *Journal of Biomedical Materials Research Part B: Applied Biomaterials*, *90*(1), pp.123-130.